



Universiteit
Leiden
The Netherlands

Glycosylation analysis of immune-related molecules

Borosak, I.

Citation

Borosak, I. (2024, October 1). *Glycosylation analysis of immune-related molecules*. Retrieved from <https://hdl.handle.net/1887/4093406>

Version: Publisher's Version

License: [Licence agreement concerning inclusion of doctoral thesis in the Institutional Repository of the University of Leiden](#)

Downloaded from: <https://hdl.handle.net/1887/4093406>

Note: To cite this publication please use the final published version (if applicable).

The background of the cover is a complex, abstract geometric pattern. It features a large, multi-colored polygonal shape at the bottom, composed of various shades of blue, green, yellow, and red. Above this shape, the background is white, scattered with numerous small, colorful geometric shapes, including squares, triangles, and circles in shades of purple, blue, green, yellow, and red. The title is centered in the upper half of the cover.

Glycosylation Analysis of Immune-Related Molecules

Iwona Borošak

*GLYCOSYLATION ANALYSIS
OF
IMMUNE-RELATED MOLECULES*

IWONA BOROŠAK

ISBN: 978-94-6510-106-4

©2024 Iwona Teresa Borošak. All rights reserved. No part of this book may be reproduced, stored in a retrieval system or transmitted in any form or by any means without permission of the author or the journals holding the copyrights of the published manuscripts. All published material was reprinted with permission.

The work presented in this thesis was performed at the Center for Proteomics and Metabolomics, Leiden University Medical Center, The Netherlands, and at Genos Ltd., Croatia.

The work was supported by the European Union Horizon 2020 Glycosylation Signatures for Precision Medicine Project, GlySign, grant number 722095.

Cover design: Iwona Borošak

Layout: Iwona Borošak

GLYCOSYLATION ANALYSIS
OF
IMMUNE-RELATED MOLECULES

Proefschrift

ter verkrijging van
de graad van doctor aan de Universiteit Leiden,
op gezag van rector magnificus prof.dr.ir. H. Bijl,
volgens besluit van het college voor promoties
te verdedigen op dinsdag 1 oktober 2024
klokke 10:00 uur

door

Iwona Borošak

geboren te Sosnowiec, Polen

in 1989

Promotores

Prof. dr. M. Wuhrer

Prof. dr. G. Lauc

*Faculty of Pharmacy and Biochemistry,
University of Zagreb, Croatia*

Co-promotor

Dr. D. Falck

Leden promotiecommissie

Prof. L.A. Trouw

Dr. J. Suurmond

Prof. dr. D.J. Lefeber

*Department of Neurology,
Donders Institute for Brain, Cognition and Behavior,
Radboud University Medical Center, The Netherlands*

*Department of Laboratory Medicine,
Translational Metabolic Laboratory,
Radboud University Medical Center, The Netherlands*

Dr. K.R. Reiding

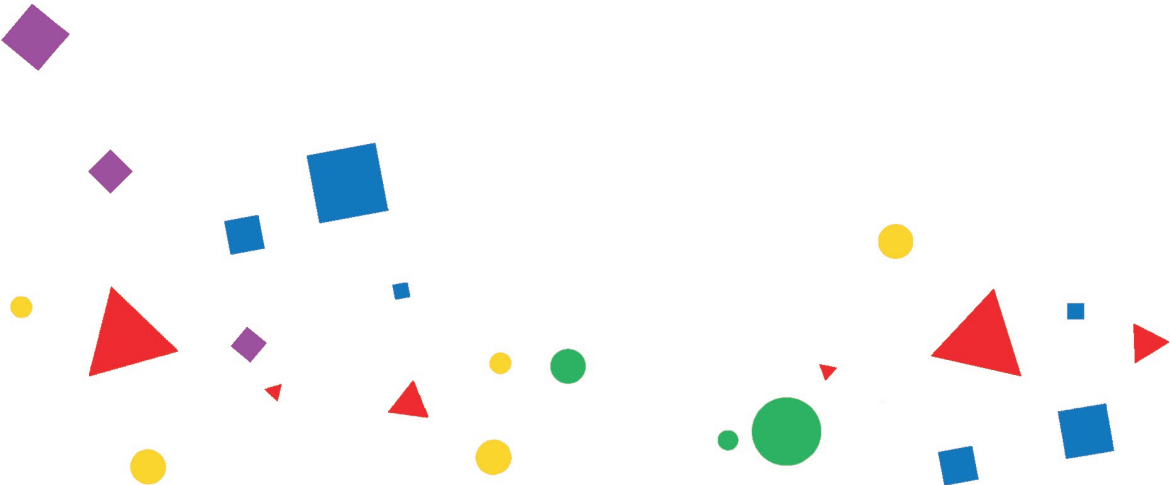
*Faculty of Science,
Pharmaceutical sciences,
Biomolecular Mass Spectrometry and Proteomics,
Utrecht University, The Netherlands*

*"I am among those who think that science has great
beauty."*

Marie Skłodowska-Curie (1934)

Table of Contents

CHAPTER 1	9
General introduction and scope of the thesis	
CHAPTER 2	31
A functional spleen contributes to afucosylated IgG in humans	
CHAPTER 3	53
Specific IgG glycosylation differences precede relapse in PR3-ANCA associated vasculitis patients with and without ANCA rise	
CHAPTER 4	85
Site-specific glycosylation mapping of Fc gamma receptor IIIb from neutrophils of individual healthy donors	
CHAPTER 5	119
High-throughput N-glycan profiling of plasma and serum using a routine and robust LC-MS analysis platform	
CHAPTER 6	139
Seminal plasma N-glycome as a new biomarker of environmental exposure associated with semen quality	
CHAPTER 7	159
Discussion and perspectives	
ADDENDUM	177
English Summary	179
Nederlandse Samenvatting	183
Curriculum Vitae	187
List of Publications	189
Acknowledgments	191



Chapter 1

General introduction and scope of the thesis



1. INTRODUCTION

Herein, I discuss the importance of glycosylation of key components/proteins of the immune system and its perturbations in autoimmune and infectious diseases. Moreover, I describe how state-of-the-art mass spectrometry (MS) technologies can be used to identify the glycan signatures of different autoimmune and infectious diseases.

1.1 BACKGROUND

Glycosylation is a common feature of the surfaces of all living organisms and most secreted proteins. Together with nucleic acids, proteins and lipids, glycans are one of the four fundamental classes of molecules that they are essential for life. In the immune system, glycans participate in nearly all immunological processes, including host-pathogen interactions, immunological recognition and activation, and differentiation between self and non-self-antigens. Proper glycosylation is crucial for maintaining homeostasis, while changes in glycosylation patterns can broadly impact fundamental immunological processes. Alterations in the glycan repertoire on various immunological components may be triggered by environmental and genetic factors. Aberrant glycosylation of immune components is associated with many inflammatory, autoimmune and oncological diseases. Though regulation of glycan changes is not well understood, current methodological advances have enabled association of glycosylation changes with the onset, progression and outcome of many pathologies. Especially, dysregulation of N-glycosylation is implicated in many immune-related disorders. Therefore, understanding the role of N-glycosylation in immunity and inflammation is important for developing new diagnostic tools, therapies and treatments for these conditions.

1.2 PROTEIN GLYCOSYLATION

Protein glycosylation is the enzyme-catalyzed process of the addition of a carbohydrate chain, or glycan, to a protein backbone. The process takes place in the endoplasmic reticulum and Golgi apparatus, where secreted and membrane proteins are being glycosylated, including key components of the immune system, such as antibodies, cytokines and chemokines as well as their receptors.(1) Protein glycosylation comes in two main classification types: N- and O-glycosylation. The glycan class is defined based on the side-chain atoms of amino acid to which glycans are linked. In N-glycosylation, glycans are attached to the nitrogen atom of an asparagine (Asn, N) side chain by a β -1N linkage, whereas in O-glycosylation glycans are attached to the oxygen atom in the side chain of serine and threonine residues.(2) Comprising often a significant proportion of the total glycoprotein size, glycans profoundly modulate physicochemical properties, structure, and function of the conjugated proteins. In addition, glycans mediate a wide range of biological roles, as well as intrinsic and extrinsic recognition.(2) Recent technological advances have provided new insights into the structure of the glycans and glycoconjugates and revealed their diversity.(3) Furthermore, an increasing number of large cohort studies have profiled and compared glycosylation in physiological and pathophysiological states, enabling glycan-based clinical marker discovery.(4)

1.2.1 Protein N-glycosylation

Whether a protein is glycosylated or not depends mainly on the presence of the consensus sequence Asn-X-Ser/Thr (X≠Pro) and occasionally Asn-X-Cys. Around 70% of proteins are estimated to contain the consensus N-glycosylation sequence. However, not all sequons are N-glycosylated and the average N-glycan site occupancy is estimated at 65%.(5)

N-glycan processing begins with the transfer of a 14-sugar oligosaccharide to the sequon. Subsequently, the attached precursor glycan is trimmed by series of glucosidases and mannosidases in the ER. It undergoes further maturation in the Golgi by adding monosaccharides, such as N-acetylglucosamine, galactose, sialic acid and fucose.(2) Based on the final structure, N-glycans can be classified into three main classes: oligomannose, hybrid and complex. The three different classes share a common pentasaccharide core consisting of two GlcNAcs and three mannose residues. Oligomannose N-glycans exist with the core structure and the addition of up to six mannose residues. These glycans undergo only incomplete processing and escape further modifications. In contrast, complex type N-glycans contain one to four additional GlcNAc residues, so-called antennae, which are often elongated with galactose and sialic acid. And as its name implies, the hybrid type is a combination of both and has one complex arm bearing at least a GlcNAc, and one arm terminated with at least one additional mannose.

Unlike genome, transcriptome or proteome biosynthesis, glycan biosynthesis is a non-templated process and thus, relies on the combinatorial activity of subsets of glycosyltransferases and glycosidases regulated by many cellular factors. These include cell type, cell signals, the availability of nucleotide sugars, and the accessibility of the N-glycosylation site. Moreover, N-glycan compositions depend on the physiological state of the cell and variations occur with almost every disease. Thus, the final N-glycan compositions on a given protein are very diverse and vary from tissue to tissue, cell to cell, protein to protein, and even site to site reflecting the overall cellular status in health and disease. To describe the variation in protein glycosylation, terms such as macro-heterogeneity and micro-heterogeneity have been introduced. Macro-heterogeneity describes the diversity in glycan occupancy, while micro-heterogeneity refers to the variations of glycan structure at a specific site. Importantly, both forms of heterogeneity strongly influence many of glycoprotein functional aspects and reflect a given physiological and pathophysiological state.

1.2.2 N-Glycosylation in immunity and inflammation

Glycans are present on key immune molecules and play a role in regulating their interaction, signal transduction and effector functions. They control molecular interactions and thus convey important functions in the innate and adaptive immune response through several basic mechanisms. The glycan recognition system, for example, promotes biological activity via binding of distinctive glycan moieties on the surface of soluble proteins or immune cells to glycan-binding proteins (GBPs), such as lectins. The intimate contact of GBPs and specific

carbohydrate determinants on respective ligands is essential for maintaining homeostasis and regulating immune and inflammatory responses, including immune cell trafficking, signalling and maintenance of self-tolerance.(6, 7)

In the adaptive immune system, glycans present on secreted or cell surface molecules can modulate signal transduction, protein-protein and cell-cell interactions necessary for humoral and cellular immunity. For instance, glycans found on T-cell (TCR) and B-cell (BCR) receptors, along with their cognate lectins are involved in the molecular mechanism that controls the threshold of TCR and BCR activation. Changes in glycan composition modify these molecular interactions, thereby influencing immunological signaling with a profound effect on the immune system.(8, 9) In addition to their presence on the cell surface molecules, glycans also regulate the immunological functions of secreted proteins such as immunoglobulins (Igs), or antibodies. Igs are essential components of humoral immunity that recognize, neutralize and mark pathogens, such as bacteria, fungi or viruses, for elimination. The glycans on Igs can affect their structure, half-life, antigen- and receptor-binding properties, ultimately influencing their effector and biological functions.(10, 11) Alterations of IgG glycosylation affect binding to Fc gamma receptors (FcγRs) and complement component 1q (C1q), and thus downstream effector signaling, such as ADCC and complement activation.(12, 13) Changes in Ig glycosylation have been linked to various diseases, including autoimmune disorders and cancer.(14)

1.3 IMMUNOGLOBULINS

Immunoglobulins are glycoproteins produced by effector B-cells (plasma cells) and constitute about 20% of the protein content of plasma. As indicated in **Figure 1A**, the immune system produces five classes or isotypes of antibodies, namely IgG, IgA, IgD, IgE, and IgM, each of which contains a distinct heavy chain – gamma, alpha, delta, epsilon, and mu, respectively.(15) In addition, there are two types of light chains - kappa and lambda, with kappa being the more common of the two in humans. The two arms of the Y-shape form the fragment antigen-binding (Fab) region, which recognizes and binds to specific epitopes on target molecules. In contrast, the fragment crystallizable (Fc) region of the molecule, located at the base of the Y, mediates different effector functions through the interaction with Fc-engaging molecules.

IgG, which is the most abundant antibody in the blood stream, is produced in response to both acute and chronic infections. It can neutralize pathogens, activate complement, and facilitate opsonization and phagocytosis by immune cells.(16). IgM is the first antibody produced in response to infectious agents and antigens and is present in a monomeric form on the surface of naïve B cells as a B-cell receptor. Secreted IgM is a pentamer and has ten antigen-binding sites, allowing it to bind multiple antigens simultaneously and initiate the classical pathway of the complement activation. IgA is primarily found in mucosal secretions such as saliva, intestinal fluid or breast milk, where it plays a critical role in preventing pathogen entry into the body. IgD is found on the surface of naïve B cells and is involved in

B cell activation and differentiation. IgE is primarily involved in allergic responses.(15). Each Ig isotype can elucidate a wide range of partially unique effector mechanisms, resulting in responses against pathogens and the maintenance of immune homeostasis.

Regardless of the isotype, all immunoglobulins are glycosylated in the constant region and glycosylation is of great importance for the appropriate function of Igs. The number and position of glycans vary between different Ig classes. While IgA, IgM, IgD and IgE have several conserved N-glycosylation sites in the Fc region, accounting for approximately 12-14% of their molecular weight, IgG is characterized by only one N-glycosylation site.(17) In addition to N-linked sugar moieties, IgA1 and IgG3 also contain O-glycans in their hinge region.

Ig effector functions are dynamically regulated by various modification of the antibody Fc region, with glycosylation being one of the factors that exerts a profound impact on the Igs' biological activity. Furthermore, glycosylation patterns on Ig molecules can vary depending on cell type, tissue location, and disease state. Such variation in glycosylation can modulate antibody effector functions, such as complement activation, antibody-dependent cellular cytotoxicity, and clearance from circulation.(18) There is no conserved N-glycosylation site in the Fab region. However, N-glycosylation sites can be generated de novo by somatic hypermutation during the antigen-specific immune responses.(19). All in all, Ig glycosylation is a highly regulated process with a strong impact on Ig effector functions.

1.3.1 IgG structure and glycosylation

Glycosylation is thus of great importance for the proper function of all Igs. The IgG class of immunoglobulins is divided into four subtypes (IgG1, IgG2, IgG3, IgG4), which can be further subdivided into their polymorphic variants, called allotypes. (20). The schematic representation of IgG subclasses and their glycosylation is shown in **Figure 1B**. IgG subclasses and allotypes differ in the amino acid sequence of the heavy chain of the Fc region, a region that interacts with Fc-engaging molecules, such as FcγRs or C-type lectins. As a result of these variations, each IgG subtype poses unique structural and functional characteristics, as well as, a unique profile with respect to triggering effector mechanisms, including antibody-dependent cytotoxicity (ADCC), antibody-dependent phagocytosis (ADCP), and complement-dependent cytotoxicity (CDC). For example, IgG1 and IgG3 have a longer hinge region that allows for increased flexibility and range motion, which is important for their ability to facilitate effector functions. IgG2 and IgG4 exhibit shorter hinge regions, which limits their ability to engage effector cells. Instead, these subtypes play a more prominent role in neutralizing toxins and antigens. IgG subclasses have different patterns of expression in response to different types of antigens. For example, IgG1 and IgG3 are more commonly produced in response to protein antigens associated with viral infections, IgG2 is produced in response to polysaccharide antigens induced by bacterial infections, and IgG4 is formed in chronic exposure to allergens.(20, 21)

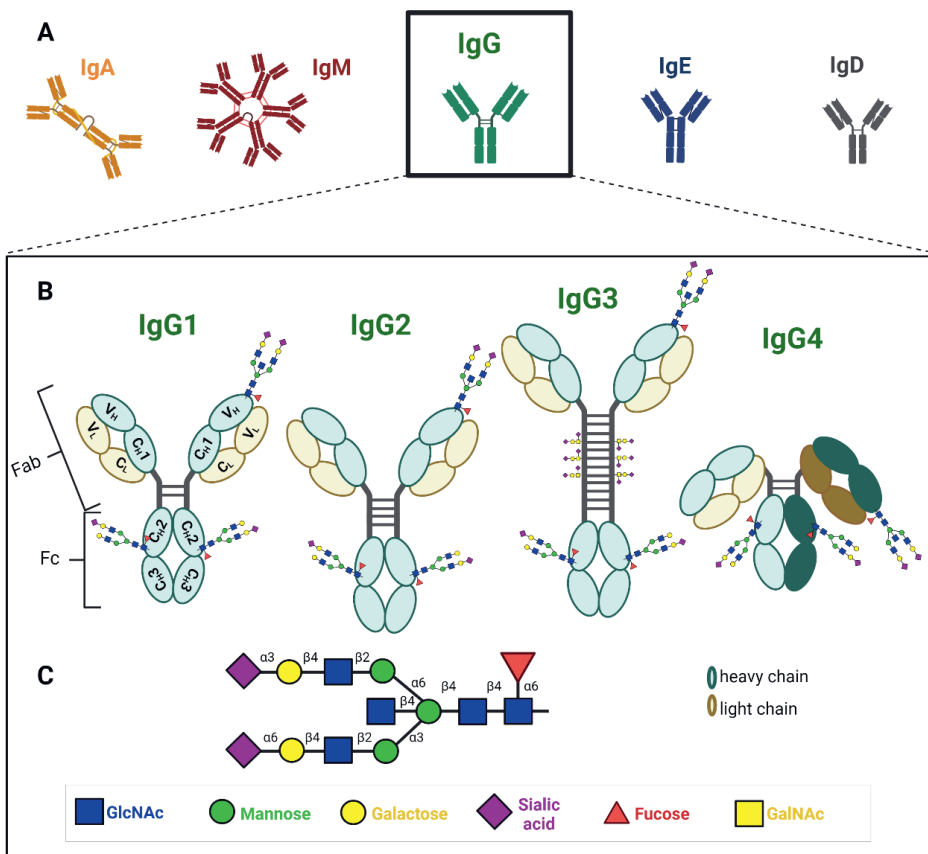


Figure 1. Immunoglobulins and their glycosylation. **(A)** Immunoglobulin (Ig) isotypes. The basic functional unit of each antibody consists of four polypeptide chains, typically two identical heavy (H) chains and two identical light (L) chains. **(B)** A structural representation of the Immunoglobulin G (IgG) subclasses and their glycosylation. Regardless of the isotype, subtype and allotype, the heavy chain consists of three constant (C) domains (C_{H1} , C_{H2} , C_{H3}), and a variable (V) domain (V_H). The light chain contains two domains, one constant (C_L) and one variable (V_L). Fab and Fc are connected via the hinge region. IgG3 has a longer hinge region bearing O-glycans. The bispecific nature of IgG4 is indicated by slightly darker colors. **(C)** Symbolic representation of the most elaborate, complex type N-glycan found on IgG. Created with Biorender.com

IgG contains an N-linked glycosylation site at the conserved asparagine 297 residue in each of the C_{H2} domains of the Fc region of the molecule. Around 30 different N-glycans decorate this single N-glycosylation site.(22) Unlike other plasma proteins which are lacking core-fucosylated glycans, plasma IgG of healthy individuals contain on average over 90% core-fucosylated glycans, that is fucose attached to the innermost GlcNAc of the N-glycan core. Moreover, these fucosylated and complex-type glycans carry intermediate levels of galactose (30-65% per antenna, low levels of bisecting GlcNAc (10-20%) and low levels of sialic acid (10-15% per antenna).(22) In addition to all IgG being glycosylated at the Fc region, 10-15% of IgG undergo glycosylation in the Fab portion.(19) The absence of a conserved N-glycosylation site complicates and therefore limits research on glycans linked

to the IgG Fab region. Nevertheless, it is established that these N-glycans are, like Fc glycans, mainly complex-type biantennary structures. However, compared to IgG Fc glycans, Fab glycans are characterized by the presence of fully processed sugar moieties, rich in sialic acid (~80%), bisecting GlcNAc (~65%) and galactose (~97%) residues in addition to exhibiting a lower fraction of core fucose (~70%).(23, 24) In addition to the impact on antigen binding, Fab glycosylation also affects the stability and half-life of IgG.(10)

Within the individual, the glycosylation profile is rather stable over time under homeostatic conditions, but it can change significantly with altered physiological or pathological states. Variations in the glycosylation profile of serum IgG have been correlated with age, inflammatory conditions, infectious diseases and cancers.(14)

1.3.2 The impact of glycosylation on the function of IgG

IgG exert their biological activity through the induction of effector mechanisms, such as complement activation and FcγR-dependent effector functions (**Figure 2**). IgG effector functions and stability are heavily influenced by the carbohydrate moiety attached to the Fc domain. Based on the composition of this moiety, IgG are capable of exerting both pro- and anti-inflammatory effector functions. The presence of N-glycans changes the conformation of the Fc region and supports its open conformation, allowing interaction with the Fc-engaging molecules.(25) Thus, the complete removal of Fc glycans changes the conformation from open to closed and diminishes the functional binding to Fc receptors and C1q.(10, 26) Alterations in the composition, size and charge of the Fc N-glycan also lead to conformational changes in the Fc region with a profound impact on binding properties to interaction partners. Thereby, Fc N-glycosylation modulates IgG's ability to activate the classical complement pathway and FcγR-expressing effector cells, impacting such effector functions as complement-dependent cytotoxicity (CDC) and antibody-dependent cellular cytotoxicity (ADCC).(18)

In recent decades, studies have demonstrated that IgG core fucosylation, which refers to the addition of a fucose residue to the innermost GlcNAc by an α 1,6-fucosyltransferase (FUT8), has a profound impact on IgG depended effector functions, especially ADCC activity mediated by natural killer (NK) cells.(13, 27) Antibodies deficient in core fucose bind with 10-100 fold higher affinity to FcγRIIIa and FcγRIIIb with respect to its fully fucosylated counterparts.(27, 28) This in turn, results in 2-40 fold increase in ADCC. Mechanistically, the higher affinity of afucosylated IgG is explained by a more favourable carbohydrate-carbohydrate interaction between the N-glycans of IgG-Fc and FcγRIIIa.(29)

IgG sialylation was shown to have anti-inflammatory effects. A classic example of anti-inflammatory activity is the discovery that infusion of high doses of intravenous immunoglobulin G suppresses a wide variety of inflammatory and autoimmune diseases.(30, 31) However, when terminal sialic acids are removed from IgG, they become more pro-inflammatory and may contribute to the development of inflammation. The precise mechanisms by which sialylated IgG interact with immune cells and modulates the balance between pro- and anti-inflammatory activity are not yet fully understood. More

functional studies are needed to resolve some of the apparent discrepancies.(32) Fc-sialylated glycovariants have been found to decrease affinity for activating FcγRs and C1q, resulting in a reduced capacity to trigger pro-inflammatory IgG effector functions, ADCC and CDC, respectively.(33, 34) Indeed, it was suggested that the sialic acid causes conformational changes that impede the binding of FcγRIIIa and FcγRIIIb. Moreover, it was suggested that IgG sialylation exert its anti-inflammatory activity through the induction of IL-33 production, which in turns upregulates FcγRIIb expression on effector cells.

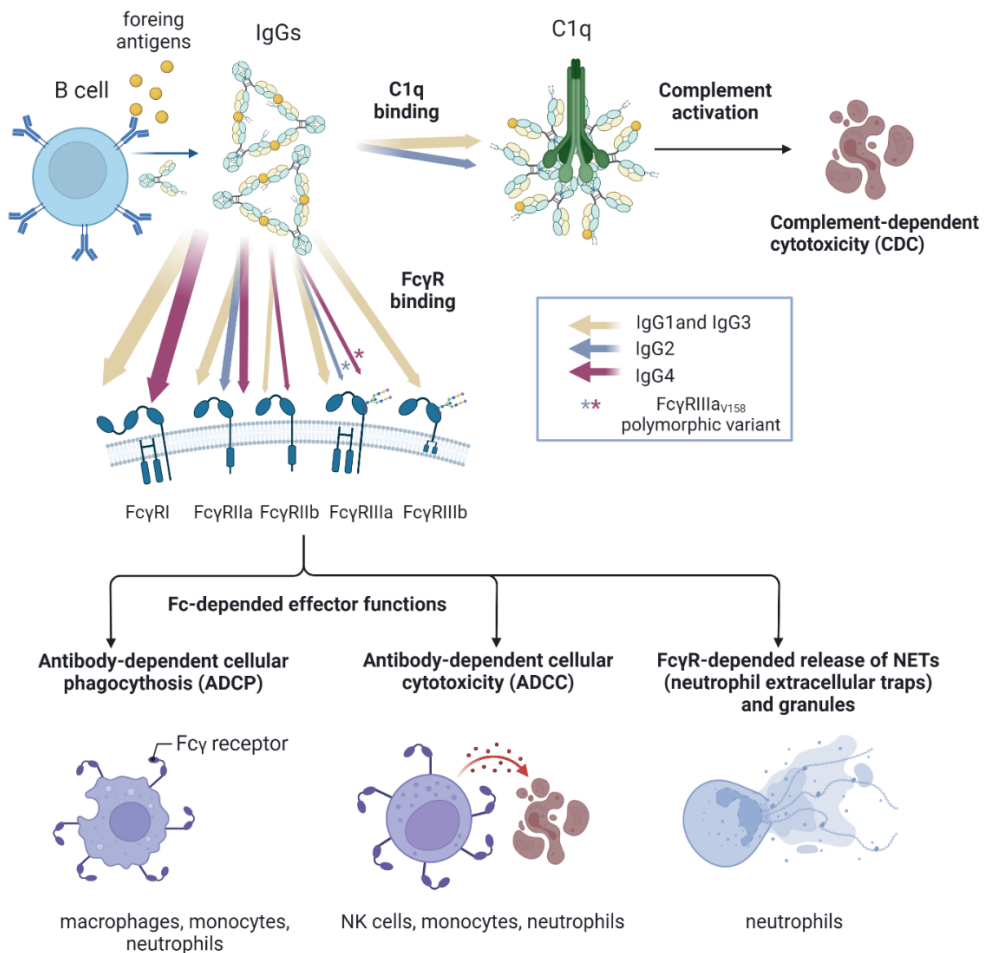


Figure 2. The diverse repertoire of immunoglobulin G effector functions. Interaction of IgG-Fc with C1q activates the classical complement pathway, while its interaction with FcγRs elicits antibody-dependent cellular cytotoxicity (ADCC) and antibody-depended cellular phagocytosis (ADCP). Human IgG subclasses have different affinity for FcγRs which is indicated by the colour of the arrows (subclass) and their thickness (thicker denotes higher affinity). IgG1 and IgG3 are highly efficient in inducing effector mechanisms, whereas IgG2 and IgG4 are much less efficient and only do so in specific cases.(20, 35) Created with Biorender.com

However, one study showed little impact of Fc-sialylation on ADCC, and another even demonstrated increased C1q binding. Some models support a role of sialic acid in promoting binding to human type II lectin receptors (DC-SIGN, CD23).(13, 36) However, there are conflicting reports and whether there is a direct interaction with DC-SIGN is under debate.(37)

The addition of a β 1,4-linked GlcNAc to the core β -mannose residue, referred to as bisection, results in a conformational alteration of the N-glycan structure.(38) However, this modification does not seem to have any significant functional consequences since it has a very limited impact on Fc γ R or C1q binding.(13, 39) Despite the uncertain significance of bisection to antibody effector functions, it appears to have an indirect effect on IgG effector functions by suppressing subsequent fucosylation during N-glycan synthesis.(40)

The role of IgG Fc-galactosylation in modulating Fc-mediated effector functions is complex and multifaceted. IgG lacking terminal galactose residues has been shown to promote pro-inflammatory activity via the lectin complement pathway upon binding to mannose-binding lectin.(41) However, later studies have challenged this observation.(42) More recent data have shown that elevated galactosylation may act in a pro-inflammatory fashion by increasing binding to Fc γ RIII and consequently NK cell-mediated ADCC, especially in synergy with afucosylation.(13) Likewise, by increasing the affinity of IgG for the C1q complement component, galactosylation enhances CDC, at least in vitro.(13, 43) Mechanistically, galactosylation enhances IgG1 hexamerization potential, and thus, subsequent downstream activation.(44)

Antibody glycosylation is largely determined by the abundance and activity of glycosyltransferases and glycosidases which, in turn, depends on the availability of sugar donors, transcription factors, and cytokines, such as the pro-inflammatory cytokine tumor necrosis factor- α (TNF α).(45, 46). Consequently, IgG glycosylation is determined by the metabolic state of the cell, enabling to adopt IgG glycosylation to altered environmental conditions. While, the regulation of glycosyltransferase expression in B cells is still not fully understood, it clearly plays a key role in various physiological and pathological processes.

1.4 THE Fc GAMMA RECEPTOR FAMILY

Fc γ Rs play a vital role in converting the recognition of antigens by IgG into various cellular immune responses. Various proteoforms of both IgG and Fc γ R influence this process because they largely determine the mutual affinity. Examples are subclass, allotype and glycosylation variations. The impact of IgG proteoforms has been elaborated on above. Fc γ Rs are classified into activating and inhibitory receptors based on the signaling properties of their intracellular domains. Among activating Fc γ Rs in humans are Fc γ RI, Fc γ RIIa, Fc γ RIIc, and Fc γ RIIIa, all of which contain an immunoreceptor tyrosine-based activation motif (ITAM). The sole inhibitory receptor is Fc γ RIIb, which transmits signals through an immunoreceptor tyrosine-based inhibitory motif (ITIM).(47) All Fc γ Rs are type I

transmembrane proteins, except FcγRIIIb, which is linked to the membrane via a glycosylphosphatidylinositol anchor.

Glycosylation of FcγRs can influence their antibody-binding properties, ultimately affecting their subsequent immune cell activation. The N-glycans on FcγRs can vary in their composition, structure, and complexity, depending on the cell type and individual. The FcγRIIIa, for example, has five N-glycan sites, of which mainly Asn162 influences IgG1 binding.(48) In vitro studies have shown that the N-glycans occupying the Asn162 site can affect the binding of FcγRs to antibodies, with different types of glycans having varying effects. FcγRIIIa with an oligomannose structure at Asn162, for example, has been shown to have increased IgG1 binding.(48, 49)

1.5 ABERRANT GLYCOSYLATION OF IMMUNE GLYCOPROTEINS AS A POTENTIAL CLINICAL MARKER

Protein glycosylation is not a DNA-template driven process, but is still partially determined by genetic factors and influenced by the microenvironment of the respective cell which produces a glycoprotein.(45, 50, 51) Any disturbances to this microenvironment due to physiological circumstances, such as disease, can alter the activity of glycosyltransferases and glycosidases. This alteration leads to a subsequent change in the glycosylation profile of immune glycoproteins. Even minor changes in glycosylation can have a profound effect on their effector functions and, in turn, deleterious consequences on both innate and adaptive immune cell activity, affecting health and disease.(52) Therefore, aberrant glycosylation of immune glycoproteins has emerged as a potential clinical marker for disease diagnosis and prognosis. In addition, manipulation of the glycosylation pattern, i.e. glycoengineering, has been incorporated in the antibody development workflow to produce glycoforms with improved therapeutic activity.

Body fluids which are relatively easy to obtain and contain various immune glycoproteins, such as plasma or seminal fluid, represent a promising source of potential clinical markers. A shift in glycosylation of plasma glycoproteins was reported in many different autoimmune and inflammatory diseases, as well as cancers.(53, 54) Based on these associations with total plasma N-glycosylation, a few potential clinical markers have been proposed.(55-59) A glycan-based diagnostic test was recently launched by Helena Biosciences and is used for the diagnosis and prognosis of various liver pathologies.(60)

One of the most extensively characterized plasma-derived glycoproteins is IgG. A reduction in galactosylation of IgG was reported across a wide spectrum of pathological conditions, suggesting that alterations in galactosylation are not a disease-specific process, but rather a general phenomenon having deleterious consequences on the adaptive immune cell activity.(14) Although the size of the drop in IgG glycosylation was associated with disease severity and poorer disease prognosis, the functional relevance of agalactosylated and

asialylated IgG is still not fully delineated. Moreover, the open question is whether aberrant glycosylation is a result of inflammatory milieu or actively drives the pathogenicity of IgG.

In addition to the glycosylation profile of bulk IgG, the glycosylation of antigen-specific IgG has been studied for several diseases. Changes in glycosylation of antigen-specific IgG have been linked to pro-inflammatory processes, disease activity and prognosis.(14, 61) For instance, alloantibodies against human platelet antigens, produced during pregnancy against fetal cells, have a reduced fucosylation which is associated with increased severity of fetal and neonatal alloimmune thrombocytopenia.(62) The biological significance of the absence of core fucose is explained by higher affinity of afucosylated IgG to FcγRIII, transforming moderate into potent mediators of immune defence mechanisms, such as ADCC.(13) Afucosylated IgG has the greatest effect on IgG effector functions, making it a potentially powerful diagnostic target for identifying ongoing inflammatory processes. Its significance is highlighted by the development of a high-throughput (ELISA)-based assay for quantifying antigen-specific IgG Fc fucosylation, a test that could facilitate the translation of glycosylation studies from research to clinical laboratories.(63)

Along with the underlying pathological condition, various population factors including age, sex, body mass index, and pregnancy, can impact the glycosylation profile of a protein, leading to inter-individual variation.(64, 65) To account for these confounding factors in cross-sectional studies, it is essential to have a considerable sample size, include sex- and age-matched control samples, and perform sample randomization. Furthermore, a longitudinal study design can be highly beneficial in exploring glycans as disease markers.

The analysis of protein N-glycosylation is critical for advancing our understanding of the role of glycans in health and disease, and for developing and validating new diagnostic and therapeutic strategies. In addition, the glycosylation analysis targeting human glycoproteins in population studies, must be of sufficient high-throughput to identify specific glycan signatures associated with various pathologies. Although studying immune protein glycosylation is a challenging analytical task, recent advances in analytical methodology facilitated the development of glycosylation analysis.

1.6 Analytical methods for N-glycosylation analysis

Recent advances in several analytical technologies including mass spectrometry (MS), liquid chromatography (LC), capillary electrophoresis (CE), carbohydrate microarrays, and nuclear magnetic resonance spectroscopy have led to the development of approaches which are suitable for both comparatively high-throughput and in-depth N-glycosylation analysis of wide range of immune molecules.(4)

Depending on the research question, protein glycosylation can be assessed at four complementary levels, that is glycan-, glycopeptide-, subunit- and intact-glycoprotein-level.(66) These approaches come with their possibilities and limitations that determine

their specific applications. The glycan-level approach relies on the chemical or enzymatic cleavage of glycans from the glycoproteins present in the sample, e.g., by peptide-*N*-glycosidase F (PNGase F) or RapidTMPNGaseF in case of *N*-glycosylation. Cleavage results in a mixture of glycans, which are subsequently labelled with a fluorescent dye and analysed. There are several analytical methods used to analyse protein *N*-glycosylation. The analysis of glycans in a high-throughput manner is currently possible using three powerful techniques: hydrophilic-interaction ultra-high-performance liquid chromatography with fluorescence detection (HILIC-UHPLC-FLD), multiplex capillary gel electrophoresis with laser-induced detection (xCGE-LIF), matrix-assisted laser ionization mass spectrometry (MALDI-MS).(4) Both HILIC-UPHLC-FLD and xCGE-LIF demonstrate remarkable repeatability and superior performance for low-complexity *N*-glycans, effectively differentiating their constitutional isomers. On the other hand, MALDI-TOF-MS stands out for its analytical throughput and comprehensive information on sialic acid linkage for all *N*-glycans. Moreover, this techniques offers more informative results for more complex glycan structures, such as tri- and tetra-antennary species.(67) While this glycan-level approach can yield the most structural information on the glycan, it fails to provide the glycan attachment site or a carrier protein, especially for multiply glycosylated proteins. This information can be retained by using a glycopeptide-level approach, where a glycoprotein is subjected to proteolytic cleavage using, for example, trypsin, endoproteinase GluC or proteinase K. The method of choice for the analysis of glycopeptides is reverse-phase-LC-ESI-MS.(4) MS analysis of the obtained (glyco)peptides, particularly tandem MS analysis, can reveal the glycosylation site, glycan composition and glycan structure. The subunit- and intact-glycoprotein-level approaches, characterize not only glycosylation, but also other post-translational modifications on a protein. While this approach provides information about different proteoforms, it requires high-resolution instruments and lacks information on site-specificity. Each of those approaches characterises glycans to a different level of detail and provides orthogonal information. Thus, a combination of these methods is required for a detailed and comprehensive glycosylation analysis.(68)

Glycosylation analysis can be further distinguished based on the analysed sample. It can be conducted on a single glycoprotein after targeted purification or on a complex mixture of glycoproteins, such as human serum.(69) An analysis of the complete repertoire of glycans has been performed for a range of single glycoproteins, such as IgG, IgA or FcγRIIIb.(70-72) However, this approach is limited since it requires the development of protein-specific purification methods. Nevertheless, new methods are being developed for the purification and analysis of glycoproteins, thereby expanding the selection of single glycoproteins that can be studied, as illustrated in **Chapter 4**. In case of clinical biofluids like serum or seminal plasma, due to the complexity of the sample and the presence of many glycoproteins, the glycan inventory is constructed for all glycoproteins in the sample on the level of released glycans, as illustrated in **Chapter 5** and **6**.

1.6.1 Mass spectrometers

Due to high sensitivity, selectivity and throughput, MS, has become a powerful tool for glycosylation profiling. MS has successfully been employed for the analysis of immune glycoproteins on all levels of characterization.(3, 73-75) MS-based analytical platforms adequately ionize glycans or glycoconjugates, detect their mass-to-charge (m/z) ratio and report ions in the form of a mass spectrum that plots the relative abundance of the ions as a function of their m/z ratio. It is highly compatible with LC.

The fragile nature of oligosaccharides, glycopeptides, and glycoproteins necessitates the use of soft ionization techniques in mass spectrometric analysis. Electrospray ionization (ESI) is often a method of choice as it avoids fragmentation, allowing the detection of the intact analyte.(76) ESI often advantageously creates ions with multiple charges, especially useful for detecting large masses. Multiple charging of large ions decreases their m/z values, making them detectable by mass analysers with a relatively narrow mass range. In the context of glycosylation analysis, ESI is especially suitable for the labile sialylated glycans.

Mass analysers distinguish ions using magnetic and/or electric fields. The performance of a mass analyser is typically characterized by mass range, analysis speed, mass accuracy and resolution. The time-of-flight (TOF) analyser is particularly suitable for high-throughput glycosylation profiling of IgG glycopeptides, due to its superior speed. In TOF analyzers, all particles are accelerated at the same time with the same energy. The resulting velocity of glycans/glycoconjugates depends on their size and charge. For more comprehensive and in-depth analyses, the latest generation of orbitrap instruments has been widely accepted, due to the ultra-high resolution.

Modern mass analysers enable the use of innovative MS hybrid fragmentation strategies. These strategies, arising from the combination and variation of multiple conventional fragmentation techniques, such as collision-induced dissociation (collision-induced dissociation, CID and higher-energy collisional dissociation, HCD) or electron-driven dissociations (electron capture dissociation, ECD and electron transfer dissociation, ETD), have been of great benefit to the field of spectrometry-based glycoproteomics, enabling high-end glycopeptide analysis.(77) Each fragmentation strategy yields distinct types of fragmentation spectra. For example, when applied to a glycopeptide analyte, CID generates B/Y-type glycan fragment ions, making it well-suited for breaking labile glycosidic bounds. On the other hand, ETD produces c/z-type ions and is more suitable for sequencing the peptide backbone. However, when these techniques are combined in the form of hybrid fragmentation, they provide information-rich fragments from both peptide and glycan moiety in a single MS/MS spectrum. This makes it a powerful tool for in-depth analysis of glycopeptides.(78, 79)

1.7 SCOPE

The aim of this thesis is to enhance the understanding of the role of glycosylation in the immune system. To achieve this, we employed high-throughput profiling methods on clinical samples, to investigate the dynamic changes in antibody glycosylation during disease and treatment processes. Furthermore, we strove to develop new methodologies for reliable characterization of N-glycosylation profiles, with the objective of expanding the range of immune glycoproteins being analysed, as well as improving existing methods. Changes in glycosylation of immune glycoproteins are typically associated with alterations in homeostasis, inflammatory processes, and disease progression. By detecting such changes in the glycosylation profiles of immune glycoproteins, researchers can identify disease-specific clinical markers, potentially enabling early diagnosis, personalized treatment, and disease progression monitoring.

The regulation of IgG glycosylation, especially fucosylation, which significantly impacts the ability of IgG to effectively trigger immune responses, remains largely elusive. To gain valuable insights into the special location of these regulatory mechanisms, we investigated the potential role of the spleen in modulating IgG glycosylation. In **Chapter 2**, we evaluated IgG-Fc glycosylation in a cohort of splenectomised individuals to address this question. Our findings reveal a shift in IgG Fc-fucosylation upon splenectomy, supporting a potential role of the spleen in regulating IgG afucosylated responses generated by B cells.

Chapter 3 describes the IgG Fc-glycosylation dynamics in a longitudinal cohort of patients with anti-neutrophil cytoplasmic antibody (ANCA)-associated vasculitis (AAV). Our findings demonstrate that IgG Fc-fucosylation differs between relapsing and non-relapsing patients already 9 months before the relapse, if a rise in ANCA titers was also observed. These results demonstrate the orthogonality of ANCA-rise and IgG fucosylation and position them as valuable components of a potential multifactor clinical marker platform for disease monitoring in AAV. Moreover, we validated the decrease in sialylation of IgG Fc N-glycans over time as a valuable glycosylation-based clinical marker for the prognosis of AAV relapse.(80)

Despite extensive research in the past decades on mapping the glycosylation profile of antibodies, there has been a lack of glycoproteomic methods for glycosylation mapping of other glycoproteins with crucial immunological functions. In **Chapter 4** of this thesis, we developed a comprehensive LC-MS method for site-specific analysis of FcγRIIIb on primary human cells. The developed methodology demonstrates the ability to identify glycosylation differences between donors, subclasses, allotypes, cells and sites of FcγRIII. Studies on FcγR glycosylation are essential, as they may provide a deeper understanding of this additional layer of regulation of the IgG-FcγR interaction and its (patho-)physiological implications.

In **Chapter 5**, we introduce a novel high-throughput method for chromatographic separation and profiling of plasma and serum N-glycans. This method utilizes hydrophilic interaction liquid chromatography-mass spectrometry and a recently introduced fluorescent label, *RapiFluor*-MS. Compared to existing methods, the developed approach allows for more rapid sample preparation. Additionally, the improved method takes advantage of the high FLR and MS sensitivity of *RapiFluor*-MS label and thus, offers a highly sensitive, rapid and robust method for detecting biological variability in clinical cohorts. With these advancements, our developed method enhanced the analysis of plasma and serum N-glycans.

Chapter 6 presents the evaluation of seminal plasma N-glycosylation using liquid chromatography-mass spectrometry to evaluate the relationship between environmental exposure and male infertility. This study identified several N-glycans with the potential for biomonitoring of exposure to different environmental factors in men with semen abnormalities.

Finally, **Chapter 7** provides a discussion of the main findings presented in this thesis, contextualizing them with the current literature in the field. Furthermore, this chapter also explores future perspectives and challenges in the analysis of glycosylation in immune molecules.

1.8 REFERENCES

1. Rabinovich GA, van Kooyk Y, Cobb BA. Glycobiology of immune responses. *Ann N Y Acad Sci.* 2012;1253:1-15.
2. Varki A, Cummings RD, Esko JD, Stanley P, Hart GW, Aebi M, et al. Essentials of Glycobiology. In: Varki A, Cummings RD, Esko JD, Stanley P, Hart GW, Aebi M, et al., editors. Essentials of Glycobiology. 4th ed. Cold Spring Harbor (NY)2022.
3. Trbojevic-Akmacic I, Lageveen-Kammeijer GSM, Heijs B, Petrovic T, Deris H, Wuhrer M, et al. High-Throughput Glycomic Methods. *Chem Rev.* 2022;122(20):15865-913.
4. de Haan N, Pucic-Bakovic M, Novokmet M, Falck D, Lageveen-Kammeijer G, Razdorov G, et al. Developments and perspectives in high-throughput protein glycomics: enabling the analysis of thousands of samples. *Glycobiology.* 2022;32(8):651-63.
5. Petrescu AJ, Milac AL, Petrescu SM, Dwek RA, Wormald MR. Statistical analysis of the protein environment of N-glycosylation sites: implications for occupancy, structure, and folding. *Glycobiology.* 2004;14(2):103-14.
6. Lubbers J, Rodriguez E, van Kooyk Y. Modulation of Immune Tolerance via Siglec-Sialic Acid Interactions. *Front Immunol.* 2018;9:2807.
7. Ereno-Orbea J, Sicard T, Cui H, Mazhab-Jafari MT, Benlekbir S, Guarne A, et al. Molecular basis of human CD22 function and therapeutic targeting. *Nat Commun.* 2017;8(1):764.
8. Demetriou M, Granovsky M, Quaggin S, Dennis JW. Negative regulation of T-cell activation and autoimmunity by Mga5 N-glycosylation. *Nature.* 2001;409(6821):733-9.
9. Hennet T, Chui D, Paulson JC, Marth JD. Immune regulation by the ST6Gal sialyltransferase. *Proc Natl Acad Sci U S A.* 1998;95(8):4504-9.
10. Arnold JN, Wormald MR, Sim RB, Rudd PM, Dwek RA. The impact of glycosylation on the biological function and structure of human immunoglobulins. *Annu Rev Immunol.* 2007;25:21-50.
11. Walker MR, Lund J, Thompson KM, Jefferis R. Aglycosylation of human IgG1 and IgG3 monoclonal antibodies can eliminate recognition by human cells expressing Fc gamma RI and/or Fc gamma RII receptors. *Biochem J.* 1989;259(2):347-53.
12. Jefferis R. Recombinant antibody therapeutics: the impact of glycosylation on mechanisms of action. *Trends Pharmacol Sci.* 2009;30(7):356-62.
13. Dekkers G, Treffers L, Plomp R, Bentlage AEH, de Boer M, Koeleman CAM, et al. Decoding the Human Immunoglobulin G-Glycan Repertoire Reveals a Spectrum of Fc-Receptor- and Complement-Mediated-Effector Activities. *Front Immunol.* 2017;8:877.
14. Gudelj I, Lauc G, Pezer M. Immunoglobulin G glycosylation in aging and diseases. *Cell Immunol.* 2018;333:65-79.
15. Schroeder HW, Jr., Cavacini L. Structure and function of immunoglobulins. *J Allergy Clin Immunol.* 2010;125(2 Suppl 2):S41-52.
16. Justiz Vaillant AA, Jamal Z, Patel P, Ramphul K. Immunoglobulin. *StatPearls.* Treasure Island (FL)2022.
17. de Haan N, Falck D, Wuhrer M. Monitoring of immunoglobulin N- and O-glycosylation in health and disease. *Glycobiology.* 2020;30(4):226-40.
18. Quast I, Peschke B, Lunemann JD. Regulation of antibody effector functions through IgG Fc N-glycosylation. *Cell Mol Life Sci.* 2017;74(5):837-47.
19. van de Bovenkamp FS, Hafkenscheid L, Rispens T, Rombouts Y. The Emerging Importance of IgG Fab Glycosylation in Immunity. *J Immunol.* 2016;196(4):1435-41.
20. Vidarsson G, Dekkers G, Rispens T. IgG subclasses and allotypes: from structure to effector functions. *Front Immunol.* 2014;5:520.
21. Ferrante A, Beard LJ, Feldman RG. IgG subclass distribution of antibodies to bacterial and viral antigens. *Pediatr Infect Dis J.* 1990;9(8 Suppl):S16-24.
22. Pucic M, Knezevic A, Vidic J, Adamczyk B, Novokmet M, Polasek O, et al. High throughput isolation and glycosylation analysis of IgG-variability and heritability of the IgG glycome in three isolated human populations. *Mol Cell Proteomics.* 2011;10(10):M111 010090.
23. Anumula KR. Quantitative glycan profiling of normal human plasma derived immunoglobulin and its fragments Fab and Fc. *J Immunol Methods.* 2012;382(1-2):167-76.
24. Bondt A, Wuhrer M, Kuijper TM, Hazes JM, Dolhain RJ. Fab glycosylation of immunoglobulin G does not associate with improvement of rheumatoid arthritis during pregnancy. *Arthritis Res Ther.* 2016;18(1):274.
25. Krapp S, Mimura Y, Jefferis R, Huber R, Sonderrmann P. Structural analysis of human IgG-Fc glycoforms reveals a correlation between glycosylation and structural integrity. *J Mol Biol.* 2003;325(5):979-89.
26. Nose M, Wigzell H. Biological significance of carbohydrate chains on monoclonal antibodies. *Proc Natl Acad Sci U S A.* 1983;80(21):6632-6.

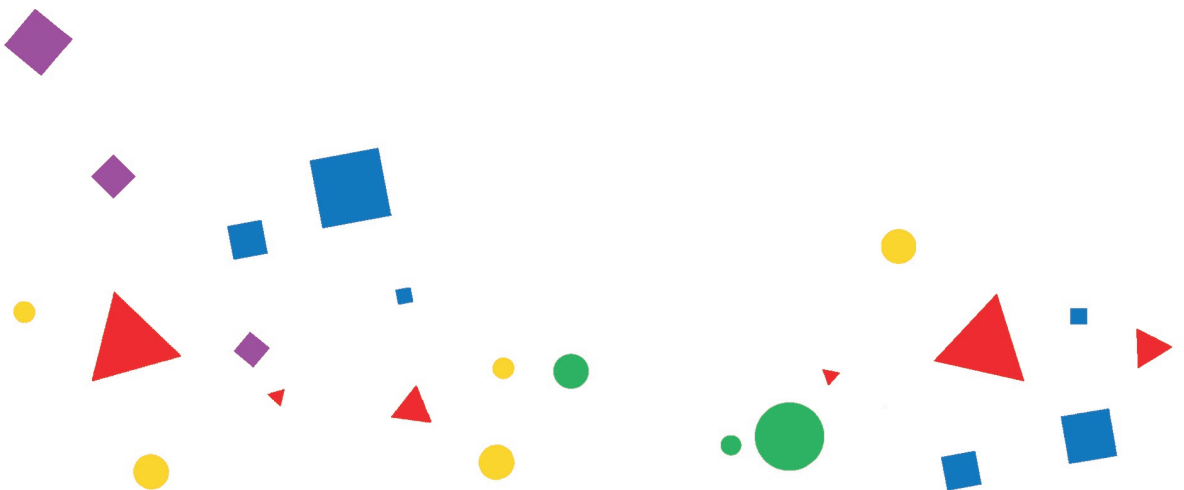
27. Shields RL, Lai J, Keck R, O'Connell LY, Hong K, Meng YG, et al. Lack of fucose on human IgG1 N-linked oligosaccharide improves binding to human Fcγ₃ and antibody-dependent cellular toxicity. *J Biol Chem.* 2002;277(30):26733-40.
28. Subedi GP, Barb AW. The immunoglobulin G1 N-glycan composition affects binding to each low affinity Fcγ₃ receptor. *MAbs.* 2016;8(8):1512-24.
29. Ferrara C, Grau S, Jager C, Sondermann P, Brunker P, Waldhauer I, et al. Unique carbohydrate-carbohydrate interactions are required for high affinity binding between Fcγ₃ and antibodies lacking core fucose. *Proc Natl Acad Sci U S A.* 2011;108(31):12669-74.
30. Schwab I, Nimmerjahn F. Intravenous immunoglobulin therapy: how does IgG modulate the immune system? *Nat Rev Immunol.* 2013;13(3):176-89.
31. Bayry J, Fournier EM, Maddur MS, Vani J, Wootla B, Siberil S, et al. Intravenous immunoglobulin induces proliferation and immunoglobulin synthesis from B cells of patients with common variable immunodeficiency: a mechanism underlying the beneficial effect of IVIg in primary immunodeficiencies. *J Autoimmun.* 2011;36(1):9-15.
32. Vattepu R, Sneed SL, Anthony RM. Sialylation as an Important Regulator of Antibody Function. *Front Immunol.* 2022;13:818736.
33. Quast I, Keller CW, Maurer MA, Giddens JP, Tackenberg B, Wang LX, et al. Sialylation of IgG Fc domain impairs complement-dependent cytotoxicity. *J Clin Invest.* 2015;125(11):4160-70.
34. Seeling M, Bruckner C, Nimmerjahn F. Differential antibody glycosylation in autoimmunity: sweet biomarker or modulator of disease activity? *Nat Rev Rheumatol.* 2017;13(10):621-30.
35. Bruhns P, Iannascoli B, England P, Mancardi DA, Fernandez N, Jorieu S, et al. Specificity and affinity of human Fcγ₃ receptors and their polymorphic variants for human IgG subclasses. *Blood.* 2009;113(16):3716-25.
36. Pincetic A, Bournazos S, DiLillo DJ, Maamary J, Wang TT, Dahan R, et al. Type I and type II Fcγ₃ receptors regulate innate and adaptive immunity. *Nat Immunol.* 2014;15(8):707-16.
37. Temming AR, Dekkers G, van de Bovenkamp FS, Plomp HR, Bentlage AEH, Szittner Z, et al. Human DC-SIGN and CD23 do not interact with human IgG. *Sci Rep.* 2019;9(1):9995.
38. Nagae M, Kanagawa M, Morita-Matsumoto K, Hanashima S, Kizuka Y, Taniguchi N, et al. Atomic visualization of a flipped-back conformation of bisected glycans bound to specific lectins. *Sci Rep.* 2016;6:22973.
39. Lippold S, Nicolardi S, Dominguez-Vega E, Heidenreich AK, Vidarsson G, Reusch D, et al. Glycoform-resolved Fcγ₃ affinity chromatography-mass spectrometry. *MAbs.* 2019;11(7):1191-6.
40. Ferrara C, Brunker P, Suter T, Moser S, Puntener U, Umana P. Modulation of therapeutic antibody effector functions by glycosylation engineering: influence of Golgi enzyme localization domain and co-expression of heterologous β_{1,4}-N-acetylglucosaminyltransferase III and Golgi α-mannosidase II. *Biotechnol Bioeng.* 2006;93(5):851-61.
41. Malhotra R, Wormald MR, Rudd PM, Fischer PB, Dwek RA, Sim RB. Glycosylation changes of IgG associated with rheumatoid arthritis can activate complement via the mannose-binding protein. *Nat Med.* 1995;1(3):237-43.
42. van de Geijn FE, de Man YA, Wuhler M, Willemsen SP, Deelder AM, Hazes JM, et al. Mannose-binding lectin does not explain the course and outcome of pregnancy in rheumatoid arthritis. *Arthritis Res Ther.* 2011;13(1):R10.
43. Peschke B, Keller CW, Weber P, Quast I, Lunemann JD. Fc-Galactosylation of Human Immunoglobulin Gamma Isotypes Improves C1q Binding and Enhances Complement-Dependent Cytotoxicity. *Front Immunol.* 2017;8:646.
44. van Osch TLJ, Nouta J, Derksen NIL, van Mierlo G, van der Schoot CE, Wuhler M, et al. Fc Galactosylation Promotes Hexamerization of Human IgG1, Leading to Enhanced Classical Complement Activation. *J Immunol.* 2021;207(6):1545-54.
45. Klaric L, Tsepilov YA, Stanton CM, Mangino M, Sikka TT, Esko T, et al. Glycosylation of immunoglobulin G is regulated by a large network of genes pleiotropic with inflammatory diseases. *Sci Adv.* 2020;6(8):eaax0301.
46. Garcia-Vallejo JJ, van Dijk W, van Die I, Gringhuis SI. Tumor necrosis factor-α up-regulates the expression of β_{1,4}-galactosyltransferase I in primary human endothelial cells by mRNA stabilization. *J Biol Chem.* 2005;280(13):12676-82.
47. Bournazos S, Gupta A, Ravetch JV. The role of IgG Fc receptors in antibody-dependent enhancement. *Nat Rev Immunol.* 2020;20(10):633-43.
48. Van Coillie J, Schulz MA, Bentlage AEH, de Haan N, Ye Z, Geerdes DM, et al. Role of N-Glycosylation in Fcγ₃ interaction with IgG. *Front Immunol.* 2022;13:987151.
49. Subedi GP, Barb AW. CD16a with oligomannose-type N-glycans is the only "low-affinity" Fcγ₃ receptor that binds the IgG crystallizable fragment with high affinity in vitro. *J Biol Chem.* 2018;293(43):16842-50.

50. Cao Y, Song Z, Guo Z, Zhao X, Gong Y, Zhao K, et al. Cytokines in the Immune Microenvironment Change the Glycosylation of IgG by Regulating Intracellular Glycosyltransferases. *Front Immunol.* 2021;12:724379.
51. Zaytseva OO, Freidin MB, Keser T, Stambuk J, Ugrina I, Simurina M, et al. Heritability of Human Plasma N-Glycome. *J Proteome Res.* 2020;19(1):85-91.
52. Reilly C, Stewart TJ, Renfrow MB, Novak J. Glycosylation in health and disease. *Nat Rev Nephrol.* 2019;15(6):346-66.
53. Pinho SS, Reis CA. Glycosylation in cancer: mechanisms and clinical implications. *Nat Rev Cancer.* 2015;15(9):540-55.
54. Dotz V, Wuhrer M. N-glycome signatures in human plasma: associations with physiology and major diseases. *FEBS Lett.* 2019;593(21):2966-76.
55. Reiding KR, Ruhaak LR, Uh HW, El Bouhaddani S, van den Akker EB, Plomp R, et al. Human Plasma N-glycosylation as Analyzed by Matrix-Assisted Laser Desorption/Ionization-Fourier Transform Ion Cyclotron Resonance-MS Associates with Markers of Inflammation and Metabolic Health. *Mol Cell Proteomics.* 2017;16(2):228-42.
56. Clerc F, Novokmet M, Dotz V, Reiding KR, de Haan N, Kammeijer GSM, et al. Plasma N-Glycan Signatures Are Associated With Features of Inflammatory Bowel Diseases. *Gastroenterology.* 2018;155(3):829-43.
57. Callewaert N, Van Vlierberghe H, Van Hecke A, Laroy W, Delanghe J, Contreras R. Noninvasive diagnosis of liver cirrhosis using DNA sequencer-based total serum protein glycomics. *Nat Med.* 2004;10(4):429-34.
58. Rudman N, Gornik O, Lauc G. Altered N-glycosylation profiles as potential biomarkers and drug targets in diabetes. *FEBS Lett.* 2019;593(13):1598-615.
59. Juszczak A, Pavic T, Vuckovic F, Bennett AJ, Shah N, Pape Medvidovic E, et al. Plasma Fucosylated Glycans and C-Reactive Protein as Biomarkers of HNF1A-MODY in Young Adult-Onset Nonautoimmune Diabetes. *Diabetes Care.* 2019;42(1):17-26.
60. Helena Biosciences Europe. Glyco Liver Profile: Helena Biosciences Europe; 2013 [Available from: <https://www.helena-biosciences.com/en/clinical-electrophoresis/v8-nexus/tests/glyco-liver-profile/>].
61. Oosterhoff JJ, Larsen MD, van der Schoot CE, Vidarsson G. Afucosylated IgG responses in humans - structural clues to the regulation of humoral immunity. *Trends Immunol.* 2022;43(10):800-14.
62. Sonneveld ME, Natunen S, Sainio S, Koeleman CA, Holst S, Dekkers G, et al. Glycosylation pattern of antiplatelet IgG is stable during pregnancy and predicts clinical outcome in alloimmune thrombocytopenia. *Br J Haematol.* 2016;174(2):310-20.
63. Sustic T, Van Coillie J, Larsen MD, Derksen NIL, Szittner Z, Nouta J, et al. Immunoassay for quantification of antigen-specific IgG fucosylation. *EBioMedicine.* 2022;81:104109.
64. Chen G, Wang Y, Qiu L, Qin X, Liu H, Wang X, et al. Human IgG Fc-glycosylation profiling reveals associations with age, sex, female sex hormones and thyroid cancer. *J Proteomics.* 2012;75(10):2824-34.
65. Kristic J, Vuckovic F, Menni C, Klaric L, Keser T, Beceheli I, et al. Glycans are a novel biomarker of chronological and biological ages. *J Gerontol A Biol Sci Med Sci.* 2014;69(7):779-89.
66. Ruhaak LR, Xu G, Li Q, Goonatilake E, Lebrilla CB. Mass Spectrometry Approaches to Glycomic and Glycoproteomic Analyses. *Chem Rev.* 2018;118(17):7886-930.
67. Reiding KR, Bondt A, Hennig R, Gardner RA, O'Flaherty R, Trbojevic-Akmacic I, et al. High-throughput Serum N-Glycomics: Method Comparison and Application to Study Rheumatoid Arthritis and Pregnancy-associated Changes. *Mol Cell Proteomics.* 2019;18(1):3-15.
68. Yang Y, Liu F, Franc V, Halim LA, Schellekens H, Heck AJ. Hybrid mass spectrometry approaches in glycoprotein analysis and their usage in scoring biosimilarity. *Nat Commun.* 2016;7:13397.
69. Pan S, Chen R, Aebersold R, Brentnall TA. Mass spectrometry based glycoproteomics--from a proteomics perspective. *Mol Cell Proteomics.* 2011;10(1):R110 003251.
70. Wojcik I, Senard T, de Graaf EL, Janssen GMC, de Ru AH, Mohammed Y, et al. Site-Specific Glycosylation Mapping of Fc Gamma Receptor IIb from Neutrophils of Individual Healthy Donors. *Anal Chem.* 2020;92(19):13172-81.
71. Novak J, Moldoveanu Z, Julian BA, Raska M, Wyatt RJ, Suzuki Y, et al. Aberrant glycosylation of IgA1 and anti-glycan antibodies in IgA nephropathy: role of mucosal immune system. *Adv Otorhinolaryngol.* 2011;72:60-3.
72. Bondt A, Selman MH, Deelder AM, Hazes JM, Willemsen SP, Wuhrer M, et al. Association between galactosylation of immunoglobulin G and improvement of rheumatoid arthritis during pregnancy is independent of sialylation. *J Proteome Res.* 2013;12(10):4522-31.
73. Chen J, Li X, Edmondson A, Meyers GD, Izumi K, Ackermann AM, et al. Increased Clinical Sensitivity and Specificity of Plasma Protein N-Glycan Profiling for Diagnosing Congenital Disorders of Glycosylation by Use of Flow Injection-Electrospray Ionization-Quadrupole Time-of-Flight Mass Spectrometry. *Clin Chem.* 2019;65(5):653-63.

74. Lippold S, Thavarajah R, Reusch D, Wuhrer M, Nicolardi S. Glycoform analysis of intact erythropoietin by MALDI FT-ICR mass spectrometry. *Anal Chim Acta*. 2021;1185:339084.
75. Selman MH, Hoffmann M, Zauner G, McDonnell LA, Balog CI, Rapp E, et al. MALDI-TOF-MS analysis of sialylated glycans and glycopeptides using 4-chloro-alpha-cyanocinnamic acid matrix. *Proteomics*. 2012;12(9):1337-48.
76. Edmond de Hoffmann VS. *Mass spectrometry: principles and applications*. 3rd edition ed2007.
77. Reiding KR, Bondt A, Franc V, Heck AJR. The benefits of hybrid fragmentation methods for glycoproteomics. *Trends in Analytical Chemistry*. 2018;108:260-8.
78. Yin H, Zhu J. Methods for quantification of glycopeptides by liquid separation and mass spectrometry. *Mass Spectrom Rev*. 2023;42(2):887-917.
79. Maliepaard JCL, Damen JMA, Boons GPH, Reiding KR. Glycoproteomics-Compatible MS/MS-Based Quantification of Glycopeptide Isomers. *Anal Chem*. 2023;95(25):9605-14.
80. Kemna MJ, Plomp R, van Paassen P, Koeleman CAM, Jansen BC, Damoiseaux J, et al. Galactosylation and Sialylation Levels of IgG Predict Relapse in Patients With PR3-ANCA Associated Vasculitis. *EBioMedicine*. 2017;17:108-18.

- ¹ Center for Proteomics and Metabolomics, Leiden University Medical Center, Leiden, The Netherlands
- ² Glycoscience Research Laboratory, Genos Ltd., Zagreb, Croatia
- ³ Department of Experimental Immunohematology, Sanquin, Amsterdam, The Netherlands
- ⁴ Department of Central Diagnostic Laboratory-Research, University Medical Center Utrecht, Utrecht University, The Netherlands
- ⁵ Department of Hematology, University Medical Center Utrecht, Utrecht University, The Netherlands
- ⁶ Department of Medical Microbiology and Immunology, St. Antonius Hospital, Nieuwegein, The Netherlands
- ⁷ Department of Internal Medicine, St. Antonius Hospital, Nieuwegein, The Netherlands
- ⁸ Center for Clinical Transfusion Research, Sanquin Research, Leiden, The Netherlands
- ⁹ Department of Hematology, Leiden University Medical Center, Leiden, The Netherlands
- ¹⁰ Department of Immunohematology Diagnostics, Sanquin, Amsterdam, The Netherlands
- ¹¹ Landsteiner Laboratory, Amsterdam UMC, University of Amsterdam, Amsterdam, The Netherlands

* Authors share co-first authorship; § Authors share co-senior authorship



Chapter 2

A functional spleen contributes to afucosylated IgG in humans

Iwona Wojcik^{1,2*}, David E. Schmidt^{3*}, Lisa A. de Neef¹,
Minke A.E. Rab^{4,5}, Bob Meek⁶, Okke de Weerd⁷, Manfred Wuhler¹,
C. Ellen van der Schoot³, Jaap J. Zwaginga^{8,9}, Masja de Haas^{8,9,10},
David Falck^{1§} and Gestur Vidarsson^{3,11§}

Reprinted and adapted with permission from

Sci Rep. 2021 Dec 15;11(1):24045. doi: 10.1038/s41598-021-03196-w. PMID: 34911982; PMCID: PMC8674363.

Copyright © 2021, Wojcik, Schmidt, de Neef, Rab, Meek, de Weerd, Wuhler, van der Schoot, Zwaginga, de Haas, Falck and Vidarsson.



2.1 ABSTRACT

As a lymphoid organ, the spleen hosts a wide range of immune cell populations, which not only remove blood-borne antigens, but also generate and regulate antigen-specific immune responses. In particular, the splenic microenvironment has been demonstrated to play a prominent role in adaptive immune responses to enveloped viral infections and alloantigens. During both types of immunizations, antigen-specific immunoglobulins G (IgGs) have been characterized by the reduced amount of fucose present on N-linked glycans of the fragment crystallizable (Fc) region. These glycans are essential for mediating the induction of immune effector functions. Therefore, we hypothesized that a spleen may modulate humoral responses and serve as a preferential site for afucosylated IgG responses, which potentially play a role in immune thrombocytopenia (ITP) pathogenesis. To determine the role of the spleen in IgG-Fc glycosylation, we performed IgG subclass-specific liquid chromatography-mass spectrometry (LC-MS) analysis of Fc glycosylation in a large cohort of individuals splenectomized due to trauma, due to ITP, or spherocytosis. IgG-Fc fucosylation was consistently increased after splenectomy, while no effects for IgG-Fc galactosylation and sialylation were observed. An increase in IgG1- and IgG2/3-Fc fucosylation levels upon splenectomy has been reported here for the first time, suggesting that immune responses occurring in the spleen may be particularly prone to generate afucosylated IgG responses. Surprisingly, the level of total IgG-Fc fucosylation was decreased in ITP patients compared to healthy controls. Overall, our results suggest a yet unrecognized role of the spleen in either the induction or maintenance of afucosylated IgG responses by B cells.

2.2 INTRODUCTION

The spleen is a key immune organ of the human body, enabling close interaction of the innate and adaptive immune system.(1) The spleen acts as a phagocytic blood filter, as splenic macrophages remove blood-borne aged cells and microorganisms. Moreover, the spleen is also a site of antibody production by long-lived memory B cells, plasmablasts and plasma cells.(1, 2) In the lymphoid white pulp, T- and B-cells interact with antigen-presenting cells such as dendritic cells or marginal zone B-cells.(1, 3) In line with these functions, surgical splenectomy is associated with several negative consequences. The reduced function or absence of the spleen can lead to infectious complications, impaired erythrocyte and iron recycling, and thromboembolic disease.(4) Immunologically, immunoglobulin M (IgM) memory B cells and switched memory B cells are markedly reduced after splenectomy.(4-6) Serum IgM is reduced following splenectomy, whereas immunoglobulin G (IgG) and immunoglobulin A (IgA) are similar to control values.(7) Generally, splenectomized individuals seem to be particularly sensitive to a drop in levels of certain antigen-specific antibodies, especially to T-cell independent antigens, such as pneumococcal polysaccharides. This is probably as the spleen is not only important for the formation of antibody-responses to both T-cell independent antigens and antigens in the blood, but also for the maintenance of those responses.(3) In line with this, the number of anti-pneumococcal polysaccharide IgM and IgG memory B cells are reduced following splenectomy.(8) For this reason, pneumococcal vaccination, especially with protein conjugated vaccine, is highly recommended before splenectomy.(9)

Antibodies represent a major effector mechanism of the adaptive immune system. Besides Fab-based affinity maturation, the effector functions of IgG antibodies are modified by N-linked glycosylation of the antibody Fc (fragment crystallizable) portion at position 297. The exact composition of this glycan branch can be affected in an antigen-specific manner.(10-14) This, in turn, modifies the binding to complement component C1q and to the IgG Fc gamma receptor III (FcγRIII) on immune cells, and determines the complement activity and antibody-dependent cellular cytotoxicity.(15) Afucosylated IgG display enhanced binding to FcγRIII expressed on CD16⁺ monocytes, macrophages, neutrophils and natural killer (NK) cells causing increased antibody-dependent cellular cytotoxicity.(15) An increase in the Fc galactosylation of IgG leads to increased C1q-mediated complement activation.(15, 16)

In autoimmune diseases, total serum IgG-Fc glycosylation is skewed, mostly with lowered galactosylation, and this is associated with increased disease progression, activity and symptoms severity.(17-20) Why this occurs is unclear, as elevated galactosylation of antigen-specific IgG is known to elevate their complement activity potential.(15, 16, 21) However, a possible explanation of the association between the lowered total IgG galactosylation and autoimmune diseases, is that the decrease in total IgG galactosylation seems to increase systemic inflammation.(20, 21) Observations in Guillain-Barré syndrome

and Kawasaki disease suggest that pre-treatment levels and normalization of Fc galactosylation and sialylation after treatment are associated with recovery.(22, 23) Interestingly, we found no biologically significant changes in IgG-Fc glycosylation were observed after CD20-targeted rituximab treatment in immune thrombocytopenia (ITP).(24)

For alloimmune responses, that is foreign antigens on cells such as platelets and anti-red blood cell antigens (RBC) in either pregnancy or after transfusion, we previously described a general reduction of antigen-specific IgG-Fc fucosylation, such as for anti-D and anti-Human Platelet Antigen-1a (HPA-1a) antibodies.(25, 26) Importantly, immunization to these alloantigens, also generally requires a functional spleen,(27) suggesting that immune responses occurring in the spleen may be particularly prone to generate afucosylated IgG responses. Similar afucosylated antigen-specific IgG responses have been observed in virus-specific IgG responses, such as for dengue virus, HIV, cytomegalovirus (CMV), hepatitis B virus (HBV), measles virus, mumps virus and severe acute respiratory syndrome coronavirus 2 (SARS-CoV-2),(12-14, 28, 29) and now recently shown by us to be a hallmark of enveloped viral infections, a response that is mimicked by alloimmunizations.(14) In theory, IgG afucosylation results in a strong humoral immune response, targeting FcγRIIIa and FcγRIIIb, potentially giving strong myeloid FcγR-mediated responses(30) that can ultimately be particularly protective as proposed for HIV.(31) On the other hand, this strong reaction can also lead to exaggerated myeloid response with elevated proinflammatory cytokine production culminating in adverse clinical reactions, as seen in Dengue and COVID-19 responses.(11, 14, 28)

The reduction in fucosylation seen in immune response to enveloped viral infections and alloimmune mediated diseases is particularly strong to CMV and many of the anti-red blood cell antigens (e.g. Rhesus D) and human platelet antigens. What these antigen responses have in common is a dominant systemic response likely to occur in the spleen.(27)

In the present study, we investigated the role of the spleen on IgG-Fc glycosylation in a large cohort of individuals splenectomized due to trauma, or due to immune thrombocytopenia, or spherocytosis, to test the hypothesis that the spleen is a primary driver of afucosylated IgG responses in humans.

2.3 EXPERIMENTAL SECTION

2.3.1 Study participants

Plasma samples from individuals with splenectomy due to trauma, spherocytosis or immune thrombocytopenia were identified by regional general practitioners and a nationwide database.(32) The study was approved by the ethical review committee of St Antonius Hospital Nieuwegein, The Netherlands. Written informed consent was obtained from the study subjects. Further samples from splenectomized ITP patients were obtained from the HOVON64 study.(33) The study was approved by the ethical review committee of Academic

Medical Center, Amsterdam, The Netherlands; subjects provided written informed consent. Age- and sex-matched control samples were obtained from healthy blood donors (Sanquin, Amsterdam, The Netherlands) and non-splenectomized ITP patients from the HOVON64 study.(33) All splenectomy samples were matched to two control samples. Patients from the HOVON64 study were splenectomized with a median interval of 12 years before blood sampling (range: 2 months - 29 years). Patients from the Utrecht study were splenectomized with a median interval of 29 years before blood sampling (range: 6 - 55 years) for trauma, 19 years (range: 5 - 51 years) for ITP and 28 years (range: 5 – 50 years) for spherocytosis. Samples were handled according to national responsible use protocols (Federation of Dutch Medical Scientific Societies Code of Conduct for responsible use; www.federa.org). All samples and data were coded for storage and analysis.

2.3.2 IgG purification and enzymatic digestion

All 254 plasma samples from splenectomized (n = 89) and non-splenectomized individuals (n = 165) were randomized through four 96-well plates, including 24 pooled plasma samples and 23 plasma standards (VisuCon_F control plasma; Affinity Biologicals Inc., Ancaster, ON, Canada). Total IgG (IgG1, IgG2, IgG3 and IgG4) was affinity-purified by protein G affinity beads (GE Healthcare, Uppsala, Sweden) and subjected to trypsin digestion in 96-well filter plates (0.7 mL wells, PE frit, Orochem, Naperville, IL) as described before,(34) see Methods in Supplementary Material. Obtained IgG glycopeptides were stored at -20°C until measurement.

2.3.3 Mass spectrometric analysis and data processing

The total IgG glycopeptides were analyzed using an Ultimate 3000 RSLC nano-liquid chromatography system (Dionex/Thermo Fisher Scientific, Sunnyvale, CA) coupled to a Maxis Impact HD quadrupole time-of-flight (QTOF)-MS instrument (micrOTOF-Q; Bruker Daltonics, Bremen, Germany) as described previously.(34) Data were processed using the highly automated LaCyTools software as previously described.(34, 35) Processing parameters and the software used to compile them are listed in the supporting information. Glycopeptide compositions were selected based on literature(36) and manual inspection with Data Analysis (version 5.0; Bruker). They were verified or rejected using quality criteria provided by LaCyTools. Per IgG subclass, samples were checked for analyte quality and total signal intensity and extreme cases removed (see Supporting Information). Total area normalization was applied. Based on the normalized, directly measured N-glycan monosaccharide composition, the following derived glycosylation traits were calculated (**Supplementary Table S2**): fucosylation (fraction of fucosylated *N*-glycopeptides), galactosylation (fraction of galactoses per antennae of biantennary glycans), bisection (fraction of *N*-glycopeptides carrying a bisecting *N*-acetylglucosamine (GlcNAc)), sialylation (fraction of sialic acids per antennae of biantennary glycans) and sialic acid per galactose (fraction of sialic acids per galactose). Fucosylation for IgG4 could not be accurately

assessed, since the exact mass of the minor IgG4 afucosylated N-glycopeptides overlapped with the more abundant IgG1 fucosylated N-glycopeptides (**Supplementary Table S1**). Moreover, the IgG4 fucosylated N-glycopeptides have the same exact mass as the afucosylated ones from IgG2/3. A study is characterized by a good analytical precision of the LC-MS method, which was assessed based on 24 replicate analysis of pool plasma standard throughout the cohort (**Supplementary Fig. S1**).

2.3.4 Statistical analysis

Analyses were performed in R version 3.6.4 (R Core Team). As the distribution of normalized glycan species and the derived traits deviates significantly from normality, further statistical analysis was performed using non-parametric tests.(37) A non-parametric Wilcoxon-rank test was used to compare relative intensities of the IgG-Fc glycosylation traits between pairs (non-splenectomized and splenectomized). A two-sided p-value below 0.05 was considered significant. Statistical tests were only performed for IgG1 glycosylation traits, other data were reported descriptively. Differences in relative intensities of IgG-Fc glycosylation traits across all patient groups were evaluated for statistical significance using the non-parametric Kruskal Wallis rank sum test followed by a post-hoc Nemenyi test for pairwise comparison.

2.4 RESULTS

We studied the impact of splenectomy on IgG-Fc N-linked glycosylation by comparing patients who had undergone splenectomy to control groups with an intact spleen. A proportion of individuals were splenectomized after trauma (n = 38), but were otherwise healthy, whereas others were splenectomized due to hematological disease (ITP, n = 35; spherocytosis, n = 16) (**Table 1**). All of the subgroups of healthy controls and ITP patients were comparable for age and sex distribution thus reducing the age- and sex-depended differences in IgG glycosylation.

Table 1. Demographics of patients splenectomized either due to trauma or hematological diseases and non-splenectomized matched controls.

	Healthy		ITP		Spherocytosis	
	Trauma splenectomized	Healthy controls	ITP splenectomized	ITP controls	Spherocytosis splenectomized	Healthy controls
N	38	76	35	57	16	32
Sex, n (%)						
Female	18 (47)	36 (47)	14 (40)	24 (42)	7 (44)	14 (44)
Male	20 (53)	40 (53)	21 (60)	33 (58)	9 (56)	18 (56)
Median age, years [IQR]	50 [39 - 56]	50 [39 - 56]	52 [44 - 62]	54 [45 - 62]	38 [30 - 53]	38 [30 - 53]
Median interval*, years [range]	29 [6 - 55]	-	HOVON64: 12 [0.2 - 29] Utrecht: 19 [5-51]	-	28 [5 - 50]	-

*Median interval between splenectomy and blood sampling

This allowed us to test our hypothesis of the effect of the spleen on IgG glycosylation in both relatively healthy individuals and individuals with an autoimmune disease.

2.4.1 Measurement of IgG-Fc glycosylation

Total IgG was affinity purified from 254 patient plasma samples, and subjected to tryptic digestion, and the resulting IgG Asn297-Fc glycopeptides were analyzed by liquid chromatography – mass spectrometry (LC-MS) (**Figure 1A**). Tryptic digestion of all four IgG subclasses (IgG1, IgG2, IgG3, IgG4) resulted in distinct peptide moieties (IgG1: EEQYNSTYR, IgG2/3: EEQFNSTFR, IgG4: EEQFNSTYR). Thus, IgG-Fc glycopeptides were separated and glycosylation patterns of individual subclasses IgG1, IgG4 as well as collective Fc glycosylation profiles of IgG2/IgG3 were analyzed by LC-MS. An example of an LC-MS sum spectrum of total IgG1 glycopeptides can be seen in **Figure 1B**. Inability to distinguish between IgG2 and IgG3 glycosylation by our profiling method is due to the fact that the amino acid sequence of the tryptic peptide including the N297-glycosylation site is identical for both IgG subclasses.(EEQFNSTFR).(38, 39) For all samples, 37 glycoforms positively passed the analyte curation, 19, 10 and 8 glycoforms for IgG1, IgG2/3 and IgG4, respectively (see **Supplementary Table S1**). For further analysis, derived glycosylation traits were calculated, including bisection, fucosylation, galactosylation and sialylation (**Figure 1C**, see **Supplementary Table S2** for the calculations of the derived traits). It should be noted that we could not assess the minor amount of IgG4 afucosylation which is a common limitation of the applied method.

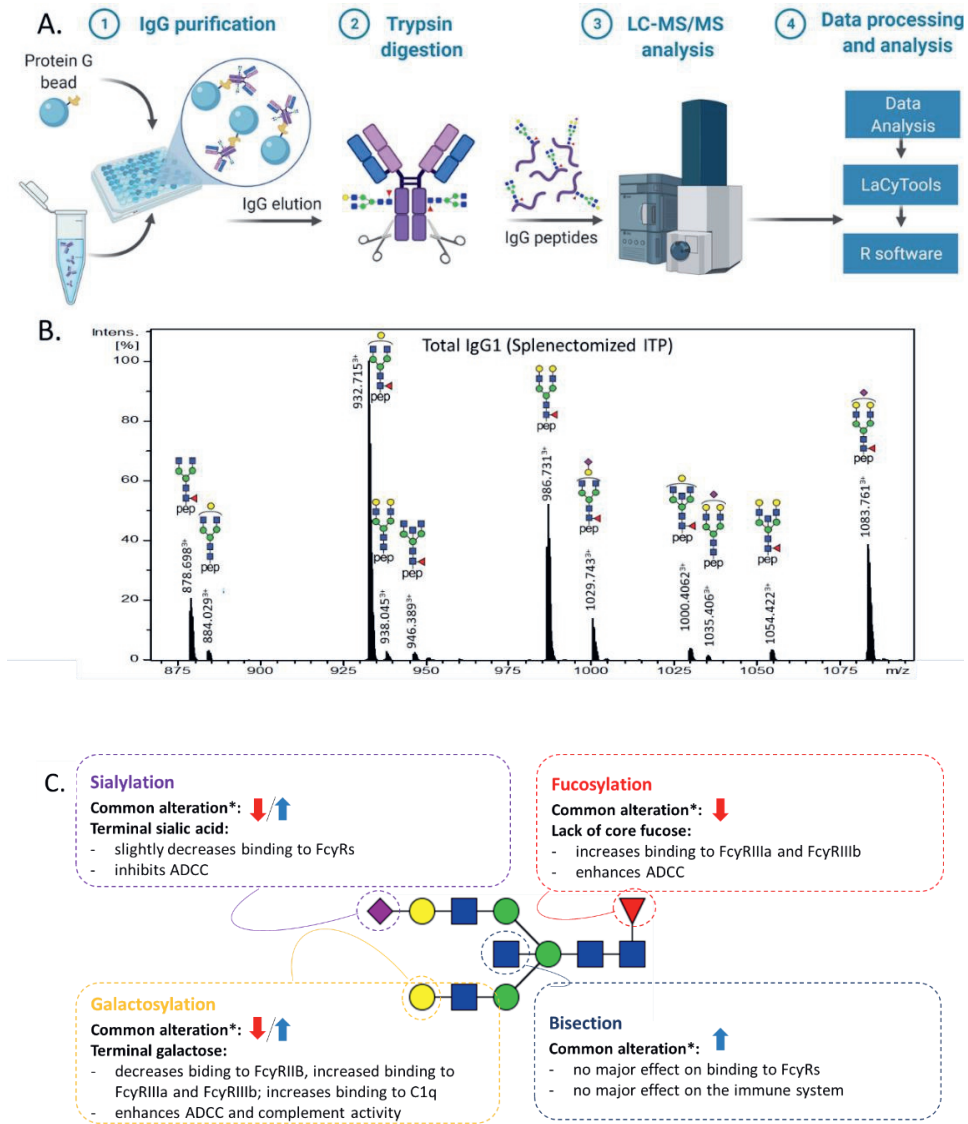


Figure 1. LC-MS analysis of IgG-Fc glycopeptides. **(A)** Schematic workflow. **(B)** Representative LC-MS summed mass spectrum of IgG1 tryptic glycopeptides obtained from a 43 year-old splenectomized ITP male. Annotated are the 11 most abundant IgG1 glycopeptides. Green circle: mannose, yellow circle: galactose, blue square: N-acetylglucosamine, red triangle: fucose, pink diamond: N-acetylneuraminic acid. **(C)** Scheme of the IgG-Fc glycan structure, common disease-related changes in total IgG and their immunological implications. It shows derived glycosylation traits representing common glycosylation features shared by glycan composition: sialylation – sialylation per antenna of biantennary glycans, fucosylation – fraction of fucosylated glycans, galactosylation – galactosylation per antenna of biantennary glycans, bisection – fraction of glycans with bisecting N-acetylhexosamine. For detailed calculation per IgG subclass see Supplementary Table S2. *Down arrow refers to a commonly observed lower and up arrow to higher proportion of the corresponding IgG glycosylation trait in patients suffering from autoimmune, infectious and inflammatory diseases compared to healthy controls; ADCC – antibody-dependent cellular cytotoxicity. The figure was created with BioRender.com

2.4.2 The Impact of Splenectomy on IgG-Fc Glycosylation

To evaluate the impact of splenectomy on total IgG-Fc glycosylation, we compared samples from three different patient groups with splenectomy with age- and sex-matched respective controls with an intact spleen. The three different splenectomized patient groups were 1) trauma-associated 2) ITP patients and 3) spherocytosis patients. For trauma splenectomized individuals, we observed a significantly higher median IgG1 fucosylation and IgG2/3 fucosylation when compared to healthy controls (**Table 2**; **Figure 2A** for IgG1; **Supplementary Fig. S2A** for IgG2/3). Likewise, the analysis of IgG-Fc glycosylation in splenectomized ITP patients revealed a higher median fucosylation for both IgG1 and IgG2/3, compared to ITP controls. For spherocytosis patients we did not observe any significant differences in the level of IgG-Fc fucosylation in splenectomized individuals compared to healthy individuals (**Figure 3A**). Bisection was significantly decreased for the trauma group and spherocytosis compared to healthy controls for both IgG1 and IgG2/3 (**Table 2**, **Figure 2B**, **Figure 3B**, see **Supplementary Fig. S2B** for IgG2/3 data). No differences were observed for any other glycan traits in any IgG subclass (**Figure 2C-E**, **Figure 3C-E**, **Supplementary Fig. S2C-E** and **Supplementary Fig. S3C-E**).

Table 2. Glycosylation comparison of two different patient groups (healthy and ITP) with splenectomy and age- and sex-matched respective controls with an intact spleen. P-values are given for a Wilcoxon-rank sum test. Only significant differences in IgG-Fc glycosylation ($P < 0.05$) are shown.

IgG subclass	Derived trait	splenectomized		Healthy controls		P-value
		median	IRQ	median	IRQ	
IgG1	fucosylation	92.9	91.5-95.2	91.4	89.1-93.6	0.026
	bisection	14.8	12.9-16.2	16.5	14.7-18.4	0.008
IgG2/3	fucosylation	99.8	99.7-99.8	99.7	99.5-99.8	0.003
	bisection	11.9	10.4-13.4	12.8	11.7-15.8	0.042
ITP						
IgG1	fucosylation	91.3	88.8-94.1	88.7	85.6-91.9	0.017
IgG2/3	fucosylation	99.6	99.5-99.8	99.5	99.4-99.7	0.016

2.4.3 ITP patients and healthy controls differ in IgG fucosylation

Comparison of the IgG-Fc glycosylation of ITP patients with healthy controls showed that the ITP patients had significantly lower median IgG1 fucosylation compared to healthy controls (**Figure 2A**). The splenectomy resulted in an elevated level of IgG1 fucosylation in ITP patients, with undistinguishable IgG1 fucosylation between splenectomized ITP patients and healthy individuals. Moreover, ITP patients had a lower IgG1-Fc fucosylation than trauma-related splenectomized patients. No other significant changes were observed comparing healthy controls for any IgG subclass or glycosylation trait (**Figure 2B-E**, **Supplementary Fig. S2B-E** for IgG2/3, **Supplementary Fig. S3A-E** for IgG4).

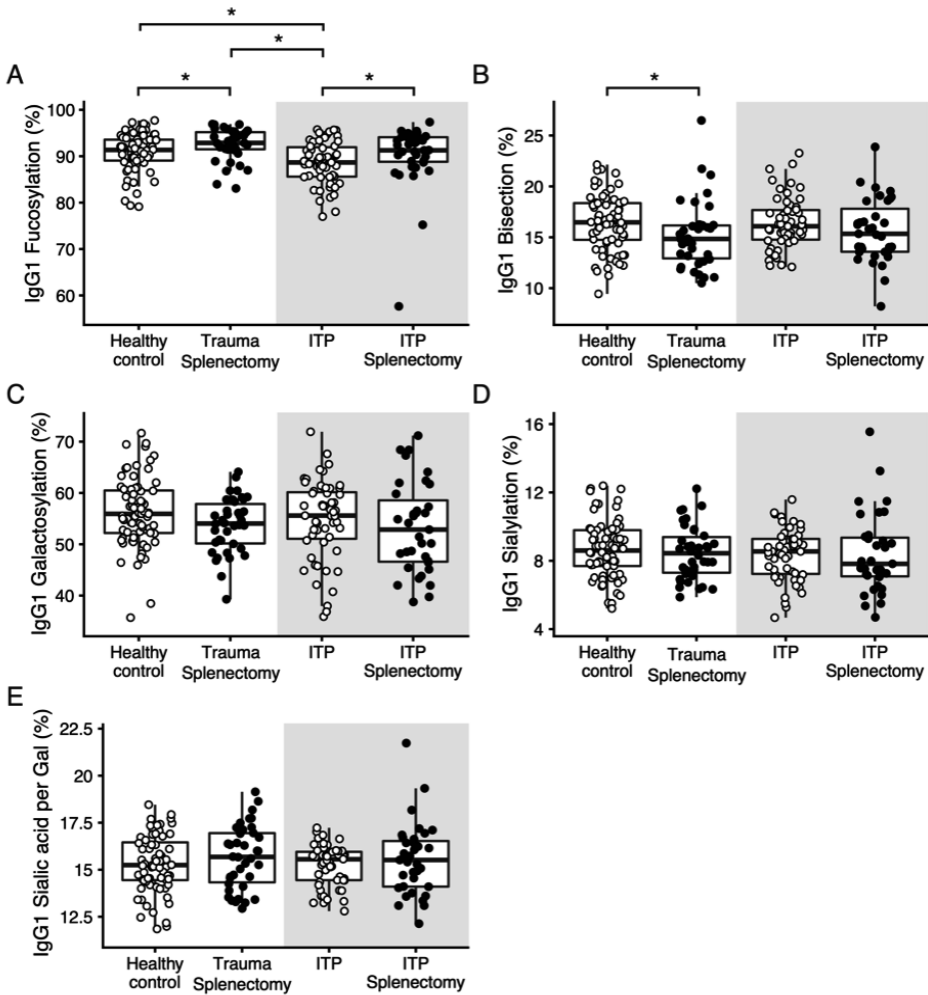


Figure 2. Effect of splenectomy on IgG1-Fc glycosylation in healthy individuals and ITP patients. Data are shown for healthy individuals with (Healthy Control, $n = 38$) or without splenectomy (Trauma Splenectomy, $n = 76$) and ITP patients with (ITP Splenectomy, $n = 35$) or without splenectomy (ITP, $n = 57$), matched for age and sex. Compared to the respective controls, IgG1-Fc fucosylation was higher in splenectomized and otherwise healthy individuals ($P = 0.026$; Wilcoxon-rank sum test), as well as in splenectomized ITP patients ($P = 0.017$; Wilcoxon-rank sum test). Regarding IgG1-Fc bisection, otherwise healthy individuals showed lower levels ($P = 0.008$; Wilcoxon-rank sum test), whereas in splenectomized ITP patients this difference was less prominent and did not result in a finding. ITP patients have reduced IgG1-Fc fucosylation compared to healthy controls ($P = 0.017$; Kruskal-Wallis rank sum test followed by a post-hoc Nemenyi test for pairwise comparison). All other glycosylation features were not significantly different between the groups. * P -values are given for a Wilcoxon-rank sum test, P -values < 0.05 ; ns, not significant.

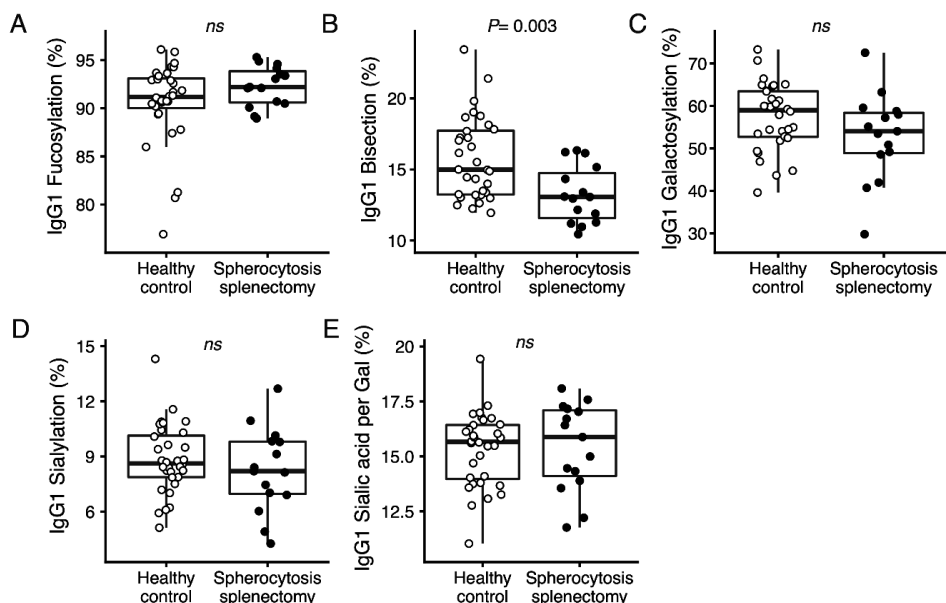


Figure 3. Effect of spherocytosis-associated splenectomy on IgG1-Fc glycosylation. Data are shown for healthy individuals without splenectomy (Healthy control, $n = 32$) and spherocytosis patients with splenectomy (Spherocytosis splenectomy, $n = 16$). Compared to the respective controls, spherocytosis-associated splenectomy individuals showed lower levels of IgG1-Fc bisection ($P = 0.003$; Wilcoxon-rank sum test), and trend towards increased IgG1-Fc fucosylation. All other glycosylation features were not significantly different between the groups.

2.5 DISCUSSION

Splenectomy performed in ITP patients and healthy individuals due to trauma represents a unique opportunity to study the role of the spleen in the control of IgG glycosylation. The key finding of our study is an increase in IgG1 fucosylation and in IgG2/3 fucosylation upon splenectomy. Although these changes in total plasma IgG are minor, with total IgG only containing ~6% of afucosylated IgG, they are likely to be larger and give rise to significant biological effects when looking at the antigen-specific level. For example, the ability to enhance the inflammatory response by afucosylated antigen-specific IgG was observed in fetal or neonatal alloimmune thrombocytopenia (FNAIT), dengue virus infection, COVID-19.(11, 14, 29, 40) Among all four patient groups, the otherwise healthy individuals after trauma-associated splenectomy showed the highest level of IgG1-Fc fucosylation. An increase in IgG-Fc fucosylation due to splenectomy was found in both healthy individuals as well as in ITP patients. Similar changes were seen in spherocytosis. This could either be due to, support of short lived afucosylated IgG responses generated by B cells in the spleen, or the spleen is a reservoir for long lived plasma cells.(2) Possibly, the less pronounced effect on IgG2/3 is because IgG2 is the more abundant subclass of these two (~32% vs 4%, respectively),(39) and because IgG2 fucosylation is generally very high, which is in line with

the predominant IgG2 response to encapsulated bacteria which do not induce afucosylated IgG responses.(14, 41, 42) However, IgG3 responses most often occur simultaneously with IgG1 responses, and the level of fucosylation of both IgG1 and IgG3 generally seem to go hand in hand.(43) It is therefore likely that the lowered effect of splenectomy on IgG2/3 afucosylation is solely due to the IgG3 fraction. Together, this points towards a pronounced role of IgG1 and IgG3 in platelet clearance compared to other IgG subclasses. Due to the prominent role and an inability to distinguish the effect size of fucosylation changes between IgG3 and IgG2, our discussion applies mainly to IgG1.

Without any intervention or emerging pathology, total IgG-Fc fucosylation is largely stable throughout the adult life.(44) The precise regulation of the IgG-Fc glycosylation, and fucosylation in particular, remains still largely unelucidated. Shortly after birth, neonates make exclusively fucosylated antibodies, but appear to gradually acquire afucosylated IgG until adulthood reaching the level of 96% of IgG-Fc fucosylation.(44) Recently, we found that only antigens expressed on the surface of host cells, such as alloantigens and proteins of enveloped viruses found on cell surfaces, seem to induce afucosylated IgG responses.(14) Based on this, it is tempting to hypothesize that the gradual accumulation of afucosylated IgG seen during childhood, is the accumulation of antigen-specific IgG to enveloped viruses. However, the tendency to generate afucosylated IgG varies vastly between targets and between individuals, with IgG1 responses to cytomegalovirus being generally low and stable in time, while responses to SARS-CoV-2 start with a relatively high level of IgG1 fucosylation in most individuals. However, in some patients afucosylated IgG1 is observed at seroconversion, which is associated with enhanced pathologies due to excessive inflammation in COVID-19, those responses quickly revert to fucosylated IgG in a matter of weeks.(11, 14) Conversely, alloantibodies specific for HPA-1a, causing FNAIT, or to RBC show remarkable low levels of fucosylation that are extremely stable for more than 10 years.(10, 25, 40) All in all, these disparate type of afucosylated IgG responses seem to favor both possible roles for the spleen in generating and maintaining IgG afucosylation. The afucosylation of anti-platelet antibodies has been recognized as a very important factor enhancing platelet-specific IgG effector functions through elevated affinity to FcγRIIIa/b and finally target destruction and production of proinflammatory cytokines.(11, 26, 45) The spleen, second to the liver, is recognized as one of the most important organs for removal of IgG-opsonized cells from the blood, with monocytes expressing FcγRIIIa being particularly abundant.(46, 47) Therefore, splenectomy has typically been seen as a resort focusing on removing the organ responsible for and thus preventing the degradation of cells in diseases like ITP. However, it is important to realize that splenectomy not only removes an important myeloid compartment responsible of removing IgG-opsonized platelets, but also removes the major site of auto-antibody production in ITP. The splenectomy removes many autoantibody-producing cells, especially in cases of autoreactive B cells to platelets in ITP.(48, 49) Accordingly, this results in the profound elimination of anti-platelet IgG

production in a splenectomized mouse model for ITP.(50) As opposed to anti-platelet IgG levels, total plasma IgG levels were not affected by splenectomy.(32) Interestingly, when targeting B cells systemically with Rituximab (anti-CD20) in ITP, afucosylated antibodies are not specifically reduced,(24) which is in line with the fact that long-lived plasma cells do not express CD20.(51) A limitation in the present study is that we did not investigate antigen-specific antibodies individually. Monitoring platelet autoantibody IgG-Fc glycosylation levels should provide further information for elucidating the mechanism of afucosylated responses in the spleen. In addition, the effect of splenectomy on the composition of antigen-specific plasma cells in the bone-marrow would be valuable in a future study.

In this study, total IgG1 and IgG2/3 purified from plasma of ITP patients showed decreased fucosylation when compared to healthy individuals, while galactosylation, sialylation and bisection remained similar. In previous studies, we found a similar result and effect size, but this was not statistically significant due to lower power.(24) This finding in ITP is in contrast to many autoimmune, inflammatory and infectious conditions, where mainly galactosylation and sialylation of total IgG1 have been described to be altered.(20, 52-54) However, afucosylation of total IgG has recently been found to be elevated in autoimmune thyroid diseases,(55) similar to our ITP findings. This may suggest that the mechanism underlying the changes in IgG glycosylation in autoimmune diseases may vary depending on the disease etiology, target tissue, or the level of antigen-specific IgG glycosylation.

2.5.1 Conclusions

Splenectomy affects total plasma IgG-Fc glycosylation. ITP patients showed a lower level of total IgG-Fc fucosylation compared to healthy controls, implying that anti-platelet autoantibodies have an afucosylation phenotype in ITP, as demonstrated for FNAIT. In addition to removing a major organ responsible for removal of IgG-autoantibody opsonized cells in ITP, we also find a general splenectomy-driven increase in IgG-Fc fucosylation in humans. Altogether, our data indicate that the spleen is a significant site to generate or maintain afucosylated IgG responses.

2.6 ACKNOWLEDGEMENTS

This research was supported by the European Union (Glycosylation Signatures for Precision Medicine Project, GlySign, Grant No. 722095), a grant from the Landsteiner Foundation for Blood Transfusion Research (LSBR, Grant No. 1546) and a scholarship from the Studienstiftung des Deutschen Volkes to David Schmidt. Neither agency had other influence on the scientific content of this manuscript.

2.7 SUPPLEMENTARY MATERIAL

A complete overview of the supplemental material is available online at <https://www.nature.com/articles/s41598-021-03196-w>.

Table S1. The list of curated glycosylation compositions detected by nano-LC-ESI-MS and the corresponding *m/z* values of exact masses of human IgG Fc glycopeptides. (*) Glycan compositions used for alignment, (bolded) Glycan structural feature used for calibration.

IgG1 P01857*			IgG2 P01859*			Ig4 P01861*		
glycoform	[M+2H] ²⁺	[M+3H] ³⁺	glycoform	[M+2H] ²⁺	[M+3H] ³⁺	glycoform	[M+2H] ²⁺	[M+3H] ³⁺
H3N3F1	1215.99	810.99	H3N3F1	1199.99	800.33	H5N4	1398.55	932.70
H3N4	1244.50	830.00	H3N4F1*	1301.53	868.02	H3N4F1*	1309.53	873.36
H4N3F1	1297.01	865.01	H4N4	1309.53	873.36	H4N4F1*	1390.56	927.37
H3N4F1*	1317.53	878.69	H4N4F1*	1382.56	922.04	H3N5F1	1411.07	941.05
H4N4	1325.52	884.02	H3N5F1	1403.07	935.72	H5N4F1	1471.58	981.39
H3N5	1346.04	897.69	H5N4F1	1463.58	976.06	H4N4F1S1	1536.10	1024.40
H4N4F1*	1398.55	932.70	H4N5F1	1484.10	989.73	H5N4S1	1544.10	1029.74
H5N4	1406.55	938.04	H4N4F1S1	1528.11	1019.07	H5N4F1S1*	1617.13	1078.42
H3N5F1	1419.07	946.38	H5N5F1	1565.12	1043.75			
H4N5	1427.06	951.71	H5N4F1S1*	1609.13	1073.09			
H5N4F1	1479.58	986.72						
H4N5F1	1500.09	1000.40						
H5N5	1508.09	1005.73						
H4N4F1S1	1544.10	1029.74						
H5N4S1	1552.10	1035.07						
H5N5F1	1581.12	1054.42						
H5N4F1S1*	1625.13	1083.75						
H5N5F1S1	1726.67	1151.45						
H5N4F1S2	1770.67	1180.79						

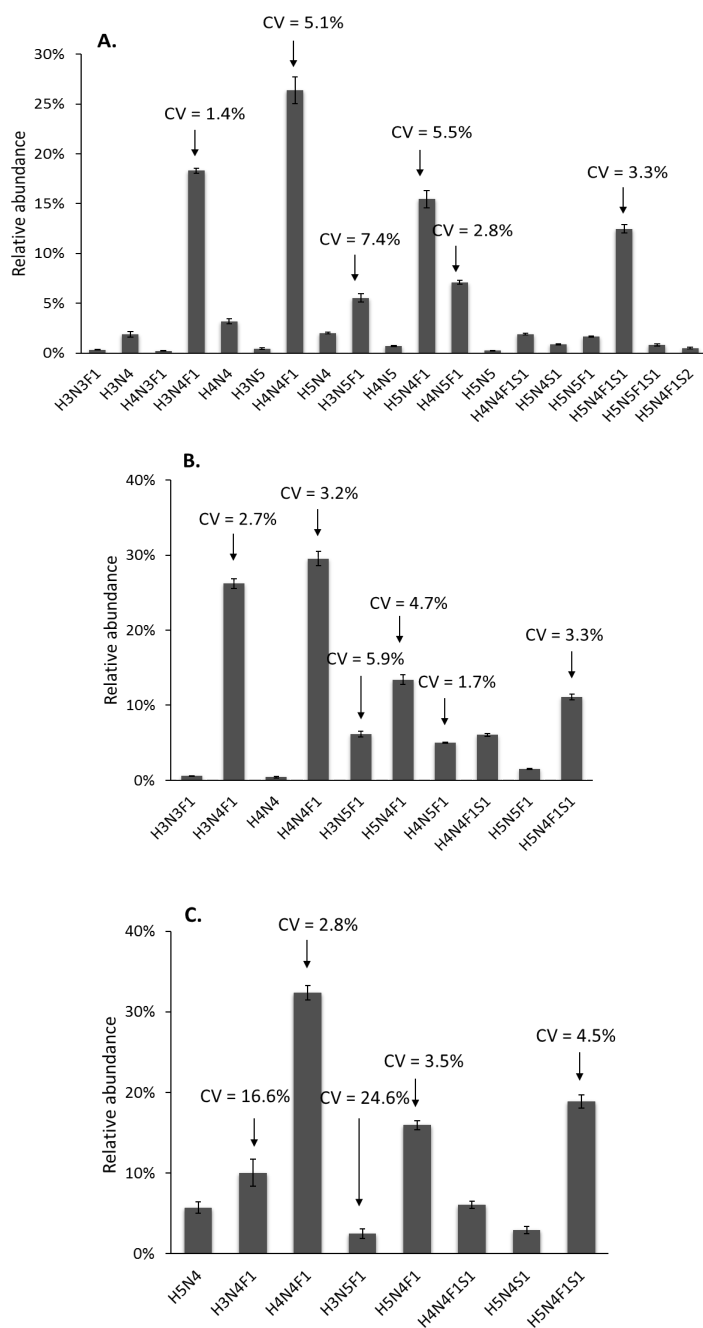


Figure S1. Repeatability of the method. Average relative abundances of A. IgG1, B. IgG2/3 and C. IgG4 glycopeptides from 24 replicates of a pooled plasma sample. The coefficient of variations (CV) is displayed for six prominent glycoforms on IgG (H3N4F1, H4N4F1, H3N5F1, H5N4F1, H4N5F1, H5N4F1S1). For those glycoforms a median coefficient of variation of 4.3%, 3.6% and 10.4% was observed for IgG1, IgG2/3 and IgG4, respectively. The error bars represent the standard deviation of the mean.

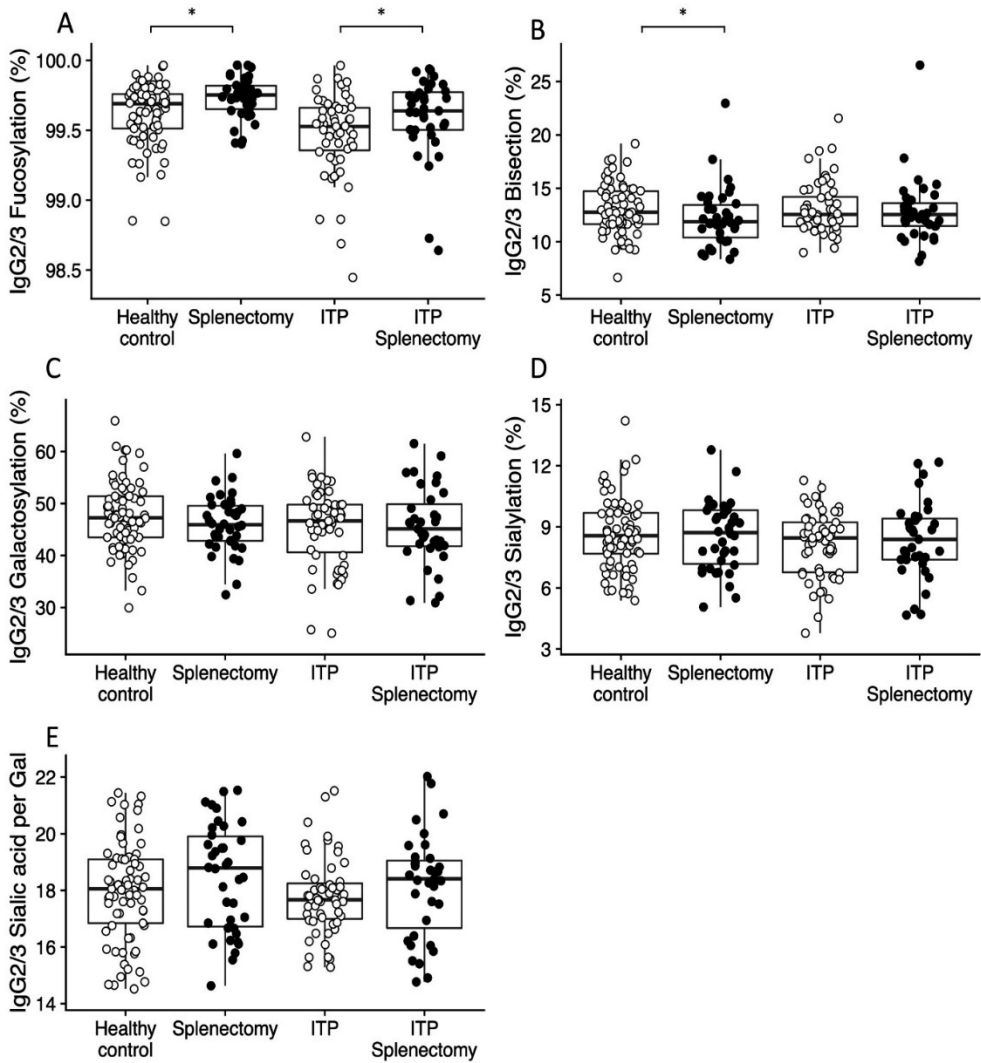


Figure S2. Comparison of IgG2/3-Fc glycosylation profiles in regard to fucosylation, bisection, galactosylation, sialylation and sialic acid per galactose after splenectomy in healthy individuals and ITP patients. Compared to the respective controls, IgG2/3 Fc fucosylation was higher in splenectomized and otherwise healthy individuals ($P = 0.006$; Wilcoxon-rank sum test), as well as in splenectomized ITP patients ($P = 0.016$; Wilcoxon-rank sum test). Regarding IgG2/3 Fc bisection, otherwise healthy individuals showed lower levels ($P = 0.042$; Wilcoxon-rank sum test), whereas in splenectomized ITP patients this difference was less prominent and not significant. All other glycosylation features were not significantly different between the groups.

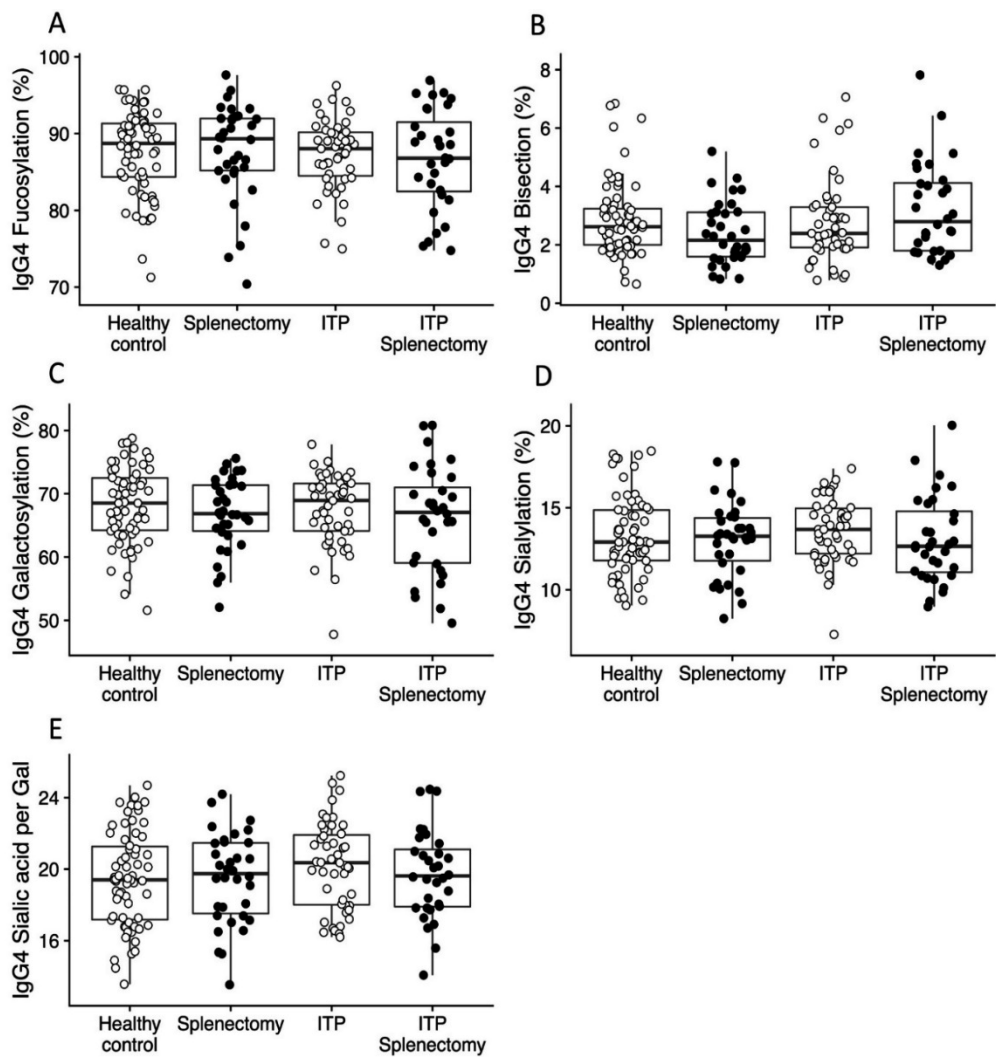


Figure S3. Comparison of IgG4-Fc glycosylation profiles in regard to fucosylation, bisection, galactosylation, sialylation and sialic acid per galactose after splenectomy in healthy individuals and ITP patients. All glycosylation features were not significantly different between the groups.

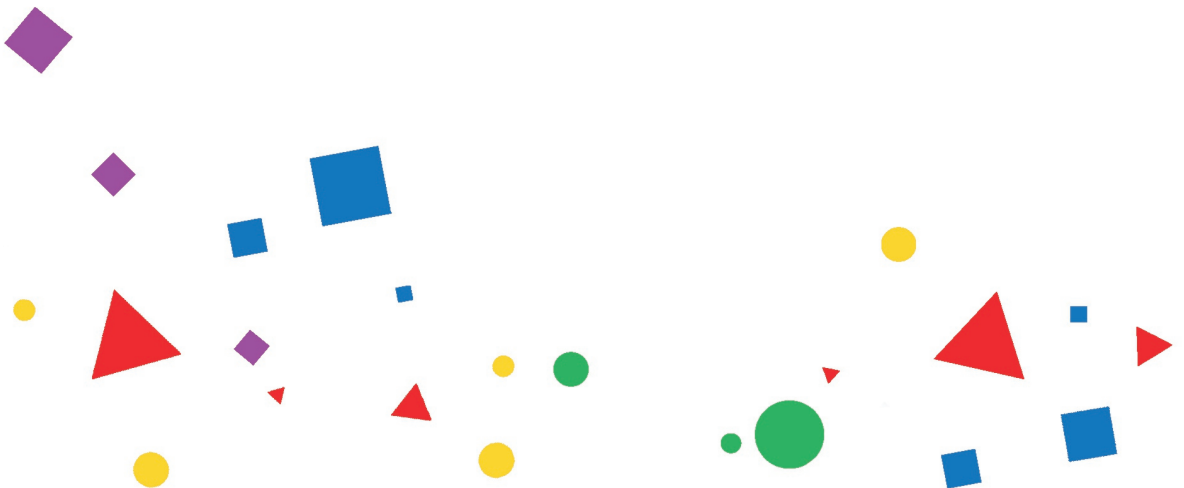
2.8 REFERENCES

1. Mebius RE, Kraal G. Structure and function of the spleen. *Nat Rev Immunol.* 2005;5(8):606-16.
2. Mamani-Matsuda M, Cosma A, Weller S, Faili A, Staib C, Garcon L, et al. The human spleen is a major reservoir for long-lived vaccinia virus-specific memory B cells. *Blood.* 2008;111(9):4653-9.
3. Cerutti A, Cols M, Puga I. Marginal zone B cells: virtues of innate-like antibody-producing lymphocytes. *Nat Rev Immunol.* 2013;13(2):118-32.
4. Di Sabatino A, Carsetti R, Corazza GR. Post-splenectomy and hyposplenic states. *Lancet.* 2011;378(9785):86-97.
5. Giordano P, Cascioli S, Lassandro G, Marcellini V, Cardinale F, Valente F, et al. B-cell hyperfunction in children with immune thrombocytopenic purpura persists after splenectomy. *Pediatr Res.* 2016;79(2):262-70.
6. Cameron PU, Jones P, Gorniak M, Dunster K, Paul E, Lewin S, et al. Splenectomy associated changes in IgM memory B cells in an adult spleen registry cohort. *PLoS One.* 2011;6(8):e23164.
7. Schumacher MJ. Serum immunoglobulin and transferrin levels after childhood splenectomy. *Arch Dis Child.* 1970;45(239):114-7.
8. Rosado MM, Gesualdo F, Marcellini V, Di Sabatino A, Corazza GR, Smacchia MP, et al. Preserved antibody levels and loss of memory B cells against pneumococcus and tetanus after splenectomy: tailoring better vaccination strategies. *Eur J Immunol.* 2013;43(10):2659-70.
9. Nived P, Jorgensen CS, Settergren B. Vaccination status and immune response to 13-valent pneumococcal conjugate vaccine in asplenic individuals. *Vaccine.* 2015;33(14):1688-94.
10. Sonneveld ME, Natunen S, Sainio S, Koeleman CA, Holst S, Dekkers G, et al. Glycosylation pattern of anti-platelet IgG is stable during pregnancy and predicts clinical outcome in alloimmune thrombocytopenia. *Br J Haematol.* 2016;174(2):310-20.
11. Hoepel W, Chen HJ, Geyer CE, Allahverdiyeva S, Manz XD, de Taeye SW, et al. High titers and low fucosylation of early human anti-SARS-CoV-2 IgG promote inflammation by alveolar macrophages. *Sci Transl Med.* 2021;13(596).
12. Ackerman ME, Crispin M, Yu X, Baruah K, Boesch AW, Harvey DJ, et al. Natural variation in Fc glycosylation of HIV-specific antibodies impacts antiviral activity. *J Clin Invest.* 2013;123(5):2183-92.
13. Wang TT, Sewatanon J, Memoli MJ, Wrammert J, Bournazos S, Bhaumik SK, et al. IgG antibodies to dengue enhanced for FcγRIIIA binding determine disease severity. *Science.* 2017;355(6323):395-8.
14. Larsen MD, de Graaf EL, Sonneveld ME, Plomp HR, Nouta J, Hoepel W, et al. Afucosylated IgG characterizes enveloped viral responses and correlates with COVID-19 severity. *Science.* 2021;371(6532).
15. Dekkers G, Treffers L, Plomp R, Bentlage AEH, de Boer M, Koeleman CAM, et al. Decoding the Human Immunoglobulin G-Glycan Repertoire Reveals a Spectrum of Fc-Receptor- and Complement-Mediated-Effector Activities. *Front Immunol.* 2017;8:877.
16. Peschke B, Keller CW, Weber P, Quast I, Lunemann JD. Fc-Galactosylation of Human Immunoglobulin Gamma Isotypes Improves C1q Binding and Enhances Complement-Dependent Cytotoxicity. *Front Immunol.* 2017;8:646.
17. Seeling M, Bruckner C, Nimmerjahn F. Differential antibody glycosylation in autoimmunity: sweet biomarker or modulator of disease activity? *Nat Rev Rheumatol.* 2017;13(10):621-30.
18. Bondt A, Selman MH, Deelder AM, Hazes JM, Willemsen SP, Wuhler M, et al. Association between galactosylation of immunoglobulin G and improvement of rheumatoid arthritis during pregnancy is independent of sialylation. *J Proteome Res.* 2013;12(10):4522-31.
19. Sonneveld ME, de Haas M, Koeleman C, de Haan N, Zeerleder SS, Ligthart PC, et al. Patients with IgG1-anti-red blood cell autoantibodies show aberrant Fc-glycosylation. *Sci Rep.* 2017;7(1):8187.
20. Gudelj I, Lauc G, Pezer M. Immunoglobulin G glycosylation in aging and diseases. *Cell Immunol.* 2018;333:65-79.
21. Dekkers G, Rispens T, Vidarsson G. Novel Concepts of Altered Immunoglobulin G Galactosylation in Autoimmune Diseases. *Front Immunol.* 2018;9:553.
22. Fokink WJ, Selman MH, Dortland JR, Durmus B, Kuitwaard K, Huizinga R, et al. IgG Fc N-glycosylation in Guillain-Barre syndrome treated with immunoglobulins. *J Proteome Res.* 2014;13(3):1722-30.
23. Ogata S, Shimizu C, Franco A, Touma R, Kanegaye JT, Choudhury BP, et al. Treatment response in Kawasaki disease is associated with sialylation levels of endogenous but not therapeutic intravenous immunoglobulin G. *PLoS One.* 2013;8(12):e81448.
24. Schmidt DE, de Haan N, Sonneveld ME, Porcelijn L, van der Schoot CE, de Haas M, et al. IgG-Fc glycosylation before and after rituximab treatment in immune thrombocytopenia. *Sci Rep.* 2020;10(1):3051.

25. Kapur R, Della Valle L, Verhagen OJ, Hipgrave Ederveen A, Ligthart P, de Haas M, et al. Prophylactic anti-D preparations display variable decreases in Fc-fucosylation of anti-D. *Transfusion*. 2015;55(3):553-62.
26. Kapur R, Della Valle L, Sonneveld M, Hipgrave Ederveen A, Visser R, Ligthart P, et al. Low anti-RhD IgG-Fc-fucosylation in pregnancy: a new variable predicting severity in haemolytic disease of the fetus and newborn. *Br J Haematol*. 2014;166(6):936-45.
27. Evers D, van der Bom JG, Tijmens J, de Haas M, Middelburg RA, de Vooght KMK, et al. Absence of the spleen and the occurrence of primary red cell alloimmunization in humans. *Haematologica*. 2017;102(8):e289-e92.
28. Chakraborty S, Gonzalez J, Edwards K, Mallajosyula V, Buzzanco AS, Sherwood R, et al. Proinflammatory IgG Fc structures in patients with severe COVID-19. *Nat Immunol*. 2021;22(1):67-73.
29. Bournazos S, Vo HTM, Duong V, Auerswald H, Ly S, Sakuntabhai A, et al. Antibody fucosylation predicts disease severity in secondary dengue infection. *Science*. 2021;372(6546):1102-5.
30. Temming AR, de Taeye SW, de Graaf EL, de Neef LA, Dekkers G, Bruggeman CW, et al. Functional Attributes of Antibodies, Effector Cells, and Target Cells Affecting NK Cell-Mediated Antibody-Dependent Cellular Cytotoxicity. *J Immunol*. 2019;203(12):3126-35.
31. Ackerman ME, Mikhailova A, Brown EP, Dowell KG, Walker BD, Bailey-Kellogg C, et al. Polyfunctional HIV-Specific Antibody Responses Are Associated with Spontaneous HIV Control. *PLoS Pathog*. 2016;12(1):e1005315.
32. Rab MAE, Meerveld-Eggink A, van Velzen-Blad H, van Loon D, Rijkers GT, de Weerd O. Persistent changes in circulating white blood cell populations after splenectomy. *Int J Hematol*. 2018;107(2):157-65.
33. Zwaginga JJ, van der Holt B, Te Boekhorst PA, Biemond BJ, Levin MD, van der Griend R, et al. Multi-center randomized open label phase II trial on three rituximab dosing schemes in immune thrombocytopenia patients. *Haematologica*. 2015;100(3):e90-2.
34. Falck D, Jansen BC, de Haan N, Wuhler M. High-Throughput Analysis of IgG Fc Glycopeptides by LC-MS. *Methods Mol Biol*. 2017;1503:31-47.
35. Jansen BC, Falck D, de Haan N, Hipgrave Ederveen AL, Razdorov G, Lauc G, et al. LaCyTools: A Targeted Liquid Chromatography-Mass Spectrometry Data Processing Package for Relative Quantitation of Glycopeptides. *J Proteome Res*. 2016;15(7):2198-210.
36. Bondt A, Rombouts Y, Selman MH, Hensbergen PJ, Reiding KR, Hazes JM, et al. Immunoglobulin G (IgG) Fab glycosylation analysis using a new mass spectrometric high-throughput profiling method reveals pregnancy-associated changes. *Mol Cell Proteomics*. 2014;13(11):3029-39.
37. Wuhler M, Stavenhagen K, Koeleman CA, Selman MH, Harper L, Jacobs BC, et al. Skewed Fc glycosylation profiles of anti-proteinase 3 immunoglobulin G1 autoantibodies from granulomatosis with polyangiitis patients show low levels of bisection, galactosylation, and sialylation. *J Proteome Res*. 2015;14(4):1657-65.
38. Zauner G, Selman MH, Bondt A, Rombouts Y, Blank D, Deelder AM, et al. Glycoproteomic analysis of antibodies. *Mol Cell Proteomics*. 2013;12(4):856-65.
39. Vidarsson G, Dekkers G, Rispen T. IgG subclasses and allotypes: from structure to effector functions. *Front Immunol*. 2014;5:520.
40. Kapur R, Kustiawan I, Vestrhaim A, Koeleman CA, Visser R, Einarsdottir HK, et al. A prominent lack of IgG1-Fc fucosylation of platelet alloantibodies in pregnancy. *Blood*. 2014;123(4):471-80.
41. Vestrhaim AC, Moen A, Egge-Jacobsen W, Reubsæet L, Halvorsen TG, Bratlie DB, et al. A pilot study showing differences in glycosylation patterns of IgG subclasses induced by pneumococcal, meningococcal, and two types of influenza vaccines. *Immun Inflamm Dis*. 2014;2(2):76-91.
42. Plomp R, Bondt A, de Haan N, Rombouts Y, Wuhler M. Recent Advances in Clinical Glycoproteomics of Immunoglobulins (Igs). *Mol Cell Proteomics*. 2016;15(7):2217-28.
43. Sonneveld ME, Koeleman CAM, Plomp HR, Wuhler M, van der Schoot CE, Vidarsson G. Fc-Glycosylation in Human IgG1 and IgG3 Is Similar for Both Total and Anti-Red-Blood Cell Anti-K Antibodies. *Front Immunol*. 2018;9:129.
44. de Haan N, Reiding KR, Driessen G, van der Burg M, Wuhler M. Changes in Healthy Human IgG Fc-Glycosylation after Birth and during Early Childhood. *J Proteome Res*. 2016;15(6):1853-61.
45. Ferrara C, Grau S, Jager C, Sondermann P, Brunker P, Waldhauer I, et al. Unique carbohydrate-carbohydrate interactions are required for high affinity binding between FcγRIII and antibodies lacking core fucose. *Proc Natl Acad Sci U S A*. 2011;108(31):12669-74.
46. Kuwana M, Kawakami Y, Ikeda Y. Suppression of autoreactive T-cell response to glycoprotein IIb/IIIa by blockade of CD40/CD154 interaction: implications for treatment of immune thrombocytopenic purpura. *Blood*. 2003;101(2):621-3.
47. Swinkels M, Rijkers M, Voorberg J, Vidarsson G, Leebeek FWG, Jansen AJG. Emerging Concepts in Immune Thrombocytopenia. *Front Immunol*. 2018;9:880.

48. Ahmed R, Devasia AJ, Viswabandya A, Lakshmi KM, Abraham A, Karl S, et al. Long-term outcome following splenectomy for chronic and persistent immune thrombocytopenia (ITP) in adults and children : Splenectomy in ITP. *Ann Hematol.* 2016;95(9):1429-34.
49. Mahevas M, Patin P, Huetz F, Descatoire M, Cagnard N, Bole-Feysot C, et al. B cell depletion in immune thrombocytopenia reveals splenic long-lived plasma cells. *J Clin Invest.* 2013;123(1):432-42.
50. Aslam R, Kapur R, Segel GB, Guo L, Zufferey A, Ni H, et al. The spleen dictates platelet destruction, anti-platelet antibody production, and lymphocyte distribution patterns in a murine model of immune thrombocytopenia. *Exp Hematol.* 2016;44(10):924-30 e1.
51. Hoyer BF, Manz RA, Radbruch A, Hiepe F. Long-lived plasma cells and their contribution to autoimmunity. *Ann N Y Acad Sci.* 2005;1050:124-33.
52. Matsumoto A, Shikata K, Takeuchi F, Kojima N, Mizuochi T. Autoantibody activity of IgG rheumatoid factor increases with decreasing levels of galactosylation and sialylation. *J Biochem.* 2000;128(4):621-8.
53. Vadrevu SK, Trbojevic-Akmacic I, Kossenkov AV, Colomb F, Giron LB, Anzurez A, et al. Frontline Science: Plasma and immunoglobulin G galactosylation associate with HIV persistence during antiretroviral therapy. *J Leukoc Biol.* 2018;104(3):461-71.
54. Ho CH, Chien RN, Cheng PN, Liu JH, Liu CK, Su CS, et al. Aberrant serum immunoglobulin G glycosylation in chronic hepatitis B is associated with histological liver damage and reversible by antiviral therapy. *J Infect Dis.* 2015;211(1):115-24.
55. Martin TC, Simurina M, Zabczynska M, Martinic Kavur M, Rydlewska M, Pezer M, et al. Decreased Immunoglobulin G Core Fucosylation, A Player in Antibody-dependent Cell-mediated Cytotoxicity, is Associated with Autoimmune Thyroid Diseases. *Mol Cell Proteomics.* 2020;19(5):774-92.

- ¹ Center for Proteomics and Metabolomics, Leiden University Medical Center, Leiden, The Netherlands
- ² Glycoscience Research Laboratory, Genos Ltd., Zagreb, Croatia
- ³ Department of Pathology and Medical Biology, University Medical Center Groningen, Groningen, The Netherlands
- ⁴ Department of Nephrology, Department of Internal Medicine, University Medical Center Groningen, Groningen, The Netherlands
- ⁵ Department of Rheumatology and Clinical Immunology, University Medical Center Groningen, Groningen, The Netherlands



Chapter 3

Specific IgG glycosylation differences precede relapse in PR3-ANCA-associated vasculitis patients with and without ANCA rise

Iwona Wojcik^{1,2}, Manfred Wuhrer¹, Peter Heeringa³, Coen Stegeman⁴, Abraham Rutgers⁵,
David Falck¹

Reprinted and adapted with permission from

SFront Immunol. 2023 Sep 29;14:1214945. doi: 10.3389/fimmu.2023.1214945. PMID: 37841251;

PMCID: PMC10570725.

Copyright © 2023 Wojcik, Wuhrer, Heeringa, Stegeman, Rutgers and Falck.



3.1 ABSTRACT

Immunoglobulin G (IgG) contains a conserved N-glycan in the fragment crystallizable (Fc), modulating its structure and effector functions. In anti-neutrophil cytoplasmic antibody (ANCA)-associated vasculitis (AAV) alterations of IgG Fc-glycosylation have been observed to correlate with the disease course. Here, we examined longitudinal changes in N-linked Fc glycans of IgG in an AAV patient cohort and its relationship with disease flares. Using liquid chromatography coupled with mass spectrometry, we analysed IgG Fc-glycosylation in 410 longitudinal samples from 96 individuals with AAV. Analysis of the cross-sectional differences as well as longitudinal changes demonstrated that IgGs of relapsing PR3-ANCA patients have higher Δ Fc-bisection at diagnosis ($P = 0.004$) and exhibit a decrease in Fc-sialylation prior to the relapse ($P = 0.0004$), discriminating them from non-relapsing patients. Most importantly, PR3-ANCA patients who experienced an ANCA rise and relapsed shortly thereafter, exhibit lower IgG Fc-fucosylation levels compared to non-relapsing patients already 9 months before relapse ($P = 0.02$). Our data indicate that IgG Fc-bisection correlates with long-term treatment outcomes, while lower IgG Fc-fucosylation and sialylation associate with impending relapse. Overall, our study replicated the previously published reduction in total IgG Fc-sialylation at the time of relapse, but showed additionally that its onset precedes relapse. Furthermore, our findings on IgG fucosylation and bisection are entirely new. All these IgG Fc-glycosylation features may have the potential to predict a relapse either independently or in combination with known risk factors, such as a rise in ANCA titre.

3.2 INTRODUCTION

Anti-neutrophil cytoplasmic antibody (ANCA) – associated vasculitis (AAV) is a group of autoimmune inflammatory diseases comprising microscopic polyangiitis (MPA), eosinophilic granulomatosis with polyangiitis (EGPA) and granulomatosis with polyangiitis (GPA). AAV is characterized by necrotizing vasculitis of small to medium-sized vessels.(1) The worldwide annual incidence rate of these diseases is estimated at 10-30 per million, with a prevalence of 50-420 per million.(2) AAV is a disease that shifts between phases of remission and relapse. Active AAV can be brought into remission with strong-acting immunosuppressive medication. Once remission is achieved, medication is tapered, and maintenance therapy is started to prevent disease relapse. In general, maintenance therapy is stopped after 1-2 years. Disease relapses occur in 50% of patients within 5 years after the original diagnosis. Disease remission is defined by the absence of active disease manifestations. In contrast, patients are considered to relapse when symptoms of active vasculitis reoccur or new onset of the disease appears.(3)

A hallmark of this vascular disease is the presence of pathogenic ANCAs targeting cytoplasmic antigens expressed in the primary granules of neutrophils, either proteinase 3 (PR3) or myeloperoxidase (MPO). PR3-ANCAs are strongly associated with GPA, while MPO-ANCAs coincide strongly with MPA.(4, 5) ANCAs are mainly of the IgG isotype, predominantly of the IgG1 and IgG4 subclass, and the pathogenic potential of ANCAs has been repeatedly demonstrated in various animal models.(6, 7) Autoantibodies contribute to the development of AAV through the excessive activation of cytokine-primed neutrophils, accompanied by the release of reactive oxygen species, proteolytic enzymes, and neutrophil extracellular trap formation, leading to endothelial damage.(8) ANCAs activate by co-ligating antigens and Fc gamma receptors (FcγRs). The Fab portion of ANCAs binds PR3 or MPO antigens, translocated from the cytoplasmic granules to the cell surface, and the crystallizable fragment (Fc) portion binds FcγRs, FcγRIIIa, and/or FcγRIIIb.(9) IgG subclass or a post-translational modification could potentially influence the activation of the inflammatory mechanism, as they strongly modulate Fc-FcγR interaction.

Human IgG carries a pair of oligosaccharides attached to Asn297 in the C_H2 domain of the Fc portion. Typical IgG Fc N-glycans consist of a heptasaccharide N-glycan core (four N-acetylglucosamine and three mannose residues), which can be elongated with various monosaccharides, such as galactose, sialic acid, fucose, and bisecting N-acetylglucosamine (see Figure 1). Glycosylation of the Fc region, along with IgG subclass, has been found to modulate IgG effector functions.(10) Altered IgG Fc-glycosylation has been demonstrated in various autoimmune diseases, including AAV.(11, 12) Moreover, IgG Fc-glycosylation has been observed to reflect the inflammation status of the body, correlate with disease activity and predict clinical outcomes in many of them.(12)

Early diagnosis and accurate disease relapse prediction can greatly contribute to the prevention of disease-related organ damage and mortality in patients with AAV. Patient stratification aims to identify patients with a low and high risk of relapse to guide maintenance therapy, thereby reducing incidences of relapses, while minimizing treatment-related side effects.(13) Nowadays, diagnosis and relapse prediction are based on clinical manifestations, histology, and the serial measurements of ANCA titre.(14) The detection of a rise in ANCA titre during remission may predict future disease flares. However, many relapses may occur without a preceding ANCA rise and in some cases, a rise in ANCA titre is not followed by a relapse. On top of that, many differences in the definition of a rise in ANCA exist, influencing the usefulness of serial ANCA measurement and making comparisons between studies difficult.(15) Thus, while the pathogenic potential of ANCAs to activate the innate immune system, leading to vasculitic damage in AAV, is undisputable, an ANCA rise by itself has a modest value for predicting relapses.(16) Therefore, it is important to study other factors involved in the final autoimmune response to arrive at a multi-marker panel with a higher predictive value. IgG Fc-glycosylation status of the antibodies is a promising candidate because of its crucial impact on the key IgG effector functions.

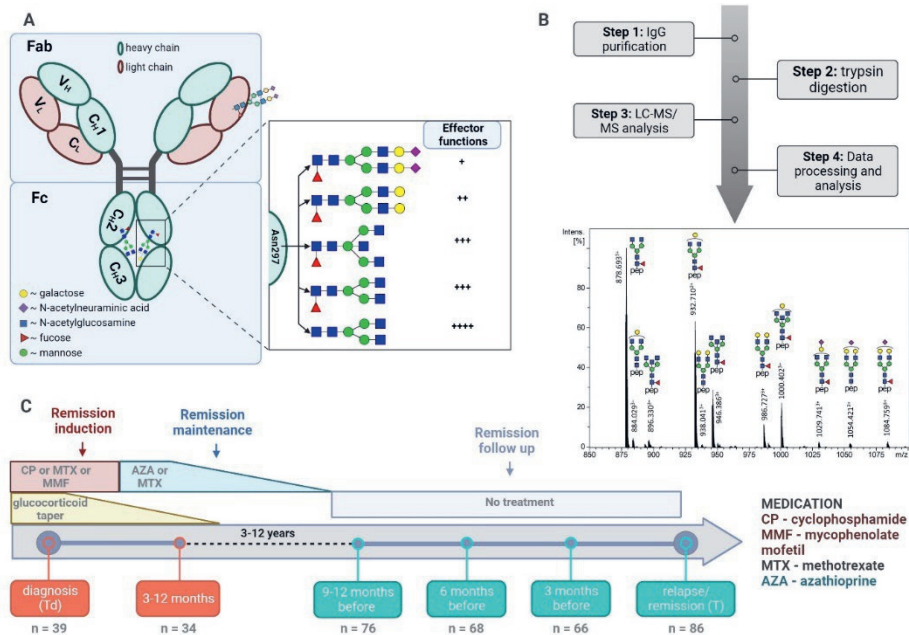


Figure 4. LC-MS analysis of total IgG Fc-glycopeptides. (A) Schematic representation of IgG N-glycosylation. The left side depicts IgG with the heavy γ chains (H) and light chains (L) composed of constant (C_H1 , C_H2 , C_H3 , C_L) and variable domains (V_H , V_L). The right side depicts the glycan features covalently attached to Asparagine 297 (Asn 297) and its implications on subsequent cellular effector functions mediated by binding to Fc receptors. (B) Schematic workflow with a representative LC-MS summed mass spectrum of IgG1 tryptic glycopeptides obtained from a 60 year-old female at the point of relapse. (C) Timeline of the study cohort. The analysed time points and number of samples analysed at each time point are specified. The major treatment regime applied in the current study is shown.(17)

Previous studies have investigated the glycosylation pattern of IgG and demonstrated significantly lower levels of IgG galactosylation in PR3-ANCA or MPO-ANCA compared to healthy individuals.(18-20) Moreover, in GPA patients, total IgG galactosylation has been shown to negatively correlate with the disease activity.(11) Kemna *et al.* have revealed that a low level of galactosylation and sialylation in total IgG predicts relapse.(21) Interestingly, glycosylation of the total serum antibody pool was a more powerful predictor than that of the ANCA antibodies themselves. These results suggest a potential for the total IgG Fc-glycosylation pattern as a prognostic marker to identify patients more prone to future relapse. Targeting such patients with more aggressive therapy could lead to a better disease prognosis while avoiding over-treatment of patients with a lower risk. Though previous studies indicated time-dependent and intra-individual differences, the longitudinal IgG Fc-glycosylation changes and their clinical relevance are insufficiently mapped, limiting the evaluation as a prognostic marker. Thus, the present work aimed to extensively characterise longitudinal changes of IgG Fc-glycosylation in a single-center AAV patient cohort by profiling changes in N-linked Fc glycans of total IgG in individual AAV patients by mass spectrometry.

3.3 EXPERIMENTAL SECTION

3.3.1 Patients Classification

For this study, 96 patients diagnosed with ANCA-AAV between 2003 and 2016 at the University Medical Groningen, were considered for inclusion. Patients were diagnosed with GPA or MPA according to the Chapel Hill Consensus Conference criteria,(1) and categorized as PR3-ANCA or MPO-ANCA based on ANCA-specificity determined using antigen specific enzyme-linked immunosorbent analysis. Disease activity states were characterized in accordance with the European League Against Rheumatism definitions. Clinical remission of the disease was defined as the absence of active vasculitic disease manifestations, with or without taking immunosuppressive therapy. In contrast, relapse was defined as the re-occurrence of symptoms or new onset of disease activity requiring augmentation of immunosuppressive therapy.(3) The severity of symptoms during the onset or reoccurrence of the disease was classified as “moderate” or “severe” based on the potential threat to organs or life.(3) Persistent positive or negative patients are defined as individuals who consistently maintain positive or negative status for ANCAs. Those initially positive, but transitioning to ANCA negativity following treatment and maintaining this negative status thereafter are classified as ANCA negative to positive patients.

All information on demographics, disease characteristics, treatment, as well as clinical outcome were collected into patient’s records according to the Dutch law on Medical Treatment Act (WGBO), the Persona Data Protection Act (Wbp), and the Code of Conduct for Health Research (Federa). Ethical approval for the study was obtained from the local Medical Ethical Committee of the University of Medical Center Groningen.

3.3.2 Measurement of ANCA and Detection of an ANCA Rise

ANCA-associated vasculitis patients were generally seen every 3 months for 2 to 3 years. At every follow-up visit, symptoms were evaluated and blood was drawn. After conversion to serum, PR3-ANCA or MPO-ANCA titres were quantified by fluorescent-enzyme immune assay on a Phadia ImmunoCAP 250 analyzer using EliA PR3S and EliA MPOS wells (Thermo Fisher Scientific, Waltham, MA).⁽²²⁾ A rise in ANCA titre was ascertained if the PR3- or MPO-ANCA level increased by at least 125% over a period of six months preceding a clinical relapse or time-matched remission.

3.3.3 Antibody Affinity Enrichment and Protease Treatment

Total IgG (IgG1, IgG2, IgG3, and IgG4) was affinity-purified and digested with trypsin in 96-well filter plates (0.7 mL wells, PE frit, Orochem, Naperville, IL) as described before.⁽²³⁾ Briefly, plasma samples (2 μ L) were diluted with 1xPBS (1:20 v/v) and applied on Protein G affinity beads (2 μ L; GE Healthcare, Uppsala, Sweden) for 1 hour with agitation. Captured IgGs were washed with 1xPBS and water (3 x 200 μ L), eluted with 100 mM FA (100 μ L) and dried in a centrifugal vacuum concentrator (Martin Christ Gefriertrocknungsanlagen GmbH, Osterode am Harz, Germany) at 50°C for approximately 2.5 h. Next, dried total IgG was dissolved by adding 0.25 mg/mL TPKK-treated trypsin (40 μ L) in 25 mM ammonium bicarbonate buffer (pH 8.0) and digested for 18 h at 37°C. Obtained IgG glycopeptides were stored at -20°C until the measurement.

3.3.4 Liquid Chromatography - Mass Spectrometry of Immunoglobulin Glycopeptides

The tryptic IgG glycopeptide separation was performed by an Ultimate 3000 HPLC nano-LC system (Thermo Fisher Scientific) as described previously.⁽²³⁾ (Glyco-)peptides (0.25 μ L) were concentrated on the trapping column (Acclaim PepMap100 C18, 5 mm x 300 μ m i.d., Thermo Fisher Scientific) and separated on the analytical column (nanoEase M/Z Peptide BEH C18, 100 mm x 75 μ m i.d., 1.7 μ m, 130 Å, 1/PK, Waters) in a linear gradient from 3% to 50% solvent B (95% acetonitrile) in 5.5 min. The separation system was coupled online by electrospray ionization (ESI) to a Maxis Impact HD quadrupole time-of-flight MS instrument (Bruker Daltonics, Bremen, Germany). The sample was nebulized and ionized in ion positive mode in a CaptiveSpray ESI source assisted by ACN-doped nitrogen gas from the nanoBooster (Bruker Daltonics). Mass spectra were acquired within a mass range m/z 550-1800 at a frequency of 1 Hz.

3.3.5 Data Analysis

The raw glycoproteomic LC-MS data were first manually inspected with Data Analysis (version 5.0; Bruker Daltonics). The separation method resulted in three subclass-specific IgG N-glycopeptide moieties that were assigned based on well-established migration orders of tryptic Fc-glycopeptides in reversed phase liquid chromatography, such as IgG1, IgG4 and

indistinguishable IgG2 and IgG3 (IgG1: EEQYNSTYR, IgG2/3: EEQFNSTFR, IgG4: EEQFNSTYR).(24, 25) Next, the LC-MS datasets were converted into the mzXML file format using MSConvert (ProteoWizard 3.0 suite). Each dataset was then automatically aligned, calibrated, and extracted using the software package LaCyTools as described previously,(26) with minor modifications in processing parameters (see **Table S1** for details). For targeted data extraction, a list of pre-defined analytes with theoretical m/z values was compiled on the basis of the literature (27) and completed by the manual annotation of summed spectra per patient group. After signal extraction, low-quality spectra with a total intensity or number of glycopeptides below a lower or above an upper threshold were discarded per subclass from further analysis. Lastly, analytes were selected based on quality control parameters provided by LaCyTools, including mass accuracy (within a ± 20 ppm range), signal to noise ratio (> 9), and isotopic pattern quality score (< 0.2). For all 37 glycopeptide species passing the analyte inclusion criteria (**Table S2**, 18 IgG1 glycoforms, 11 IgG2 glycoforms, 8 IgG4 glycoforms), relative intensities within each IgG subclass were obtained by integrating and summing signal intensities of doubly- and triply-protonated glycan species followed by normalization to the total signal intensity per IgG subclass. From the individual glycopeptides, four glycosylation traits were calculated (**Table S3**): galactosylation, fucosylation, bisection, and sialylation. Due to the overlap of m/z values of the minor afucosylated IgG4 glycopeptides with tailing and more abundant IgG1 fucosylated glycopeptide peaks, fucosylation levels for IgG4 were not quantified.

3.3.6 Statistical Analysis

All statistical analysis and data visualization were performed using R Statistical Software (version 4.1.3; R Core Team 2022) and RStudio (version 1.4.1717; RStudio, Boston, MA). Both age and sex have been shown to influence IgG glycosylation.(28) To focus on longitudinal changes and reduce the impact of such inter-individual differences, glycosylation was normalized within each individual to the final timepoint, being relapse or time-matched remission. Delta (Δ) values were calculated by subtracting IgG glycosylation levels at the time of relapse or time-matched remission – T(Rel) – from each time point of follow-up – Tx –, according to Formula 1. Pairwise comparison with a non-parametric Wilcoxon rank-sum test between relapsing and non-relapsing patients was used to determine differences in Δ glycosylation traits and relative intensities of the glycosylation traits in patients with an ANCA rise across all time points. A two-sided p-value was considered significant when below 0.05. For multiple testing correction, a 5% false discovery rate was applied throughout using the Benjamini-Hochberg method. An ANOVA F-test, comparing glm models with and without ANCA positivity, was used to assess the confounding effects of this feature. The Wilcoxon sign-ranked test was used to test changes within Δ glycosylation over time. Longitudinal glycosylation trait data were evaluated by means of Restricted Maximum Likelihood with the post-hoc Tukey test. Spearman's correlation was used to explore the association between IgG1, IgG2/3, and IgG4

glycosylation. The average coefficient of variation (CV) of the relative intensities was calculated in 94 replicate measurements of a pooled sample to further assess the quality of the data (**Figure S1**). A spread was measured by means of the interquartile range and the Kolmogorov-Smirnov test was used to determine differences in the distribution of the data.

$$\Delta = T_x - T(Rel) \quad (1)$$

3.4 RESULTS

In this study, we explored changes in total serum IgG Fc-glycosylation over the course of AAV treatment (see **Figure 1**). To this end, IgG was affinity-purified from 410 longitudinal samples collected from 89 individual patients. Of these 89 patients, 63 were PR3-positive and 26 were MPO-positive. The patient demographics and comprehensive cohort characteristics are presented in **Table 1**. IgG Fc-glycosylation profiles were determined by LC-MS glycopeptide analysis individually for IgG1 and IgG4 (tryptic peptides IgG1: EEQYNSTYR, IgG4: EEQFNSTYR), as well as collectively for IgG2 and IgG3 (shared peptide sequence EEQFNSTFR). LC-MS analysis allowed the identification of 18, 11, and 8 Fc-glycopeptides for IgG1, IgG2/3, and IgG4, respectively (**Table S2**). 94 replicates of a patient plasma pool demonstrated low technical variability. Average coefficient of variation (CV) was 6.5%, 7.2%, and 6.4% for IgG1, IgG2/3, and IgG4 glycopeptides, respectively (**Figure S1**). To reflect the various enzymatic steps involved in glycosylation, derived glycosylation traits, including galactosylation, sialylation, fucosylation and bisection, were calculated from individual glycoforms (**Table S3**). There was a strong correlation between derived traits of IgG1 and IgG2/3, as well as IgG4 in the study patients (**Figure S2**), indicating that all IgG subclasses follow the same general trend in glycosylation changes. Therefore, IgG2/3 and IgG4 data are shown in the **Supplemental data**.

3.4.1 Changes in IgG Fc-glycosylation

Differences in total IgG Fc-glycosylation relative to the timepoint of relapse or time-matched remission (Δ values) were observed between relapsing patients and patients in remission in GPA with PR3-ANCA or MPA with MPO-ANCA. At the time of diagnosis in GPA-PR3-ANCA patients, Δ IgG1 bisection of relapsing patients was higher than in non-relapsing patients (IgG1 0.8% vs. -3.9%; $P = 0.004$, **Table S4** and **Figure 2A**). A similar trend in medians was also found to a lower extent 9 to 12 months before relapse. These differences were not confounded by ANCA positivity as no significant differences between the glm models was observed. Bisection increased by 4.7% upon initial treatment in non-relapsing PR3-ANCA patients (**Figure S3D**). For these patients, the spread in Δ bisection ([IQR = $Q3 - Q1$] 4.42 vs. 1.53, $P = 0.0003$) appeared to be higher at diagnosis (Td) when compared to an early treatment phase, 3 to 12 months after diagnosis (Td+(3-12m)) (**Table S5**). Glycosylation data on IgG2/3 and IgG4 data are shown in the **Figure S4**.

Δ IgG1 sialylation of the GPA-PR3-ANCA relapsing patients was increased in the year leading up to the relapse and differed from non-relapsing patients at 6 months (and potentially at 3 months) before relapse (IgG1 0.6% vs. 0.0%; $P = 0.002$, 0.4% vs. -0.1%; $P = 0.044$, **Table S4** and **Figure 2D**). Also, these findings were not confounded by ANCA positivity. Moreover, the longitudinal analysis revealed a decrease in Δ IgG1 sialylation over 6 months preceding relapse ($P = 0.0004$, **Figure S3A**), whereas Δ IgG1 sialylation in non-relapsing patients remained constant. No differences between relapsing and non-relapsing GPA-PR3-ANCA patients were observed for Δ fucosylation and Δ galactosylation (**Figure 2B, C**).

Table 2. Patient characteristics of the study group.

	Total (n = 89)			
	MPO-ANCA		PR3-ANCA	
	Remission (n = 15)	Relapse (n = 11)	Remission (n = 42)	Relapse (n = 21)
Demographics				
Age (average in years + SD)	67 (17)	67 (12)	61 (12)	59 (15)
Male	9 (60%)	6 (55%)	16 (38%)	9 (43%)
Disease subtype				
GPA	0 (0%)	0 (0%)	42 (100%)	21 (100%)
MPA	15 (100%)	11 (100%)	0 (0%)	0 (0%)
ANCA^a				
Increase in titre	0 (0%)	3 (25%)	8 (20%)	13 (62%)
ANCA positivity				
Persistent ANCA positive	2 (16%)	4 (36%)	26 (62%)	18 (86%)
Persistent ANCA negative	11 (68%)	4 (21%)	9 (21%)	2 (9%)
Inconclusive data	2 (16%)	2 (43%)	7 (17%)	1 (5%)
Severity^b				
Moderate	2 (13%)	4 (36%)	3 (7%)	1 (5%)
Severe	13 (87%)	5 (46%)	32 (76%)	19 (90%)
No information	-	2 (18%)	7 (7%)	1 (5%)
Induction treatment^c				
Glucocorticoid therapy (GC)	2 (13%)	0 (0%)	4 (10%)	-
Cyclophosphamide + GC	10 (67%)	5 (46%)	29 (69%)	13 (62%)
Mofetil mycophenolate (MMF) + GC	3 (20%)	1 (9%)	3 (7%)	6 (28%)
Methotrexate (MTX) + GC	-	2 (18%)	-	1 (5%)
Rituximab (RTX) + GC	-	1 (9%)	-	-
No information		2 (18%)	6 (14%)	1 (5%)
Organ involvement^d				
Ear, nose, throat	2 (13%)	1 (9%)	32 (76%)	19 (90%)
Lung	7 (47%)	3 (27%)	22 (52%)	20 (95%)
Renal	13 (87%)	7 (64%)	22 (52%)	15 (71%)
No information		3 (27%)	6 (14%)	1 (5%)

Abbreviations: SD, standard deviation

^a A rise in ANCA titre preceding relapse determined using a highly sensitive capture enzyme-linked immunosorbent assay (ELISA)

^b Severity of symptoms at previous disease flare (diagnosis or any previous relapse)(3)

^c Medication scheme used to induce remission

^d Organ-threatening manifestation of disease at previous disease flare (diagnosis or any previous relapse)

Sialylation and galactosylation of both IgG1 and IgG2/3 showed a negative correlation with the level of PR3-ANCAs (IU/mL) in the plasma of relapsing patients (**Figure S5A, B, E, F**). In contrast, the levels of bisection of both IgG1 and IgG2/3 showed a positive relationship with the PR3-ANCA concentration in relapsing GPA patients (**Figure S5D, H**). Regression analysis of IgG4 galactosylation as well as the sialylation versus PR3-ANCA titre did not show an ANCA titre dependence (**Figure S5I, J**).

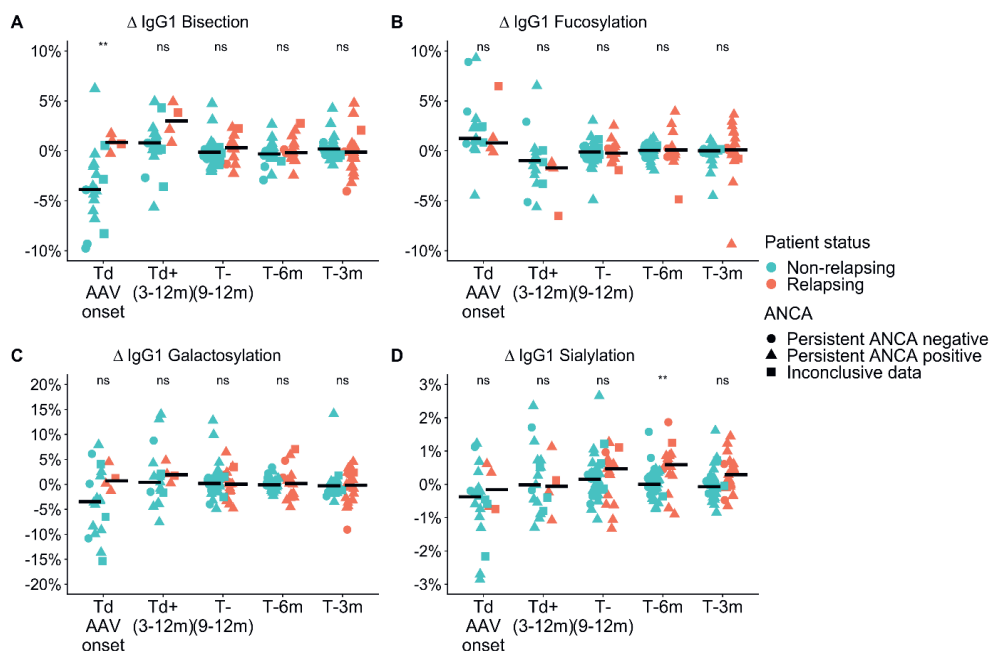


Figure 5. Cross-sectional differences in IgG1 glycosylation features for GPA-PR3-ANCA patients. Differences compared to the point of relapse or time-matched remission are displayed as Δ values, separately for patients who either relapsed (orange) or stayed in remission (green). The shapes represent patients who are persistently ANCA positive (circle), persistently ANCA negative (triangle), or show inconclusive results (square). Time points range from disease diagnosis (Td AAV onset), and 3-12 months after diagnosis (Td+(3-12m)), to 9-12 months (T-(9-12m)), 6 months (T-6m), and 3 months (T-3m) before relapse or time-matched during remission. Median values are indicated by black horizontal bars. A Wilcoxon signed-rank test was used to compare IgG1 glycosylation traits. Findings are indicated by two asterisks ($p < 0.005$); ns, not significant (see also Table S4). An ANOVA F-test showed that these findings were independent of ANCA positivity.

Conversely, relapsing MPA-MPO-ANCA patients showed a trend towards a more pronounced lowering in Δ bisection at diagnosis compared to non-relapsing patients (IgG1 - 3.5% vs. -1.05% **Table S6** and **Figure S6A**). Subsequently, relapsing MPA-MPO-ANCA patients experienced an increase in Δ bisection by 3.9% up to the second follow-up (**Figure S7**; $P = 0.002$). Notably, the Δ sialylation effects are not observed for the MPA-MPO-ANCA group (**Figures S6D**). Δ fucosylation, as well as Δ galactosylation of the IgG Fc glycoforms, did not

differ during the course of disease treatment between relapsing and non-relapsing MPA-MPO-ANCA patients (**Figures S6B, C**).

There were no correlations between IgG1, IgG2/3, and IgG4 glycosylation traits and MPO-ANCA titre MPA-MPO-ANCA patients (**Figure S8**).

3.4.2 IgG Fc-glycosylation changes associate with an ANCA rise

We separately analysed a subset of GPA-PR3-ANCA patients who experienced an ANCA rise that was defined as at least 125% elevation in ANCA level relative to the previous titre measurement (**see Figure 3**). Only in the subset of GPA-PR3-ANCA patients with an ANCA rise, relapsing patients showed a lower fucosylation compared to patients in remission in the year before relapse (T-9 months 91.6% vs. 94.6%, $P = 0.02$; T-6 months 91.6% vs. 94.2%, $P = 0.01$; T-3 months 91.7% vs. 95.0%, $P = 0.02$) and at the point of relapse or time-matched during remission (91.9% vs. 94.4% $P = 0.02$) (**Figure 4, Table S7**). Neither bisection, galactosylation, nor sialylation differed between patients relapsing or in remission (**Figure S9A-C**). Longitudinal changes were not appreciated at all (**Figure S10**).

Interestingly, the IgG fucosylation difference in GPA-PR3-ANCA patients between relapsing patients and patients in remission was limited to patients with an ANCA rise. It did not emerge in patients without an ANCA rise (**Figure S11B**) nor when looking at the whole GPA-PR3-ANCA patient group (**Figure 2B**), even though patients experiencing an ANCA rise were in the majority.

RELATIVE VALUES	PR3 & MPO-positive patients					
	PR3			MPO		
	ANCA rise	no ANCA rise	all	ANCA rise	no ANCA rise	all
Δ VALUES						
IgG1-Fc bisection	Figure S9A Figure S10	Figure S11A	Figure 2A Figure S3D	-	-	Figure S6A Figure S7
IgG1-Fc fucosylation	Figure 4 Figure S10	Figure S11B	Figure 2B	-	-	Figure S6B
IgG1-Fc galactosylation	Figure S9B Figure S10	Figure S11C	Figure 2C	-	-	Figure S6C
IgG1-Fc sialylation	Figure S9C Figure S10	Figure S11D	Figure 2D Figure S3A	-	-	Figure S6D

Figure 6. Figure layout of the IgG glycosylation analyses for GPA-PR3-ANCA and MPA-MPO-ANCA patients with and without an ANCA rise. Cells are colored based on the IgG glycosylation values (Blue rectangles correspond to the analysis based on relative levels of IgG glycosylation, while green rectangles correspond to Δ values). Dark colors indicate figures with statistically significant findings, longitudinally (Figures S3, 7, 10,) or between relapsing and non-relapsing patients (other figures).

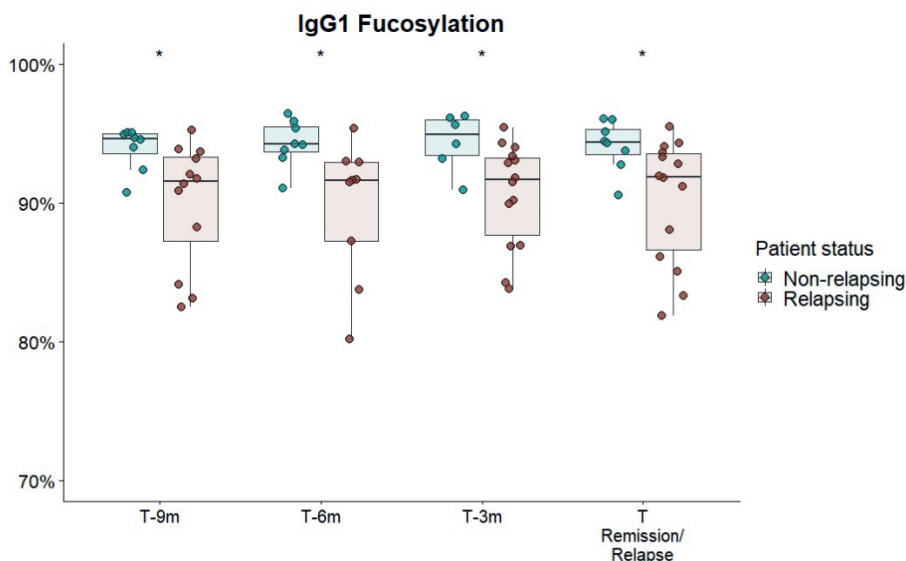


Figure 7. Cross-sectional differences in IgG1 Fc-fucosylation for GPA-PR3-ANCA patients with an ANCA rise. Total serum IgG1 fucosylation of GPA-PR3-ANCA patients who either relapse (brown) or stayed in remission (green), was compared at 9 months, 6 months before, 3 month before and at the time of relapse or time-matched points during remission. A Wilcoxon signed-rank test was used to compare IgG1 glycopeptide traits. * T-6m is a finding after multiple testing correction ($p=0.011$; see Table S7). However, since there is an according trend in all timepoints ($p=0.02$), the probability of the trends being false negative findings (should they be excluded) is more than 99.99%.

3.5 DISCUSSION

GPA and MPA are distinct disease subtypes, but are highly associated with PR3- and MPO-ANCA, respectively. Previous studies additionally indicated that PR3-ANCA and MPO-ANCA-associated diseases are significantly different.(29, 30). Consequently, we analysed data from GPA-PR3-ANCA and MPA-MPO-ANCA patients separately throughout this investigation. Our study indicates distinct cross-sectional differences in IgG Fc-glycosylation between GPA-PR3-ANCA and MPA-MPO-ANCA patients. Unfortunately, we are not able to determine whether the disease subtype or ANCA-type is dominant in these differences. Comparing relapsing with non-relapsing patients, GPA-PR3-ANCA patients exhibited a higher degree of Δ IgG1 bisection at diagnosis, while MPA-MPO-ANCA patients showed a trend towards a lower degree of Δ IgG1 bisection if they would relapse (**Figure 2 and Figure S6**). The trend in MPA-MPO-ANCA patients is confirmed by an increase in Δ IgG1 bisection from diagnosis to 9 to 12-month follow-up in relapsing patients which is not observed in non-relapsing patients (Figure S7). Δ IgG1 sialylation only associated with relapse in GPA-PR3-ANCA, but not in MPA-MPO-ANCA patients (**Figure 2 and Figure S6**).

In our study, the focus on total serum IgG Fc-glycosylation is justified by the stronger associations with relapse, as compared to ANCA glycosylation, demonstrated previously.(21) A cross-sectional comparison revealed that Δ IgG1 bisection and Δ IgG1

sialylation of total serum IgG Fc N-glycans differed between GPA-PR3-ANCA patients who relapsed and those who stayed in remission (**Figure 2**). Interestingly, while bisection differed mainly at the time of diagnosis, sialylation only differed in the year leading up to relapse. Accordingly, the longitudinal analysis showed that a decrease in sialylation precedes relapse in GPA-PR3-ANCA patients, while there are no changes in sialylation for non-relapsing patients. (**Figure S3**). Similarly, Kemna *et al.* showed a reduction in sialylation at relapse compared to an ANCA-rise time point, whereas patients who stayed in remission had unchanged sialylation levels.(21) Our analysis replicates this finding, but additionally demonstrates that the reduction starts before the reoccurrence of symptoms. Moreover, sialylation negatively correlated with the level of pathogenic PR3-ANCA titre in relapsing GPA patients (**Figure S5**). Reduced sialylation indicates a general inflammatory environment which may be the cause and/or effect of enhanced antibody production.(31) Thus, a longitudinal reduction in total IgG Fc-sialylation may be a potential clinical marker of relapse risk. Sialylation on IgG has been reported to have anti-inflammatory potential through a shift in IgG conformation, preventing the antibody from binding to activating type I Fc receptors and C1q protein and enabling interaction with type II Fc receptors DC-SIGN and CD23, which in turn induces the loss of the cytotoxic capability and FcγR-mediated anti-inflammatory activities, respectively.(32-34) Lower amounts of sialylated IgGs during inflammation have further been correlated with enhanced activity of autoimmune diseases, including GPA.(11, 21) Intriguingly, this potential marker may thus be directly involved in the disease mechanism. It has been suggested that a higher sialylation could counterbalance the autoimmune cascade induced by ANCA, and a subsequent shift towards a lower degree of sialylated IgGs would reduce its protective anti-inflammatory effect, possibly contributing to disease reactivation.(21) Therefore, we speculate that IgG Fc-sialylation could be used for monitoring relapse risk in patients with PR3-AAV. Longitudinal monitoring of the patient's level of IgG Fc-sialylation and detecting its drop, could aid in initiating appropriate treatment to prevent disease recurrence. Such clinical marker guided preemptive therapy could prevent further damage to the patient's vasculature. However, more data – ideally with an even higher time-resolution – would be needed to conclude whether sialylation changes occur sufficiently early prior to relapse to be of diagnostic value. We did not observe any differences in IgG Fc-galactosylation, which contradicts previous reports.(18, 21) For example, Lardinois *et al.* showed that terminal galactose was reduced in GPA-PR3-ANCA patients with active disease compared to patients in remission.(18) Moreover, Kemna *et al.* revealed a reduced galactosylation and sialylation in total IgG Fc of relapsing patients compared to non-relapsing patients.(21) However, their cohort was focused exclusively on GPA patients with PR3-ANCA experiencing an ANCA rise, which means that our study is likely underpowered regarding this very specific finding. Due to the complexity of AAV, for example in antigen specificity, definitions of an ANCA rise and disease phenotype, differences between studies in terms of study design, clinical cohort

characteristics, and the definition of the relapse and an ANCA rise, have to be carefully considered when comparing them and may explain observed differences.

This study identified, for the first time, a persistently lowered IgG Fc-fucosylation as a feature of relapsing GPA-PR3-ANCA patients experiencing an ANCA rise, discriminating them from non-relapsing ones (**Figure 4**). Interestingly, no differences in IgG1 fucosylation were observed for relapsing patients without a preceding rise in the ANCA titre (**Figure S11**). This may indicate differences in pathological mechanisms between AAV patients with and without an ANCA rise. These observations lead us to speculate on the potential utility of differences in IgG Fc-fucosylation as an orthogonal biomarker, enhancing the specificity of ANCA rise in clinical practice for predicting relapse. Importantly, differences in IgG Fc-fucosylation between relapsing and non-relapsing patients can be detected as early as nine months prior relapse if a rise in ANCA titer was also observed. Consequently, an ANCA rise and IgG Fc-fucosylation could potentially be integrated into a multiplex biomarker platform. Due to the limited number of MPA-MPO-ANCA patients, the study was underpowered to detect differences within the MPA-MPO-ANCA vasculitis patient population who experienced an ANCA rise. A predominantly afucosylated IgG response may occur naturally during the B-cell immune responses and has been mostly found for antigen-specific IgG1 against enveloped viruses and intracellular parasites, as well as for IgG1 alloantibodies causing fetal and neonatal alloimmune thrombocytopenia and hemolytic disease of the fetus and newborn.(35-37) Since afucosylated IgG1 seem to be specific for membrane-bound antigens (36) and PR3-/MPO-antigens are found on neutrophil plasma membranes in AAV,(9, 38) afucosylated IgG responses could be present in AAV. Though other factors will likely contribute to the observed differences in afucosylation, the association with an ANCA rise would suggest that such afucosylated autoantibody responses may be a relevant risk factor for relapse. However, Kemna et al. observed high fucosylation of PR3-ANCA antibodies.(21) Thus, the observed afucosylation differences are more likely due to changes in IgGs of other specificities (non-autoantigen specific IgG). The same immune activation, which leads to increased production of PR3-ANCA, could specifically stimulate B cells with a low fucosylation programming to differentiate and produce predominantly afucosylated antibodies. Such preferential co-activation of afucosylated antibody producing cells could, for example, result from the co-localization of antibody producing cells in the spleen.(39) Another explanation would be a globally altered regulation of Fc-fucosylation, for example changes in cytokine composition in the B cell microenvironment,(40, 41) initiated by an increased activity of inflammatory processes. Non-autoantigen specific IgG might be more affected by these changes, as it already has a higher propensity for afucosylated responses than PR3-ANCA.

IgG Fc-fucosylation has been shown to have a significant impact on IgG effector functions by sterically disturbing the interaction between the Fc region and FcγRIIIa/b, a receptor expressed on various effector cells. Thus, fucosylation may act as a safety switch hampering

potentially harmful cellular immune functions.(42, 43) It has been shown that ANCAs bind to and activate neutrophils and monocytes by initial Fab binding to MPO or PR3 expressed on the cell surface and subsequent Fc binding to FcγRs (FcγRIIa and FcγRIIb), which induces neutrophil and monocyte activation leading to endothelial cell death and inflammation.(44, 45) The complete removal of the Fc N-glycans has been shown to attenuate FcγRIIb-mediated neutrophil respiratory burst and degranulation whilst reducing the disease progression.(46) The importance of the IgG Fc-FcγRIIb interaction for the disease progression of AAV has also been evidenced by the association of the FcγRIIb-NA1 allele with the development of severe renal disease.(47) Moreover, as reported in studies involving therapeutic antibodies, decreased levels of IgG Fc-fucosylation induced a more rapid inflammatory cytokine release and cell activation.(48) As opposed to afucosylation of ANCA IgG, afucosylation of IgG with other specificities (aspecific IgG) will also have anti-inflammatory effects. Monomeric, afucosylated, aspecific IgG will compete with the ANCA immune complexes for FcγRIII-binding. Since monomeric IgG will not activate receptor signaling, this competition should reduce FcγRIII-dependent pro-inflammatory signaling.(49) While the lower fucosylation of aspecific IgG could be a bystander effect of differences in general inflammation, it may also affect the disease mechanism of ANCA-AAV by reducing the interaction between PR3-ANCA and activating FcγRs on neutrophils.

We revealed a markedly lower bisection for non-relapsing GPA-PR3-ANCA patients at diagnosis (**Figure 1**). Moreover, the longitudinal analysis demonstrated a 4.7% increase in bisection between diagnosis and first follow-up for non-relapsing GPA-PR3-ANCA patients (**Figure S3**). This is likely due to treatment effects. Interestingly, we found that the cross-sectional differences, as well as longitudinal changes, reversed for MPA-MPO-ANCA patients, where relapsing patients showed a trend towards lower bisection at diagnosis followed by a significant increase in bisection up to the second follow-up (**Figure S6 and Figure S7**). We hypothesize that the treatment effect observed for bisection could be useful to screen patients for their risk of relapse. However, due to the limited number of available samples for GPA-PR3-ANCA patients at early time points, the discriminative potential of bisection needs further justification. The current understanding of the functional relevance of IgG Fc-bisection is limited. At least for the complement activation and FcγR-mediated effector functions no significant impact of the observed differences would be expected.(50) However, IgG Fc-bisection plays a role in other aspects, such as higher-order protein structure and stability.(51)

IgG Fc-glycosylation trades of IgG2/3 subclasses showed a high correlation with IgG1 and consistent effects to those observed for IgG1. This indicates that alteration of IgG Fc-glycosylation is most likely a common event in all IgG subclasses, perhaps as a result of an identical stimulation of IgG-secreting plasma cells.

The limitations of this study include the absence of glycosylation analysis of anti-PR3 and anti-MPO specific antibodies. Ultimately, only a direct analysis of autoantibody glycosylation would confirm or exclude afucosylated ANCA responses in AAV. Importantly, this does not limit the clinical relevance of our study, as total serum IgG Fc-glycosylation has demonstrated superior performance as a potential clinical marker.(21) Another limitation of the study is the sample collection, where not all 89 AAV patients were sampled on six occasions from diagnosis to relapse or time-matched remission, leading to missing time points and temporal spread of the time points. The statistical analysis of relatively small groups of patients constitutes another limitation of the study. However, this is strongly mitigated by the longitudinal setup of the cohort. The possibility to partially correct for inter-individual differences in the longitudinal analyses and the repeated observation of the same cross-sectional differences at different time points greatly enhance the statistical confidence in our findings. Nonetheless, for novel findings, which are not a validation or extension of previous studies, external validation with a larger cohort would be prudent to evaluate if these glycosylation differences also enable relapse risk stratification.

In conclusion, our study confirmed several IgG Fc-glycosylation features that may have the potential to predict relapse either independently or in combination with known risk factors. We were able to replicate the reduced IgG Fc-sialylation at relapse reported by Kemna et al. Importantly, we have additionally demonstrated that this gradual decrease in IgG Fc-sialylation happens over a period of six months and could be detected before relapse occurs, irrespective of the rise in ANCA titre. Our study has revealed previously unreported associations with IgG Fc-fucosylation and IgG Fc-bisection as well. Namely, increased afucosylation in combination with an ANCA rise correlated with relapse risk. This correlation might originate from and/or contribute to enhanced inflammation in the wake of a rise in ANCA titre which ultimately leads to relapse. Moreover, our results have indicated changes in IgG Fc-bisection that accompany treatment. Bisection thus correlates with long-term treatment outcomes, while fucosylation and sialylation associate with impending relapse. Consequently, all these features might be used to develop novel predictors of relapse risk.

3.6 ACKNOWLEDGMENTS

We thank Oleg Mayboroda for discussions on statistical analysis.

3.7 SUPPLEMENTARY MATERIAL

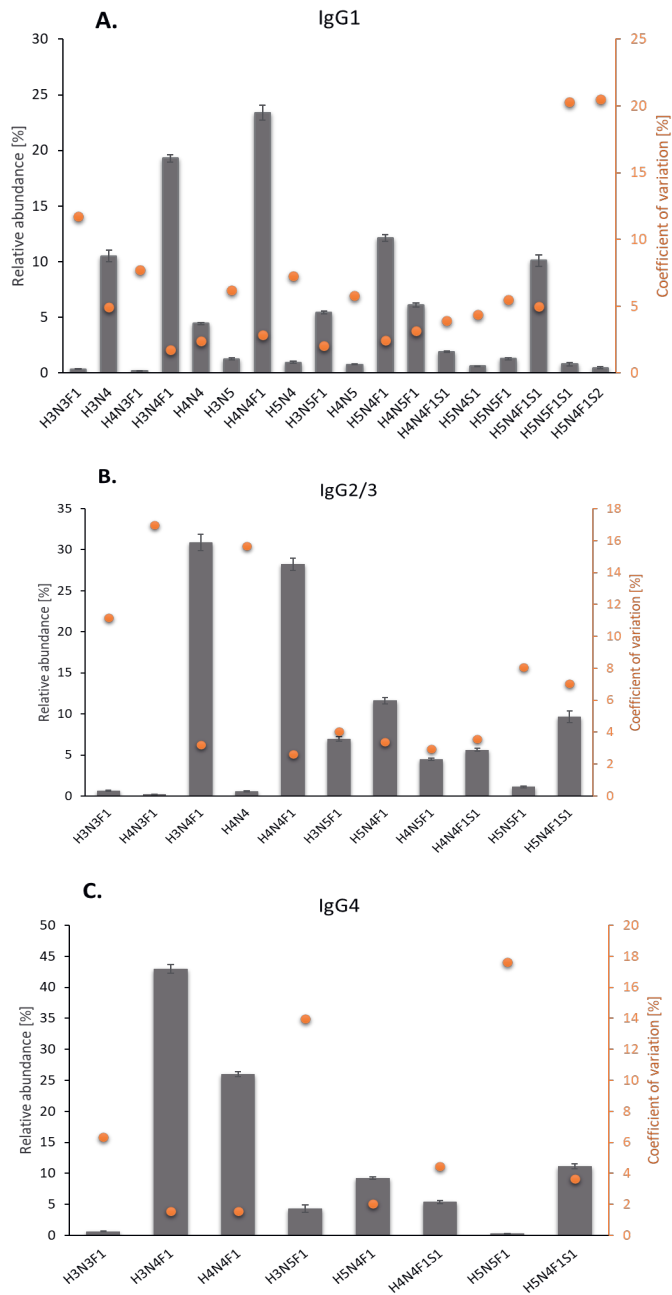
A complete overview of the supplementary material is available online at <https://www.frontiersin.org/articles/10.3389/fimmu.2023.1214945/full#B21>.

Supplementary Table 2. Compositions of human IgG Fc glycans quantified by nano-LC-ESI-MS and the theoretical *m/z* values corresponding to the most abundant isotopologue of tryptic glycopeptides.

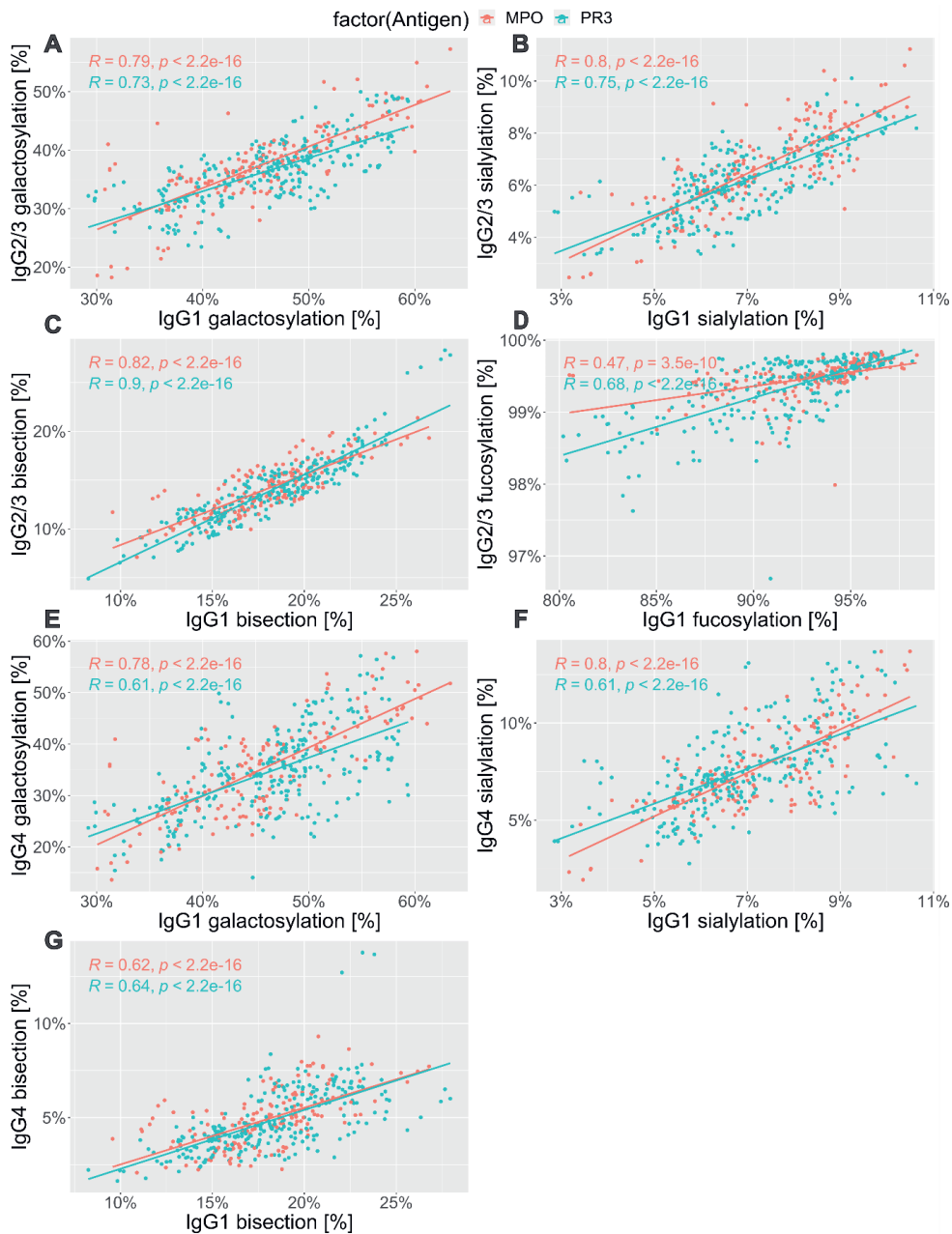
Glycan composition	Alternative nomenclature	Proposed structure	IgG1 P01857*		IgG2 P01859*		IgG4 P01861*	
			[M+2H] ²⁺	[M+3H] ³⁺	[M+2H] ²⁺	[M+3H] ³⁺	[M+2H] ²⁺	[M+3H] ³⁺
H3N4	G0		1244.50	830.00				
H3N5	G0N		1346.04	897.69				
H4N4	G1		1325.52	884.02	1309.53	873.36		
H4N5	G1N		1427.06	951.71				
H5N4	G2		1406.55	938.04				
H3N3F1	G0FN		1215.99	810.99	1199.99	800.33	1207.99	805.66
H4N3F1	G1FN		1297.01	865.01	1281.02	854.35		
H3N4F1	G0F		1317.53	878.69*	1301.53	868.02*	1309.53	873.36*
H4N4F1	G1F		1398.55	932.70*	1382.56	922.04*	1390.56	927.37*
H5N4F1	G2F		1479.58	986.72	1463.58	976.06	1471.58	981.39
H3N5F1	G0FN		1419.07	946.38	1403.07	935.72	1411.07	941.05
H4N5F1	G1FN		1500.09	1000.40	1484.10	989.73		
H5N5F1	G2FN		1581.12	1054.42	1565.12	1043.75	1573.12	1049.08
H5N4S1	G2S		1552.10	1035.07				
H4N4F1S1	G1FS		1544.10	1029.74	1528.11	1019.07	1536.10	1024.40
H5N4F1S1	G2FS		1625.13	1083.75*	1609.13	1073.09*	1617.13	1078.42*
H5N4F1S2	G2FS2		1770.67	1180.79				
H5N5F1S1	G2FNS		1726.67	1151.45				

(*) Glycan compositions used for alignment

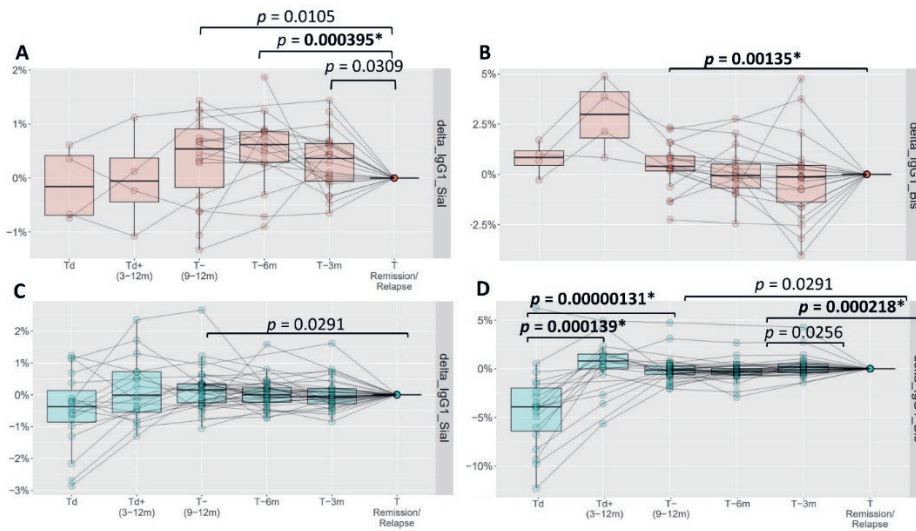
(bold) Glycan structural feature used for calibration.



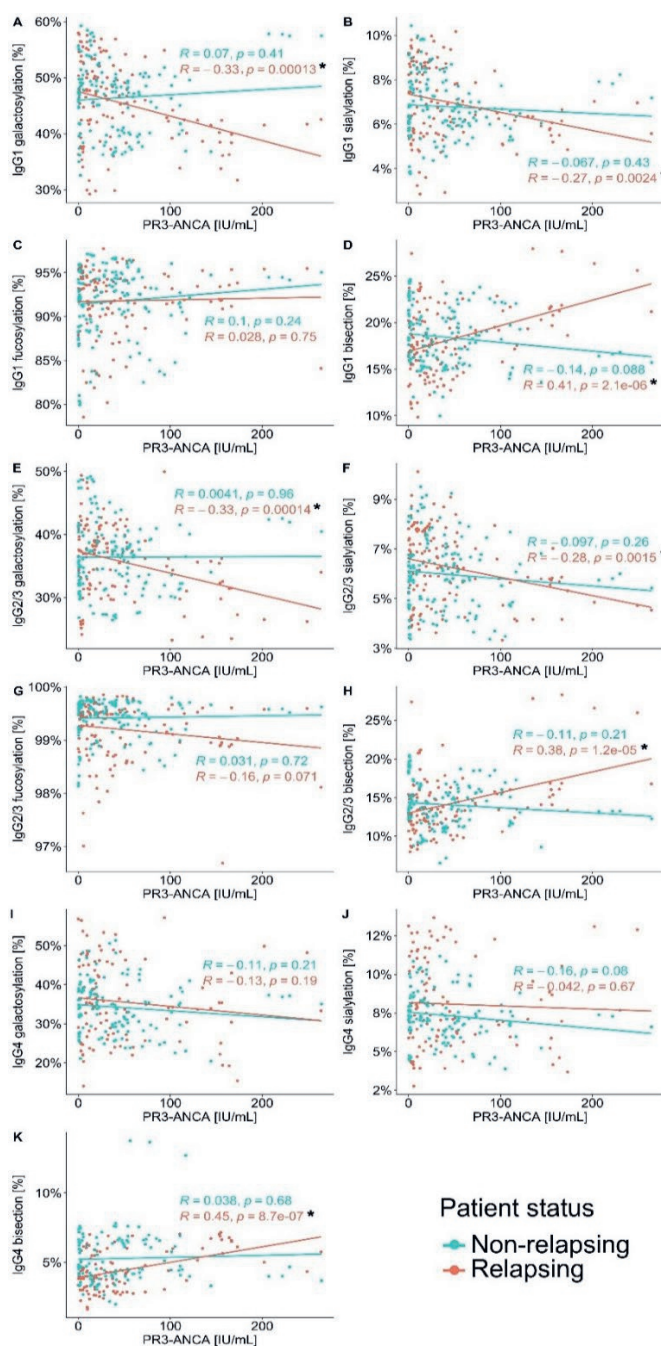
Supplementary Figure 1. Technical variability. Average and coefficient of variation of relative abundances of (A) IgG1, (B) IgG2/3 and (C) IgG4 glycopeptides from 94 replicates of a pooled plasma sample. A median coefficient of variation of 6.5%, 7.2% and 6.4% was observed for IgG1, IgG2/3 and IgG4, respectively. The error bars represent the standard deviation of the mean.



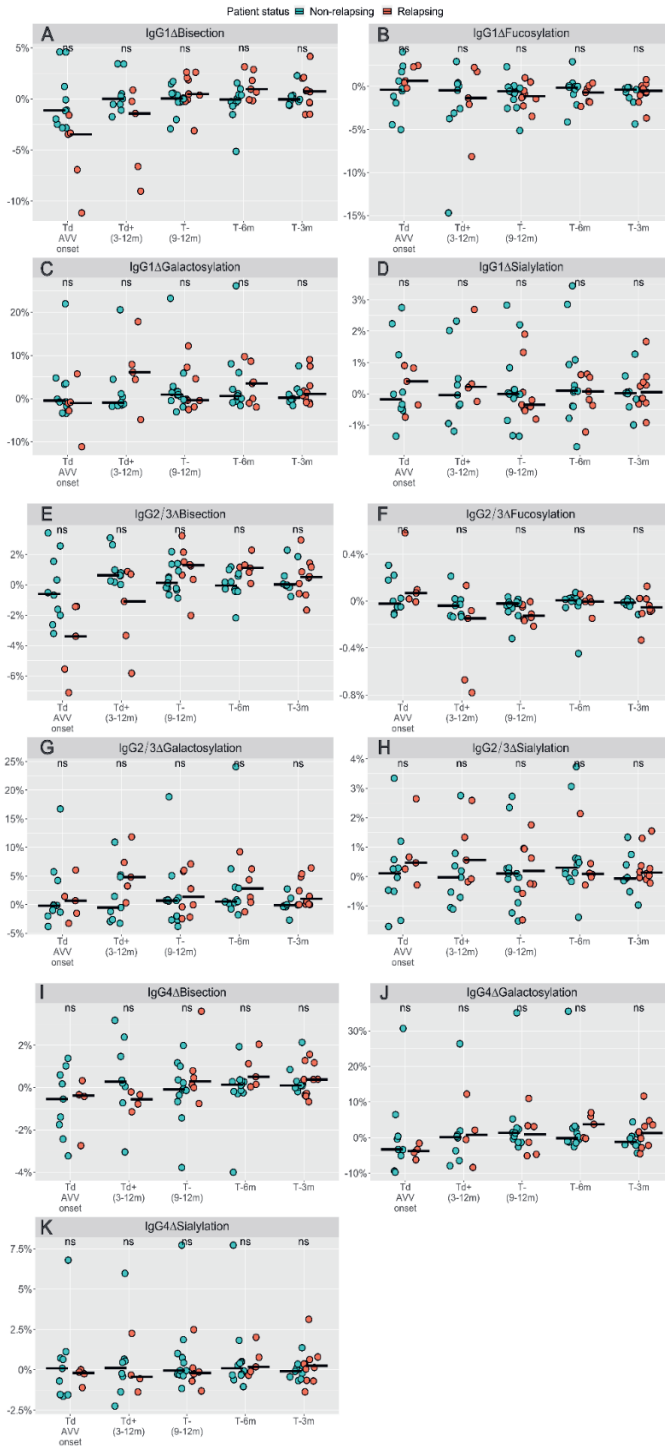
Supplementary Figure 2. Correlation analysis between IgG1 and IgG2/3 Fc (A-D), as well as IgG1 and IgG4 (E-G) Fc glycosylation traits. Data are shown for the regression analysis of the galactosylation, sialylation, bisection, and fucosylation (only for IgG1 and IgG2/3). Spearman's correlation coefficient and *p* values are shown for MPO- and PR3-ANCA separately.



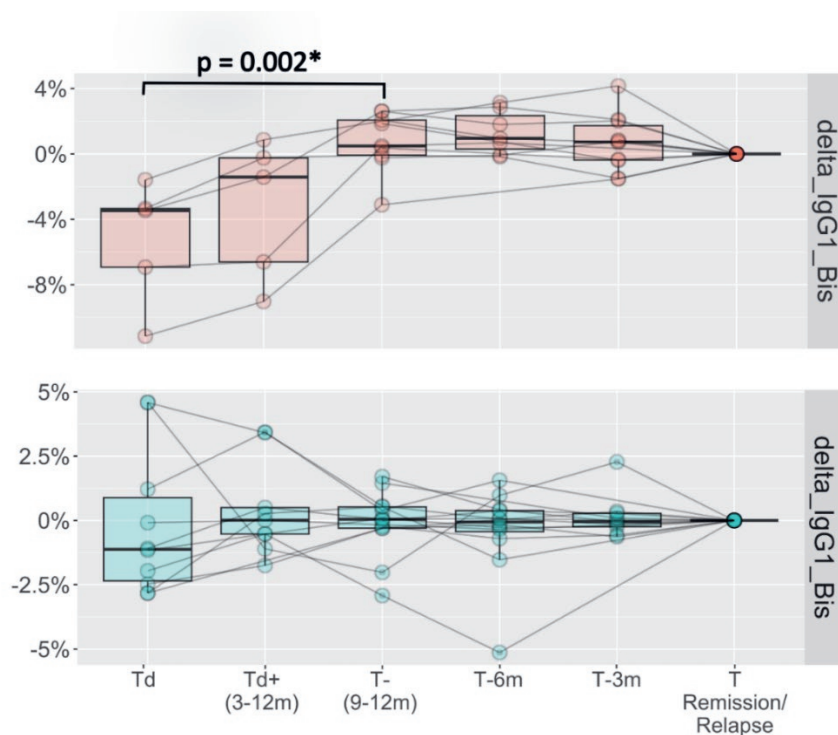
Supplementary Figure 3. Longitudinal changes in Δ IgG1-Fc sialylation (A, C) and Δ IgG1-Fc bisection (B, D) in PR3-positive patients. Differences compared to the point of relapse or time-matched remission are displayed as Δ values, separately for patients who either relapsed (upper panel in red) or stayed in remission (lower panel in green). Significant differences ($p < 0.0035$) are marked with asterisk *. For relapsing patients note: Td and Td+(3-12m) could not be analyzed due to a lack of power.



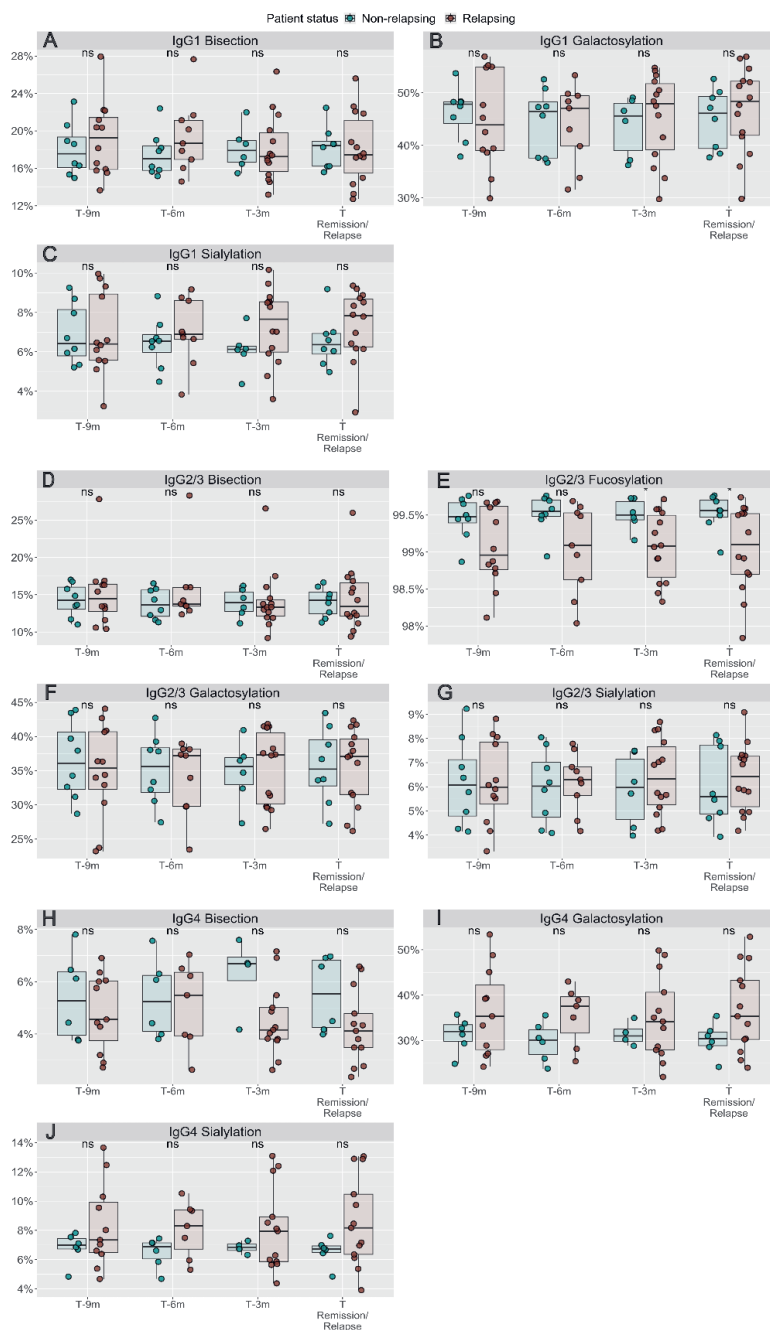
Supplementary Figure 5. Correlation analysis between the level of PR3-ANCA titer and IgG glycosylation. Regression analysis was done for IgG Fc-galactosylation, sialylation, fucosylation, and bisection of IgG1 (A-D), IgG2/3 (D-H), IgG4 (I-K), respectively, versus PR3-ANCA titer. Spearman's correlation coefficient and p values are shown for non-relapsing and relapsing PR3-positive patients separately. Significant differences are indicated by one asterisk ($p < 0.05$).



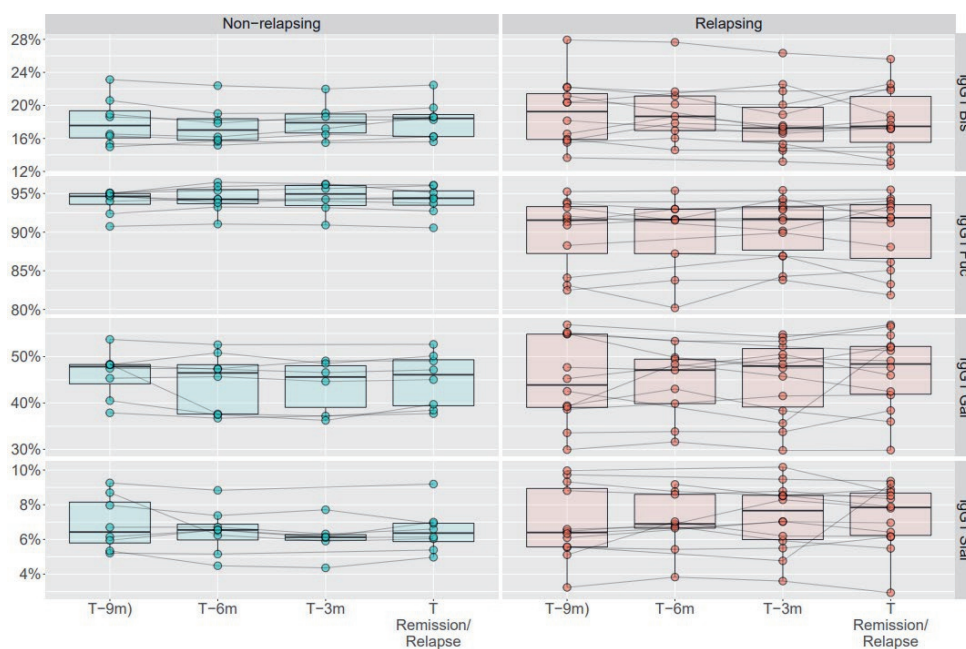
Supplementary Figure 6. Cross-sectional differences in Δ IgG1 (A-D), Δ IgG2/3 (E-F), Δ IgG4 (I-K) Fc glycosylation traits (bisection, fucosylation, galactosylation, and sialylation) for MPO-ANCA patients. Differences compared to the point of relapse or time-matched remission are displayed as Δ values, separately for patients who either relapsed (orange) or stayed in remission (green). Time points range from disease diagnosis (Td AVV onset), and 3-12 months after diagnosis (Td+(3-12m)), 9-12 months (T-(9-12m)), 6 months (T-6m), and 3 months (T-3m) before relapse or time-matched during remission. Median values are indicated by black, horizontal bars. ns, not significant. For Δ bisection of IgG1 and IgG2/3 the same difference at Td AVV onset was observed as a trend (Table S6) which was found in GPA-PR3-ANCA patients (Figure 2).



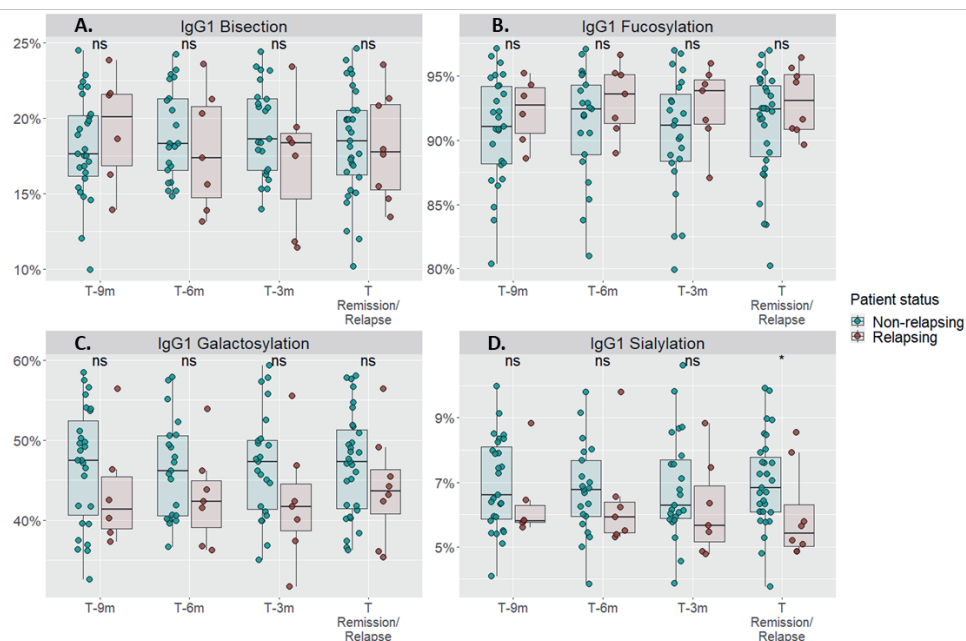
Supplementary Figure 7. Longitudinal changes in Δ IgG1-Fc bisection in MPO-positive patients. Differences compared to the point of relapse or time-matched remission are displayed as Δ values, separately for patients who either relapsed (upper panel in red) or stayed in remission (lower panel in green). Significant differences ($p < 0.0035$) are marked with asterisk *. For relapsing patients note: Td and Td+(3-12m) could not be analyzed due to a lack of power.



Supplementary Figure 9. Cross-sectional differences in IgG1 (A-C), IgG2/3 (D-G) and IgG4 (H-J) Fc glycosylation traits bisection, galactosylation, sialylation, and fucosylation (only for IgG2/3) for PR3-ANCA patients with an ANCA rise. Total serum IgG1 galactosylation of PR3-ANCA patients who either relapse (brown) and stayed in remission (green), was compared at 9 months, 6 months before, 3 months before and at the time of relapse or remission. Significant differences are indicated by an asterisk ($p < 0.05$); ns, not significant.



Supplementary Figure 10. Longitudinal analysis of IgG1-Fc glycosylation changes for PR3-ANCA relapsing and non-relapsing patients, who experienced a rise in the ANCA titre. IgG1-Fc glycosylation changes are shown for the time points preceding relapse or time-matched remission. Significant differences were evaluated by means of Restricted Maximum Likelihood (REML) with post-hoc Tukey test. There were no significant differences. IgG1 Bis – Bisection of IgG1; IgG1 Fuc – Fucosylation of IgG1; IgG1 Gal – Galactosylation of IgG1; IgG1 Sial – Sialylation of IgG1.



Supplementary Figure 11. Cross-sectional differences in IgG1-Fc bisection (A), fucosylation (B), galactosylation (C), and sialylation (D) for PR3-ANCA patients without an ANCA rise. Total serum IgG1 glycosylation of PR3-ANCA patients who either relapse (brown) and stayed in remission (green), was compared at 9 months, 6 months before, 3 months before and at the time of relapse or remission. Significant differences are indicated by an asterisk ($p < 0.05$); ns, not significant.

3.8 REFERENCES

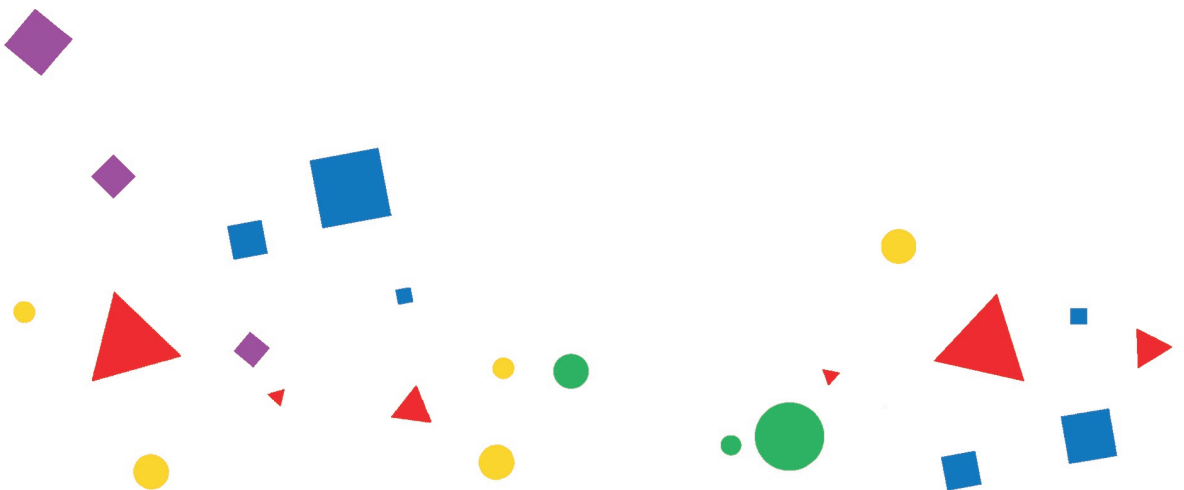
- Jennette JC, Falk RJ, Bacon PA, Basu N, Cid MC, Ferrario F, et al. 2012 revised International Chapel Hill Consensus Conference Nomenclature of Vasculitides. *Arthritis Rheum.* 2013;65(1):1-11.
- Berti A, Dejaco C. Update on the epidemiology, risk factors, and outcomes of systemic vasculitides. *Best Pract Res Clin Rheumatol.* 2018;32(2):271-94.
- Hellmich B, Flossmann O, Gross WL, Bacon P, Cohen-Tervaert JW, Guillevin L, et al. EULAR recommendations for conducting clinical studies and/or clinical trials in systemic vasculitis: focus on anti-neutrophil cytoplasm antibody-associated vasculitis. *Ann Rheum Dis.* 2007;66(5):605-17.
- Alba MA, Jennette JC, Hu Y, Poulton CJ, Blazek L, Derebail VK, et al. Relevance of Combined Clinicopathologic Phenotype and Antineutrophil Cytoplasmic Autoantibody Serotype in the Diagnosis of Antineutrophil Cytoplasmic Autoantibody Vasculitis. *Kidney Int Rep.* 2022;7(12):2676-90.
- Lyons PA, Rayner TF, Trivedi S, Holle JU, Watts RA, Jayne DR, et al. Genetically distinct subsets within ANCA-associated vasculitis. *N Engl J Med.* 2012;367(3):214-23.
- Little MA, Smyth L, Salama AD, Mukherjee S, Smith J, Haskard D, et al. Experimental autoimmune vasculitis: an animal model of anti-neutrophil cytoplasmic autoantibody-associated systemic vasculitis. *Am J Pathol.* 2009;174(4):1212-20.
- Segelmark M, Wieslander J. IgG subclasses of antineutrophil cytoplasm autoantibodies (ANCA). *Nephrol Dial Transplant.* 1993;8(8):696-702.
- Falk RJ, Terrell RS, Charles LA, Jennette JC. Anti-neutrophil cytoplasmic autoantibodies induce neutrophils to degranulate and produce oxygen radicals in vitro. *Proc Natl Acad Sci U S A.* 1990;87(11):4115-9.
- Nakazawa D, Masuda S, Tomaru U, Ishizu A. Pathogenesis and therapeutic interventions for ANCA-associated vasculitis. *Nat Rev Rheumatol.* 2019;15(2):91-101.
- Bournazos S, Ravetch JV. Diversification of IgG effector functions. *Int Immunol.* 2017;29(7):303-10.
- Wuhrer M, Stavenhagen K, Koeleman CA, Selman MH, Harper L, Jacobs BC, et al. Skewed Fc glycosylation profiles of anti-proteinase 3 immunoglobulin G1 autoantibodies from granulomatosis with polyangiitis patients show low levels of bisection, galactosylation, and sialylation. *J Proteome Res.* 2015;14(4):1657-65.
- Gudelj I, Lauc G, Pezer M. Immunoglobulin G glycosylation in aging and diseases. *Cell Immunol.* 2018;333:65-79.
- Emejuiwe N. Treatment Strategies in ANCA-Associated Vasculitis. *Curr Rheumatol Rep.* 2019;21(7):33.
- Kidney Disease: Improving Global Outcomes Glomerular Diseases Work G. KDIGO 2021 Clinical Practice Guideline for the Management of Glomerular Diseases. *Kidney Int.* 2021;100(4S):S1-S276.
- Kemna MJ, van Paassen P, Damoiseaux JGMC, Tervaert JWC. Maintaining remission in patients with granulomatosis with polyangiitis or microscopic polyangiitis: the role of ANCA. *Expert Opin Orphan D.* 2017;5(3):207-18.
- Al-Soudi A, Vegting Y, Klarenbeek PL, Hilhorst ML. Do Relapses Follow ANCA Rises? A Systematic Review and Meta-Analysis on the Value of Serial ANCA Level Evaluation. *Front Med (Lausanne).* 2022;9:844112.
- Yates M, Watts RA, Bajema IM, Cid MC, Crestani B, Hauser T, et al. EULAR/ERA-EDTA recommendations for the management of ANCA-associated vasculitis. *Ann Rheum Dis.* 2016;75(9):1583-94.
- Lardinois OM, Deterding LJ, Hess JJ, Poulton CJ, Henderson CD, Jennette JC, et al. Immunoglobulins G from patients with ANCA-associated vasculitis are atypically glycosylated in both the Fc and Fab regions and the relation to disease activity. *PLoS One.* 2019;14(2):e0213215.
- Holland M, Takada K, Okumoto T, Takahashi N, Kato K, Adu D, et al. Hypogalactosylation of serum IgG in patients with ANCA-associated systemic vasculitis. *Clin Exp Immunol.* 2002;129(1):183-90.
- Holland M, Yagi H, Takahashi N, Kato K, Savage CO, Goodall DM, et al. Differential glycosylation of polyclonal IgG, IgG-Fc and IgG-Fab isolated from the sera of patients with ANCA-associated systemic vasculitis. *Biochim Biophys Acta.* 2006;1760(4):669-77.
- Kemna MJ, Plomp R, van Paassen P, Koeleman CAM, Jansen BC, Damoiseaux J, et al. Galactosylation and Sialylation Levels of IgG Predict Relapse in Patients With PR3-ANCA Associated Vasculitis. *EBioMedicine.* 2017;17:108-18.
- Land J, Abdulhad WH, Arends S, Sanders JF, Stegeman CA, Heeringa P, et al. Prospective monitoring of in vitro produced PR3-ANCA does not improve relapse prediction in granulomatosis with polyangiitis. *PLoS One.* 2017;12(8):e0182549.
- Falck D, Jansen BC, de Haan N, Wuhrer M. High-Throughput Analysis of IgG Fc Glycopeptides by LC-MS. *Methods Mol Biol.* 2017;1503:31-47.
- Dard P, Lefranc MP, Osipova L, Sanchez-Mazas A. DNA sequence variability ofIGHG3 alleles associated to the main G3m haplotypes in human populations. *Eur J Hum Genet.* 2001;9(10):765-72.

25. Vidarsson G, Dekkers G, Rispens T. IgG subclasses and allotypes: from structure to effector functions. *Front Immunol.* 2014;5:520.
26. Jansen BC, Falck D, de Haan N, Hipgrave Ederveen AL, Razdorov G, Lauc G, et al. LaCyTools: A Targeted Liquid Chromatography-Mass Spectrometry Data Processing Package for Relative Quantitation of Glycopeptides. *J Proteome Res.* 2016;15(7):2198-210.
27. Selman MH, Derks RJ, Bondt A, Palmblad M, Schoenmaker B, Koeleman CA, et al. Fc specific IgG glycosylation profiling by robust nano-reverse phase HPLC-MS using a sheath-flow ESI sprayer interface. *J Proteomics.* 2012;75(4):1318-29.
28. Kristic J, Vuckovic F, Menni C, Klaric L, Keser T, Beceheli I, et al. Glycans are a novel biomarker of chronological and biological ages. *J Gerontol A Biol Sci Med Sci.* 2014;69(7):779-89.
29. Lionaki S, Blyth ER, Hogan SL, Hu Y, Senior BA, Jennette CE, et al. Classification of antineutrophil cytoplasmic autoantibody vasculitides: the role of antineutrophil cytoplasmic autoantibody specificity for myeloperoxidase or proteinase 3 in disease recognition and prognosis. *Arthritis Rheum.* 2012;64(10):3452-62.
30. Walsh M, Flossmann O, Berden A, Westman K, Hoglund P, Stegeman C, et al. Risk factors for relapse of antineutrophil cytoplasmic antibody-associated vasculitis. *Arthritis Rheum.* 2012;64(2):542-8.
31. Wu RQ, Lao XM, Chen DP, Qin H, Mu M, Cao WJ, et al. Immune checkpoint therapy-elicited sialylation of IgG antibodies impairs antitumorigenic type I interferon responses in hepatocellular carcinoma. *Immunity.* 2023;56(1):180-92 e11.
32. Kaneko Y, Nimmerjahn F, Ravetch JV. Anti-inflammatory activity of immunoglobulin G resulting from Fc sialylation. *Science.* 2006;313(5787):670-3.
33. Quast I, Keller CW, Maurer MA, Giddens JP, Tackenberg B, Wang LX, et al. Sialylation of IgG Fc domain impairs complement-dependent cytotoxicity. *J Clin Invest.* 2015;125(11):4160-70.
34. Wang TT, Ravetch JV. Functional diversification of IgGs through Fc glycosylation. *J Clin Invest.* 2019;129(9):3492-8.
35. Kapur R, Kustiawan I, Vestreheim A, Koeleman CA, Visser R, Einarsdottir HK, et al. A prominent lack of IgG1-Fc fucosylation of platelet alloantibodies in pregnancy. *Blood.* 2014;123(4):471-80.
36. Larsen MD, de Graaf EL, Sonneveld ME, Plomp HR, Nouta J, Hoepel W, et al. Afucosylated IgG characterizes enveloped viral responses and correlates with COVID-19 severity. *Science.* 2021;371(6532).
37. Kapur R, Della Valle L, Sonneveld M, Hipgrave Ederveen A, Visser R, Ligthart P, et al. Low anti-RhD IgG-Fc fucosylation in pregnancy: a new variable predicting severity in haemolytic disease of the fetus and newborn. *Br J Haematol.* 2014;166(6):936-45.
38. Jennette JC, Falk RJ. Pathogenesis of antineutrophil cytoplasmic autoantibody-mediated disease. *Nat Rev Rheumatol.* 2014;10(8):463-73.
39. Wojcik I, Senard T, de Graaf EL, Janssen GMC, de Ru AH, Mohammed Y, et al. Site-Specific Glycosylation Mapping of Fc Gamma Receptor IIb from Neutrophils of Individual Healthy Donors. *Anal Chem.* 2020;92(19):13172-81.
40. Wang J, Balog CI, Stavenhagen K, Koeleman CA, Scherer HU, Selman MH, et al. Fc-glycosylation of IgG1 is modulated by B-cell stimuli. *Mol Cell Proteomics.* 2011;10(5):M110 004655.
41. Cao Y, Song Z, Guo Z, Zhao X, Gong Y, Zhao K, et al. Cytokines in the Immune Microenvironment Change the Glycosylation of IgG by Regulating Intracellular Glycosyltransferases. *Front Immunol.* 2021;12:724379.
42. Shinkawa T, Nakamura K, Yamane N, Shoji-Hosaka E, Kanda Y, Sakurada M, et al. The absence of fucose but not the presence of galactose or bisecting N-acetylglucosamine of human IgG1 complex-type oligosaccharides shows the critical role of enhancing antibody-dependent cellular cytotoxicity. *J Biol Chem.* 2003;278(5):3466-73.
43. Shields RL, Lai J, Keck R, O'Connell LY, Hong K, Meng YG, et al. Lack of fucose on human IgG1 N-linked oligosaccharide improves binding to human FcγRIII and antibody-dependent cellular toxicity. *J Biol Chem.* 2002;277(30):26733-40.
44. Rarok AA, Limburg PC, Kallenberg CG. Neutrophil-activating potential of antineutrophil cytoplasm autoantibodies. *J Leukoc Biol.* 2003;74(1):3-15.
45. Tsukui D, Kimura Y, Kono H. Pathogenesis and pathology of anti-neutrophil cytoplasmic antibody/ANCA-associated vasculitis. *J Transl Autoimmun.* 2021;4:100094.
46. van Timmeren MM, van der Veen BS, Stegeman CA, Petersen AH, Hellmark T, Collin M, et al. IgG glycan hydrolysis attenuates ANCA-mediated glomerulonephritis. *J Am Soc Nephrol.* 2010;21(7):1103-14.
47. Kelley JM, Monach PA, Ji C, Zhou Y, Wu J, Tanaka S, et al. IgA and IgG antineutrophil cytoplasmic antibody engagement of Fc receptor genetic variants influences granulomatosis with polyangiitis. *Proc Natl Acad Sci U S A.* 2011;108(51):20736-41.

48. Golay J, Da Roit F, Bologna L, Ferrara C, Leusen JH, Rambaldi A, et al. Glycoengineered CD20 antibody obinutuzumab activates neutrophils and mediates phagocytosis through CD16B more efficiently than rituximab. *Blood*. 2013;122(20):3482-91.
49. Nimmerjahn F, Ravetch JV. Fcγ receptors as regulators of immune responses. *Nat Rev Immunol*. 2008;8(1):34-47.
50. Dekkers G, Treffers L, Plomp R, Bentlage AEH, de Boer M, Koeleman CAM, et al. Decoding the Human Immunoglobulin G-Glycan Repertoire Reveals a Spectrum of Fc-Receptor- and Complement-Mediated-Effector Activities. *Front Immunol*. 2017;8:877.
51. Falck D, Jansen BC, Plomp R, Reusch D, Habberger M, Wuhrer M. Glycoforms of Immunoglobulin G Based Biopharmaceuticals Are Differentially Cleaved by Trypsin Due to the Glycoform Influence on Higher-Order Structure. *J Proteome Res*. 2015;14(9):4019-28.

- ¹ *Center for Proteomics and Metabolomics, Leiden University Medical Center, Leiden, The Netherlands*
- ² *Glycoscience Research Laboratory, Genos Ltd., Zagreb, Croatia*
- ³ *Department of Experimental Immunohematology, Sanquin Research, and Landsteiner Laboratory, Academic Medical Center, University of Amsterdam, Amsterdam, The Netherlands*

** Authors share co-first authorship*



Chapter 4

Site-specific glycosylation mapping of Fc gamma receptor IIIb from neutrophils of individual healthy donors

Iwona Wojcik^{1,2*}, Thomas Sénard^{1*}, Erik L de Graaf³, George MC Janssen¹, Arnoud H de Ru¹,
Yassene Mohammed¹, Peter A van Veelen¹,
Gestur Vidarsson³, Manfred Wuhrer¹ and David Falck¹

Reprinted and adapted with permission from

Anal Chem. 2020 Oct 6;92(19):13172-13181. doi: 10.1021/acs.analchem.0c02342. Epub 2020 Sep 22. PMID:
32886488; PMCID: PMC7547861.

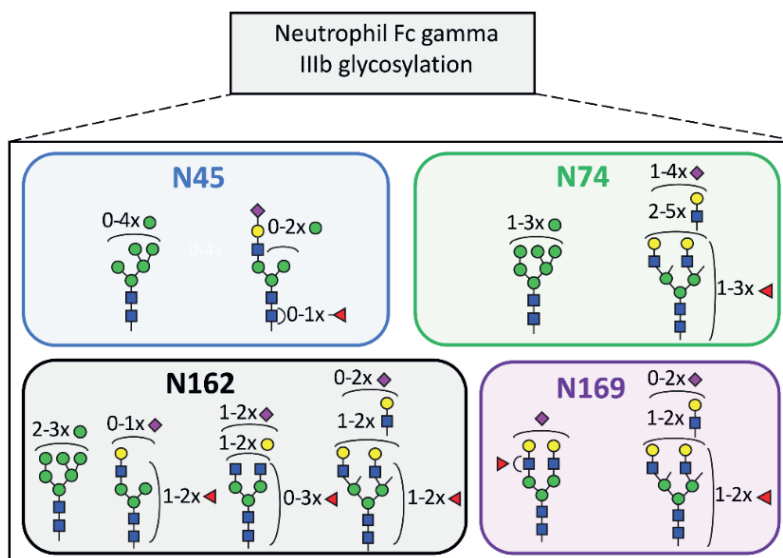
Copyright © 2020, American Chemical Society.



4.1 ABSTRACT

Fc gamma receptors (FcγRs) translate antigen-recognition by immunoglobulin G (IgG) into various immune responses. A better understanding of this key element of immunity promises novel insights into mechanisms of (auto-/allo-)immune diseases and more rationally designed antibody-based drugs. Glycosylation on both IgG and FcγR impacts their interaction dramatically. Regarding FcγR glycosylation profiling, major analytical challenges are associated with the presence of multiple glycosylation sites in close proximity and the large structural heterogeneity. In order to address these challenges, we developed a straightforward and comprehensive analytical methodology to map FcγRIIIb glycosylation from primary human cells. After neutrophil isolation and immunoprecipitation, glycopeptides containing a single site each were generated by a dual-protease in-gel digestion. The complex mixture was resolved by liquid chromatography - tandem mass spectrometry (LC-MS/MS) providing information on the level of individual donors. In contrast to recently published alternatives for FcγRIIIb, we assessed its site-specific glycosylation in a single LC-MS/MS run and simultaneously determined the donor allotype. Studying FcγRIIIb derived from healthy donor neutrophils, we observed profound differences as compared to the soluble variant and the homologous FcγRIIIa on natural killer cells. This method will allow assessment of FcγRIII glycosylation differences between individuals, cell types, subcellular locations and pathophysiological conditions.

GRAPHICAL ABSTRACT



4.2 INTRODUCTION

Binding of immunoglobulin G (IgG) to Fc gamma receptors (FcγRs) initiates and regulates important immune responses.(1, 2) Therefore, FcγRs have a key role in homeostasis and in many pathological conditions.(3, 4) This is widely exploited for therapeutic purposes, for example with monoclonal antibodies or polyclonal intravenous IgG.(5-7) The key interaction between IgG and FcγRs is heavily regulated by the proteoform distribution of either binding partner, e.g. through post-translational modifications. The impact of IgG proteoforms has been extensively studied in the last decades.(8, 9) Subclass, allotype and glycosylation, especially (α)fucosylation, of IgG impact FcγR binding.(10-12) FcγR-mediated IgG effector functions are partially regulated by varying FcγR expression on different immune cells.(13) For example, FcγRIIIb or CD16b is exclusively expressed as a monomeric protein mainly on granulocytes, while the homologous FcγRIIIa or CD16a is expressed on NK cells, monocytes, macrophages and dendritic cells. Unlike all other transmembrane FcγRs, the human FcγRIIIb is GPI-anchored and lacks a transmembrane and cytoplasmic signalling domain. FcγRIIIb is an 233 amino acid protein which consists of N-terminal signal peptide (18 amino acids) cleaved during protein processing and two domains in the extracellular region.(14) Those domains share 97% sequence homology with FcγRIIIa.(15) Despite the homology, FcγRIIIa binds IgG stronger than FcγRIIIb due to a single amino acid difference, G₁₂₉ versus D₁₂₉.(16) FcγRIIIb seems to affect signalling of other Fc-receptors through accumulation in lipid rafts which are enriched in kinases (Src) and required for ITAM-phosphorylation and signalling.(17) Given the relatively high expression levels of FcγRIIIb on neutrophils with 120,000 to 300,000 copies per cell,(18) and the dominance of neutrophils amongst white blood cells, FcγRIIIb can be considered the most abundant FcγR in circulation. Known functions include activation of neutrophil degranulation, cell adhesion, calcium mobilization and neutrophil tethering to soluble immune complexes.(19-21)

Despite recent advances, the role of FcγR proteoforms is only poorly understood.(14) Allotypes lead to differentially active proteoforms. There are three known allotypes of FcγRIIIb, neutrophil antigen 1 (NA1) and 2 (NA2), and SH (SH being uncommon). They vary in their affinity for IgG and capacity to induce phagocytosis of IgG-opsonized targets.(22) The two major FcγRIIIb allotypes, NA1 and NA2 differ in four amino acids, resulting in four and six potential *N*-glycosylation sites for NA1 (N₃₈, N₇₄, N₁₆₂, N₁₆₉) and NA2 (N₃₈, N₄₅, N₆₄, N₇₄, N₁₆₂, N₁₆₉), respectively.(23) Five of the potential *N*-glycosylation sites are conserved between FcγRIIIa and FcγRIIIb, namely N₃₈, N₄₅, N₇₄, N₁₆₂ and N₁₆₉. The vast majority of glycan data on FcγRIII derives from the endogenous FcγRIIIa from NK cells(24) and monocytes,(25) as well as recombinant protein expressed in human embryonic kidney (HEK), Chinese hamster ovary (CHO) cells,(26) Baby Hamster Kidney Cells (BHK)(27) and murine cell line NS0.(28) Both variants, endogenous as well as a recombinant FcγRIIIa/b are modified by *N*-glycans, but only for recombinant FcγRIIIa a single *O*-glycan modification has been detected.(26) FcγR glycosylation strongly impacts the interaction with IgG. Some

receptor glycans have direct glycan-glycan and glycan-protein interactions with bound IgG.(29, 30) Deglycosylation of site N₁₆₂ (unique to FcγRIIIa and FcγRIIIb), strongly elevates affinity of FcγRIIIa to IgG, but also alleviates sensitivity to IgG-core-fucosylation.(31, 32) Furthermore, differences in FcγRIIIb glycosylation in different cell models, have been shown to impact IgG binding.(33, 34) The available studies underline the importance of FcγR glycosylation, but can so far only sketch a very rough picture of its functional impact.

A prominent reason for this lack of functional understanding is the limited available data on FcγR glycosylation of primary human cells.(14) While the great heterogeneity of proteoforms, especially in FcγRIIIb, was already apparent in early studies,(18) glycomics studies on primary human cells only became possible in recent years.(35) However, owing to the great complexity and differential functional impact of glycosylation sites, only site-specific glycoproteomics studies can characterize FcγR glycosylation to the necessary extent. Recent studies on healthy volunteers revealed FcγRIIIa glycosylation of NK cells(24) and monocytes(25) and FcγRIIIb glycosylation of neutrophils(36). Therein, cells were purified by negative selection with magnetic beads, followed by immunoprecipitation of FcγR. Additionally, the soluble FcγRIIIb,(37) which originates from shedding from neutrophils upon their activation, has been studied in plasma. The purified receptor from all sources was analysed by bottom-up glycoprotein analysis / glycoproteomics following protease cleavage with chymotrypsin and/or endoproteinase Glu-C (GluC).(26) Targeted analysis of FcγRIIIb using immunoprecipitation (IP) offers important advantages, because it increases the depth of analysis, and hence the number of identified and quantified glycoforms. Untargeted glycoproteomics strategies possess the advantage that they provide a glimpse on the glycosylation of many proteins. While they may overcome potential proteoform-biases in antibody-specificity for IP, the increased sample complexity and resulting co-elution of (glyco-)peptides in such approaches introduce significant biases due to ion-suppression and undersampling.(38, 39)

While ground-breaking, the two previous studies on site-specific glycosylation of FcγRIIIb had some limitations.(36, 37) They relied on two independent proteolytic cleavages, thus necessitating multiple liquid chromatography – mass spectrometry (LC–MS) runs to cover the whole receptor. Yagi *et al.* focused on soluble FcγRIIIb whose function is largely unknown.(37) They used pooled blood from multiple donors, losing inter-donor variability. Washburn *et al.* only analysed three of the six potential N-glycosylation sites, but accumulated strong data on inter-donor variability of 50 donors.(36) Nonetheless, we still know too little about the functional and clinical impact of FcγR glycosylation to prefer a method focussing only on certain glycosylation sites. Other existing strategies covering all sites of FcγRIIIb or FcγRIIIa are quite complicated to apply to clinical investigations where eventually large numbers of samples need to be detected in a robust way.(24, 37)

Here, we present a method for the site-specific analysis of all glycosylation sites of FcγRIIIb in a single LC-MS/MS experiment. With it, we identified and relatively quantified neutrophil-derived FcγRIIIb glycosylation individually for multiple donors. Additionally, our approach allowed a qualitative overview of site occupancy and the determination of donor allotypes. This was enabled by avoiding glycopeptide enrichment which also promises more robustness. Additionally, interferences from endogenous IgG and from leaking capturing antibody are avoided by a simple non-reducing SDS-PAGE step. Additionally, our method is generic for FcγRIIIa and FcγRIIIb, making it potentially applicable to a wide range of leukocytes. Moving towards clinical investigations of FcγR glycosylation will be essential for a complete understanding of the (patho-)physiological role of IgG-FcγR interactions. Our methodology presents a uniquely suited starting point, as it is unprecedented in its ability to simultaneously cover individual donor, subclass, allotype, cell and site differences of FcγRIII glycosylation comprehensively.

4.3 EXPERIMENTAL SECTION

4.3.1 Buffers and reagents

Trizma hydrochloride, Tris(hydroxymethyl)aminomethane, Protease Inhibitor Cocktail (Set V, EDTA-Free), phenylmethylsulfonyl fluoride (PMSF), ethylenediaminetetraacetic acid (EDTA), glycerol were obtained from Sigma-Aldrich (Steinheim, Germany). Di-sodium hydrogen phosphate dihydrate ($\text{Na}_2\text{HPO}_4 \cdot 2 \text{H}_2\text{O}$), potassium dihydrogen phosphate (KH_2PO_4), and NaCl were obtained from Merck (Darmstadt, Germany). CARIN lysis buffer (pH 8.0) was prepared in-house with 20 mM Tris-HCl, 137 mM NaCl, 10 mM EDTA, 0.1 M NaF, 1% NP-40 and 10% glycerol. Protease Inhibitor Cocktail and PMSF were added to prevent unwanted proteolysis. Phosphate-buffered saline (PBS, 0.035 M, pH 7.6) was prepared in-house with 5.7 g/L of Na_2HPO_4 , 2 H₂O, 0.5 g/L of KH_2PO_4 , and 8.5 g/L of NaCl. Coomassie staining was prepared in-house according to Candiano et al.(40) using Coomassie Blue G-250 (Sigma-Aldrich). SDS-PAGE reagents were of the NuPAGE™ series (ThermoFisher Scientific) and included: LDS Sample Buffer (4x) (non-reducing loading buffer), a PageRuler Prestained Protein Ladder (protein standard), 4-12% Bis-Tris gel and a 4 Morpholinepropanesulfonic acid (MOPS) SDS running buffer.

4.3.2 Materials

GluC (Staphylococcus aureus Protease V8) and chymotrypsin were obtained from (Worthington Biochemical Corp., Lakewood, USA). The ultrapure deionized water (MQ) was generated using a Q-Gard 2 system (Millipore, Amsterdam, Netherlands). MS grade acetonitrile (ACN) was acquired from Biosolve B.V. (Valkenswaard, The Netherlands). Iodoacetamide (IAA), dithiothreitol (DTT), ethylenediaminetetraacetic acid (EDTA), analytical grade formic acid (FA) and LC-MS grade water were obtained from Sigma-Aldrich (Steinheim, Germany). More information on buffers and reagents can be found in the

Supplementary Information. FcγRIIIb were immunoprecipitated from the neutrophil cell lysate using a mouse anti-CD16 monoclonal IgG2a antibody (Ref M9087, Clone CLB-FcR gran/1, 5D2, Sanquin, Amsterdam, The Netherlands). Prior to usage, antibodies were labelled with biotin.

4.3.3 Antibody biotinylation

At first, antibodies were buffer exchanged from Tris buffer to PBS buffer using the Zeba spin protocol (ThermoFisher Scientific, Rockford, IL, USA), as amine-containing buffers may interfere with biotinylation. Subsequently, the Z-link™ Sulfo-NHS-Biotinylation protocol (ThermoFisher Scientific) was followed. The level of biotin incorporation was measured with a HABA Assay (ThermoFisher Scientific).

4.3.4 Neutrophil cell isolation and FcγRIIIb purification

Neutrophils were isolated from whole blood of three healthy volunteers as described previously.⁽⁴¹⁾ Briefly, the blood was collected from healthy donors into tubes coated with spray dried EDTA for anticoagulation (VACUETTE TUBE 9ml K3E K3EDTA, Greiner Bio-One, Amsterdam, Netherlands). Mononuclear leukocytes and platelets were removed by centrifugation (2,000 rpm, 18 min, 25°C) using a Ficoll gradient with a specific density of 1.077 g/mL (Ficoll-Paque PLUS, GE Healthcare, Freiburg, Germany). Erythrocytes were subsequently lysed with isotonic NH₄Cl solution at 4°C. With this standard method, a high degree of depletion of other cell types is obtained and neutrophils are isolated with a typical purity of over 95%. The isolated neutrophils were washed two times with 1 mL of cold PBS. The cells were counted on a CASY automated cell counter (Thermo Fisher Scientific, Rockford, IL, USA) followed by centrifugation (1,200 rpm, 4 minutes, 4°C). The neutrophils were resuspended in CARIN Buffer at a final concentration of 50 x 10⁶ cells/mL (**Table S1**). The cells were then incubated on ice for 5-10 min. Lastly, cell lysates were sonicated for 30 seconds at 20 kHz. The cell lysate was centrifuged at 13000 x *g* for 15 min at 4°C. The cellular debris pellet was discarded. The total protein content of the supernatant was measured with a NanoDrop™ 2000 spectrophotometer (Thermo Fisher Scientific, Rockford, IL, USA). For FcγRIII identification and purification, respectively, an amount of ~3 or ~16 million primary human neutrophils from healthy donors was used for immunoprecipitation (**Table S1**). 100 µg or 500 µg of neutrophil proteins were incubated, while rotating, with 5 µg or 25 µg of biotinylated antibodies in the total volume of 1 mL CARIN lysis buffer overnight at 4°C. A rough estimate of the antibody: FcγRIII ratio was 2,500:1. 10 µL of High Capacity Streptavidin Agarose Resin beads (Thermo) were washed twice in 1 mL CARIN buffer and incubated with the pre-formed FcγRIII-anti-CD16 immune complexes for 1 hour at 4°C and rotating. The beads were centrifuged for 2 min at 2500 x *g*, removing supernatant, and washed four times with 1 mL CARIN buffer. Finally, FcγRIII was eluted from the beads with

two times 150 μ L of 200 mM FA. The eluates were then dried by vacuum centrifugation at 60°C for 2 hours.

4.3.5 SDS-PAGE

The immunoprecipitation of Fc γ RIIIb from 100 μ g of total neutrophil proteins was evaluated by sodium dodecyl-sulfate-polyacrylamide gel electrophoresis (SDS-PAGE). The dried samples were resuspended in 20 μ L of non-reducing loading buffer, incubated at 95°C for 5 min and applied to a 4-12% Bis-Tris gel. The migration was performed at 200 V constant voltage for 50 min in 4-Morpholinepropanesulfonic acid (MOPS) SDS running buffer. Gels were stained using Coomassie blue. The presence of CD16 was confirmed by western blotting, using an anti-CD16 mouse monoclonal IgG1 conjugated to horseradish peroxidase (DJ130c, sc-20052 HRP, Lot #D2617, Santa Cruz Biotech; see also Supplementary Information).

4.3.6 In-gel proteolytic digest and LC-MS glycopeptide analysis

For the in-gel LC-MS workflow, 500 μ g of total neutrophil proteins were used for immunoprecipitation. The subsequent SDS-PAGE was performed at 200 V constant voltage for only 15 min. The obtained gels were silver stained (SilverQuest™ Staining Kit, Invitrogen) and the protein of interest was cut out from the gel. Excised bands were subjected to in-gel digestion with endoproteinase GluC and chymotrypsin which was performed on a Proteineer DP digestion robot (Bruker, Bremen, Germany). (26, 42, 43) Reduction with 10 mM DTT was followed by alkylation with 50 mM IAA(44) and 3 wash and shrink cycles with 25 mM ammonium bicarbonate (pH 8.4) and neat acetonitrile, respectively. The shrunken gel bands were soaked for 45 min at 10°C in 25 mM ammonium bicarbonate, containing both proteases at a concentration of 12.8 ng/ml each. Excess protease solution was removed, followed by overnight digestion at 37°C. Peptides were extracted with 100 μ L H₂O/acetonitrile/ formic acid (50/50/1), lyophilized and dissolved in solvent A (3% ACN/95% water containing 0.1% FA (v/v)) prior to injection. The liquid chromatography-tandem mass spectrometry (LC-MS/MS) analysis was performed on a nanoLC-MS system composed of an Easy nLC 1000 gradient HPLC system (Thermo, Bremen, Germany) and a LUMOS mass spectrometer (Thermo). Prior to sample injection, the peptides and glycopeptides extracted from the bands were lyophilized and dissolved in solvent A (water containing 0.1% FA (v/v)). The samples were then loaded onto an in-house packed C18 precolumn (100 μ m \times 15 mm; Reprosil-Pur C18-AQ 3 μ m, Dr. Maisch, Ammerbuch, Germany) and separated on a homemade analytical nanoLC column (30 cm \times 75 μ m; Reprosil-Pur C18-AQ 3 μ m). The digested (glyco-)peptides were eluted using a linear gradient from 10 to 40% solvent B (80% ACN/20% water containing 0.1% FA (v/v)) over 20 min, followed by a column washing step with solvent B to 100% (at 25 min) and reconditioning with solvent A for 12 min. The nanoLC column was drawn to a tip of \sim 5 μ m and acted as the electrospray needle of the MS source. The Orbitrap Fusion LUMOS mass spectrometer was operated in data-dependent MS/MS

(top-20 mode) with the collision energy set at 32% normalized collision energy (NCE) and recording the MS/MS spectrum in the Orbitrap. The MS¹ full scan spectra were acquired within a mass range of m/z of 400–1500 and MS/MS was set to auto (i.e. depending on the m/z of the selected precursor ion). The resolution setting for MS¹ scans was 12×10^4 and an AGC target value of 4×10^4 for an accumulation time of a maximum 50 ms. Dynamic exclusion duration was 10 s with a single repeat count, and charge states in the range 1–5 were included for MS/MS. The resolution of MS/MS scans was 3×10^4 with an AGC target of 5×10^4 with a maximum fill time of 60 ms. MS/MS spectra were generated from precursors isolated with the quadrupole with an isolation width of 1.2 Da. During acquisition, a product ion trigger was set on the HexNAc oxonium ion at m/z 204.087. Upon the detection of the oxonium ion, three additional data-dependent MS/MS scans of the same precursor were executed in the ion-routing multipole with higher-energy collisional dissociation (HCD) collision energies of 32%, 37%, and 42% NCE, respectively, at an AGC target of 5×10^5 with a maximum fill time of 200 ms. In addition, the acquisition of collision-induced dissociation (CID) spectra in the linear ion trap was performed for the precursor and recorded at 35% NCE. The presented results on protein identification, coverage and purity are from a standard data-dependent HCD run (without exclusive m/z 204.087 triggering). For the identification of glycopeptides in these runs, MS/MS spectra containing the specific HexNAc oxonium ion at m/z 204.087 (HexNAc, $[C_8H_{14}NO_5]^+$) were extracted from the raw data and written to a .mgf file using in-house routines. This filtering step also ensured to include only spectra containing the HexNAc oxonium ion with a strong signal (among top 30 peaks).

4.5.7 Identification and quantification of site-specific glycosylation

Initially, LC-MS/MS data were processed with Byonic (Protein Metrics, Cupertino, CA v3.2-38).(45) MS/MS spectra were searched against an extensive human proteome database combined with a pre-defined glycan list (**Table S2**). Glycopeptides identification with Byonic scores below 150 were removed from the analysis. Digestion specificity was set as non-specific (slowest), allowing for both specific and miscleaved peptides. Glycosylation was set as a common modification and other modifications were anticipated upon prevalence: Glycan modification/ + [glycan composition] Da @ NGlycan | common1; carbamidomethyl/ +57.021 Da @C | fixed; oxidation/ +15.995 Da @M | common2; acetyl/ +42.011 Da @Protein N-term | rare1. The Byonic search allowed one common modification and one rare modification per peptide. For more parameters refer to **Table S3**. Byonic identifications were manually verified and extended using Xcalibur (Thermo). **Table S4** gives an overview of the identification level of individual glycoforms (Byonic, manual MS/MS, manual MS). Regarding the manual identification, MS¹ sum spectra were generated — around the retention times reported by Byonic — and searched for expected monosaccharide differences. This was done per combination of unique peptide backbone and number of sialic acids, the main two retention time determinants. Some sialic acid variants were

inferred, improving the identification of multisialylated glycan compositions. Annotation of MS¹ spectra was based on precursor mass with a tolerance of ± 0.05 Th. Manual MS/MS interpretation was based on, firstly the clear presence of an m/z corresponding to a peptide or peptide+HexNAc fragment ion of a previously identified glycosylated sequence and secondly the presence of a dominating pattern of oxonium ions. During the manual interpretation, differences in (glyco-)peptide sequences between the FcγRIIIb allotypes, NA1 and NA2, were taken into consideration.

For automatic alignment, integration and extraction of LC-MS data, the in-house software LacyTools (Version 1.1.0-alpha) was used as described previously.⁽⁴⁶⁾ As an input, the raw data files were converted to mzXML files and a list of identified glycopeptides along with their retention times was created. For the area integration of the sum spectra, the following settings were applied: sum spectrum resolution of 100, extraction mass window of 0.07 Th, extraction time window of 15 s, percentage of the theoretical isotopic pattern of 95%, min charge stage 2, max charge stage 4. This resulted in integrated signal intensities for each glycopeptide per charge stage (from $[M+2H]^{2+}$ to $[M+4H]^{4+}$). After extraction, analytes were curated from the identification list, if the average mass error was outside ± 20 ppm and the isotopic pattern deviated more than 20% from the theoretical one. This resulted in the exclusion of signals for all doubly charged glycopeptides and inclusion of signals for triply and some quadruply charged analytes. All included charge stage signals for the same glycopeptide were summed, the absolute intensities were corrected for the fraction of isotopes integrated and used for relative quantification. Total area normalization per glycosylation site was used for relative quantitation. The intensities of the iron adduct ($[M+Fe^{III}]^{3+}$) and ammonia adduct ($[M+2H+NH_4]^{3+}$) signals were significant. Hence, the relative quantification was performed on extracted areas of protonated, iron adduct and ammonia adduct peaks. The *N*-glycosylation site occupancy was determined as the fraction of all glycopeptide signals in the sum of glycopeptide and non-glycosylated peptide signals.

4.4 RESULTS AND DISCUSSION

4.4.1 FcγRIIIb purification and identification

Similar to previous reports,⁽⁴⁷⁾ the western blot showed a smear from 50 to 80 kDa, confirming the presence of FcγRIIIb with its abundant and diverse glycosylation pattern (**Figure 1**). A comparison of total cell lysate, flow-through and eluate demonstrates the efficacy of the purification. The non-reducing SDS-PAGE allowed the separation of FcγRIIIb from interferences derived, for example, from the capturing antibody or endogenous IgG (**Figure S1**). This is simple and preferable to an affinity removal of IgG which may lose specific FcγR proteoforms due to high affinity interactions.⁽²⁴⁾ In the eluate, the FcγRIIIb could not be detected by Coomassie blue staining (LOD ca. 25 ng for well-defined bands). This indicated a recovery value below 4 to 20%, determined by the percentage ratio of the eluted FcγRIIIb (< 25 ng) to the theoretical amount of FcγRIIIb on the neutrophil surface

(160-630 ng). This is consistent with the western blot, where the eluate fraction is significantly lower from the neutrophils signal corresponding to the $\frac{1}{4}$ of the expected optical density at 100%. Despite the low recovery, the purification scheme resulted in enough material for LC-MS(/MS) analysis after in-gel digestion. Furthermore, MS/MS analysis of the purified protein yielded a sequence coverage of approximately 80% and did not indicate any major interferences in the relevant gel band (**Table S5**). Thus, a strong enrichment of Fc γ RIIIb from neutrophil lysate was achieved.

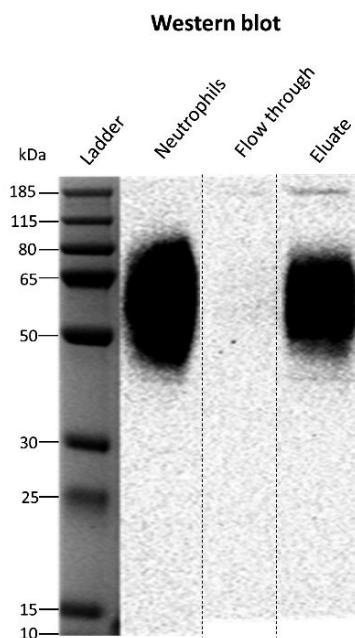


Figure 1. Western blot of human neutrophil lysate before and after Fc γ RIII immunoprecipitation. The identity of Fc γ RIIIb was confirmed with an anti-CD16 antibody. The flow-through lanes show the diluted unbound fraction of the immunoprecipitation while the eluate lanes present the purified Fc γ RIIIb protein. The neutrophil lanes represent $\sim 25 \mu\text{g}$ of total protein content from the neutrophil cell lysate from donor 2. Apparent differences in the western blot are due to concentration differences. The weaker signal of extreme low and high MW proteoforms is lost at lower concentrations after IP. The cropping area is indicated by striated lines. The complete gel and blot are presented in Figure S1 and Figure S2.

4.4.2 Coverage and protein identity

Isolated Fc γ RIIIb was subjected to an in-gel endoproteinase GluC and chymotrypsin treatment prior to the LC-MS(/MS) analysis.(26) This approach was sufficient to generate and identify unique peptides for all six glycosylation motifs. FHN₄₅ESLISSQASSY (NES), FIDAATVN₆₄DSGEY (NDS), RCQTN₇₄LSTLSDPVQLE (NLS), CRGLVGSKN₁₆₂VSSE (NVS) and TVN₁₆₉ITITQGLAV (NIT) were found in human neutrophils (**Table S6**), while SPEDN₃₈ESQW was only detected in recombinant receptor (**Figure S3 and S4**). An overview of Fc γ RIIIb

glycopeptides is depicted in **Figure 2**. Our method required only one LC-MS/MS run to obtain full coverage of all glycosylation sites.

FcγRIIIb showed lower electrophoretic mobility for Donor 1, suggesting the less glycosylated NA1 allotype (**Figure S2**). The allotype can be determined by proteomics,(36) which we achieved simultaneously with the glycoprofiling. The assignments were based on the intensity ratios of allele-specific peptides: for example, FHN₄₅ENLISSQASSY (NEN), FIDAATVD₆₄DSGEY (DDS) for NA1, and FHN₄₅ESLISSQASSY (NES), FIDAATVN₆₄DSGEY (NDS) for NA2 (**Table S7**). Indeed, Donor 1 was an NA1/NA2 individual, with a 1:5 ratio of NA2 N₄₅ oligomannose glycopeptides (NES/(NES+NEN)). Relative quantitation may be biased by the reduced ionization efficiency of glycopeptides compared to non-glycosylated peptides. However, a similar ratio (1:4) for unoccupied NA2 N₆₄ peptide (NDS/(DDS+ NDS)) was observed. Thus, the 1:5/1:4 ratio likely reflects the real expression levels between NA2 and NA1, potentially caused by naturally occurring gene copy number variation of FcγRIIIb.(48) Donors 2 and 3 were NA2 homozygous, since they contained approximately 98% of FHN₄₅ESLISSQASSY and FIDAATVN₆₄DSGEY peptides (**Table S7**). The residual 2% was explained by shared peptides sequences between FcγRIIIb NA1 and FcγRIIIa (FHN₄₅ENLISSQASSY, FIDAATVD₆₄DSGEY and FIDAATVD₆₄DSGEYR). We cannot exclude that these signals may be derived from contamination by NK cells, macrophages and/or monocytes. Additionally, deamidation of site N₆₄ may contribute to the D₆₄ peptide signals, but does not explain the N₄₅ signals. Importantly, at these low levels, the impact of FcγRIIIa glycopeptides on FcγRIIIb glycosylation profiling can be neglected. Therefore, co-isolation is preferred as it enables the use of the same sample preparation protocol for FcγRIIIa-dominated cell types.

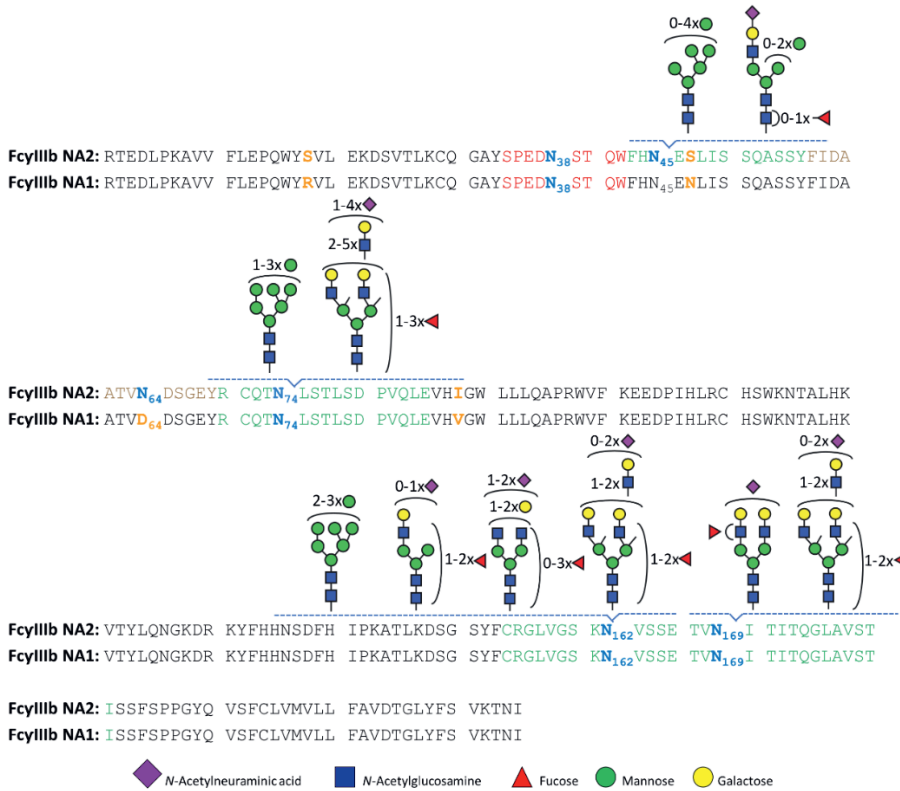


Figure 2. A schematic representation of site-specific N-glycosylation of endogenous FcγRIIb NA1 and NA2 from human neutrophils. N-glycosylation sites are noted in bold, blue letters. All determined and occupied glycopeptides are depicted in green with their corresponding set of glycans. A peptide with an unoccupied N-glycosylation site (site N₆₄ NA2) is marked in brown, while the sequence of a peptide containing site N₃₈, that was only detected in recombinant receptor, is indicated in red. Amino acids in yellow show the sequence variations between NA1 and NA2.

Neither peptides nor glycopeptides corresponding to the glycosylation site N₃₈ were observed in our LC-MS/MS data of the healthy donors. Of note, we were able to detect complex glycans occupying site N₃₈ on recombinant FcγRIIb (Figure S3 and S4). Yagi *et al.* previously reported on site N₃₈ large, highly elaborated glycan structures in the range of *m/z* 1400 to *m/z* 2000.(37) The identified features on recombinant FcγRIIb possess on average less antennae which are also less processed.

4.4.3 Glycopeptide identification

10 N-glycan compositions at N₄₅, 15 at N₇₄, 30 at N₁₆₂ and 6 at N₁₆₉ were identified. Of these 61 compositions, 36 glycoforms were confirmed by tandem mass spectrometry (Table S4). Based on glycopeptide fragmentation data, mass accuracy, isotopologue pattern and biosynthetic pathways, we propose the N-glycan structures shown in Figure 2 and S5.

Numerous structural isomers could be present for the same *N*-glycan composition. We identified multiple isomeric structures, but were not able to resolve them quantitatively. We confirmed the presence of sialic acid by the diagnostic ion at m/z 292.103. Antennary fucosylation was confirmed by presence of a B-ion at m/z 512.197 [hexose+N-acetylhexosamine+fucose+H]⁺. In contrast, core fucosylation was indicated by the formation of the ion assigned as [peptide+N-acetylhexosamine+fucose+H]⁺. *N*-glycans containing *N*-acetylglucosamine (GlcNAc) repeats, were indicated by signals at m/z 731.272 [*N*-acetylhexosamine₂+hexose₂+H]⁺.

Two novel (N₇₄, N₁₆₉) and three already described (N₄₅, N₆₄, N₁₆₂) *N*-glycosylation sites of neutrophil-derived FcγRIIIb were identified. Per site, the nature and number of the glycans differ, and, among other things reflect the extent of biosynthetic processing. The glycan heterogeneity ranges from oligomannose type glycans to highly processed complex type glycans with GlcNAc extensions. Three *N*-glycosylation sites, N₄₅, N₁₆₂ and N₁₆₉, were found to be fully occupied. Glycosylated and non-glycosylated forms of the peptide containing site N₇₄ indicated partial occupancy. This peptide was estimated to be glycosylated at 80%, 64% and 58% for donors 1, 2 and 3, respectively. Site N₆₄ was known to be unoccupied(36) and indeed corresponding peptides were exclusively non-glycosylated. Molecular dynamics simulations of the highly homologous FcγRIIIa (V158 allotype) have shown intramolecular interactions between the peptide backbone residues 60 to 70 and glycans at N₄₅, which may explain a preference for an unoccupied site N₆₄.(30) Moreover, this intramolecular interaction may inhibit enzymatic *N*-glycan processing in the Golgi, explaining the restricted processing at site N₄₅. The occupancy of site N₆₄ appears to be the most prominent difference between neutrophil-bound and soluble FcγRIIIb (**Table S8**); the former unoccupied, the latter displaying highly branched glycans on site N₆₄.(37) Different glycosylation profiles of resting neutrophil-bound FcγRIIIb and soluble FcγRIIIb, released by activated neutrophils,(23) may warrant further study.

MS spectra obtained for sites N₁₆₂ and N₄₅ with annotation of the major glycoforms are given in **Figure 3** and **Figure S6**. For site N₁₆₂, complex di- and triantennary glycans were found accompanied by a small percentage of oligomannose glycans. Site N₄₅ mainly showed oligomannosidic glycans with a significant fraction of hybrid and complex structures. N₇₄ predominantly elaborated as di- to tetraantennary complex glycans with a small amount of oligomannose type glycans. N₁₆₉ was found to exclusively carry di- and triantennary complex glycans.

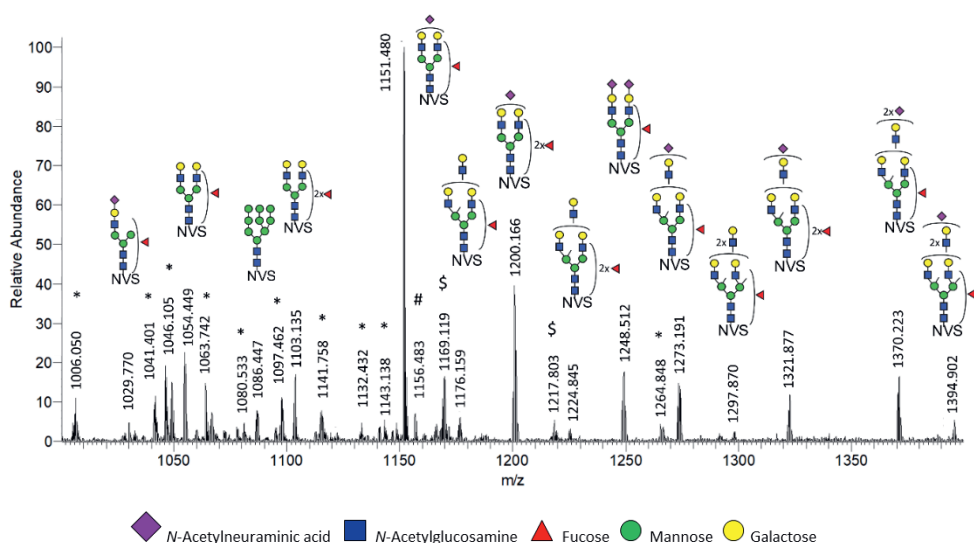


Figure 3. Sum spectra showing the major glycoforms of the N₁₆₂ site. MS sum spectrum (retention time 10.2 to 14.4 min; 94 spectra) showing the major glycoforms of the N₁₆₂ site. Interestingly, ammonia adducts were exclusively observed for glycopeptides carrying an oligomannose glycan, while iron adducts were detected for both oligomannose and complex structures. For more details on MS/MS spectrum see **Figure S9**. *: N₁₆₂ glycopeptides with a miscleaved peptide backbone; #: unidentified glycopeptide (z=2); \$: iron adducts [M+Fe^{III}]³⁺. NVS: CRGLVGSKN₁₆₂VSSE peptide backbone.

4.4.4 Site-specific quantification of FcγRIIIb N-glycans from human neutrophils

The 61 identified glycopeptides were targeted for relative quantification in a site-specific manner (**Figure 4**). FcγRIIIb glycosylation of the three healthy donors displayed very similar glycosylation patterns (**Figure S7**). Derived glycosylation traits — complexity, number of fucoses per glycan and number of sialic acids per glycan — were calculated to facilitate the comparison of the different sites (**Figure S8**) and with other studies (**Table S9**).

As shown in **Figure 4a** and **Table S8**, site N₄₅ was decorated with 86% oligomannose type glycans (M6, M7, M8, M9). Remainders were 7% hybrid (M4A1G1S1, M5A1G1S1, FM4A1G1S1) and 8% complex (A1G1S1, FA1G1S1) type glycans, with and without core fucose. In contrast to soluble FcγRIIIb, containing only oligomannose N-glycans,(36) the neutrophil-bound N₄₅ contains a significant amount of sialylated hybrid and monoantennary complex N-glycans.

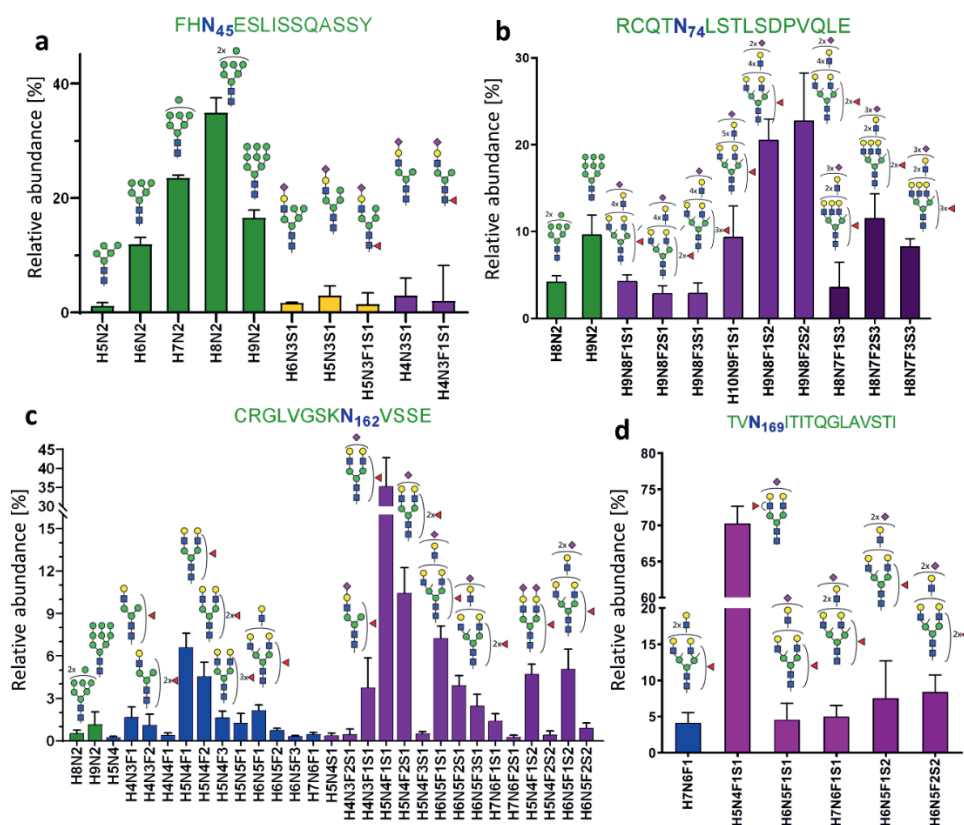


Figure 4. Site-specific, relative quantification of *FcγRIIIb* glycoforms. (a) 10 different glycan compositions occupy the glycosylation site *N*₄₅, (a) 11 compositions on *N*₇₄, (c) 29 compositions on *N*₁₆₂ and (d) 6 compositions on *N*₁₆₉. Mean and SD of three donors are shown. Bar colours indicate glycan classes: Green, oligomannose type; orange, hybrid type; blue, neutral complex; purple, sialylated complex, with one (light), two (medium) or three (dark) sialic acids per glycan.

Site *N*₁₆₂ contained 98% of sialylated, complex, mono- up to triantennary glycans, with some evidence of LacNAc repeats, and 2% of oligomannose glycans (**Figure 4c**). The derived traits revealed a high level of galactosylation and fucosylation, which indicate a high expression of both galactosyltransferases and fucosyltransferases (**Figure S8**). On average, 1.3 fucoses per glycan were displayed on *N*₁₆₂ glycans. Diagnostic ions indicated core fucosylation and antennary fucosylation. Some monofucosylated compositions (H5N4F1S1, H5N4F1) also showed evidence of both core and antennary fucosylated isomers. In comparison to the other glycosylation sites, *N*₁₆₂ possesses the lowest amount of sialic acids per glycan (0.9), which implies poorer accessibility for sialyltransferases.

On site *N*₇₄, sialylated, fucosylated, complex *N*-glycans with multiple LacNAc extensions represent the largest group (86%) of structures (**Figure 4b**). Fragmentation of these glycans resulted in the formation of the oxonium ion of *m/z* 657.237, assigned as [*N*-

acetylglucosamine+galactose+N-acetylneuraminic acid]⁺ (**Table S4**). No evidence for the presence of oligosialylated antennae was seen in the fragments indicating that the tri-sialylated structures are at least triantennary. Even though N₇₄ is not directly involved in antibody binding,(49) there are some speculations regarding LacNAc repetition in cell activation regulation through the modulation of receptor clustering.(50) This site is characterized by the highest numbers of sialic acids (2.1) and fucoses (1.5) per glycan, which implies a high accessibility for sialyltransferases and fucosyltransferases.

Site N₁₆₉ is mainly occupied by a diantennary and monosialylated (H5N4F1S1) structure (**Figure 4d**). Interestingly, core fucosylation at N₁₆₉ was reported for soluble FcγRIIIb, whereas we only observed evidence for antennary fucosylation (**Table S4**). In general, as depicted in **Figure S8**, *N*-glycans modifying N₁₆₉ were fully galactosylated and exhibited a moderate number of sialic acids (1.1) and fucoses (1.1) per glycan.

Overall, we confirmed the presence of antennary fucosylated glycans for three *N*-glycosylation sites, namely N₇₄, N₁₆₂, and N₁₆₉ (**Table S4**). N₇₄ and N₁₆₉ were annotated as predominantly occupied by antennary fucosylated structures, lacking evidence for core fucosylation. In contrast, glycans on N₁₆₂ presented a mixture of both core and antennary fucosylated isomers. In addition to complex type species, oligomannose structures (M8, M9) complement the repertoire of N₇₄ (14%) and N₁₆₂ (2%). For N₇₄, oligomannose structures are being reported for the first time. Interestingly, LacNAc repeats were also detected for some N₁₆₂ glycans (**Table S4**). Generally, the presence of oligomannose type glycoforms is not expected among highly processed glycopeptides. However, it is consistent with a recent glycomics study of FcγRIIIa(24) and with a recent study mapping subcellular glycans during cell maturation in healthy human neutrophils,(51) where different stages of *N*-glycan processing within one site may reflect the developmental stage of granulopoiesis.(51) *N*-glycan processing is initially influenced by the protein expression and precursor availability. Differential processing of the sites, however, is influenced by transferase accessibility which seems to correlate with solvent accessibility. The more exposed an *N*-glycosylated asparagine residue is, the more processed its glycans generally are.(52) Additionally, the large biosynthetic gap between the oligomannose type glycans and the large, (at least partially) tetraantennary glycans may indicate different subcellular fractions. Considering the overall glycosylation pattern of FcγRIIIb in neutrophils, we estimated that nearly all glycans of FcγRIIIb were fully galactosylated, indicating a high activity of galactosyltransferases. Consequently, the partially sialylated and core fucosylated glycans suggest a moderate activity of sialyltransferases and α1,6-fucosyltransferases. Lastly, the high average number of fucose per glycan and MS/MS data for antennary fucosylation were evidence for a high activity of α1,2, α1,3 or α1,4 fucosyltransferases in the neutrophils (**Figure S8b**, **Table S9**).

4.4.5 Comparison of site-specific *N*-glycosylation of FcγRIIIb

Sites N₇₄ and N₁₆₉ of neutrophil-bound FcγRIIIb are profiled for the first time. Otherwise, glycosylation profiles were, both qualitatively and quantitatively, highly consistent between the study of Washburn *et al.* and ours (**Table S8 and Table S9**).⁽³⁶⁾ A minor difference is the observation of oligomannose *N*-glycans at site N₁₆₂ in our study.

Recently, the site-specific glycosylation of human NK cell FcγRIIIa was published.⁽²⁴⁾ Major glycosylation differences in sites N₄₅, N₇₄ and N₁₆₉ clearly distinguish the two FcγRIII isoforms (**Table S8 and S9**). FcγRIIIb showed less processing than FcγRIIIa on N₄₅, having mainly oligomannose glycans, while FcγRIIIa expressed mainly hybrid type glycans. The most pronounced differences were observed in the levels of antennary fucosylation. FcγRIIIb had on average more than one fucose per glycan, up to 1.5 on N₇₄. Moreover, only antennary fucosylation was observed for monofucosylated glycans at site N₁₆₉. In stark contrast, glycoforms of FcγRIIIa are reported to be almost exclusively core fucosylated, except small amounts of antennary fucosylation on sites N₇₄ and N₁₆₂. This hints at a higher activity of α1,2, α1,3 or α1,4 fucosyltransferases in the neutrophils versus NK cells. *N*-glycans at N₁₆₂ showed the highest similarity between the two receptor isotypes. This observation suggests that the glycosylation profiles of this functionally relevant site are conserved among FcγRIII isoforms and cells. However, sialylation of N₁₆₂ appeared lower in neutrophil FcγRIIIb than in NK cell FcγRIIIa with 0.9 and 1.3 sialic acids per glycan at N₁₆₂, respectively.

Notably, glycosylation differences influence FcγRIII properties and function.⁽³⁴⁾ Thus, it is important to use an expressing system that assembles an endogenous-like glycosylation profile for *in-vitro* studies. Among all four mammalian systems producing differently processed *N*-glycans (HEK293, CHO, BHK, NS0),⁽²⁶⁻²⁸⁾ CHO cells constitute a good expression vehicle, where the highly-branched N₇₄ glycans in FcγRIII were carrying LacNAc repetitions. However, to produce antennary fucosylation, prevalent in FcγRIIIb, the HEK293 system constitutes a better vehicle. Additionally, glycoengineering allows to create specific FcγRIIIb structures for functional studies.^(53, 54) The present data indicate that neutrophil-derived FcγRIIIb *N*-glycosylation is rather consistent between healthy individuals, but significantly differs from soluble FcγRIIIb, recombinant or serum-derived, and NK cell-derived FcγRIIIa profiles.

4.5 CONCLUSION

In this study, we describe a straightforward and comprehensive site-specific profiling of FcγRIIIb *N*-glycosylation with a resolution of a single donor. However, by design the approach may be applicable to many different leukocytes.

The observed differences between the plasma-derived and the neutrophil-derived FcγRIIIb demonstrate a significant biological diversity. It would be of great interest to compare FcγRIIIb glycosylation profiles of subcellular fractions or FcγRIIIb from resting neutrophils to soluble receptors in the same donor. The source and impact of the simultaneous similarity,

site N₁₆₂, and dissimilarity, other sites, between FcγRIIIb and FcγRIIIa glycosylation warrants further study as well.

Additional isomer differentiation would also be desirable, but would likely need a separation method with a higher degree of isomers separation.

We believe that a throughput-optimized adaptation of the presented approach could be used in defining glycan signatures of FcγRIII for different pathophysiological conditions in various cell types or even subcellular compartments. This would reveal a yet hidden layer of regulation of antibody-mediated (auto-)immune responses. However, sensitivity should be further improved for such aims. A better understanding of glycosylation as an additional layer of regulation of FcγR activity is likely to improve the performance of antibody-based therapeutic interventions and provide clinical markers for personalized medicine in the long run.

4.6 ACKNOWLEDGMENTS

We thank Gillian Dekkers for expressing the recombinant receptors used in the initial development of the method. This research was supported by the European Union (Glycosylation Signatures for Precision Medicine project, GlySign, Grant No.722095), and the Netherlands Organization for Scientific Research (NWO) via Vernieuwingsimpuls Veni (Project No.722.016.008) and Medium Investment (to P.A.V.; 91116004; partly financed by ZonMw) grants.

4.7 SUPPLEMENTARY MATERIAL

A complete overview of the supplementary material is available online at <https://pubs.acs.org/doi/10.1021/acs.analchem.0c02342>.

Table S1. Information on healthy donors and separated neutrophils cells used for FcγRIIIb isolation.

	Donor 1	Donor 2	Donor 3
Sex	female	male	female
Cell type	neutrophils	neutrophils	neutrophils
Cell count [cell/mL]	50x10 ⁶	50x10 ⁶	50x10 ⁶
Total protein con. [mg/mL]	1.61	1.72	1.51
Amount of cells for isolation [cell/mL]	16x10 ⁶	15x10 ⁶	17x10 ⁶
Volume of lysate for isolation [μL]	310	291	331
Amount of total protein for isolation [μg]	500	500	500

Table S3. The search parameters used for initial analysis using Byonic (Protein Metrics, Cupertino, CA v3.2-38).

Search parameter	Value
Protein database	UniProt human protein database
Glycan database	User defined, see Table S2
Precursor mass tolerance	5 ppm
Fragmentation type	QTOF/HCD
Parent tolerance	0.005 <i>m/z</i>
Fragment mass tolerance	20 ppm
Recalibration (lock mass)	none
Maximum precursor mass	10,000
Precursor and mass charge assignments	compute from MS1
Max # of precursor per scan	2
Smoothing width	0.01 <i>m/z</i>

Table S5. Byonic output of critical parameters reflecting the quality of the peptide-spectrum matches (PSMs) of identified FcγRIIb for each donor. The list of parameters includes: protein p-value (the likelihood of the PSMs to be the identified protein). # unique peptides (total number of PSMs). coverage % (percent of the protein sequence covered by PSMs).

Donor	Protein Identifier	Protein p-value (Log base 10)	# unique peptides	Ranking place	Coverage
1	Low affinity immunoglobulin gamma Fc region receptor III-B UNIPROT: O75015 (FCG3B_HUMAN)	362.01	131	1	77.8 %
2		268.28	127	1	80.3 %
3		250.22	114	1	71.2 %

Table S6. Characterization of predominant human FcγRIIb (UniProtKB - O75015) site-specific peptides and glycopeptides generated from Endoproteinase Glu-C and chymotrypsin cleavage. C, carboxymethyl cysteine

Site	Peptide sequence	Glycosylation	m/z peptide [M+H]	m/z peptide [M+GlcNAc]	RT [min]
Asn 38	missing peptide	NA	NA	NA	NA
Asn 45	FHN(45)ES(47)LISSQASSY	+	1569.708	1772.787	17 - 23
Asn 64	FIDAATVN(64)DSGEY	-	1401.617	1604.696	19
Asn 74	R _C QTN(74)LSTLSDPVQLE	+	1860.901	2063.980	20-28
	R _C QTN(74)LSTLSDPVQLE	-	1860.901	-	25
Asn 162	C _R GLVGSKN(162)VSSE	+	1392.679	1595.758	10 - 14
Asn 169	TVN(169)ITITQGLAV	+	1229.706	1432.779	28 - 32

Table S7. Allelic peptide and glycopeptide sequences containing N45 and N64/D64 used for polymorphic variant assessment. *Uniprot identifiers.

FcγRIII variant	N ₄₅ peptide	N ₆₄ peptide	
NA1 *O75015 (FCG3B*01)	FHN ₄₅ EN(47)LISSQASSY	FIDAATVD ₆₄ DSGEY	
NA2 *O75015 (FCG3B*02)	FHN ₄₅ ES(47)LISSQASSY	FIDAATVN ₆₄ DSGEY	
FcγRIIIa *P08637	FHN ₄₅ ES(47)LISSQASSY	FIDAATVD ₆₄ DSGEY	
DONOR	RATIO ALLOTYPIC		ALLOTYPE
	NES/(NES+NEN)	NDS/(DDS+NDS)	
Donor 1	0.2	0.26	NA1/NA2
Donor 2	0.99	0.98	NA2/NA2
Donor 3	0.99	0.98	NA2/NA2

Table S8. The glycosylation profiles of endogenous neutrophil-derived FcγRIIIb, soluble FcγRIIIb and NK-derived FcγRIIIa. The different glycoforms are displayed as defined derived traits (high mannose, complex, hybrid). *the corresponding glycopeptides were not detected in this study **potential glycosylation site was not occupied by oligosaccharides, only corresponding peptide observed.

Sites	FcγRIIIb – our study (human neutrophils)	sFcγRIIIb(37) (human serum)	FcγRIIIb(36) (human neutrophils)	FcγRIIIa(24) (human natural killer cells)
N ₃₈	-*	Complex (LacNAc repeats) > 99%	- *	Complex (LacNAc repeats) > 99%
N ₄₅	Complex (monoantennary) 8% Hybrid 7% High mannose 86%	High mannose >99%	Complex (monoantennary) 16% Hybrid < 30% High mannose 54%	Complex (di-, tri-, tetra antennary) 22% Hybrid 71% High mannose 2%
N ₆₄	-** (not glycosylated)	Complex (LacNAc repeats) > 99%	- ** (not glycosylated)	-
N ₇₄	Complex (LacNAc repeats) 86% High mannose 14%	Complex (LacNAc repeats) > 99 %	- *	Complex (LacNAc repeats) > 99%
N ₁₆₂	Complex (mono-, di-, tri antennary) 98% High mannose 2%	Complex (di-, tri-, tetraantennary) > 99%	Complex (di-, tri antennary) > 99%	Complex (di-, tri-antennary) 66% Hybrid 22% High mannose 12%
N ₁₆₉	Complex (di-, tri-, tetrantennary) > 99%	Complex (di-, tri-, tetrantennary) > 99%	- *	Complex (di-, tri-, tetrantennary) > 99%

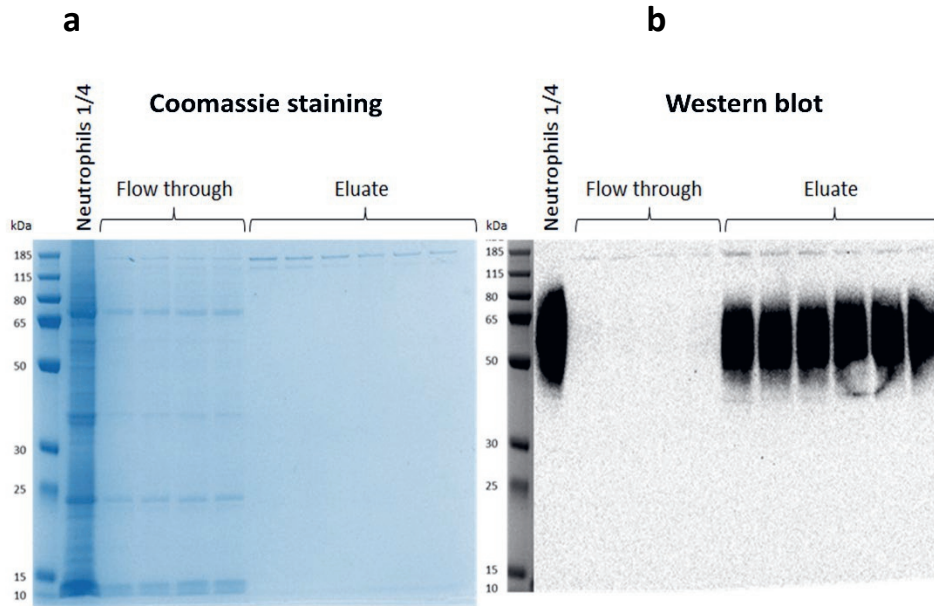


Figure S1. The whole non-reducing SDS-PAGE and western blot of human neutrophil lysate before and after FcγRIIIb immunoprecipitation. Protein contaminations and FcγRIIIb were detected with (a) coomassie staining and (b) western blot, respectively. The neutrophil lanes represent ~25 µg of total protein content from the neutrophil cell lysate from donor 2. In this experiment, the immunoprecipitation was done from 100 µg and the eluate was split between the two gels (50 µg per gel). The flow-through lanes show the unbound diluted fraction of the immunoprecipitation while the eluate lanes present the purified FcγRIIIb protein. As expected, FcγRIIIb exhibits an elongated band from 50 to 80 kDa, visible after western blotting. Despite high dilution, the flow-through mirrors the major bands from the total cell lysate. In contrast, the eluate exhibits none of those bands and thus any interfering proteins of 50-80 kDa above the limit of detection (LOD; 25 ng protein). Two bands around 150 kDa appear in the flow-through and eluate. They are likely derived from the capturing antibody, as an in-solution proteolytic cleavage of the eluate revealed immunoglobulin G glycopeptide masses (data not shown). Whatever the identity of the contamination, it is the main reason to prefer an in-gel proteolytic cleavage.

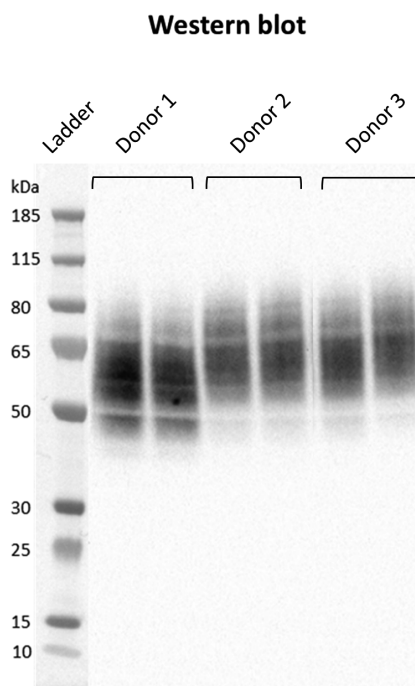


Figure S2. The immunoblot shows FcγRIIIb immunoprecipitated from the lysate of neutrophils. Lanes contain material from donor 1 (NA1/NA2), donor 2 (NA2/NA2) and donor 3 (NA2/NA2) in duplicate. Size markers are indicated on the left. FcγRIIIb showed a smear from 50 to 80 kDa indicating the heterogeneity of the N-glycosylation pattern of the receptor. Differential electrophoretic mobility of the receptor from NA1/NA2-heterozygous and NA2-homozygous is likely mainly due to NA polymorphism and distinct number of N-glycosylation sites.(23) Larger proteoforms attributed to NA2, may not be visible in the first donor, because the protein expression is skewed towards NA1.

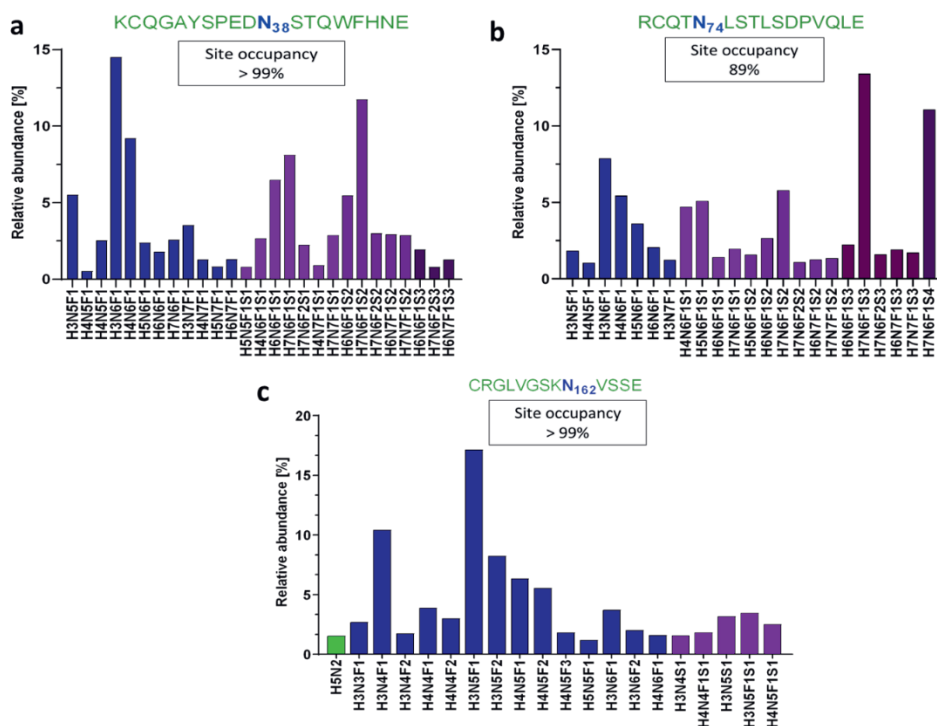


Figure S3. Bar graphs showing the relative abundances of identified glycopeptides for recombinant NA1 allotype of FcγRIIIB(55). Site-specific analysis revealed (a) 27 different glycan compositions occupying the glycosylation site N₃₈, (b) 54 compositions on site N₇₄ and (c) 65 compositions on site N₁₆₂. For sites N₇₄ and N₁₆₂ only compositions above a 1% cut-off of relative abundance were visualized, amounting to 23 and 20 glycans respectively. Full glycosylation site occupancy was observed for N₃₈ and N₁₆₂, while site N₇₄ was partially occupied. 11% relative signal intensity of the non-glycosylated peptide were detected. Sulphated and multifucosylated N-glycan compositions were detected below 1% relative intensity for N₇₄, as were sulphated and disialylated N-glycans for N₁₆₂. Bar colours indicate glycan classes: Green, oligomannose type; blue, neutral complex; purple, sialylated complex, with one (light), two (medium) or three (dark) sialic acids per glycan.

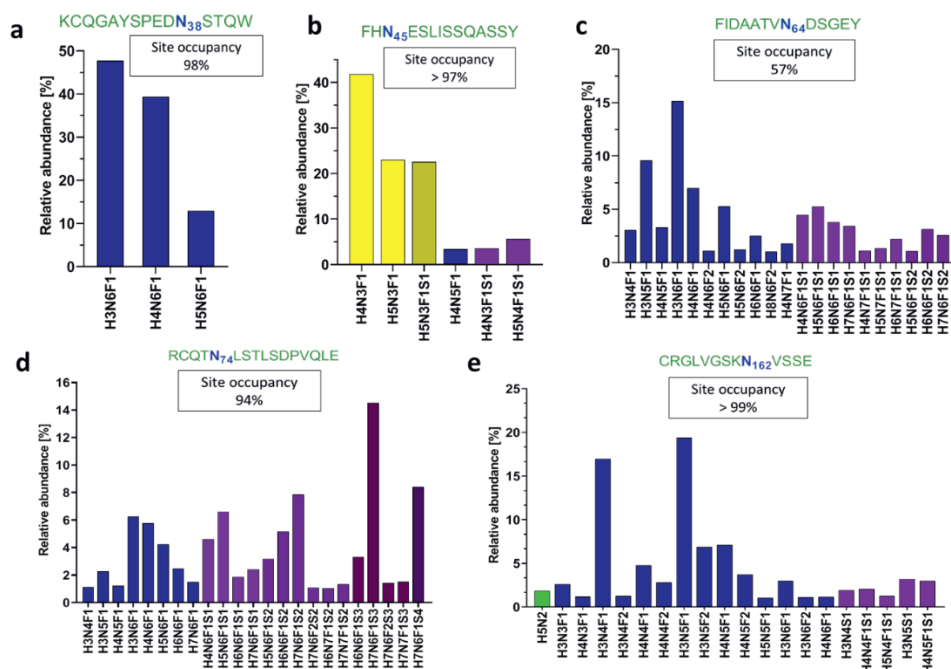


Figure S4. Bar graphs showing the relative abundances of identified glycopeptides for the recombinant NA2 allotype of FcγRIIb(55). Site-specific analysis revealed (a) 3 different glycan compositions occupying the glycosylation site N₃₈, (b) 6 compositions on site N₄₅, (c) 35 compositions on site N₆₄, (d) 49 compositions on site N₇₄ and (e) 69 compositions on site N₁₆₂. For sites N₆₄, N₇₄ and N₁₆₂ only compositions above a 1% cut-off of relative abundance were visualized, amounting to 21, 23 and 20 glycans respectively. Full glycosylation site occupancy was observed for N₄₅ and N₁₆₂, while sites N₃₈, N₆₄ and N₇₄ were partially occupied. 2%, 46% and 7% relative signal intensity of the non-glycosylated peptide for sites N₃₈, N₆₄ and N₇₄ were detected respectively. Multifucosylated N-glycan compositions for N₆₄, sulfated N-glycans for N₇₄ and sulphated and disialylated N-glycans for N₁₆₂ were detected below 1% relative intensity. Bar colours indicate glycan classes: Yellow, hybrid, sialylated hybrid (medium); Green, oligomannose type; blue, neutral complex; purple, sialylated complex, with one (light), two (medium) or three (dark) sialic acids per glycan.

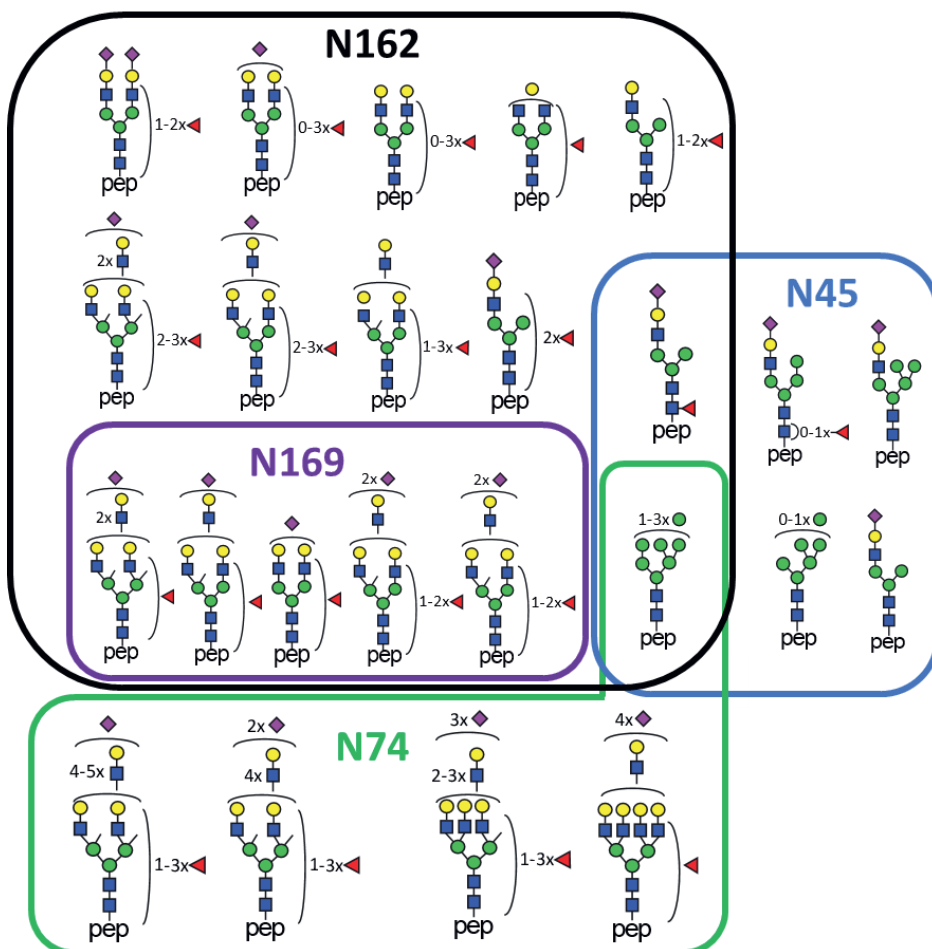


Figure S5. Putative structures of N-glycans identified on the four occupied N-glycosylation sites, namely 10 at N₄₅, 15 at N₇₄, 30 at N₁₆₂ and 6 at N₁₆₉. Isomeric structures co-occur and are discussed in the text. The scheme underlines the diversity, overlap and uniqueness of glycans compositions.

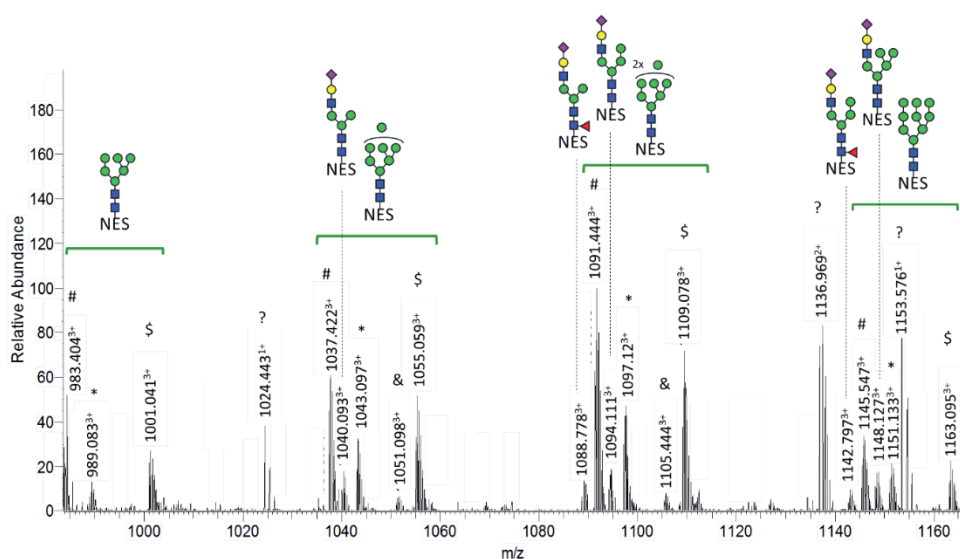


Figure S6. Sum spectra showing the different ions observed for the N_{45} glycoforms of Fc γ RIIb. The mass spectrum was generated for donor 2 within the following retention time range: 17.4-19.4 min. NES: FHN $_{45}$ ESLISSQASSY peptide backbone. The MS spectra revealed satellite peaks for some triply-charged protonated species with a difference of 55.934 Da and 18.033 Da. These were identified by accurate mass (± 5 ppm) as iron ($[M+Fe^{III}]^{3+}$) and ammonia ($[M+2H+NH_4]^{3+}$) adducts, respectively. They also presented the same retention time as the respective protonated glycopeptide. Additionally, the presence of the ammonia adducts was confirmed by MS/MS spectra, as the comparison of the b- and y-ion series provided evidence for the same peptide backbone without additional modification. #: the triply protonated N_{45} glycopeptides $[M+3H]^{3+}$. *: the triply charged ions of protonated N_{45} glycopeptides with ammonia adducts $[M+2H+NH_4]^{3+}$. \$: N_{45} glycopeptides charged by iron ions $[M+Fe^{III}]^{3+}$. &: misscleaved glycopeptide. ?: unidentified glycopeptide.

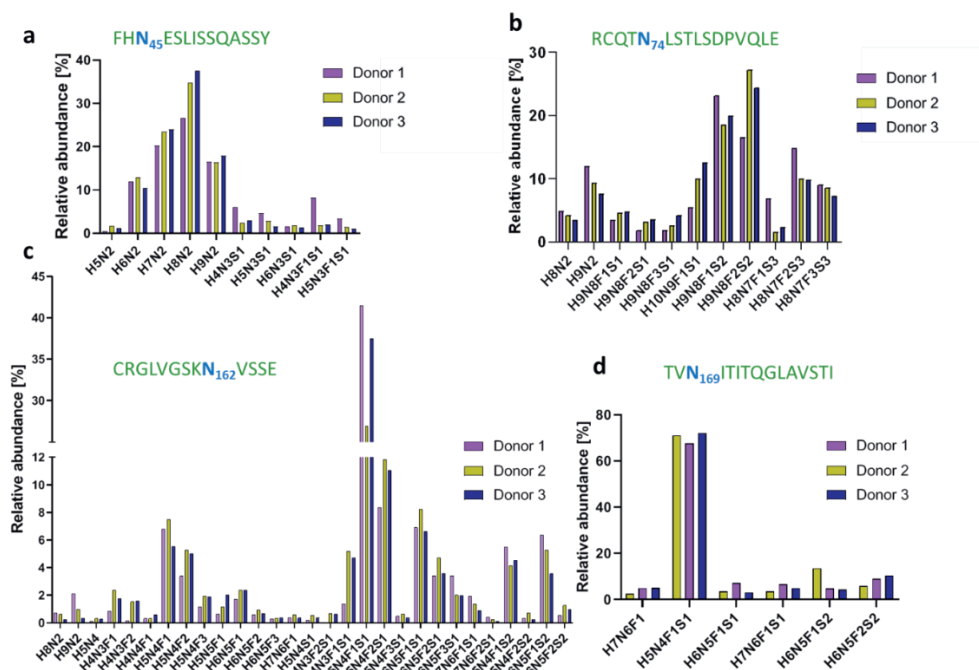


Figure S7. Site-specific relative quantification of FcγRIIIb glycoforms. Bar graphs show the relative abundance of identified glycopeptides for individual donors, donor 1 (NA1/NA2), donor 2 (NA2/NA2) and donor 3 (NA2/NA2). (a) 10 different glycan compositions occupy glycosylation site N₄₅, (b) 11 site N₇₄, (c) 30 site N₁₆₂ and (d) 6 site N₁₆₉.

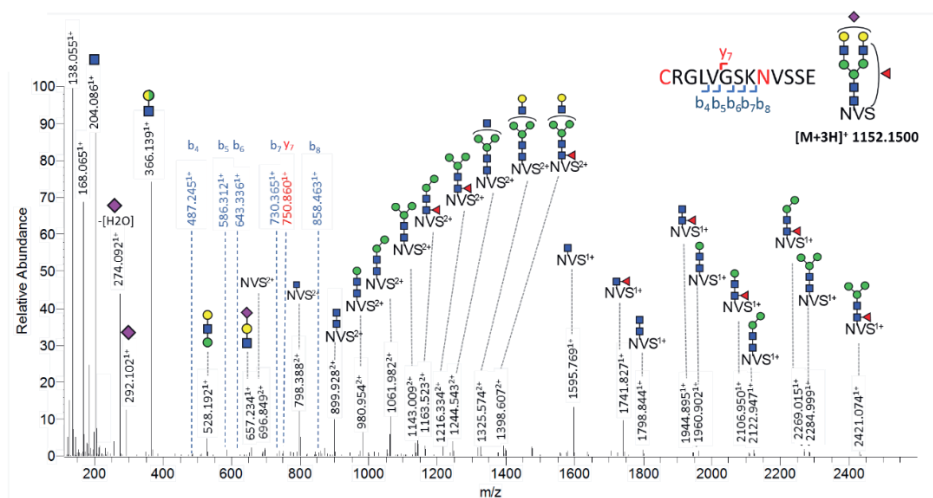


Figure S9. Stepping-energy HCD MS/MS sum spectrum of the precursor ion 1152.1503⁺ [second isotopologue] of the most abundant N₁₆₂ glycopeptide (H5N4F1S1). The MS/MS spectrum was generated for three stepping energies (32%, 37%, 42% NCE) at retention time 11.0 min.

4.8 REFERENCES

1. Nimmerjahn F, Ravetch JV. Fcγ receptors as regulators of immune responses. *Nat Rev Immunol*. 2008;8(1):34-47.
2. Kapur R, Einarsdottir HK, Vidarsson G. IgG-effector functions: "the good, the bad and the ugly". *Immunol Lett*. 2014;160(2):139-44.
3. Ben Mkaddem S, Benhamou M, Monteiro RC. Understanding Fc Receptor Involvement in Inflammatory Diseases: From Mechanisms to New Therapeutic Tools. *Front Immunol*. 2019;10:811.
4. Bournazos S, Woof JM, Hart SP, Dransfield I. Functional and clinical consequences of Fc receptor polymorphic and copy number variants. *Clin Exp Immunol*. 2009;157(2):244-54.
5. Hogarth PM, Pietersz GA. Fc receptor-targeted therapies for the treatment of inflammation, cancer and beyond. *Nat Rev Drug Discov*. 2012;11(4):311-31.
6. Hudis CA. Trastuzumab--mechanism of action and use in clinical practice. *N Engl J Med*. 2007;357(1):39-51.
7. Schwab I, Nimmerjahn F. Intravenous immunoglobulin therapy: how does IgG modulate the immune system? *Nat Rev Immunol*. 2013;13(3):176-89.
8. Cobb BA. The history of IgG glycosylation and where we are now. *Glycobiology*. 2020;30(4):202-13.
9. de Haan N, Falck D, Wuhler M. Monitoring of immunoglobulin N- and O-glycosylation in health and disease. *Glycobiology*. 2020;30(4):226-40.
10. Vidarsson G, Dekkers G, Rispens T. IgG subclasses and allotypes: from structure to effector functions. *Front Immunol*. 2014;5:520.
11. Yamaguchi Y, Barb AW. A synopsis of recent developments defining how N-glycosylation impacts immunoglobulin G structure and function. *Glycobiology*. 2020;30(4):214-25.
12. de Taeye SW, Bentlage A, Mebius MM, Meesters JI, Lissenberg S, Falck D, et al. FcγR binding and ADCC activity of human IgG allotypes *Front Immunol*. 2020.
13. Rosales C. Fcγ gamma Receptor Heterogeneity in Leukocyte Functional Responses. *Front Immunol*. 2017;8:280.
14. Hayes JM, Cosgrave EF, Struwe WB, Wormald M, Davey GP, Jefferis R, et al. Glycosylation and Fc receptors. *Curr Top Microbiol Immunol*. 2014;382:165-99.
15. Bruhns P, Iannascoli B, England P, Mancardi DA, Fernandez N, Jorieux S, et al. Specificity and affinity of human Fcγ gamma receptors and their polymorphic variants for human IgG subclasses. *Blood*. 2009;113(16):3716-25.
16. Roberts JT, Barb AW. A single amino acid distorts the Fc gamma receptor IIIB/CD16b structure upon binding immunoglobulin G1 and reduces affinity relative to CD16a. *J Biol Chem*. 2018;293(51):19899-908.
17. Kara S, Amon L, Luhr JJ, Nimmerjahn F, Dudziak D, Lux A. Impact of Plasma Membrane Domains on IgG Fc Receptor Function. *Front Immunol*. 2020;11:1320.
18. Huizinga TW, Kleijer M, Tetteroo PA, Roos D, von dem Borne AE. Biallelic neutrophil Na-antigen system is associated with a polymorphism on the phospho-inositol-linked Fc gamma receptor III (CD16). *Blood*. 1990;75(1):213-7.
19. Coxon A, Cullere X, Knight S, Sethi S, Wakelin MW, Stavrakis G, et al. Fc gamma RIII mediates neutrophil recruitment to immune complexes. a mechanism for neutrophil accumulation in immune-mediated inflammation. *Immunity*. 2001;14(6):693-704.
20. Chen K, Nishi H, Travers R, Tsuboi N, Martinod K, Wagner DD, et al. Endocytosis of soluble immune complexes leads to their clearance by Fcγ gammaRIIB but induces neutrophil extracellular traps via Fcγ gammaRIIA in vivo. *Blood*. 2012;120(22):4421-31.
21. Wang Y, Jonsson F. Expression, Role, and Regulation of Neutrophil Fcγ gamma Receptors. *Front Immunol*. 2019;10:1958.
22. Salmon JE, Edberg JC, Kimberly RP. Fc gamma receptor III on human neutrophils. Allelic variants have functionally distinct capacities. *J Clin Invest*. 1990;85(4):1287-95.
23. Huizinga TW, de Haas M, Kleijer M, Nuijens JH, Roos D, von dem Borne AE. Soluble Fc gamma receptor III in human plasma originates from release by neutrophils. *J Clin Invest*. 1990;86(2):416-23.
24. Patel KR, Nott JD, Barb AW. Primary human natural killer cells retain proinflammatory IgG1 at the cell surface and express CD16a glycoforms with donor-dependent variability. *Mol Cell Proteomics*. 2019.
25. Roberts JT, Patel KR, Barb AW. Site-specific N-glycan Analysis of Antibody-binding Fc gamma Receptors from Primary Human Monocytes. *Molecular & Cellular Proteomics*. 2020;19(2):362-74.
26. Zeck A, Pohlentz G, Schlothauer T, Peter-Katalinic J, Regula JT. Cell type-specific and site directed N-glycosylation pattern of Fcγ gammaRIIA. *J Proteome Res*. 2011;10(7):3031-9.
27. Kawasaki N, Okumoto T, Yamaguchi Y, Takahashi N, Fridman W, Sautès-Fridman C, et al. Site-Specific Classification of N-Linked Oligosaccharides of the Extracellular Regions of Fcγ Receptor IIIB Expressed in Baby Hamster Kidney Cells. *Journal of Glycomics & Lipidomics*. 2014;4.

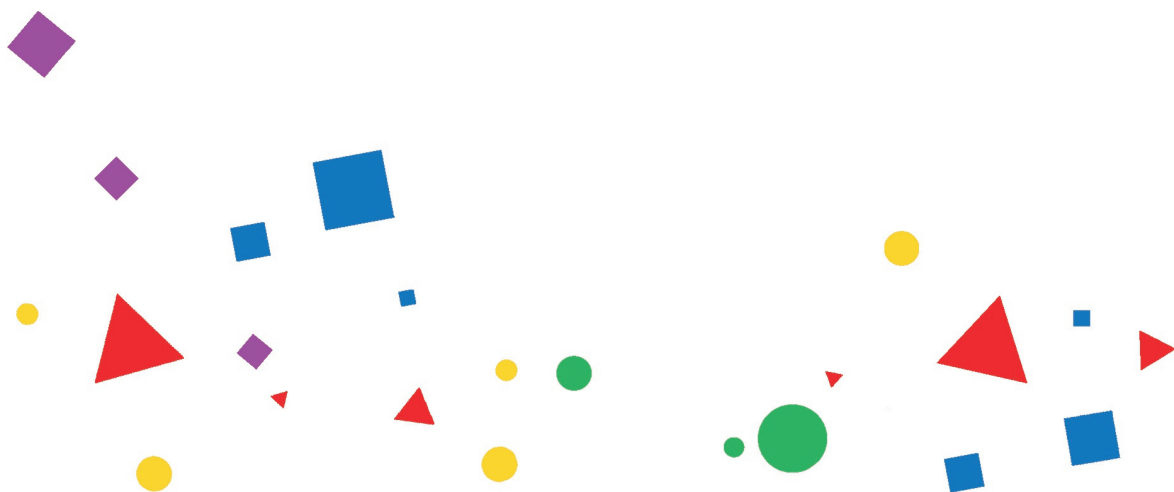
28. Cosgrave EF, Struwe WB, Hayes JM, Harvey DJ, Wormald MR, Rudd PM. N-linked glycan structures of the human Fcγ receptors produced in NS0 cells. *J Proteome Res.* 2013;12(8):3721-37.
29. Ferrara C, Grau S, Jager C, Sondermann P, Brunker P, Waldhauer I, et al. Unique carbohydrate-carbohydrate interactions are required for high affinity binding between FcγRIII and antibodies lacking core fucose. *Proc Natl Acad Sci U S A.* 2011;108(31):12669-74.
30. Subedi GP, Falconer DJ, Barb AW. Carbohydrate-Polypeptide Contacts in the Antibody Receptor CD16A Identified through Solution NMR Spectroscopy. *Biochemistry.* 2017;56(25):3174-7.
31. Shibata-Koyama M, Iida S, Okazaki A, Mori K, Kitajima-Miyama K, Saitou S, et al. The N-linked oligosaccharide at Fc gamma RIIIA Asn-45: an inhibitory element for high Fc gamma RIIIA binding affinity to IgG glycoforms lacking core fucosylation. *Glycobiology.* 2009;19(2):126-34.
32. Dekkers G, Bentlage AEH, Plomp R, Visser R, Koeleman CAM, Beentjes A, et al. Conserved FcγRIIIA-glycan discriminates between fucosylated and afucosylated IgG in humans and mice. *Mol Immunol.* 2018;94:54-60.
33. Hayes JM, Frostell A, Karlsson R, Muller S, Martin SM, Pauers M, et al. Identification of Fc Gamma Receptor Glycoforms That Produce Differential Binding Kinetics for Rituximab. *Mol Cell Proteomics.* 2017;16(10):1770-88.
34. Subedi GP, Barb AW. CD16a with oligomannose-type N-glycans is the only "low-affinity" Fc gamma receptor that binds the IgG crystallizable fragment with high affinity in vitro. *J Biol Chem.* 2018;293(43):16842-50.
35. Patel KR, Roberts JT, Subedi GP, Barb AW. Restricted processing of CD16a/Fc gamma receptor IIIa N-glycans from primary human NK cells impacts structure and function. *J Biol Chem.* 2018;293(10):3477-89.
36. Washburn N, Meccariello R, Duffner J, Getchell K, Holte K, Prod'homme T, et al. Characterization of Endogenous Human FcγRIII by Mass Spectrometry Reveals Site, Allele and Sequence Specific Glycosylation. *Mol Cell Proteomics.* 2019;18(3):534-45.
37. Yagi H, Takakura D, Roumenina LT, Fridman WH, Sautes-Fridman C, Kawasaki N, et al. Site-specific N-glycosylation analysis of soluble Fcγ receptor IIIb in human serum. *Sci Rep.* 2018;8(1):2719.
38. Riley NM, Hebert AS, Westphall MS, Coon JJ. Capturing site-specific heterogeneity with large-scale N-glycoproteome analysis. *Nat Commun.* 2019;10(1):1311.
39. Zhu J, Lin YH, Dingess KA, Mank M, Stahl B, Heck AJR. Quantitative Longitudinal Inventory of the N-Glycoproteome of Human Milk from a Single Donor Reveals the Highly Variable Repertoire and Dynamic Site-Specific Changes. *J Proteome Res.* 2020;19(5):1941-52.
40. Candiano G, Bruschi M, Musante L, Santucci L, Ghiggeri GM, Carnemolla B, et al. Blue silver: a very sensitive colloidal Coomassie G-250 staining for proteome analysis. *Electrophoresis.* 2004;25(9):1327-33.
41. Kuijpers TW, Tool AT, van der Schoot CE, Ginsel LA, Onderwater JJ, Roos D, et al. Membrane surface antigen expression on neutrophils: a reappraisal of the use of surface markers for neutrophil activation. *Blood.* 1991;78(4):1105-11.
42. Shevchenko A, Wilm M, Vorm O, Mann M. Mass spectrometric sequencing of proteins silver-stained polyacrylamide gels. *Anal Chem.* 1996;68(5):850-8.
43. Shevchenko A, Tomas H, Havlis J, Olsen JV, Mann M. In-gel digestion for mass spectrometric characterization of proteins and proteomes. *Nat Protoc.* 2006;1(6):2856-60.
44. Gundry RL, White MY, Murray CI, Kane LA, Fu Q, Stanley BA, et al. Preparation of proteins and peptides for mass spectrometry analysis in a bottom-up proteomics workflow. *Curr Protoc Mol Biol.* 2009;Chapter 10:Unit10 25.
45. Bern M, Kil YJ, Becker C. Byonic: advanced peptide and protein identification software. *Curr Protoc Bioinformatics.* 2012;Chapter 13:Unit13 20.
46. Jansen BC, Falck D, de Haan N, Hipgrave Ederveen AL, Razdorov G, Lauc G, et al. LaCyTools: A Targeted Liquid Chromatography-Mass Spectrometry Data Processing Package for Relative Quantitation of Glycopeptides. *J Proteome Res.* 2016;15(7):2198-210.
47. Galon J, Moldovan I, Galinha A, Provost-Marloie MA, Kaudewitz H, Roman-Roman S, et al. Identification of the cleavage site involved in production of plasma soluble Fc gamma receptor type III (CD16). *Eur J Immunol.* 1998;28(7):2101-7.
48. Breunis WB, van Mirre E, Geissler J, Laddach N, Wolbink G, van der Schoot E, et al. Copy number variation at the FCGR locus includes FCGR3A, FCGR2C and FCGR3B but not FCGR2A and FCGR2B. *Hum Mutat.* 2009;30(5):E640-50.
49. Sondermann P, Huber R, Oosthuizen V, Jacob U. The 3.2-A crystal structure of the human IgG1 Fc fragment-Fc gammaRIII complex. *Nature.* 2000;406(6793):267-73.
50. Demetriou M, Granovsky M, Quaggin S, Dennis JW. Negative regulation of T-cell activation and autoimmunity by Mgat5 N-glycosylation. *Nature.* 2001;409(6821):733-9.
51. Venkatakrishnan V, Dieckmann R, Loke I, Tjondro H, Chatterjee S, Bylund J, et al. Glycan analysis of human neutrophil granules implicates a maturation-dependent glycosylation machinery. *J Biol Chem.* 2020.

52. Thaysen-Andersen M, Packer NH. Site-specific glycoproteomics confirms that protein structure dictates formation of N-glycan type, core fucosylation and branching. *Glycobiology*. 2012;22(11):1440-52.
53. Hayes JM, Wormald MR, Rudd PM, Davey GP. Fc gamma receptors: glycobiology and therapeutic prospects. *J Inflamm Res*. 2016;9:209-19.
54. Buettner MJ, Shah SR, Saeui CT, Ariss R, Yarema KJ. Improving Immunotherapy Through Glycodesign. *Front Immunol*. 2018;9:2485.
55. Dekkers G, Treffers L, Plomp R, Bentlage AEH, de Boer M, Koeleman CAM, et al. Decoding the Human Immunoglobulin G-Glycan Repertoire Reveals a Spectrum of Fc-Receptor- and Complement-Mediated-Effector Activities. *Front Immunol*. 2017;8:877.

¹ *Center for Proteomics and Metabolomics, Leiden University Medical Center, Leiden,
The Netherlands*

² *Glycoscience Research Laboratory, Genos Ltd., Zagreb, Croatia*

³ *Faculty of Pharmacy and Biochemistry, University of Zagreb, Zagreb, Croatia.*



Chapter 5

High-throughput N-glycan profiling of plasma and serum using a routine and robust LC-MS analysis platform

Iwona Wojcik^{1,2}, Maja Pučić-Baković², Gordan Lauc^{2,3}

Manuscript to be submitted



5.1 ABSTRACT

Alterations in the composition of plasma and serum N-glycome have been linked to many diseases, such as metabolic, autoimmune and infectious diseases. As a result, the discovery and detailed characterization of clinically relevant N-glycome signatures is a primary interest of biomedical research. While the complexity of the plasma and serum samples makes comprehensive analysis challenging, the recent advances in released N-glycan analysis have greatly simplified sample preparation and increased analytical sensitivity, specificity and throughput. Here we describe the development and optimization of a 96-well plate format method to chromatographically separate and profile plasma and serum N-glycans labeled with *RapiFluor*-MS by hydrophilic interaction liquid chromatography-mass spectrometry (HILIC-LC-MS) using a routine LC-MS analysis platform (BioAccord LC-MS system, Waters Corporation). The improved method for plasma and serum N-glycan profiling takes advantage of rapid protein denaturation, deglycosylation, and fluorescent derivatization with *RapiFluor*-MS label and offers a high sensitivity and reproducibility of the N-glycan profile. The HILIC-UPLC-MS profile of total N-glycome comprised 44 individual glycan peaks with 72 assigned N-glycan compositions. We also demonstrated its capability to reveal the biological variability of the serum N-glycome in a robust and high-throughput manner. This improved methodology provides a powerful tool in support of the rapid advancement of glycan analysis for biopharmaceutical development and biomarker discovery.

5.2 INTRODUCTION

Protein glycosylation is an enzymatic process catalyzing the addition of monosaccharides to create a variety of glycan structures on protein molecules. As an integral part of proteins, glycans modulate their physical and biological properties, including folding, solubility, stability, binding affinity and specificity, and biological activity.(1) In addition, glycosylation is recognized to play an essential role in almost every aspect of biological processes, such as cell migration, cell differentiation, inflammatory response and immune regulation.(2) In clinics, growing attention has been directed to an easily obtainable biofluid like plasma or serum (the fluid left after the plasma has clotted) since changes in plasma and serum N-glycome have been linked to many diseases, such as metabolic, autoimmune and infectious diseases, and cancer.(3, 4) All of this opens up the possibility to use plasma and serum N-glycans as potential biomarkers of major diseases. Thus, there is a great deal of interest in the development of a simple, robust and high-throughput methodology for the rapid analysis of total plasma/serum protein glycosylation.

The analysis of protein N-glycosylation can be performed at various levels of characterization, ranging from the analysis of an intact purified glycoprotein to the analysis of the total released glycome of complex biological matrices. Released N-glycan profiling has become the most prevalent strategy for high-throughput analysis of total plasma and serum N-glycome.(5) This strategy includes an enzymatic release of N-glycans, labeling of released N-glycans with a fluorescent dye, purification, and finally profiling of fluorescently labeled N-glycans using hydrophilic interaction chromatography (HILIC).(6) Chromatographic separation can be complemented with the orthogonal method, such as mass spectrometry (MS) analysis which provides rapid and confident identification of glycan structures based on accurate mass measurements.(5) Recent advances in sample preparation have driven the progression in the released N-glycan analysis. For example, the effort needed for released glycan sample preparation has been reduced by the recent introduction of the surfactant-assisted deglycosylation and the novel *RapiFluor*-MS (RF-MS) labeling reagent incorporated in the available GlycoWorks RF-MS N-glycan Kit (Waters Corporation).(7) With this, the standard sample preparation procedure has been simplified, sample preparation time reduced from two days to 1.5 h for 96 samples, and both fluorescence and mass spectrometric sensitivity enhanced, facilitating glycan characterization and peak identification.(8, 9) However, while the applicability of the GlycoWorks RF-MS N-glycan Kit has only been established in small and large-scale studies of isolated glycoproteins, such as Immunoglobulin G,(8, 10) it has not been validated for its applicability in the glycosylation analysis of complex sample types, such as plasma or serum.

Thus, we developed and optimized a method to chromatographically separate and profile plasma and serum N-glycans labeled with RF-MS by hydrophilic interaction liquid chromatography-mass spectrometry (HILIC-LC-MS) on a BioAccord LC-MS System. Using

this method, serum N-glycans from 483 individual/biological samples were profiled with a very good chromatographic resolution and repeatability enabling a robust and high-throughput detection, identification and quantification of the plasma and serum N-glycome.

5.3 EXPERIMENTAL SECTION

5.3.1 Sample description

The pooled plasma standard was used for the method development and all optimization experiments. For the method validation, 483 serum samples were obtained longitudinally from 89 patients with asymptomatic and mild COVID-19 from the Injury, Inflammation and Recovery Unit, School of Medicine, University of Nottingham, Nottingham (UK). The serum samples were collected within two months, with a one-week interval. All of the participants provided written informed consent to participate in the study. The baseline characteristics of the study participants are summarized in **Table S1**.

5.3.2 Enzymatic release and labeling of plasma and serum N-glycans

The N-glycans from total plasma or serum proteins were released, labeled, and purified with the HILIC solid phase extraction (HILIC-SPE) in a 96-well format using the GlycoWorks *RapiFluor*-MS N-Glycan Kit obtained from Waters Corporation (Milford, MA, USA). All steps were done in accordance with the Waters Corporation protocol (“GlycoWorks *RapiFluor*-MS N-Glycan Kit Care and Use Manual”; p/n 715004793). The only modification was that all plasma and serum samples (10 µL) were aliquoted to 1 mL 96-well collection plates and diluted 70x with ultrapure water (690 µL) prior to the deglycosylation step. The dilution was made to ensure the sample's recommended protein concentration of 15 µg. Next, 10 µL of the diluted sample was loaded into a 96-well PCR plate (Eppendorf, Hamburg, Germany). GlycoWorks kit reagents including *RapiGest* surfactant, Rapid PNGase F enzyme, and *RapiFluor*-MS labeling agent were subsequently added to each sample for protein denaturation, deglycosylation, and labeling, respectively. After the glycan labeling, the HILIC-SPE step was performed using GlycoWorks µElution Plate. *RapiFluor*-MS labeled glycans were eluted with 90 µL of the GlycoWorks SPE Elution Buffer (200 mM ammonium acetate in 5% acetonitrile). After elution, 310 µL of the GlycoWorks Sample Diluent-DMF/ACN was added to each sample and frozen at -80 °C until LC-MS run.

5.3.3 Liquid chromatography method optimization

RF-MS labeled plasma and serum N-glycans were analyzed via HILIC-LC-MS with a BioAccord LC-MS System consisting of an ACQUITY UPLC I-Class PLUS and an ACQUITY RDa time-of-flight (TOF) mass spectrometer (Waters Corporation). The separation was carried out on an ACQUITY UPLC Glycan BEH Premier Amide chromatography column (130Å, 1.7 µm, 2.1 x 150 mm; Waters Corporation). To improve the chromatographic separation, parameters

including mobile phase ionic strength, column temperature, gradient, and flow rate were optimized through the study. The following concentrations of aqueous mobile phase A (ammonium formate in ultrapure water, pH 4.4) were evaluated: 50 mM, 100 mM and 200 mM. Mobile phase B was 100% acetonitrile (ACN, Honeywell, USA), and a number of linear gradient ranges of solvents in 35 min analytical run were explored: (I) 75-54%, (II) 73-54 %, (III) 72-54%, (IV) 71-54%, and (V) 70-54% of solvent B. Several analytical column temperatures were tested: 60, 45, and 30 °C. Two different analytical flows were used: 0.4 and 0.5 mL/min. The detailed gradient conditions of both the Universal N-Glycan Profiling Method and the optimized Plasma/Serum N-Glycome Profiling Method are listed in the **Supporting Information**.

5.3.4 Mass spectrometric analysis

The released and separated N-glycans were analyzed on-line via electrospray ionization in a positive mode using an ACQUITY RDa (TOF) mass spectrometer. The settings were as follows: range, 50–2000 m/z ; capillary voltage, 1.5 kV; cone voltage, 45 V; desolvation temperature, 300 °C; and sampling rate, 2 Hz. Mass spectra were acquired under the “Full MS scan” mode. *RapiFluor-MS* Dextran Calibration Ladder (Waters Corporation) was injected into LC-MS to calibrate the retention time of glycan peaks. The retention times were normalized using the dextran calibration curve to Glucose Units (GU).

5.3.5 Linearity

Assuming that the protein content of the plasma/serum is 70 $\mu\text{g}/\mu\text{L}$, (Anderson et al., 2004; Leeman et al., 2018) dilution series of the plasma donor sample were prepared in triplicates resulting in theoretical protein amounts ranging from 0.6 to 15.3 μg (**Table S3**). To determine linearity, a curve was obtained by plotting the fluorescent signal as a function of the theoretical protein amount (**Figure S1 – S5**). The results were investigated for five different types of N-glycans by linear regression and the linear regression coefficient was determined to assess the linearity of the system.

5.3.6 Validation

The utility of the optimized Plasma/Serum N-Glycome Profiling Method was evaluated by determining the total serum protein N-glycosylation in a cohort of patients with asymptomatic and mild COVID-19. In addition to 483 biological samples, 36 in-house plasma standards and 6 blanks (ultrapure water) were included in the study to serve as positive and negative controls. All samples were randomized and distributed over six 96-well plates. Subsequently, samples were subjected to N-glycan release and RF-MS labeling followed by HILIC-LC-MS analysis utilizing the optimized LC method for human plasma/serum N-glycans.

5.3.7 Data analysis

Chromatographic and MS data were processed using UNIFI Scientific Information System (Waters Corporation). The chromatograms were integrated in a semi-automated way into 44 peaks (**Figure 3**), and the relative quantification of glycans in each peak was obtained by area-under-curve measurements and expressed as a percentage of the total integrated area (% Area). Initially, the N-glycan structural assignment was done automatically by the waters_connect software (UNIFI application) based on the obtained glucose units (GU) matched to the reference values in the relevant waters_connect library. Additionally, all N-glycan identifications were further manually verified and extended based on the recorded *m/z* values in MS1 sum spectra generated for each chromatographic peak. The manually detected *m/z* values were converted to singly charged ions and characterized with the aid of the glycobioinformatics tools GlycoMod (<https://web.expasy.org/glycomod/>) and according to previously published and annotated plasma and serum N-glycome profiles.(11, 12) Based on the 44 directly measured N-glycan-containing peaks, 16 derived glycosylation traits reflecting the main structural characteristics and common enzymatic activities were calculated (**Table S2**). The repeatability of the method was assessed by measuring the coefficient of variation (CV) of the pooled plasma standard technical replicates. Data were analyzed and visualized using R Statistical Software (version 4.2.1, R Core Team 2021).

5.4 RESULTS and DISCUSSION

5.4.1 Optimization of the HILIC-LC-MS separation method for plasma and serum N-glycans

To develop a reproducible and robust HILIC-LC-MS separation method specifically tailored for N-glycans released from total proteins of human plasma and serum, we used the Universal N-glycan profiling method from Waters as a starting point.(13) The universal method was established for the separation of all types of N-glycans on an ACQUITY UPLC Glycan BEH Amide columns. However, it is not optimized for any particular N-glycan sample and optimization of chromatographic conditions might be necessary. Thus, the initial fluorescence (FLR) chromatograms of *Rapi*Fluor-MS labeled plasma N-glycans, which were generated with 60 °C column temperature, 50 mM ammonium formate as a mobile phase A, and a gradient from 75% to 54% of LC-MS grade ACN (mobile phase B), showed substantial peak broadening, considerable tailing, and inadequate peak resolution (**Figure 1**).

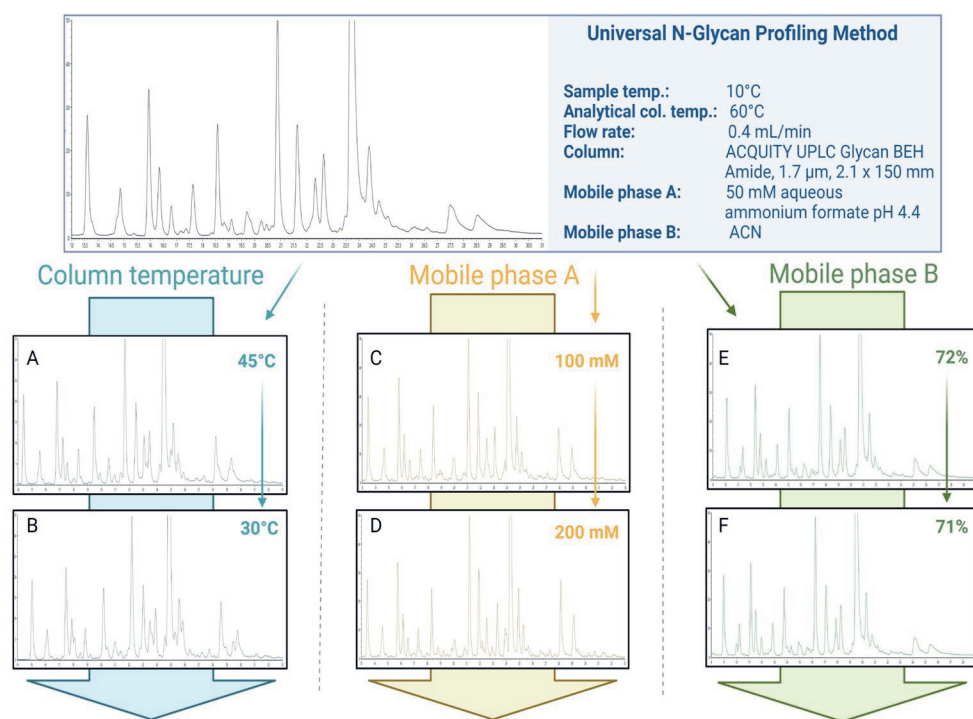


Figure 1. Optimization of HILIC-UPLC-FLR conditions to improve peak separation of plasma N-glycans labeled with RF-MS. Initial FLR chromatograms (first row) of RF-MS labeled N-glycans were obtained at 60 °C column temperature, with 50 mM ammonium formate, pH 4.4, as a mobile phase A, and a gradient from 75% to 54% LC-MS grade ACN (mobile phase B). The following chromatograms (second and third row) present the effect of the reduced column temperature: 45 °C (A) and 30 °C (B); higher aqueous mobile phase ionic strengths: 100 mM (C) and 200 mM (D) ammonium formate; and the lowered initial concentration of mobile phase B: 72% (E) and 71% (F) on FLR plasma N-glycome separation profile.

In order to improve the chromatographic separation and facilitate reliable quantification of plasma and serum N-linked glycans, the benchmark method was subjected to further optimization, where several factors such as temperature, mobile phase ionic strength, flow rate, and the gradient slope have been modified (**Figure 1, A-F**). All the modified factors, except for the flow rate, resulted in improved chromatographic separation. The mobile phase flow rate adjustment from initial 0.4 to 0.5 mL/min had a minimal effect on the N-glycan profile (data not shown), which is why the flow rate as a factor was excluded from further optimization. Regarding the temperature, we observed that reducing the column temperature from 60 °C to 30 °C improved resolution in the second part of the chromatogram (peak GP25 to GP44), but at the cost of peak capacity at the beginning of the chromatogram (GP6, 7 and 8). Hence, to allow for improved resolution and at the same time to preserve peak capacity we chose 45 °C as column temperature. In the context of peak shape, numerous glycan structures were shown to have sharper peaks as the column temperature decreased (GP25, GP26, GP37, GP38). Next, in order to explore the influence

of the ionic strength of aqueous mobile phase A, the concentration of ammonium formate was increased from 50 mM to 100 and 200 mM. As shown in previous studies,(14) increasing ammonium formate concentration improved both the peak shape and chromatographic resolution of sialylated glycans (GP37, GP38). However, mobile phases with high concentrations of ion pairing reagent may lead to a shortened column lifetime, hence, we chose 100 mM ammonium formate as a final concentration. Next, we modified the slope of the gradient by reducing the initial % of mobile phase B from 75 to 70%. Compared to the universal method, a new, reduced gradient slope running from 71% - 54% mobile phase B resulted in significant improvement in peak resolution observed for two co-eluting glycans at the beginning of the chromatogram (GP2 and GP3).

The improvements in the HILIC-LC-MS method outlined above, such as the column temperature at 45 °C, 100 mM ammonium formate as a mobile phase A, gradient slope from 71% to 54% mobile phase B, and 0.4 mL/min flow rate resulted in a number of significant improvements in chromatographic separation of plasma N-glycans labeled with *Rapi*Fluor-MS compared to the Universal profiling method. Therefore, they were chosen as the final conditions for the HILIC-LC-MS separation. The most prominent improvements were seen for high mannose and sialylated glycan structures. For example, peaks GP3, GP9, and GP21, corresponding to high mannose (M5, M6) and disialylated glycans (FA2G2S2), co-eluted with other glycan structures when analyzed by the universal method, but they were resolved when the optimized method was used (**Figure 2**). Moreover, the adjustments of the benchmark method resulted in reduced peak broadening of sialylated structures, such as A2G2S2 (GP25), FA2G2S2 (GP26), FA2BG2S2 (GP27), as well as A3G3S3 (GP37) and A3F1G3S3 (GP38). This, in turn, facilitated the enhanced resolution of the aforementioned sialylated N-glycans.

With the use of the developed method, plasma N-glycome was integrated and separated into 44 chromatographic peaks (**Figure 3**). Next, by using the MS data simultaneously generated by the BioAccord system, we could determine N-glycan compositions that elute in each chromatographic peak. A total of 54 major and 15 minor N-glycan compositions were successfully identified (**Table S4**). To a large extent, the RF-MS plasma N-glycan profile deciphered in this study matched with the previously profiled plasma N-glycans labeled with 2-AB, with A2G2S2, A2G2S1, FA2G1, FA2, FA2G2, FA2G2S1, and A3G3S3 species being the most abundant in the spectrum.(11) However, previous studies quantified only 39 glycan peaks. This is due to the fact that the hydrophobicity of the RF-MS label is different from 2-AB resulting in the different migration patterns of several high mannose species, such as M5 (GP3), M6 (GP9), and M8 (GP19) (**Figure 3**). Notably, using optimized conditions those high mannose species appeared as individual peaks and did not co-elute with FA2B or FA2[3]BG1 as was the case in the previous study.

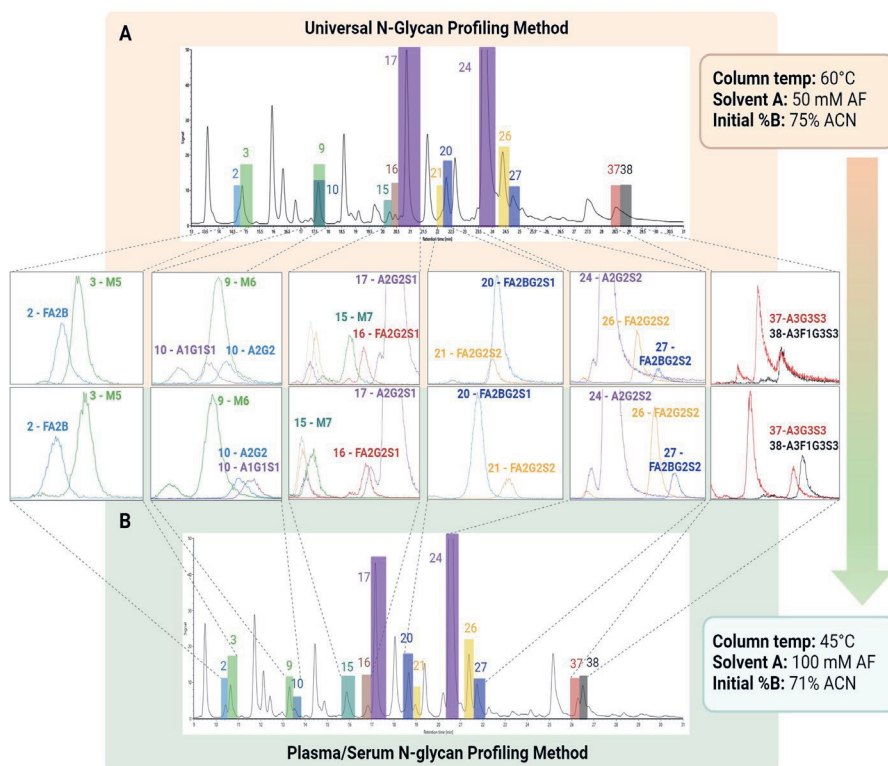


Figure 2. Improvements in RF-MS labeled plasma N-glycan peak separation obtained using the optimized N-glycan profiling method. (A) Fluorescence (FLR) chromatogram and extracted ion chromatograms (XICs) obtained with the universal N-glycan profiling method (60 °C column temperature, 50 mM mobile phase A, gradient from 75% to 54% ACN). (B) FLR chromatogram and XICs obtained with the optimized method for plasma N-glycan profiling (45°C column temperature, 100 mM mobile phase A, gradient from 71% to 54% ACN). The six most prominent differences in glycan separation are shown.

Finally, to examine potential differences in HILIC-LC-MS profiles between plasma and serum RF-MS labeled N-glycans, we compared the profiles of a pooled plasma standard and three randomly chosen serum samples from the validation cohort (data not shown). Our analysis revealed no difference in N-glycome composition (the same structures were observed in both types of samples). There were only minor differences in the abundances of certain N-glycan structures within the same peak, suggesting that the developed separation method is suitable for both plasma and serum N-glycome profiling.

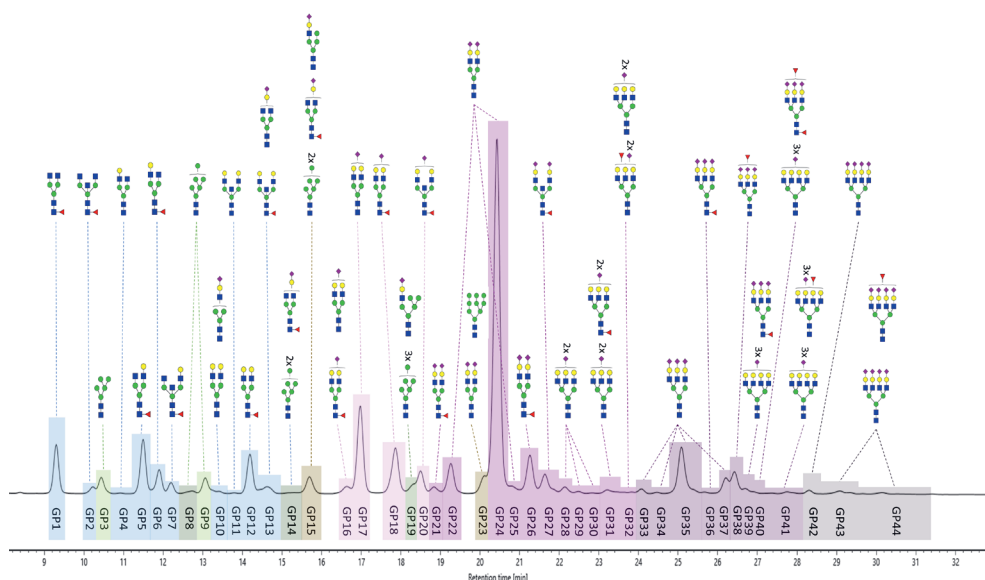


Figure 3. HILIC-UPLC-FLR separation of total N-glycans released from human plasma glycoproteins and labeled with RF-MS. The chromatograms were separated into 44 chromatographic glycan peaks (GP1-GP44). The N-glycans in each chromatographic peak were assigned based on respective MS1 sum spectra and established literature on plasma N-glycosylation. The structures of the most abundant glycans are shown for each peak. For the complete assignment of the glycan peaks, see **Supplementary Table S4**.

5.4.2 Linearity of the HILIC-LC-MS separation method

Equally important as HILIC separation conditions, is the amount of plasma and serum proteins used for the sample preparation step. The recommended amount of glycoproteins for the enzymatic release and RF-MS labeling of N-glycans using Waters GlycoWorks RF-MS N-Glycan Kit is 15 μg . The protein concentration in plasma and serum is approximately 60–80 $\mu\text{g}/\mu\text{L}$.^(15, 16) Hence, according to the theoretical protein concentration, we determined a range of the starting volume of plasma and serum which results in robust release and labeling of N-glycans. The linear range of detection for the FLR signal was determined for various N-glycan structures in the standard sample (**Figure S1–S5**). The linear response of the selected glycan peaks ($R \geq 0.9879$) demonstrated the applicability of the optimized method for profiling plasma and serum N-glycans labeled with RF-MS. The linearity was already achieved with the theoretical amount of 0.6 μg of proteins. However, to facilitate the robustness of the method, the protein amount of 9.5 μg in the middle of the linear range was chosen for further experiments.

5.4.3 Validation of the HILIC-LC-MS separation method

To elucidate the applicability of the developed Plasma/Serum N-glycan Profiling Method and especially its ability to reveal clinically relevant glycosylation changes, the total serum

N-glycome from 483 biological samples was analyzed. Next to the cohort samples, 36 replicates of pooled plasma standard samples were distributed throughout six sample plates.

For all samples, the analysis was performed in a 96-well based-format and 44 glycan chromatographic peaks were quantified. Furthermore, the individual peaks were systematized into 16 glycosylation traits reflecting a common biosynthetic pathway: high-mannose (HM), low branching (LB), high branching (HB), agalactosylation (G0), monogalactosylation (G1), digalactosylation (G2), trigalactosylation (G3), tetragalactosylation (G4), core fucosylation (CF), antennae fucosylation (AF), bisection (B), and asialylation (S0), monosialylation (S1), disialylation (S2), trisialylation (S3), and tetrasialylation (S4) (**Table S2**). The repeatability of the method was assessed by measuring the coefficient of variation (CV) for 36 replicates of pooled plasma standard samples. The average coefficient of variation for all 44 glycan peaks was only 4.7% indicating a very good analytical precision (**Figure S6**).

In order to demonstrate the potential of the method to detect biological variability among individuals in the cohort, we calculated relative abundances for each glycosylation trait in total serum N-glycome for each analyzed sample (**Figure 4**). We observed that the biological variability of all the glycosylation traits among the study population is higher than the technical variation of the standard samples. Thus, the optimized HILIC profiling method would be suitable to capture potential changes in serum and plasma N-glycome composition.

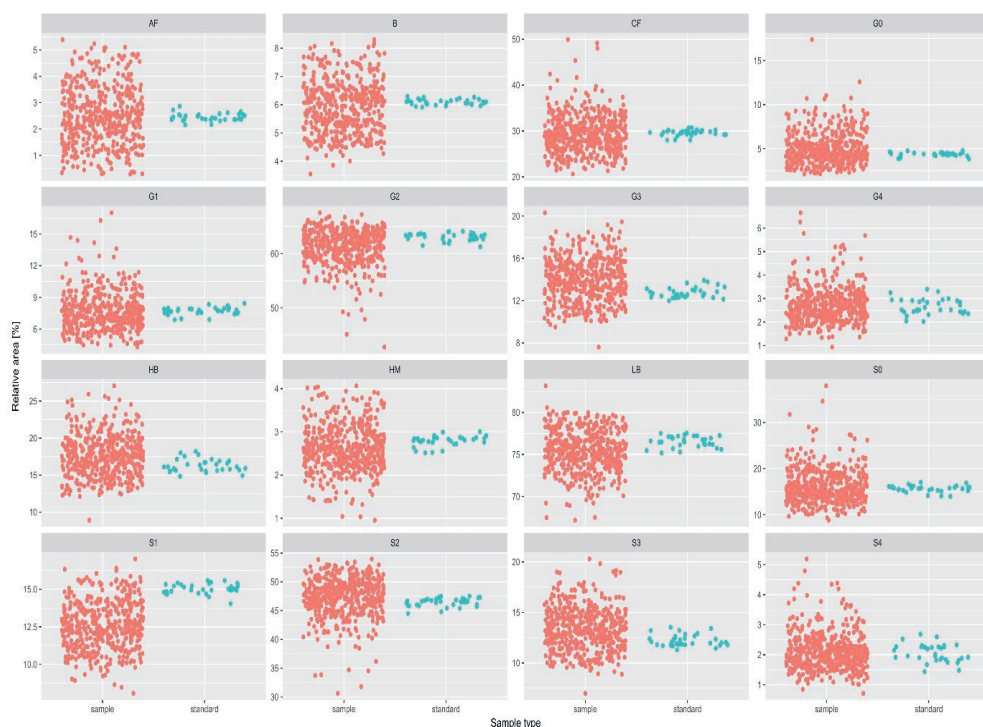


Figure 4. Biological and technical variability of studied individuals (red) and standard samples (blue), respectively, for major traits of serum N-glycans (antennary fucosylation (AF), bisection (B), core fucosylation (CF), agalactosylation (G0), monogalactosylation (G1), digalactosylation (G2), trigalactosylation (G3), tetragalactosylation (G4), high branching (HB), high mannosylation (HM), low branching (LB), asialylation (S0), monosialylation (S1), disialylation (S2), trisialylation (S3) and tetrasialylation (S4)). Relative abundances of derived glycan traits in total serum N-glycome are shown.

5.5 CONCLUSION

We have optimized the HILIC-LC-MS method to analyze N-glycans released from total human plasma and serum proteins and labeled with *RapiFluor*-MS. The developed approach combining the advantages of GlycoWorks N-glycan sample preparation with the separation capabilities of HILIC-UPLC and an integrated and routine high resolution mass spectrometer like the BioAccord LC-MS system allows for identifying clinically relevant changes in plasma and serum N-glycome in a simple, robust and high-throughput manner.

5.6 ACKNOWLEDGMENTS

We thank Marleen van Wingerden, Dr. Guillaume Bechade, Nick Pittman, Evelien Dejaegere, and WatersCorporation for their support in this work. We also thank Prof Ana M. Valdes from the School of Medicine, University of Nottingham, for obtaining biological samples from COVID-19 patients.

5.7 SUPPLEMENTARY MATERIAL

LC conditions – Universal N-Glycan Profiling Method

LC system: ACQUITY UPLC I-Class

Sample temp.: 10 °C

Column temp.: 60 °C

Injection volume: 25 µL

Fluorescence detection: Ex 265 nm/Em 425 nm, 2 Hz

Mobile phase A: 50 mM ammonium formate, pH 4.4 (LC-MS grade water)

Mobile phase B: ACN (LC-MS grade)

Gradient used for the chromatographic separation:

Time (min)	Flow rate (mL/min)	%A	%B	Curve
0.00	0.400	25.0	75.0	Initial
35.00	0.400	46.0	54.0	6
36.50	0.200	100.0	0.0	6
39.50	0.200	100.0	0.0	6
43.10	0.200	25.0	75.0	6
46.60	0.400	25.0	75.0	6
55.00	0.400	25.0	75.0	6

LC conditions – Plasma and Serum N-Glycan Profiling Method

LC system: ACQUITY UPLC I-Class

Sample temp.: 10 °C

Column temp.: 45 °C

Injection volume: 25 µL

Fluorescence detection: Ex 265 nm/Em 425 nm, 2 Hz

Mobile phase A: 100 mM ammonium formate, pH 4.4 (LC-MS grade water)

Mobile phase B: ACN (LC-MS grade)

Gradient used for the chromatographic separation:

Time (min)	Flow rate (mL/min)	%A	%B	Curve
0.00	0.400	29.0	71.0	Initial
35.00	0.400	46.0	54.0	6
36.50	0.200	100.0	0.0	6
39.50	0.200	100.0	0.0	6
43.10	0.200	29.0	71.0	6
46.60	0.400	29.0	71.0	6
55.00	0.400	29.0	71.0	6

Table S1. Overview of the baseline characteristics of the study cohort.

Characteristics	Observation
Longitudinal samples, N	483
Individuals, N	89
Age, years (mean ± SD)	42 ± 11
Sex, N (%)	
Male	20 (22)
Female	69 (78)

Table S3. The theoretical amount and concentration of plasma proteins in serially diluted samples. The calculation was based on the value of 70 mg/mL, the theoretical total protein concentration in human plasma.

Sample	Theoretical protein amount [µg]	Theoretical protein concentration [µg/µL]
Tpng_1	0.6	0.05
Tpng_2	0.9	0.08
Tpng_3	1.5	0.13
Tpng_4	2.3	0.22
Tpng_5	3.7	0.34
Tpng_6	6	0.55
Tpng_7	9.5	0.88
Tpng_8	15.3	1.41

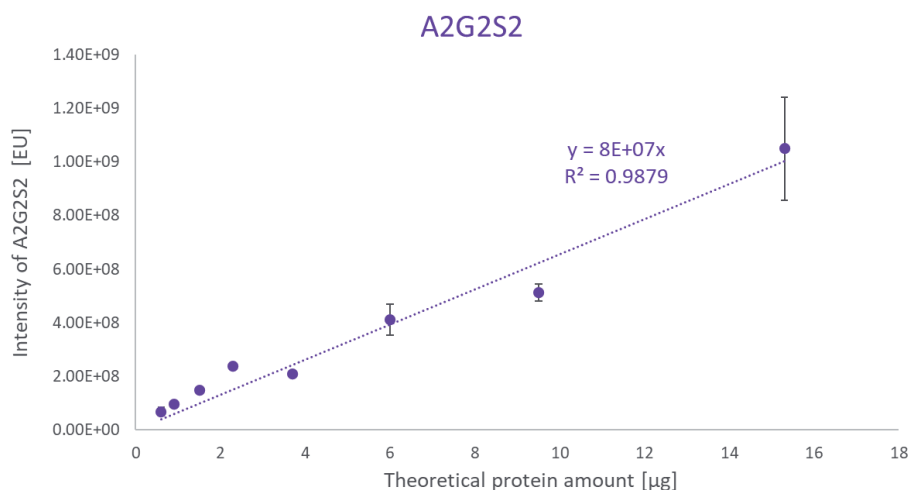


Figure S1. The linear range of detection for the A2G2S2 glycan labeled with RapiFluor-MS. FLR signal intensities for the series dilutions of plasma proteins are shown. Standards plasma samples were analyzed in triplicate. Error bars represent the standard deviation of the triplicates.

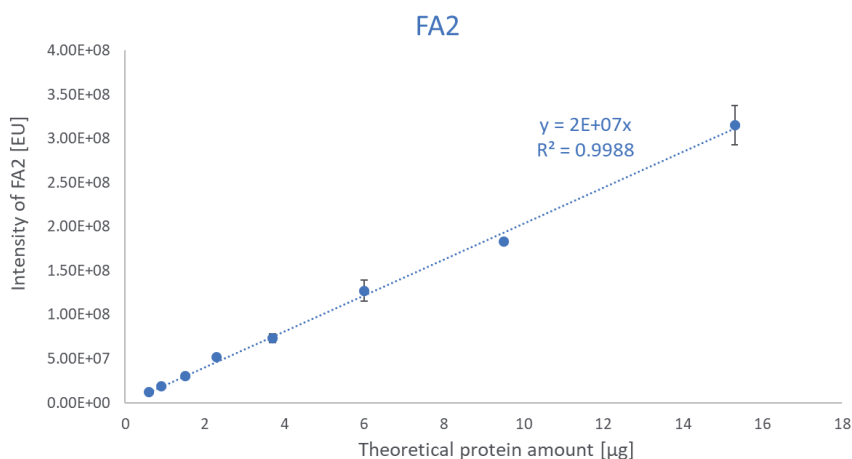


Figure S2. The linear range of detection for the FA2 glycan labeled with RapiFluor-MS. FLR signal intensities for the series dilutions plasma proteins are shown. Standards plasma samples were analyzed in triplicate. Error bars represent the standard deviation of the triplicates.

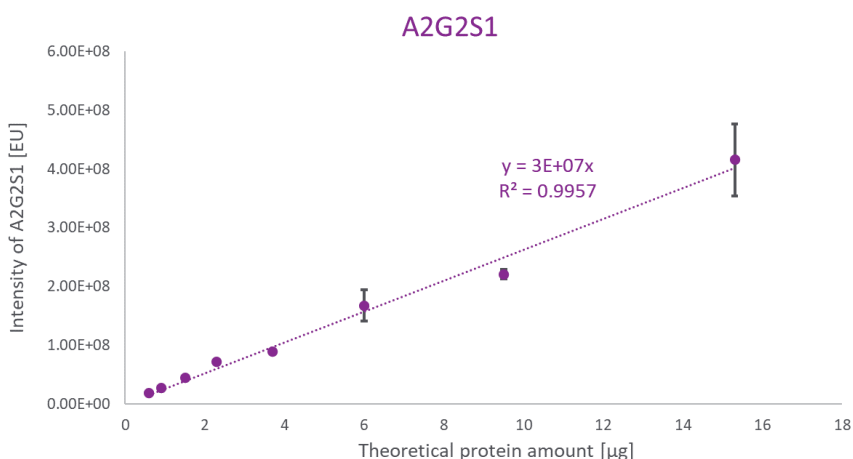


Figure S3. The linear range of detection for the A2G2S1 glycan labeled with RapiFluor-MS. FLR signal intensities for the series dilutions of plasma proteins are shown. Standards plasma samples were analyzed in triplicate. Error bars represent the standard deviation of the triplicates.

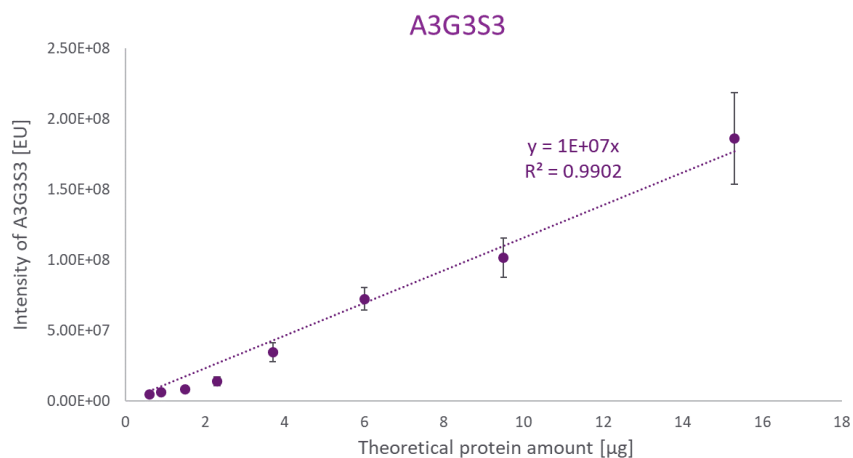


Figure S4. The linear range of detection for the A3G3S3 glycan labeled with RapiFluor-MS. FLR signal intensities for the series dilutions of plasma proteins are shown. Standards plasma samples were analyzed in triplicate. Error bars represent the standard deviation of the triplicates.

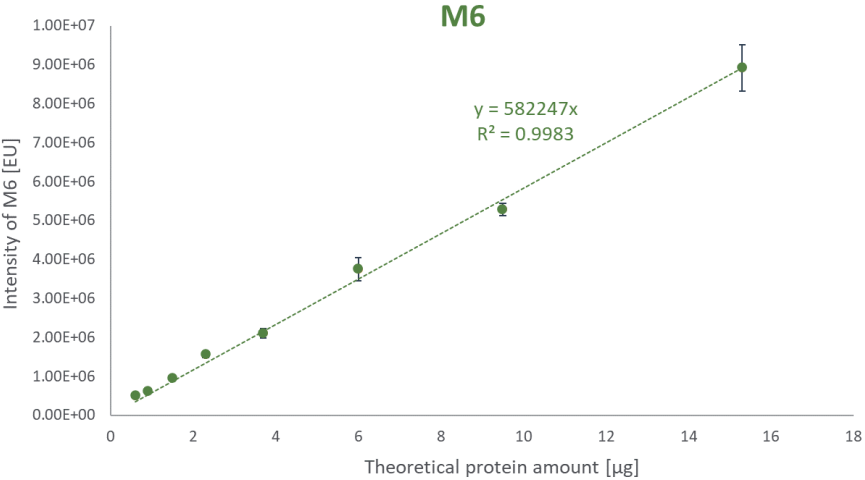


Figure S5. The linear range of detection for the M6 glycan labeled with RapiFluor-MS. FLR signal intensities for the series dilutions of plasma proteins are shown. Standards plasma samples were analyzed in triplicate. Error bars represent the standard deviation of the triplicates.

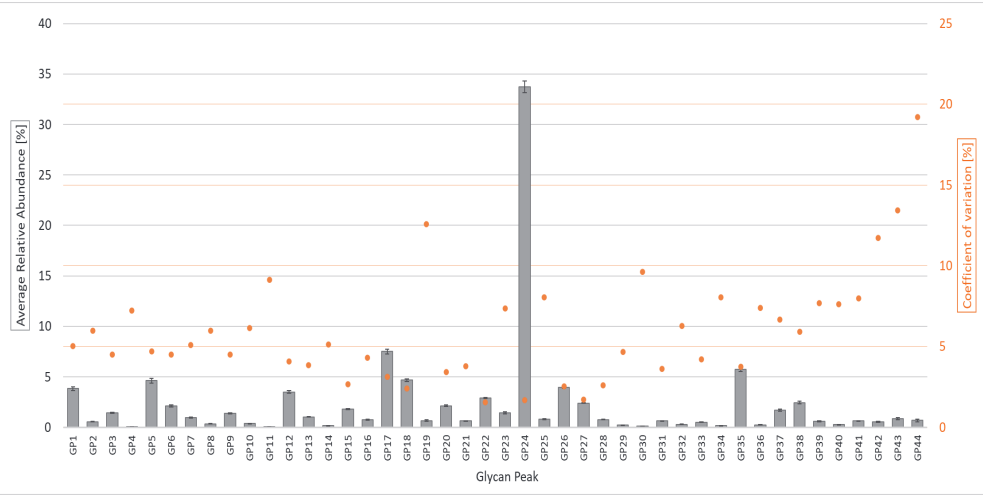


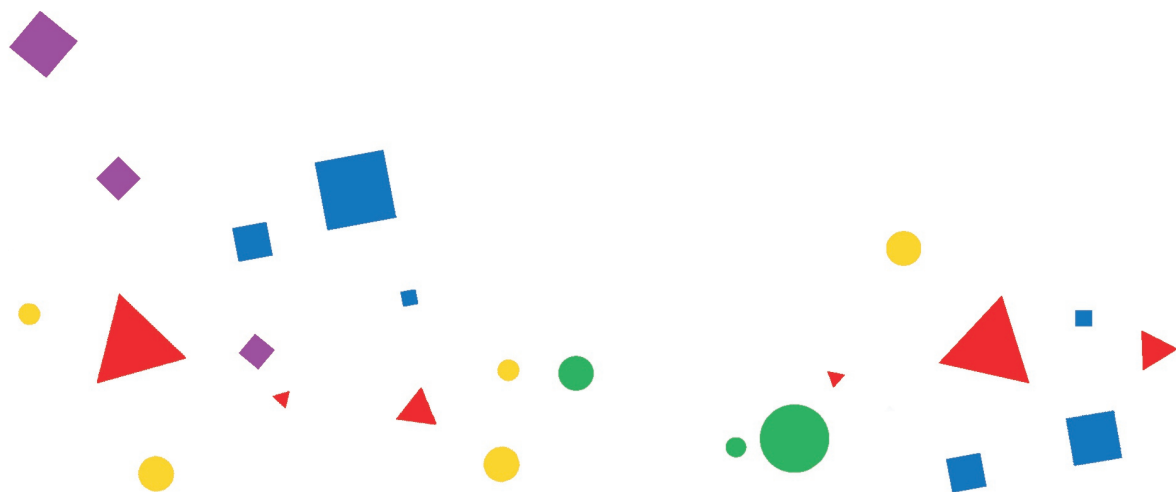
Figure S6. Technical variability. Average relative abundances (primary y axis on the left) and coefficients of variation (secondary y axis on the right) of RF-MS labeled N-glycans from 36 replicates of a standard plasma sample. The error bars represent the standard deviation of the mean while the coefficients of variation for each glycan peak are shown as orange dots.

5.8 REFERENCES

1. Sola RJ, Rodríguez-Martínez JA, Griebenow K. Modulation of protein biophysical properties by chemical glycosylation: biochemical insights and biomedical implications. *Cell Mol Life Sci.* 2007;64(16):2133-52.
2. Pascal Gagneux TH, and Ajit Varki. Biological Functions of Glycans. In: Ajit Varki RDC, Jeffrey D. Esko, Pamela Stanley, Gerald W. Hart, Markus Aeby, Debra Mohnen, Taroh Kinoshita, Nicolle H. Packer, James H. Prestegard, Ronald L. Schnaar, and Peter H. Seeberger., editor. *Essentials of Glycobiology*. NY: Cold Spring Harbor Laboratory Press; 2022.
3. Reilly C, Stewart TJ, Renfrow MB, Novak J. Glycosylation in health and disease. *Nat Rev Nephrol.* 2019;15(6):346-66.
4. Dotz V, Wührer M. N-glycome signatures in human plasma: associations with physiology and major diseases. *FEBS Lett.* 2019;593(21):2966-76.
5. Trbojevic-Akmacic I, Lageveen-Kammeijer GSM, Heijs B, Petrovic T, Deris H, Wührer M, et al. High-Throughput Glycomic Methods. *Chem Rev.* 2022;122(20):15865-913.
6. Adamczyk B, Stockmann H, O'Flaherty R, Karlsson NG, Rudd PM. High-Throughput Analysis of the Plasma N-Glycome by UHPLC. *Methods Mol Biol.* 2017;1503:97-108.
7. Lauber MA, Yu YQ, Brousmiche DW, Hua Z, Koza SM, Magnelli P, et al. Rapid Preparation of Released N-Glycans for HILIC Analysis Using a Labeling Reagent that Facilitates Sensitive Fluorescence and ESI-MS Detection. *Anal Chem.* 2015;87(10):5401-9.
8. Deris H, Cindric A, Lauber M, Petrovic T, Bielik A, Taron CH, et al. Robustness and repeatability of GlycoWorks RapiFluor-MS IgG N-glycan profiling in a long-term high-throughput glycomic study. *Glycobiology.* 2021;31(9):1062-7.
9. Keser T, Pavic T, Lauc G, Gornik O. Comparison of 2-Aminobenzamide, Procainamide and RapiFluor-MS as Derivatizing Agents for High-Throughput HILIC-UPLC-FLR-MS N-glycan Analysis. *Front Chem.* 2018;6:324.
10. Alley WR, Qing YY. Combining RapiFluor-MS and UNIFI Scientific Information System for a Total N-linked Glycan Solution for Innovator vs. Biosimilar Infliximab Comparisons. *Waters Application Notes Glycans.* 2016.(720005532EN).
11. Zaytseva OO, Freidin MB, Keser T, Stambuk J, Ugrina I, Simurina M, et al. Heritability of Human Plasma N-Glycome. *J Proteome Res.* 2020;19(1):85-91.
12. Saldova R, Asadi Shehni A, Haakensen VD, Steinfeld I, Hilliard M, Kifer I, et al. Association of N-glycosylation with breast carcinoma and systemic features using high-resolution quantitative UPLC. *J Proteome Res.* 2014;13(5):2314-27.
13. McCall SA, Lauber M, Koza SM. Profiling Released High Mannose and Complex N-Glycan Structures from Monoclonal Antibodies Using RapiFluor-MS Labeling and Optimized Hydrophilic Interaction Chromatography. *Waters Application Notes Glycans.* 2015.(720005516).
14. Wang Q, Lauber MA. Optimizing HILIC-based Analyses of RapiFluor-MS Labeled Sialylated N-Glycans. *Waters Application Notes Glycans.* 2016. (720005850EN).
15. Anderson NL, Polanski M, Pieper R, Gatlin T, Tirumalai RS, Conrads TP, et al. The human plasma proteome: a nonredundant list developed by combination of four separate sources. *Mol Cell Proteomics.* 2004;3(4):311-26.
16. Leeman M, Choi J, Hansson S, Storm MU, Nilsson L. Proteins and antibodies in serum, plasma, and whole blood-size characterization using asymmetrical flow field-flow fractionation (AF4). *Anal Bioanal Chem.* 2018;410(20):4867-73.

- ¹ *Scientific Centre of Excellence for Reproductive and Regenerative Medicine, University of Zagreb School of Medicine, 10 000 Zagreb, Croatia*
- ² *University of Zagreb School of Medicine, 10 000 Zagreb, Croatia*
- ³ *Genos Glycoscience Research Laboratory, 10 000 Zagreb, Croatia*
- ⁴ *University Hospital Centre Zagreb, Department of Laboratory Diagnostics, 10 000 Zagreb, Croatia*
- ⁵ *Clinical Epidemiology Unit, IRCCS Ospedale Policlinico San Martino, 16 132 Genova, Italy*
- ⁶ *Cryogonia Cryopreservation Bank, 11 526 Athens, Greece*
- ⁷ *University of Zagreb, Faculty of Pharmacy and Biochemistry, 10 000 Zagreb, Croatia*
- ⁸ *Institute for Medical Research and Occupational Health, 10 000 Zagreb, Croatia*

** Authors share co-first authorship*



Chapter 6

Seminal plasma N-glycome as a new biomarker of environmental exposure associated with semen quality

Maric T^{1,2*}, Wojcik I^{3*}, Katusic Bojanac A^{1,2}, Matijevic A⁴, Ceppi M⁵,
Bruzzzone M⁵, Evgeni E⁶, Petrovic T³, Trbojevic-Akmacic I³, Lauc G^{3,7}, Jezek D^{1,2} and Fucic A^{1,8}

Reprinted and adapted with permission from
Reprod Toxicol. 2022 Oct;113:96-102. doi: 10.1016/j.reprotox.2022.08.005. Epub 2022 Aug 10.

PMID: 35961531.

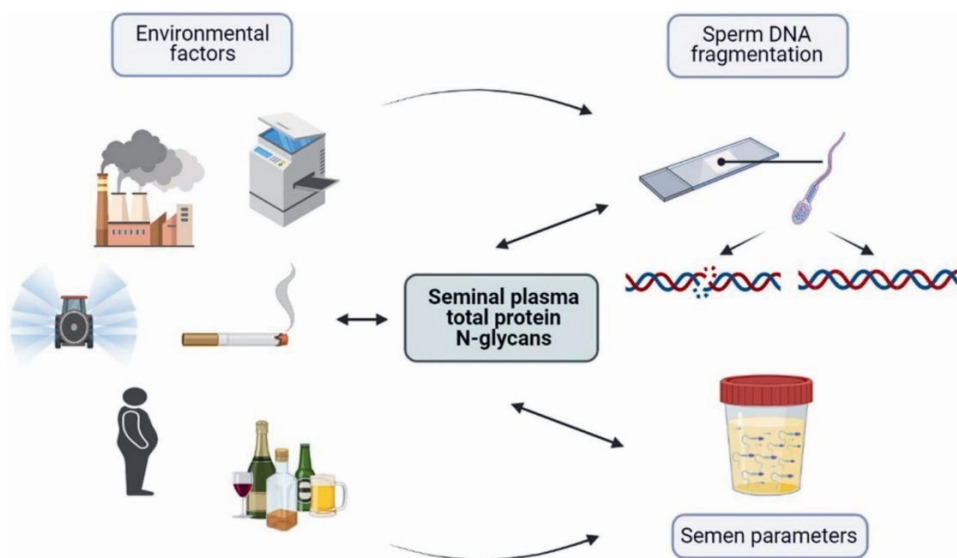
Copyright © 2022, Elsevier Inc.



6.1 ABSTRACT

Male infertility, a condition that has during the last decade raised significant concern, is a diagnostically demanding and socially sensitive topic. The number of unsolved issues on infertility etiology, especially potential environmental causes, in couples, demonstrates the need for further investigations into infertility biomarkers. Semen parameters are often insufficient for reliable profiling of male infertility. Thus, this study aims to evaluate for the first time seminal plasma N-glycosylation as a biomarker of environmental exposure in semen samples from 82 normozoospermic men and 84 men with abnormal semen parameters and compare it with genome damage measured by DNA fragmentation. We obtained information about chronic exposure to environmental factors from the self-reported questionnaire, and determined sperm DNA fragmentation by sperm chromatin dispersion, while N-glycans were characterized with liquid chromatography-mass spectrometry (LC-MS). Based on previously published results, ten N-glycans were selected. Results show that the selected seminal plasma N-glycans were significantly associated with smoking, exposure to pesticides, air pollution, agents emitted during photocopying, alcohol consumption, and obesity. Some N-glycans showed a simultaneous association with DNA fragmentation, semen parameters, and environmental stressors. These subgroups of N-glycans are new potential candidates for biomonitoring of exposure to different environmental factors in men with semen abnormalities.

GRAPHICAL ABSTRACT



6.2 INTRODUCTION

Reproduction is one of the most sensitive components of human social and personal life and it has been challenged during the last decades due to the significant rise of reproductive disorders in both sexes.(1) Male infertility, a condition characterized by failure to achieve pregnancy with a healthy female, may have a hormonal or genetic background, but can also be associated with lifestyle habits such as smoking, alcohol consumption, or excess caloric intake leading to overweight and obesity.(2-4) Moreover, exposure to environmental and occupational factors including pesticides, bisphenols, perfluoroalkyl chemicals, phthalates, heavy metals, etc can also negatively affect fertility.(5-8) Many of these factors act as endocrine disruptors (EDs), compounds with the ability to interfere with hormones, which may lead to disrupted hormonal balance and fertility.(9)

Since male infertility is a very complex condition with multiple molecular pathways involved, its diagnostics is highly demanding and novel biomarkers are constantly investigated. Currently, the golden standard in male infertility diagnostics is an assessment of basic semen parameters including sperm count, morphology, motility, and semen volume.(10) Besides semen analysis, additional sperm quality assay may improve infertility diagnostics.(11) Due to the highly condensed packaging of sperm DNA,(12) the assessment of sperm chromatin integrity through sperm DNA fragmentation (SDF) with a relatively simple sperm chromatin dispersion (SCD) assay, provides useful insight into sperm quality.(6, 13) Previous studies have shown the association of increased sperm DNA fragmentation with exposure to different environmental factors and obesity.(14-17)

N-linked protein glycosylation is a post-translational mechanism that can influence the structure and activity of secretory, transmembrane, and intracellular proteins.(18) Various N-glycosylated proteins are found in sperm and seminal plasma, with the proposed role in spermatogenesis, sperm maturation, capacitation, and sperm-egg interaction.(19) Precisely, seminal plasma N-glycoproteins facilitate sperm transportation in the female reproductive tract and maintain the spermatozoa in a decapacitated state until they reach the egg.(20) Several studies showed that the N-glycosylation pattern of seminal plasma can be altered in men with disrupted fertility.(18, 21-23) Hence, glycosylation patterns have been proposed as potential biomarkers of different semen abnormalities, although the current knowledge is still very limited.(24-26)

Currently, there are no data on the association of N-glycosylation changes in seminal plasma total proteins in men with disrupted semen parameters with DNA damage and environmental exposure. Our previous study(27) has shown the significant association of ten seminal plasma N-glycan peaks (SPGPs) with sperm quality parameters which are further investigated herein. Because there is a constant demand for the development of novel biomonitoring and diagnostic tools for male infertility, the current study aims to investigate for the first time (a) the association between the specific seminal plasma N-glycans, DNA damage, and the exposure to environmental factors in men with

normozoospermic (N) and abnormal (Ab) semen parameters, and (b) potential of seminal plasma N-glycans as a biomarker of environmental exposure in infertile men.

6.3 EXPERIMENTAL SECTION

6.3.1 Subjects

All procedures were conducted according to the regulations of the Declaration of Helsinki. The study was approved by the Ethics Committee of the University Hospital Zagreb, Croatia under reference number 021–1/41–18. The study cohort and the sampling of study subjects were described in our previous study.(27) Briefly explained, the study participants were recruited at the University Hospital Zagreb, Croatia. Informed consent for the use of patients' clinical data for scientific purposes was signed voluntarily by all of the study participants. After 2–7 days of abstinence, samples were obtained by masturbation in a sterile container, liquefied for 30–60 min, and analyzed by computer-aided sperm analysis (CASA). According to World Health Organization (WHO) recommendations and criteria for semen parameters, the semen analysis was conducted.(11) Exclusion criteria were the absence of sperm in the neat ejaculate, cryptozoospermia, leukocytospermia, and previous chemo- or radiation therapy. Sperm parameters including volume, pH, concentration, motility and morphology were determined and study participants were grouped as normozoospermic (N = 82), oligozoospermic (N = 21), asthenozoospermic (N = 29) and oligoasthenozoospermic (N = 34).

6.3.2 Assessment of exposure to environmental factors

All of the participants were offered a self-reported questionnaire for the assessment of lifestyle habits and the frequent environmental and occupational factors they are exposed to. The questionnaire was used in previously published studies and adapted for the infertility population.(28-30) The questionnaire included questions that assessed chronic exposures to various environmental factors containing endocrine-disrupting agents, such as pesticides, solvents, dyes, and plastics in the last year (yes/no). Information about the lifestyle habits of participants including smoking (yes/no), alcohol consumption (yes/no), red meat ($n \geq 3$ per week/less than 3/no), poultry ($n \geq 3$ per week/less than 3/no), vegetable (everyday/less/no), fruit (everyday/less/no), fish ($n \geq 1$ per week /no), and dairy consumption (yes/no) were also obtained. Moreover, the participants self-reported whether they live near the industry (distance ≤ 500 m) or highway (distance ≤ 500 m). Obesity was characterized as BMI ≥ 30 . The questionnaire served as an initial robust screening of the most common environmental factors and lifestyle habits that participants were exposed to in the last year.

6.3.3 DNA fragmentation test

According to the manufacturer's instructions, the percentage of sperm with fragmented DNA was determined by sperm chromatin dispersion (SCD) assay (GoldCyto Sperm® Kit, Goldcyto Biotech corp., China). Briefly, samples were diluted with a concentration of 5 million per ml with PBS, mixed with agarose, and 30 µl of the mixture was added to the slide and cooled for 10 min at 4 °C. Next, slides were incubated with the acidic denaturation solution for 7 min, for 25 min with lysis solution, washed in dH₂O for 5 min, and fixed in 70%, 90%, and 100% ethanol for 2 min each at RT. Slides were then air-dried, and incubated with commercial staining solution A for 1 min, then solution B was added and altogether was incubated for 10 min. Then, slides were washed with tap water, air-dried, and analyzed with the CASA system in the *SCA evolution* software's *DNA fragmentation* module.

6.3.4 Isolation of N-glycans from total seminal plasma proteins

Semen samples were aliquoted in 1.5 ml tubes and centrifuged for 10 min at RT 650 rpm. Seminal plasma was separated from the pellet, centrifuged once more at 3550 rpm, and again separated from the pellet. All samples were stored at – 80 °C until the subsequent N-glycan analysis. Throughout the entire analysis, in-house seminal plasma standards were used as a control and were prepared by pooling 5 µl of each sample. Samples were then randomized on a 96-well plate, using 5 µl of each sample. For isolation of N-glycans from seminal plasma total proteins, 200 µl of 50 mg/ml Chromabond C-18 beads (Marcherey-Nagel, Germany) suspension in acetonitrile (ACN, Carlo Erba, Italy)/0.1% trifluoroacetic acid (TFA, Sigma-Aldrich, USA) (80:20) was added to each well of an Orochem plate (Orochem, USA). Using a vacuum manifold (Pall Corporation, USA), the beads were washed three times with 200 µl ACN/0.1% TFA (80:20), and three times with 200 µl ACN/0.1% TFA (5:95). Samples were diluted with 45 µl of ACN/0.1% TFA (5:95), transferred to the preconditioned C-18 beads, and resuspended with 150 µl of ACN/0.1% TFA (5:95), and incubated for 2 min. Samples were centrifuged (centrifuge 5804 with a rotor A-2-DWP, Eppendorf, Germany) for 5 min, at increasing speeds from 300 to 800 rpm for the removal of free seminal plasma glycans. Next, 200 µl of 80% ACN was added to each well of the Orochem plate, samples were incubated for 2 min and the centrifugation step was repeated. Glycoproteins were then eluted from the C-18 beads, collected in a 96-well plate (Thermo Fisher Scientific, USA), and incubated overnight at 37 °C. Glycoproteins were denatured with 30 µl of 1.33% SDS (Carl Roth, Germany) and incubated, for 10 min at 65 °C. Then 10 µl of 4% non-denaturing detergent Igepal CA-630 (Sigma-Aldrich) was added to each well. After incubation for 30 min, 1.25 mU PNGase F (Promega, USA) in 10 µl of 5 x PBS was added to each well and incubated for 18 h at 37 °C.

6.3.5 Fluorescent labeling of N-glycans from seminal plasma total proteins

Fluorescent labeling of N-glycans released from seminal plasma total proteins was performed using procainamide. Briefly, 4.32 mg of procainamide (Sigma-Aldrich) was dissolved in glacial acetic acid (Honeywell, USA)/dimethylsulfoxide (Sigma-Aldrich) (30:70),

and 25 µl of the mixture was added to each sample. The plate was sealed and incubated for 1 h at 65 °C. The solution containing the reducing agent was prepared by dissolving 4.48 mg of 2-picoline borane (J&K Scientific, China) in 25 µl of glacial acetic acid /dimethylsulfoxide (30:70) per sample. The reducing agent was then added to each well and incubated for 1.5 h at 65 °C. The samples were then cooled for 30 min at RT and the labeled N-glycans were cleaned up as previously described.(31) The only modification in the protocol was the usage of a 0.2 µm Supor AcroPrep filter plate (Pall Corporation) as a stationary phase.

6.3.6 Detection and measurement of N-Glycans

Separation of labeled N-glycans was conducted with hydrophilic interaction liquid chromatography (HILIC) on a Waters Acquity ultra-high-performance liquid chromatography (UHPLC) H-class UPLC instrument (Milford, MA, USA). The procedure was previously described.(27)

6.3.7 Structural characterization of N-Glycans

The compositional characterization was conducted for glycans eluting in peaks SPGP2, SPGP4, SPGP6, SPGP14, SPGP17, SPGP18, SPGP26, SPGP32, and SPGP35 as described previously in a sister study(27) from the seminal plasma standard representing the average of a cohort (prepared as described above). Briefly explained, N-glycan compositions were identified manually by averaging the MS scans over the chromatographic retention time in which the glycan peaks of interest were eluted. The detected glycan ions inferred from their *m/z* values were characterized with the aid of the glycobioinformatics tools GlycoMod (<https://web.expasy.org/glycomod/>). Determinations of N-glycan compositions were done based on their accurate mass. The putative glycan structures were assigned from compositional information and the recently published reference library of seminal plasma N-glycans.(32) Mass accuracy was set within 10 ppm for assigning the glycan compositions. Putative glycan structures were visualized using the GlycoWorkbench 2.1 software.(33)

6.3.8 Statistical analysis

Statistical analysis was performed using STATA software (StataCorp. 2021. *Stata Statistical Software*: Release 17. College Station, TX: StataCorp LLC.). As for the descriptive analysis, the non-parametric Mann-Whitney test was employed.

Multivariate analysis was performed using the log-normal regression model. This statistical model allows for the estimation of the percentage change in the mean frequency of the studied variable in each group, compared to the reference group. To select the environmental factors related to the outcomes of interest a stepwise backward procedure was employed. To verify if the assumptions of the log-normal model were violated, the residual-versus-fitted plot and the test for heteroskedasticity were performed. Bonferroni's correction for multiple comparisons was applied.

6.4 RESULTS

The study included men whose semen parameters were within WHO's recommended normal range, normozoospermic (N) and abnormal (Ab) range. Abnormal sub-groups were defined according to the WHO limits for basic sperm parameters. The univariate statistical comparison between these two groups regarding age, BMI, semen parameters, and sperm DNA fragmentation is presented in **Table 1**. A comparative statistical analysis between N and Ab sub-groups – asthenozoospermic (A), oligozoospermic (O), and oligoasthenozoospermic (OA) was presented in our previous paper.(27) Subjects' age and semen volume did not significantly differ between the N and Ab or between the sub-groups.

To explore whether the N-glycan features identified in our previous study(27) showed an association between self-reported exposure to environmental factors and acted differentially between N and Ab subjects, a log-normal regression model stratified by diagnosis was applied. In N subjects SPGP5, SPGP17, and SPGP26 significantly decreased as sperm genome damage increased, and in infertile men only SPGP18 significantly decreased as sperm genome damage increased (**Table 2a and 2b**). Exposure to a mixture of chemicals for photocopying, industrial dyes, motors oils, insecticides, fish consumption, neoplastic disease in the family, residence near factories and highways, and smoking were significantly associated with SPGPs in the N group. In normozoospermic men, when the DNA fragmentation increased by the mean ratio (MR) of 10 units, SPGP5 decreased by 16% and was negatively associated with smoking and positively with industrial dyes. Similarly, SPGP17 and SPGP26 were negatively correlated with DNA fragmentation and positively with residence near industry, photocopying, while SPGP26 was also positively correlated with motor oils, and smoking. In subjects with abnormal semen parameters, only SPGP18 was negatively associated with DNA fragmentation and positively with smoking (**Table 2b**).

To compare the SPGP between normozoospermic and the three abnormal sub-groups, we refitted the log-normal regression model by adjusting for selected environmental factors (**Table 3**). It was observed that SPGP2 and SPGP4 were negatively associated with the OA group and smoking, while positively associated with pesticides. SPGP5 was associated with the O group using latex dyes and photocopying and was negatively associated with smoking. SPGP6 was negatively associated with the OA group. SPGP14 was negatively associated with the OA and O groups and with inguinal hernia. SPGP18 was positively associated with the OA group. SPGP26 was associated with the A group and with photocopying and smoking. SPGP32 was negatively associated with the OA group and pesticides and positively with fish consumption.

Table 1. Descriptive analysis of men diagnosed with normozoospermic (N) and abnormal (Ab) semen parameters. P-value was achieved using the Mann-Whitney test.

	N (N=82)		Ab (N=84)		P-value
	Mean	SD	Mean	SD	
Age	34.5	6.4	36.0	6.8	0.178
Sperm concentration (10 ⁶ /ml)	59.1	29.0	33.4	92.9	< 0.001
Total sperm count (10 ⁶ /sample)	188.3	116.1	72.4	115.4	< 0.001
Volume (ml)	3.3	1.3	3.2	1.8	0.269
Rapid progressive (%)	15.7	7.2	8.6	7.7	< 0.001
Slow progressive (%)	35.7	11.1	17.1	11.0	< 0.001
Non-progressive (%)	16.1	4.9	13.1	7.4	0.004
Motile (%)	67.4	10.8	37.9	16.8	< 0.001
Immotile (%)	32.7	11.0	62.1	16.8	< 0.001
Abnormal morphology (%)	90.2	4.0	93.4	4.2	< 0.001
Dead (%)	25.6	8.7	47.6	16.3	< 0.001
Non-fragmented sperm (%)	82.2	9.2	69.3	17.5	< 0.001
Fragmented sperm (%)	17.8	9.2	30.7	17.5	< 0.001
Big halo sperm (%)	58.1	18.7	42.1	20.3	< 0.001
Medium halo sperm (%)	24.1	15.4	27.4	12.3	0.010
Small halo sperm (%)	3.6	2.1	5.4	5.3	0.019
Sperm without halo (%)	13.6	8.4	24.7	14.2	< 0.001
Degraded sperm (%)	0.6	0.8	0.6	0.8	0.421
BMI	26.7	4.1	27.1	4.5	0.754

Table 3a. Association of SPGP, DNA fragmentation and exposure to environmental factors in normozoospermic subjects: log-normal regression model adjusted for the selected confounders.

SPGP	DNA fragmentation		Significantly associated factors: (+ / -) positive / negative association
	MR ^a	p-value	
2	1.08	0.082	Residence near industry (+), Photocopying (+), Smoking (-)
4	1.00	0.907	Smoking (-), Photocopying (+)
5	0.84	0.006	Smoking (-), Industrial Dyes (+), Photocopying (+)
6	1.11	0.071	Motor oils (-),
14	1.03	0.262	Residence near highway (+),
17	0.89	0.025	Residence near industry (+), Photocopying (+)
18	0.99	0.861	none
26	0.89	0.038	Motor oils (+), Smoking (+), Photocopying (+)
32	1.03	0.515	Smoking (+), Insecticides (-), Fish consumption (+)
35	1.12	0.108	Pesticides (-), Industrial Dyes (-), Smoking (+), neoplastic diseases in the family (+)

^a: MR when the variable increased by 10 units

Table 2b. Association of SPGP, DNA fragmentation, and exposure to environmental factors in subjects with abnormal semen parameters: log-normal regression model adjusted for the selected confounders.

SPGP	DNA fragmentation		Significantly associated factors: (+ / -) positive / negative association
	MR ^a	p-value	
2	1.02	0.319	Lubricating oil (+)
4	1.05	0.068	Residence Near Factories (+),
5	0.99	0.655	Disinfection (-)
6	1.02	0.412	Alcohol consumption (+), Obesity (-), Drug consumption (-)
14	1.02	0.240	Obesity(-)
17	0.98	0.323	Lacquers (+)
18	0.91	0.001	Smoking (+)
26	0.97	0.316	Glues (-), Lacquers (+)
32	0.99	0.867	Smoking (+)
35	1.04	0.259	Residence near highway (+)

^a: MR when the variable increased by 10 units

Table 3. Mean Ratio of SPGPs in subgroups of subjects with abnormal semen parameters. A – asthenozoospermia, O – oligozoospermia, OA – oligoasthenozoospermia.

SPGP	A		O		OA		Significantly associated factors: (+ / -) positive/negative association
	MR*	p-value	MR*	p-value	MR*	p-value	
2	0.85	0.060	1.01	0.909	0.78	0.006	Pesticides (+), smoking (-)
4	0.96	0.625	1.03	0.696	0.78	0.003	Pesticides (+), smoking(-)
5	1.11	0.415	1.41	0.011	1.11	0.412	Latex dyes (+), photocopying (+), smoking (-)
6	0.92	0.464	0.83	0.108	0.70	0.002	
14	0.97	0.683	0.85	0.021	0.76	< 0.001	
17	1.19	0.066	1.15	0.169	0.87	0.176	Industrial dyes (+), neoplastic diseases in the family(-)
18	0.93	0.444	1.03	0.754	1.27	0.018	
26	1.42	0.001	1.23	0.076	1.02	0.882	Photocopying (+), smoking (+)
32	1.02	0.873	0.95	0.642	0.80	0.036	Pesticides (-), fish (+)
35	0.86	0.266	1.13	0.376	0.79	0.083	Industrial dyes (-)

According to the investigation for correlations between semen characteristics and SPGPs, the most frequently associated N-glycans with sperm quality parameters were those with significant associations with exposure to environmental factors (Table 4).

Table 4. Association between sperm quality parameters and selected SPGPs. N – normozoospermic and Ab - abnormal semen parameters.

Empty Cell	Associated N-glycan peaks Total	Associated N-glycan peaks (N)	Associated N-glycan peaks (Ab)
M/ml (≥ 15 M/ml)	none	6 (+)	none
M/sample (≥ 39 M/sample)	6 (+)	none	6 (+)
Volume (ml)	2 (-), 4 (-), 14 (-), 17 (-), 18 (+)	5 (-),	4 (-), 14 (-), 17 (-), 18 (+)
Rapid progressive (≥32%)	none	none	5 (+), 32 (-)
Slow progressive (%)	2 (+), 5 (+)	none	2 (+), 4 (+), 5 (+)
Non-progressive (%)	32 (+)	none	14 (+), 18 (-), 32 (+)
Immotile (%)	35 (-)	none	2 (-), 4 (-), 5 (-), 35 (-)
Abnormal (%)	none	none	none
Dead (%)	none	none	5 (-)

Associations with a nominal p-value < 0.05; positive or negative (+/-).

Moreover, we structurally characterized selected N-glycan peaks that showed significant associations with environmental factors by liquid chromatography-mass spectrometry (LC-MS). Proposed structures are described and presented in **Table 5**.

Table 5. Compositions and proposed structures of N-glycans identified in the glycan peaks SPGP2, SPGP4, SPGP5, SPGP6, SPGP14, SPGP17, SPGP18, SPGP26, SPGP32, and SPGP35 of HILIC-UHPLC profile of seminal plasma N-glycome. Blue square: N-acetylglucosamine, red triangle: fucose, green circle: mannose, yellow circle: galactose, pink diamond: N-acetylneuraminic acid (sialic acid).

Glycan peak	Observed m/z	z	Glycan composition	Proposed structure	Description
SPGP2	1641.70	1	H4N3F1		Complex type glycan, monoantennary monogalactosylated glycan with core fucose or Hybrid type glycan, monoantennary agalactosylated glycan with core fucose and one terminal mannose
	1698.71	1	H4N4		Complex type glycan, diantennary monogalactosylated glycan without fucose
SPGP4	922.90	2	H4N4F1		Complex type glycan, diantennary monogalactosylated glycan with core fucose
	1844.77	1			
SPGP5	966.89	2	H4N3F1S1		Complex type glycan, monoantennary monogalactosylated monosialylated glycan with core fucose
	1932.78	1			
	1024.42	2	H4N5F1		Complex type glycan, diantennary monogalactosylated with bisected N-acetylglucosamine and core fucose
SPGP6	966.89	2	H4N3F1S1		Complex type glycan, monoantennary monogalactosylated monosialylated glycan with core fucose
	1932.78	1			
	1295.01	2	H5N4F1S2		Complex type glycan, diantennary digalactosylated disialylated glycan with core fucose
SPGP14	1221.98	2	H5N4S2		Complex type glycan, diantennary digalactosylated disialylated glycan without fucose
	1221.98	2	H5N4S2		Complex type glycan, diantennary digalactosylated disialylated glycan without fucose
SPGP17	1221.98	2	H5N4S2		Complex type glycan, diantennary digalactosylated disialylated glycan without fucose
SPGP18	1223.02	2	H5N4F4		Complex type glycan, diantennary digalactosylated glycan with core and antennary fucose

Glycan peak	Observed m/z	z	Glycan composition	Proposed structure	Description
SPGP26	1033.75	3	H6N5S3		Complex type glycan, triantennary trigalactosylated trisialylated glycan without core fucose
SPGP32	1301.16	3	H7N6F1S4		Complex type glycan, tetraantennary tetragalactosylated tetrasialylated glycan with core fucose
	1551.62	2	H6N5F6		Complex type glycan, triaantennary trigalactosylated glycan with core and antennary fucose
SPGP35	1107.78	3	H7N6F5		Complex type glycan, tetraantennary tetragalactosylated glycan with core and antennary fucose

6.5 DISCUSSION

Protein N-glycans are a highly dynamic and diverse system, and their pattern in various pathological conditions, including disorders of the male reproductive system, has strong biomarker potential.(34) Since seminal plasma is a rich source of N-linked glycoproteins, in this study we found statistically significant correlations of specific N-glycan peaks with semen parameters, sperm DNA fragmentation (SDF), and environmental exposure in men with normozoospermic and abnormal semen parameters.

Structural characterization of SPGP18 showed the presence of biantennary digalactosylated glycans with core fucose and antenna fucose, which are linked to both GlcNAc forming Lewis^x (Le^x), or both GlcNAc and Gal forming Lewis^y (Le^y) structures. These results are in contrast with the observation that seminal plasma of O, A, and OA patients is enriched with Le^x and Le^y epitopes compared to normozoospermic men,(25) and lower semen quality is associated with increased SDF.(27) It is suggested that these epitopes contribute to the low immunogenicity of seminal plasma and induce tolerance of the female adaptive immune system, hence their quantitative changes could considerably impact male fertility.(32)

In subjects with normal semen parameters, we found a significant association between highly sialylated N-glycans SPGP5 ($p = 0.006$), SPGP17 ($p = 0.025$), and SPGP26 ($p = 0.038$), increased SDF, exposure to photocopying, and smoking. This may be because working next to a photocopy machine on an everyday basis represents a mixture of several possible substances such as ozone, electro-magnetic fields, volatile organic compounds, heavy metals, particulate matter, and increased temperature, all of which may have hazardous effects on male infertility.(35) Similarly, increased genome damage in newborns was

reported to be associated with sialylated glycans in blood plasma.(28) Association of smoking with significant changes in N-glycosylation is expected since smoking was already shown as a risk factor for disrupted sperm quality, including genome damage, motility, and morphology.(36) Smoking has a dual effect as a source of genotoxic compounds and EDs, such as cotinine, an aromatase inhibitor causing a decrease in estradiol.(37) Smoking was previously described to change the pattern of N-glycosylation in blood serum proteins in lung cancer patients.(38) A positive association of SPGP5 with industrial dyes, SPGP17, and residence near industry, as well as SPGP26 and usage of motor oils, together with increased SDF indicate the potential of N-glycans as biomarkers of exposure in men with disrupted semen parameters. An association of N-glycans with residence near industry (SPGP2, SPGP17) or highways (SPGP14), an effect potentially caused by air pollution, a factor shown to negatively impact fertility is detected in the current study.(39) Similarly, the changes in N-glycosylation of immunoglobulin G were previously associated with exposure to a traffic air pollutant.(40-42)

Considering the subjects with abnormal semen parameters, a significant negative association of SPGP18 with increased SDF ($p = 0.001$) and an association with smoking is detected. These results confirm smoking as a risk factor in men with disrupted sperm quality, however, the effect was observed for different N-glycans than those in normozoospermic men.

Other exposures to environmental stressors were also associated with specific N-glycans in men with abnormal semen parameters, although not with SDF. An interesting observation was an association of obesity with SPGP6 and SPGP14 in men with abnormal, but not in men with normal semen parameters, and in abnormal sub-groups, indicating the importance of participants sub-grouping for detection of the environmental effect. Moreover, lubricating oil, rich in petroleum (crude oil),(43) was associated with SPGP2, the N-glycan was also negatively associated with semen volume and immotile sperm, while positively with slow progressive motility in total and Ab subjects. Studies on animal models also showed that petroleum can negatively affect sperm motility, concentration, and velocity.(44, 45)

Classification of the subjects with abnormal semen parameters into A, O, and OA sub-groups yielded different environmental factors as significant. A significant association between exposure to photocopying, smoking, and the glycan peak SPGP26 in the A sub-group, the same effect that was observed in the normozoospermic group was observed. In the O group, the SPGP5 showed a significant positive association with photocopying and latex dyes and a negative with smoking, again similarly to the normozoospermic group, shown to be associated with sperm chromatin maturity,(27) which might be sperm characteristics affected by these environmental stressors. In the OA group, pesticides, known as risk factors for sperm quality,(46, 47) showed a significant association with SPGP2 and SPGP4, while a negative association with SPGP32. These glycans were also associated with decreased

motility and semen volume, parameters previously associated with pesticide exposure.(48, 49)

Seminal plasma total protein N-glycans might be potentially used as biomarkers for sperm quality affected by environmental exposure. In favor of the introduction of N-glycans is that clusterin (CLU), one of the main glycoproteins in seminal plasma and a biomarker of oxidative stress has already been investigated as a potential male infertility biomarker.(50) The large-scale proteomic analysis revealed clusterin has the same N-glycan composition as detected in SPGP14, SPGP17, and SPGP26 from our study, indicating the potential origin of these N-glycans. Moreover, seminal plasma glycoproteins fibronectin, prostatic acid phosphatase, metalloproteinase inhibitor, and semenogelin-2 were shown to have the highest number of glycoforms. SPGP2 and SPGP4 were found on fibronectin, and in the metalloproteinase inhibitors together with SPGP14 and SPGP17. Furthermore, abnormal semen parameters were associated with decreased fibronectin sialylation, lower expression of the α -2,3-sialylated fibronectin, and the existence of the asialo-fibronectin glycoforms, indicating the importance of glycosylation pattern in a specific protein, which could be reflected also in our study.(21)

Seminal plasma proteins are secretory, hence they are rich in post-translational modifications such as N-glycosylation. Previous studies have demonstrated that N-glycans and N-glycosidic bonds may differentiate between men with abnormal and normal semen parameters.(23, 26, 51) For example, lowered sialylation was demonstrated in O, A, and OA men. Moreover, the absence of glycans with sialic acid and an increase in fucosylation was detected in A men.(51) Next, sperm DNA damage can occur post-testicularly potentially from oxidative stress. That can affect not only sperm DNA integrity but also the pattern of seminal plasma protein N-glycans.(52) Since N-glycan composition can be highly dynamic also due to the environmental effects on the organism, the pattern of N-glycans from seminal plasma total proteins can change. The environmental toxicants can also induce oxidative stress, which can altogether lead to an altered N-glycan profile and sperm DNA damage.(53, 54)

Our study has certain limitations that should be addressed. Exposure to environmental factors was assessed with a questionnaire, which is a robust screening method. The more accurate recent data on exposure to different environmental stressors would be obtained by the direct measurements of xenobiotics in the participants' urine or blood samples. This also presents a potential future study direction, where precisely measured individual exposures to environmental factors in patients' samples and their correlation with seminal plasma N-glycans can be further studied. Based on the results, we suggest that the altered glycosylation in seminal plasma may reflect environmental exposures associated with sperm pathology. Further research is required on large cohorts which will enable additional profiling of N-glycans predictability of association between infertility in men and

environmental exposure which in some cases may be corrected and reflected in the improvement of sperm quality.

6.6 CONCLUSION

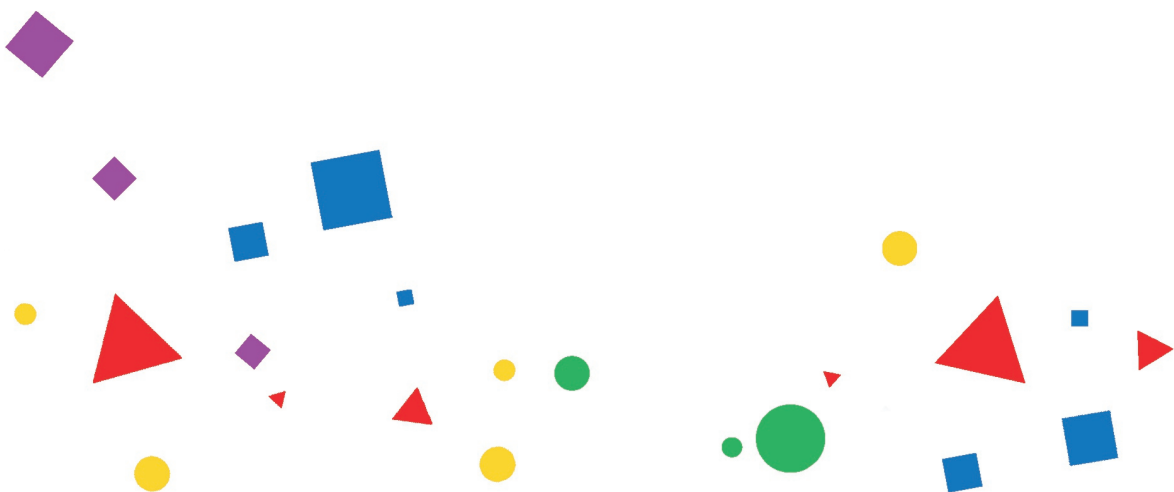
Seminal plasma N-glycan profile disturbances and sperm genome damage were shown to be associated with reduced semen quality and exposure to environmental factors. A significant association of these glycan features with smoking, exposure to complex mixtures such as working next to a photocopy machine, air pollution, industrial oils, and smoking is presented. The application of a battery of selected seminal plasma glycans may become a reliable predictor of infertility risk. Future investigations could also focus on the potential of N-glycans as biomarkers of assisted reproduction success.

6.7 REFERENCES

1. Sun H, Gong TT, Jiang YT, Zhang S, Zhao YH, Wu QJ. Global, regional, and national prevalence and disability-adjusted life-years for infertility in 195 countries and territories, 1990-2017: results from a global burden of disease study, 2017. *Aging (Albany NY)*. 2019;11(23):10952-91.
2. Fucic A, Duca RC, Galea KS, Maric T, Garcia K, Bloom MS, et al. Reproductive Health Risks Associated with Occupational and Environmental Exposure to Pesticides. *International Journal of Environmental Research and Public Health*. 2021;18(12):6576.
3. Hauser R, Skakkebaek NE, Hass U, Toppari J, Juul A, Andersson AM, et al. Male reproductive disorders, diseases, and costs of exposure to endocrine-disrupting chemicals in the European Union. *J Clin Endocrinol Metab*. 2015;100(4):1267-77.
4. Rehman I, Ahmad G, Alshahrani S. Chapter 10 - Lifestyle, Environment, and Male Reproductive Health: A Lesson to Learn. In: Sikka SC, Hellstrom WJG, editors. *Bioenvironmental Issues Affecting Men's Reproductive and Sexual Health*. Boston: Academic Press; 2018. p. 157-71.
5. Jeseta M, Navratilova J, Franzova K, Fialkova S, Kempisty B, Ventruha P, et al. Overview of the Mechanisms of Action of Selected Bisphenols and Perfluoroalkyl Chemicals on the Male Reproductive Axes. *Front Genet*. 2021;12:692897.
6. Maric T, Fucic A, Aghayanian A. Environmental and occupational exposures associated with male infertility. *Arh Hig Rada Toksikol*. 2021;72(3):101-13.
7. Zhang T, Ru YF, Wu B, Dong H, Chen L, Zheng J, et al. Effects of low lead exposure on sperm quality and sperm DNA methylation in adult men. *Cell Biosci*. 2021;11(1):150.
8. Cui F-P, Liu C, Deng Y-L, Chen P-P, Miao Y, Luo Q, et al. Urinary and seminal plasma concentrations of phthalate metabolites in relation to spermatogenesis-related miRNA106a among men from an infertility clinic. *Chemosphere*. 2022;288:132464.
9. Fucic AMA. *Challenges in Endocrine Disruptor Toxicology and Risk Assessment: The Royal Society of Chemistry*; 2021.
10. Agarwal A, Baskaran S, Parekh N, Cho C-L, Henkel R, Vij S, et al. Male infertility. *The Lancet*. 2021;397(10271):319-33.
11. World Health Organization H. *WHO laboratory manual for the examination and processing of human semen*. Manual. World Health Organization; 2021.
12. Ioannou D, Tempest HG. Does genome organization matter in spermatozoa? A refined hypothesis to awaken the silent vessel. *Systems Biology in Reproductive Medicine*. 2018;64(6):518-34.
13. Fernández JL, Muriel L, Goyanes V, Segrelles E, Gosálvez J, Enciso M, et al. Halosperm® is an easy, available, and cost-effective alternative for determining sperm DNA fragmentation. *Fertility and Sterility*. 2005;84(4):860.
14. Evgeni E, Charalabopoulos K, Asimakopoulos B. Human sperm DNA fragmentation and its correlation with conventional semen parameters. *J Reprod Infertil*. 2014(2228-5482 (Print)).
15. Jurewicz J, Radwan M, Wielgomas B, Dziewirska E, Karwacka A, Klimowska A, et al. Human Semen Quality, Sperm DNA Damage, and the Level of Reproductive Hormones in Relation to Urinary Concentrations of Parabens. *J Occup Environ Med*. 2017;59(11):1034-40.
16. Kiwitt-Cárdenas J, Adoamnei E, Arense-Gonzalo JJ, Sarabia-Cos L, Vela-Soria F, Fernández MF, et al. Associations between urinary concentrations of bisphenol A and sperm DNA fragmentation in young men. *Environmental Research*. 2021;199:111289.
17. Pearce KL, Hill A, Tremellen KP. Obesity related metabolic endotoxemia is associated with oxidative stress and impaired sperm DNA integrity. *Basic and Clinical Andrology*. 2019;29(1):6.
18. Lan R, Xin M, Hao Z, You S, Xu Y, Wu J, et al. Biological Functions and Large-Scale Profiling of Protein Glycosylation in Human Semen. *J Proteome Res*. 2020;19(10):3877-89.
19. Aebi M. N-linked protein glycosylation in the ER. *Biochim Biophys Acta*. 2013;1833(11):2430-7.
20. Seppala M, Koistinen H, Koistinen R, Chiu PC, Yeung WS. Glycosylation related actions of glycodeclin: gamete, cumulus cell, immune cell and clinical associations. *Hum Reprod Update*. 2007;13(3):275-87.
21. Kątnik-Prastowska I, Kratz EM, Faundez R, Chełmońska-Soyta A. Lower expression of the α 2,3-sialylated fibronectin glycoform and appearance of the asialo-fibronectin glycoform are associated with high concentrations of fibronectin in human seminal plasma with abnormal semen parameters. *Clinical Chemistry and Laboratory Medicine (CCLM)*. 2006;44(9):1119-25.
22. Kratz EM, Kaluza A, Zimmer M, Ferens-Sieczkowska M. The analysis of sialylation, N-glycan branching, and expression of O-glycans in seminal plasma of infertile men. *Dis Markers*. 2015;2015:941871.

23. Olejnik B, Kratz EM, Zimmer M, Ferens-Sieczkowska M. Glycoprotein fucosylation is increased in seminal plasma of subfertile men. *Asian Journal of Andrology*. 2015;17(2).
24. Janiszewska E, Kokot I, Gilowska I, Faundez R, Kratz EM. The possible association of clusterin fucosylation changes with male fertility disorders. *Sci Rep*. 2021;11(1):15674.
25. Kaluza A, Jarzab A, Gamian A, Kratz EM, Zimmer M, Ferens-Sieczkowska M. Preliminary MALDI-TOF-MS analysis of seminal plasma N-glycome of infertile men. *Carbohydr Res*. 2016;435:19-25.
26. Olejnik B, Jarzab A, Kratz EM, Zimmer M, Gamian A, Ferens-Sieczkowska M. Terminal Mannose Residues in Seminal Plasma Glycoproteins of Infertile Men Compared to Fertile Donors. *Int J Mol Sci*. 2015;16(7):14933-50.
27. Maric T, Katusic Bojanac A, Matijevic A, Ceppi M, Bruzzone M, Evgeni E, et al. Seminal Plasma Protein N-Glycan Peaks Are Potential Predictors of Semen Pathology and Sperm Chromatin Maturity in Men. *Life (Basel)*. 2021;11(9).
28. Fucic A, Guszak V, Keser T, Wagner J, Juretić E, Plavec D, et al. Micronucleus, cell-free DNA, and plasma glycan composition in the newborns of healthy and diabetic mothers. *Mutation Research/Genetic Toxicology and Environmental Mutagenesis*. 2017;815:6-15.
29. Fucic A, Katic J, Fthenou E, Kogevinas M, Plavec D, Koppe J, et al. Increased frequency of micronuclei in mononucleated lymphocytes and cytome analysis in healthy newborns as an early warning biomarkers of possible future health risks. *Reprod Toxicol*. 2013;42:110-5.
30. Fucic A, Starcevic M, Dessardo NS, Batinic D, Kralik S, Krasic J, et al. The Impact of Mother's Living Environment Exposure on Genome Damage, Immunological Status, and Sex Hormone Levels in Newborns. *Int J Environ Res Public Health*. 2020;17(10).
31. Trbojević-Akmačić I, Ugrina I, Lauc G. Chapter Three - Comparative Analysis and Validation of Different Steps in Glycomics Studies. In: Shukla AK, editor. *Methods in Enzymology*. 586: Academic Press; 2017. p. 37-55.
32. Pang PC, Tissot B, Drobnis EZ, Morris HR, Dell A, Clark GF. Analysis of the human seminal plasma glycome reveals the presence of immunomodulatory carbohydrate functional groups. *J Proteome Res*. 2009;8(11):4906-15.
33. Ceroni A, Maass K, Geyer H, Geyer R, Dell A, Haslam SM. GlycoWorkbench: a tool for the computer-assisted annotation of mass spectra of glycans. *J Proteome Res*. 2008;7(4):1650-9.
34. Drabovich AP, Saraon P, Jarvi K, Diamandis EP. Seminal plasma as a diagnostic fluid for male reproductive system disorders. *Nature Reviews Urology*. 2014;11(5):278-88.
35. Nandan A, Siddiqui NA, Kumar P. Assessment of environmental and ergonomic hazard associated to printing and photocopying: a review. *Environ Geochem Health*. 2019;41(3):1187-211.
36. Ranganathan P, Rao KA, Thalaivarasai Balasundaram S. Deterioration of semen quality and sperm-DNA integrity as influenced by cigarette smoking in fertile and infertile human male smokers-A prospective study. *J Cell Biochem*. 2019;120(7):11784-93.
37. Barbieri RL, Gochberg J, Ryan KJ. Nicotine, cotinine, and anabasine inhibit aromatase in human trophoblast in vitro. *J Clin Invest*. 1986;77(6):1727-33.
38. Vasseur JA, Goetz JA, Alley WR, Jr., Novotny MV. Smoking and lung cancer-induced changes in N-glycosylation of blood serum proteins. *Glycobiology*. 2012;22(12):1684-708.
39. Sun S, Zhao J, Cao W, Lu W, Zheng T, Zeng Q. Identifying critical exposure windows for ambient air pollution and semen quality in Chinese men. *Environ Res*. 2020;189:109894.
40. Liu J, Liu S, Huang Z, Fu Y, Fei J, Liu X, et al. Associations between the serum levels of PFOS/PFOA and IgG N-glycosylation in adult or children. *Environmental Pollution*. 2020;265:114285.
41. Calogero AE, La Vignera S, Condorelli RA, Perdichizzi A, Valenti D, Asero P, et al. Environmental car exhaust pollution damages human sperm chromatin and DNA. *J Endocrinol Invest*. 2011;34(6):e139-43.
42. Chaemfa C, Barber JL, Huber S, Breivik K, Jones KC. Screening for PFOS and PFOA in European air using passive samplers. *J Environ Monit*. 2010;12(5):1100-9.
43. Nowak P, Kucharska K, Kamiński M. Ecological and Health Effects of Lubricant Oils Emitted into the Environment. *International Journal of Environmental Research and Public Health*. 2019;16(16):3002.
44. Bamiro SA, Elias SO, Ajonuma LC. Sperm motility characteristics and oxidative stress in crude oil exposed rats. *Fertility and Sterility*. 2018;110(4, Supplement):e173.
45. Obidike IR, Maduabuchi IU, Olumuyiwa SS. Testicular morphology and cauda epididymal sperm reserves of male rats exposed to Nigerian Qua Iboe Brent crude oil. *J Vet Sci*. 2007;8(1):1-5.
46. Ghafouri-Khosrowshahi A, Ranjbar A, Mousavi L, Nili-Ahmadabadi H, Ghaffari F, Zeinvand-Lorestani H, et al. Chronic exposure to organophosphate pesticides as an important challenge in promoting reproductive health: A comparative study. *J Educ Health Promot*. 2019;8:149.

47. Manikandan I, Bora S, Adole PS, Thyagaraju C, Nachiappa Ganesh R. Assessment of Organophosphate Pesticides Exposure in Men with Idiopathic Abnormal Semen Analysis: A Cross-Sectional Pilot Study. *Int J Fertil Steril*. 2021;15(3):219-25.
48. Abou Ghayda R, Sergeyev O, Burns JS, Williams PL, Lee MM, Korrick SA, et al. Peripubertal serum concentrations of organochlorine pesticides and semen parameters in Russian young men. *Environ Int*. 2020;144:106085.
49. Giulioni C, Maurizi V, Scarcella S, Di Biase M, Iacovelli V, Galosi AB, et al. Do environmental and occupational exposure to pyrethroids and organophosphates affect human semen parameters? Results of a systematic review and meta-analysis. *Andrologia*. 2021;53(11):e14215.
50. Janiszewska E, Kratz EM. Could the glycosylation analysis of seminal plasma clusterin become a novel male infertility biomarker? *Molecular Reproduction and Development*. 2020;87(5):515-24.
51. Ka UAA, Ferens-Sieczkowska MA, Olejnik B, Ko Odziejczyk J, Zimmer M, Kratz EM. The content of immunomodulatory glycoepitopes in seminal plasma glycoproteins of fertile and infertile men. *Reprod Fertil Dev*. 2019;31(3):579-89.
52. Khoder-Agha F, Kietzmann T. The glyco-redox interplay: Principles and consequences on the role of reactive oxygen species during protein glycosylation. *Redox Biology*. 2021;42:101888.
53. Kumar N, Singh AK. Impact of environmental factors on human semen quality and male fertility: a narrative review. *Environmental Sciences Europe*. 2022;34(1):6.
54. Spiro RG. Protein glycosylation: nature, distribution, enzymatic formation, and disease implications of glycopeptide bonds. *Glycobiology*. 2002;12(4):43R-56R.



Chapter 7

Discussion and perspectives



7.1 MASS SPECTROMETRY IS OF PARAMOUNT IMPORTANCE IN GLYCOMICS DISCOVERY STUDIES

Mass spectrometry (MS) has emerged as a method of choice for clinical marker discovery studies. It provides precise mass information and structurally informative fragments with high sensitivity and specificity. Moreover, it enables the quantitative analysis of glycoform abnormalities. Clinical marker discovery only became practical with the introduction of high-throughput and robust mass spectrometry-based methodologies into glycomic studies.(1-3) Nowadays, a wide range of high-throughput analytical strategies is available for glycan-orientated clinical evaluation.(4, 5)

In this thesis, the glycan-orientated research studies were conducted using three types of mass spectrometers. In **Chapters 2 and 3**, IgG glycopeptides were analyzed by reversed-phase nano-liquid chromatography coupled to electrospray ionisation quadrupole time-of-flight mass spectrometry (RP-nLC-ESI-QTOF-MS). Finally, in **Chapter 5 and 6** hydrophilic interaction liquid chromatography hyphenated with electrospray ionisation time-of-flight mass spectrometry (HILIC-LC-ESI-TOF-MS) was utilized to analyze released N-glycans from either serum or seminal plasma. In **Chapter 4**, we employed reversed-phase nano liquid chromatography coupled to electrospray ionisation quadrupole Kingdon trap, commercially referred to as Orbitrap™ mass spectrometry (RP-nLC-ESI-KT-MS), to analyze FcγRIIIb glycopeptides. The glycopeptide workflow involved protein purification, enzymatic digestions, purification of glycopeptides, and their analysis by either RP-LC-ESI-TOF-MS or RP-LC-ESI-KT-MS. For the released N-glycan analysis, glycans were released from either a purified protein or total glycoproteins in the sample. Subsequently, the released N-glycans were labeled with a fluorescent tag, separated by HILIC-LC and analyzed by on-line ESI-TOF-MS. It is important to note, that each of the aforementioned LC-MS strategies is suitable for separating ions according to their mass-to-charge ratio, each with its own set of advantages and disadvantages in terms of mass resolution, accuracy, ion fragmentation capabilities, user-friendliness, throughput and level of structural information content.

The mass spectrometry instrumentation mentioned above involved ESI as a preferable soft ionization technique. Although not used in this thesis, there is another technique called matrix-assisted laser desorption/ionization (MALDI) widely used to ionize glycoforms. Both ESI-MS and MALDI-MS are attractive methods for clinical marker discovery on the level of released N-glycans, glycopeptides, as well as intact glycoproteins profiled from human biofluids.(6) They offer powerful and in-depth characterization of glycoforms with high-sensitivity and specificity. ESI-MS can be easily hyphenated with various separation techniques to further enhance the sensitivity, specificity and precision of the MS analysis. On the other hand, MALDI-MS includes a simpler sample preparation workflow that can be fully automated.(7, 8) Additionally, it eliminates the need for a separation system prior to

measurement, enhancing its throughput capacity, and making it a popular choice among researchers for high-throughput analysis.(8) However, limitation of MALDI-MS include the inability to separate glycan isomers, as well as the need for a derivatization strategy to preserve labile sialic acids.(8) Numerous studies have used these methods to identify altered glycosylation patterns in various diseases.(1, 9, 10) Mass spectrometry-based assays for glycan screening using either MALDI-MS or ESI-MS analysis are well-suited for clinical laboratories.(6, 11) However, despite the great potential, the clinical utility of these techniques is still in its early stages. Further research and development are needed to fully harness their power for clinical applications.

MS is an essential tool in glycan analysis, but it comes with inherent limitations. Since it relies solely on mass accuracy measurements, MS struggles to distinguish between structural isomers of glycoforms. The differentiation of isomers is important because distinct structural isomers can have varying biological relevance.(12, 13) To provide the capability to separate isomeric glycans and glycopeptides, MS is often coupled with various chromatography techniques, such as porous graphitized carbon, capillary electrophoresis, ion exchange, reverse phase (RP) and hydrophilic liquid chromatography (HILIC). Among these, HILIC and RP have shown great promise for high-throughput applications due to their robustness and reproducibility, as demonstrated in the aforementioned studies. Hydrophilic interaction liquid chromatography (HILIC) is primarily used for separating released glycans.(14) Alternatively, HILIC can also be applied for glycopeptide analysis, resolving glycan linkage isomers. On the other hand, reverse-phase liquid chromatography (RP-LC) has become the most widely used method for glycopeptide separation.(15) RP-LC has likewise been shown to resolve glycan isomers and to be also employed for analyzing released glycans.(16) These chromatography techniques, when combined with MS offer a more comprehensive and versatile approach to glycan analysis, addressing challenges posed by structural isomers.

In **Chapter 3**, we employed a nLC-qTOF-MS to investigate the IgG glycosylation patterns of IgG in patients with ANCA-associated vasculitis (AAV). The results revealed specific glycomics markers that are closely linked to disease relapse. These findings contribute to the growing body of evidence indicating the significant role of glycosylation in maintaining overall health, and its association with the occurrence, progression and outcome of various diseases.(17-19) As a consequence, glycans have emerged as promising clinical markers with the potential to be utilized in disease diagnosis, prognosis and monitoring.(20) However, despite the rapidly growing body of evidence supporting the clinical value of glycan markers, there are challenges associated with the translation of the glycomic MS-based approaches into clinical laboratories.

The path from the discovery of a glycan marker to its successful clinical implementation involves a series of steps and requirements that must be fulfilled. The development of a method that reliably identifies a candidate clinical marker is just the initial phase in this process. Subsequent steps include the clinical validation of the marker and analytical validation of the method, demonstrating their sensitivity and specificity, obtaining regulatory agency approval, gaining acceptance from healthcare practitioners, and ultimately, their inclusion in appropriate medical guidelines. In the field of proteomics, a three-tier classification system (Tier 1, Tier 2, Tier 3) has been developed to outline the prerequisites for protein quantification assays in both protein biomarker discovery and well as their anticipated clinical integration.(21) These tiers represent the stringency of requirements for various assay performance metrics, including precision, accuracy, repeatability as well as the extend of analytical validation. As the tier decreases, the requirements become more stringent, indicating distinct characteristics of the analytical performance and preferred applications for each tier. Specifically, Tier 3 methods are primarily used for clinical markers discovery, Tier 2 for clinical marker quantification and validation, and Tier 1 for clinical implementation. To facilitate the transfer and implementation of quantitative MS-based glycomics assays across different clinical laboratories, glycan and glycopeptide markers could be subjected to standardized strategies similar to those developed for protein markers. A comparable Tier 1 for glycan and glycopeptide markers would necessitate absolute quantification through the use of stable isotope-labeled (SIL) internal standards. Indeed, the incorporation of stable isotope-labeled internal standards into glycans and glycopeptides methods would enable improved absolute quantification of individual glycoforms in a standardized manner, facilitating the establishment of consistent reference ranges for diagnostic purposes.(22). However, the current absence of well-established synthetic SIL analogs for released glycans, glycopeptides, and intact glycoproteins impedes the translation of glycomics and glycoproteomics profiling into standardized clinical assays. Consequently, most MS-based glycomic approaches are currently better suited for clinical marker discovery studies, where relative quantification of individual glycoforms in relation to the total glycoform signal intensity is deemed acceptable.(6) Nonetheless, the growing interest in clinical glycoscience will drive further advancements in the development of internal standards necessary to facilitate the translation of these approaches to clinical laboratories.(23) Alternatively, the clinical translation of glycan-based markers can be facilitated through the implementation of proposed tiers tailored for glycan-multimarker panels, especially with the regard to quantification.(24)

The analytical methods anticipated to translate clinical markers from discovery studies to clinical practice must deliver excellent diagnostic performance and undergo rigorous validation. Additionally, these methods should be fit-for-purpose, robust and cost-effective. Ideally, these methods should be straightforward enough for healthcare providers to

perform. While mass spectrometry offers numerous advantages in discovery glycomics analysis, it also comes with completely opposite characteristics, such as high operational costs, complex sample preparation procedures and the requirement for sophisticated instrumentation and skillful personnel, particularly when analyzing glycans. One elegant solution to this challenge is to simplify the analysis approach and shift away from MS-based methods which are used for clinical marker discovery, towards non-MS-based platforms for clinical deployment.⁽²⁵⁾ By transitioning to non-MS-based platforms, particularly immunoassays and plate-based assays, the barriers associated with cost, complexity and expertise can be overcome, making the glycan-based clinical marker analysis more accessible. When established with a high level of accuracy and precision, these non-MS-based platforms have the potential to be easily and successfully implemented in existing molecular diagnostic laboratories. The transition of glycomic assays between platforms is exemplified by the development of an immunoassay for relative and absolute quantification of antigen-specific IgG fucosylation, which serves as a clinically relevant marker for altered IgG effector functions, such as antibody-dependent cellular cytotoxicity.⁽²⁶⁾ Initially, LC-MS-based methods were used to characterize antigen-specific IgG Fc-fucosylation in alloimmune diseases or viral infections ^(27, 28) Subsequently, a fucose-sensitive ELISA-based method for quantifying antigen-specific IgG (FEASI) was developed for assay validation and potential clinical utilization. FEASI is a high-throughput assay that can be implemented in diagnostic laboratories, for example, for screening patients with lower IgG Fc fucosylation on anti-S antibodies, which has the potential to guide the treatment of conditions such as COVID-19.⁽²⁶⁾ This approach eliminates the need for sophisticated equipment and complex analytical and computational processing required for antigen-specific IgG Fc glycosylation analysis. While plate-based glycomics assays are sensitive and relatively costs-effective, and therefore well suited for the clinical laboratory, they are challenged by technological limitations. These limitations include cross-reactivity, limited specificity, interference and low multiplexing capability. This becomes crucial as often multiple glycosylation features, need to be analyzed simultaneously as a panel of structures rather than individually. However, with the current availability of novel antigen preparations (recombinant, highly purified proteins, synthetic oligosaccharides) along with other methodological improvements, a new generation of immunoassay-based and plate-based methods is being developed, enabling the investigation of glycan structures even in minute amounts of antigen-specific responses.^(26, 29)

Immunoassays are one of the main diagnostics tools in today's clinical laboratories, offering several distinct advantages. They stand out primarily for their minimal sample preparation requirements and the absence of the need for sophisticated instrumentation. Instead, immunoassays rely on straightforward detection methods, such as photo-, fluoro-, or luminometric techniques, replacing chromatographic approaches in clinical diagnostics. These methods benefit from simplicity, rapidity, sensitivity, and potential for automation,

making them less dependent on the operator's skill. For example, the measurement of the carbohydrate antigen 19-9 (CA 19-9), also known as sialyl-Lewis^a antigen, is commonly conducted using immunoassays.(30, 31) Within clinical laboratories, a range of immunoassay techniques, including electrochemiluminescence immunoassay, enzyme immunoassay or microparticle-enhanced enzyme immunoassay, is employed to assess elevated CA 19-9 levels in circulation.(32) Notably, elevated CA 19-9 levels are indicative of pancreatic cancer and are instrumental in monitoring the effectiveness of therapy.(33)

7.2 GLYCAN SIGNATURES AS POTENTIAL CLINICAL MARKERS

Glycomics and glycoproteomics have emerged as promising sources of clinical markers, and this expansion shows no sign of slowing down as new technologies come into play.(24, 34, 35) Among the most extensively studied glycan markers are the glycosylation of total plasma proteins (plasma total N-glycome, TPNG) and the glycosylation of the most abundant plasma glycoprotein, immunoglobulin G (IgG N-glycome).(18, 36) Both plasma and IgG N-glycans can offer valuable insight, for example distinguishing between states of health and disease, discerning different disease subtypes or predicting disease outcomes. The growing availability of data from retrospective cohorts, as exemplified in **Chapters 2, 3, and 6**, has led to significant advances in our comprehension of how alterations in N-glycosylation are associated with the onset, progression and severity of various diseases, shedding light on pathophysiological processes. Notably, as demonstrated in **Chapter 3**, glycans can be tracked longitudinally to monitor treatment response and predict the likelihood of disease relapse. Glycan markers are explored for multiple clinical purposes, including diagnosis, prediction, prognosis, guiding treatment decisions, and assessing treatment response.(17, 24)

7.2.1 Plasma glycan-based clinical markers

Plasma serves not only as the primary clinical specimen but also as a readily accessible source for the discovery of novel clinical markers.(18, 37) Given that the vast majority of plasma proteins undergo glycosylation, exploring plasma protein N-glycosylation holds enormous potential for identifying specific glycosylation signatures associated with a wide range of diseases.(18) **Chapter 5** describes an optimization of a novel profiling approach for total plasma N-glycome. This method utilizes user-friendly LC-MS instrumentation and a novel fluorescent label with an *N*-hydroxysuccinimide carbamate tag, quinolone fluorophore, and tertiary amine to enhance ionisation efficiency.(38) With its simplicity and robustness, the method opens exciting avenues for translating glycomic profiling into clinical practise.

Profiling of total plasma N-glycans, encompassing the release and analysis of N-glycans bound to all plasma proteins, and provides data on alterations in glycan structures. Changes in plasma protein glycosylation constitute an important phenotypic feature of both health

and disease and hold potential as differential clinical markers. The vast majority of glycoproteins in plasma, including acute phase proteins and apolipoproteins, originate from liver. Therefore, it does not come as a surprise that these plasma glycosylation patterns predominantly mirror liver (patho)physiology.(37, 39) The differences in the level of bisection and galactosylation are indicative of an individual's liver health status, and methods quantifying these differences are currently being applied for the differential diagnosis of liver fibrosis.(40). This success story exemplifies a plasma glycomics-based test, readily available for clinical use.

In addition to its relevance in liver disorders, the plasma N-glycome holds the potential for differential diagnosis of pathologies arising from mutations in genes which are implicated or directly involved in glycosylation processes. This includes conditions such as congenital disorder of glycosylation (CDG) and maturity-onset diabetes of the young type 3 (MODY3). Notably, disease-causing mutations in these diseases exert systemic effects on the glycosylation processes. MODY3, a subtype of maturity-onset diabetes of the young, is caused by mutations in the *HNF1A* gene, which encodes hepatocyte nuclear factor-1 α (HNF1 α). HNF1 α regulates the expression of several liver-specific genes, including those encoding fucosyltransferases.(41) Genome-wide association studies (GWAS) showed that the lower activity of HNF1A leads to the downregulation of α 1-3 and α 1-4 fucosyltransferase. Subsequent studies proposed a reduction in antennary fucosylation levels of plasma N-glycans as a hallmark of HNF1A-MODY.(42) Subsequently, the antennary fucosylation signature of plasma proteins demonstrated high differential diagnostic performance in distinguishing HNF1A-MODY using glycomics workflows. (43) A novel exoglycosidase plate-based assay, has been developed for the quantification of antennary fucosylation markers, offering a straightforward diagnostic tool.(29) This assay paves the way toward integrating N-glycomic approaches into clinical practice for the diagnosis of individuals with deleterious HNF1A variants.

In the context of CDG diagnosis, the exploration of plasma N-glycan differences shows promise for improving the diagnostic process. CDG are rare inherited conditions caused by recessive mutation that affect protein N-glycosylation. Currently, CDG diagnostic relies on carbohydrate-deficient transferrin (CDT) profiling, typically by isoelectric focusing. However, CDT has limited diagnostic value. For instance, in cases of SLC35A2-CDG, which are caused by genetic defects in the uridine diphosphate (UDP)-galactose transporter, classical transferrin analysis often fails to detect the disease due to an unchanged transferrin glycosylation profile in the majority of patients. As a result, researchers have broadened their focus and look at plasma N-glycans, which encompass alterations in the glycosylation of the most abundant glycoproteins.(44) Recently, Chen et al. identified potential new N-glycan markers by employing a fast and semi-quantitative MS-based technique using flow-injection ESI-QTOF.(45) They pinpointed oligomannose N-glycans as

potent clinical markers for screening different CDG subtypes. Moreover, by making use of an isotope-labeled sialylated glycopeptide they were able to semi-quantitatively assess N-glycans. Their approach proved efficient for the diagnosis of certain CDGs and demonstrated superiority over alternative methods, particularly in terms of robustness and turnaround time.

Although very promising in detecting some genetic diseases, a wide variety of diseases associate with similar changes in plasma protein glycosylation. Generally, an aberrant plasma N-glycome such as an increase in fucosylation, branching or sialylation, has been cross-sectionally linked to numerous pathological states. These range from diabetes, and inflammation to even cancer.(18, 46) Thus, specificity and sensitivity as a stand-alone clinical marker are missing. Moreover, total plasma N-glycan profiling is biased by the variation in protein concentration. When studying total plasma N-glycome with glycomics methods, we are not able to determine if the observed glycosylation changes originate from variations in protein concentration and/or variations in protein glycosylation.

To eliminate this variation and to increase the sensitivity and specificity of glycan-based markers derived from plasma, an approach that involves protein-specific and site-specific glycosylation analysis is being explored. This method includes the isolation of the protein of interest and the analysis of both the protein backbone and the attached glycans. By specifically targeting the glycosylation patterns of certain plasma glycoproteins, such as alpha-fetoprotein (AFP), there is great promise for improving the accuracy of differential diagnosis. AFP is a plasma marker for diagnosing hepatocellular carcinoma (HCC). However, its performance in early HCC detection is limited by low specificity, especially in patients with benign liver disease. In light of this limitation, a particular proteoform of AFP, fucosylated alpha-fetoprotein-L3 (AFP-L3) has proved to be more specific and sensitive, making it a promising new generation HCC marker that allows for earlier diagnosis, assessment of therapeutic effects and evaluation of the biological malignancy.(47, 48) The test, which evaluates both the percentage of AFP-L3 and the AFP concentration is now FDA-approved for use as a marker for determining the risk of HCC in clinical settings. By delving deeper into protein-specific glycosylation analysis and exploring specific proteoforms like AFP-L3, we are making substantial progress in developing glycan-based clinical markers for targeted disorders. This advancement holds potential for disease diagnosis and personalized medicine, ultimately leading to improved patients outcomes.

Another way to increase the specificity of plasma-derived markers is to conduct site- and protein-specific analysis of glycosylation, for instance, based on intact glycopeptide workflows. The ideal scenario would entail the simultaneous site-specific examination of protein glycosylation across total plasma proteins using a multiplexed analysis method. Recent efforts have been directed toward optimising the analysis of a large number of

glycopeptides within a single glycoproteomics workflow for plasma samples, using different tandem mass spectrometry approaches.(49) As such, individual glycopeptide differences can serve as highly specific signatures, thus improving the specificity of plasma glycans and their clinical utility in monitoring and improving CDG diagnostics.(49) Insights gained from this innovative large-scale site-specific glycosylation analysis provide an exciting perspective toward understanding disease processes, and designing individualized diagnostics based on glycosylation status. Nevertheless, a current challenge lies in the availability of bioinformatic tools capable of handling the extensive and intricate site-specific glycosylation data and correlating meaningful glycoproteomic changes with clinical phenotypes, thereby ensuring its practical clinical application.

7.2.2 Immunoglobulin G glycosylation-based clinical markers

N-glycans of immunoglobulin G, the most abundant immunoglobulin in human plasma and a key component of the adaptive immune response, have emerged as potential clinical markers. Years of research in profiling IgG glycosylation revealed alterations in IgG glycosylation profiles in various clinical conditions, enabling differentiation between healthy controls and individuals with disease, patient stratification and disease prediction.(20, 36) For instance, profiling of IgG glycosylation has shown promise in distinguishing early-stage thyroid cancer from non-cancer controls by utilizing several N-glycan structures as differential markers. (50)

While glycan-based markers demonstrate high accuracy in disease detection, they often lack sensitivity, leading to a risk of false-positive findings. This limitation is particularly concerning when using IgG N-glycans as a stand-alone clinical marker. Many disparate diseases very often exhibit similar IgG N-glycan trends, showing changes in galactose, sialic acid, fucose and bisected GlcNAc content that move in the same direction. Consequently, changes in total IgG glycosylation do not appear to be disease-specific but rather represent non-specific effects, reflecting a general immune activation or common underlying inflammatory mechanisms.(51)

Despite the limitations of IgG N-glycans as stand-alone clinical markers in clinical practice, their integration with other diagnostic measures can improve diagnostic sensitivity and specificity, addressing clinical needs. For instance, a promising complementary analysis involves the combination of glycoprotein cancer antigen 125 (CA-125), an FDA-approved serum clinical marker for ovarian cancer detection, with IgG N-glycans. While CA-125 is frequently used, its performance in diagnosing ovarian cancer is only modest due to poor specificity, as it often increases in benign gynaecological pathologies. However, incorporating the quantification of IgG (a)galactosylation, which has been found to differentiate between benign and malignant stages, in multiplex clinical marker platforms improves the specificity from 62.2% to 84.6%.(52) This combined approach refines the

differential diagnosis of ovarian cancer, highlighting the importance of combining clinical markers in future diagnostic and prognostic strategies. A similar strategy to enhance the robustness of existing clinical markers is demonstrated in **Chapter 3**, where the performance of an ANCA rise for detecting AAV relapse could potentially be improved by considering IgG fucosylation. Given the complex nature of various disease responses and the heterogeneity of patient responses, combinations or panels of clinical markers have the highest potential to become a key aspect of future diagnostic and prognostic strategies. However, further research is needed to determine the most effective panels for each purpose. Additionally, to enable this shift, technology needs to be developed that allows for the simultaneous assessment of multiple markers from a single blood sample.

While this thesis is focused on the evaluation of longitudinal and cross-sectional alterations in total IgG glycosylation, another very promising approach to improving the specificity of glycan-based clinical markers involves isolating and analysing the glycosylation of antibodies against specific antigens. Especially those produced in response to infectious agents, as well as those playing a central role in the pathogenesis of autoimmune and alloimmune diseases are interesting targets. Profiling the glycosylation of these antigen-specific antibodies not only holds the potential to predict disease activity, but also provides valuable insights into the immunological response and the underlying mechanisms driving the pathologies. By focusing on these specific antibodies, we can gain a deeper understanding of disease progression and the factors influencing it. Indeed, in many cases of infectious, autoimmune and alloimmune diseases, the N-glycosylation of these antigen-specific antibodies has been reported to be altered and different from the total IgG.(28, 53, 54) Specifically, IgG Fc-fucosylation has emerged as a critical pathological feature in infectious diseases and alloimmune diseases.(55) Mechanistically, the low core fucose content on IgG amplifies affinity to Fc-gamma receptor IIIa (FcγRIIIa) and IIIb (FcγRIIIb), thereby increasing downstream signalling and escalating antibody-dependent cell-mediated cytotoxicity (ADCC). These changes can profoundly impact the effector functions of IgG and trigger pro-inflammatory responses of the immune system, ultimately leading to disease exacerbation. Recent studies have pointed towards low fucosylation levels on antigen-specific as a hallmark of severe disease and demonstrated their potential to stratify patients upon diagnosis of coronavirus disease 2019 (COVID-19) infection.(56) Consequently, future tests monitoring antigen-specific IgG N-glycosylation features can aid in patient stratification and assessing the effectiveness of specific treatments. This can potentially lead to adjustments or alterations in therapy to maximise the beneficial effect on the patients' health.

The integration of established clinical markers like proteins and cytokines with newer omics markers, such as glycans, is both exciting and promising. Glycomics-based clinical markers have the potential to advance personalized medicine significantly. Notably, IgG glycosylation cannot only aid in diagnosing diseases but also predict the disease

development as well as the risk of developing certain conditions.(36) However, there are still many challenges to overcome before moving from the discovery phase to clinical use. The current limitations of the field include 1) the lack of an internal standard enabling absolute quantification and control for technical variability; 2) the need for validation of the primary results on the larger population in multicentre analysis and prospective cohorts; 3) the development of assays that can be easily transferred to clinical settings. To unlock the full potential of IgG N-glycomics and make significant strides in discovery and innovation, further research is required to address these limitations. By doing so, we can pave the way for incorporating glycomics into clinical practice, ultimately improving patient outcomes and advancing personalized medicine.

7.3 FcγRIIIb GLYCOSYLATION AND ITS FUNCTIONAL RELEVANCE

IgG antibodies play a pivotal role in triggering antigen-specific immune responses by binding to FcγRs located on the surface of various effector cells. This binding event initiates a cascade of downstream effector signalling events. For example, in human neutrophils, the interaction of IgG with FcγRs can trigger processes such as phagocytosis, NET formation, and degranulation.(57) The strength of this immunologically relevant IgG-FcγR interaction is profoundly influenced by the proteoform distribution of both binding partners. Notably, N-glycosylation of not only IgG but also FcγR has been found to modulate the binding affinity between IgG and FcγR.(58, 59) Despite the significance of glycosylation in this context, comprehensive profiling of endogenous FcγR was limited. These constraints arise from various analytical challenges, including the scarcity of endogenous FcγR material, substantial structural diversity of glycans, and the presence of multiple glycosylation sites in close proximity.

In an effort to address this issue, **Chapter 4** outlines the analytical method designed to enable the straightforward and comprehensive site-specific profiling of vastly understudied N-glycosylation of FcγRIIIb isolated from a primary human cell material from a single donor. While other research groups have also developed analytical methods for site-specific glycosylation profiling of FcγRIIIb, our analytical approach overcomes several limitations of prior studies.(60-62) In particular, it allowed for the individual assessment of all glycosylation sites across multiple donors in a single LC-MS run. The results revealed an extensive compositional heterogeneity, spanning from oligomannosidic structures to complex sialylated tetra-antennary glycans with LacNAc extensions. While this method has allowed for a comprehensive and in-depth characterization of glycopeptides structures, uncovering the intricate details of glycan structures still remains a challenge. The study would benefit from an orthogonal method addressing for instance, isomer separation. Recently, progress has been made and new LC-MS/MS-based workflows showed the capability to determine glycan structural isomerism at the glycopeptide level, thereby achieving a higher degree of isomer separation.(63)

Furthermore, by incorporating several modifications into our method, it has the potential not only to improve isomer separation resolution but also to become a sensitive, robust and powerful workflow for high-throughput FcγRIII glycopeptide analysis. For instance, the initial glycopeptide identification was performed using the Byonic software. A substantial part of the process involved manual interpretation of both MS and MS/MS data. While effective for smaller sets, this approach becomes progressively more time-consuming and less efficient when analysing larger sample sets. Recent advancements in bioinformatic tools have partially addressed this challenge through the use of GlycopeptideGraphMS, which streamlines glycopeptide identification, curation and quantification following LC-MS(/MS) analysis.(64, 65) The manual identification process can now be semi-automated by integrating multiple software packages, such as Byonic, GlycopeptideGraphMS and LaCyTools. This integrated approach would reduce the time and effort required for manual analysis, thereby enabling the efficient processing of larger and more complex data sets.

There are also several unexplored aspects regarding the functional and clinical impact of FcγRIII glycosylation. Despite recent studies implicating the active role of glycosylation of the FcγRIII in the interaction with IgG,(58) there remains a notable scarcity of information regarding the glycosylation profile of the receptor in both healthy and diseased states. The potential application of this method to clinical samples would enhance our understanding of the clinical significance of differential FcγRIII glycosylation in healthy and diseased individuals. One compelling example is ANCA-associated vasculitis, a condition where the neutrophil activation plays a key role in damaging surrounding vessels and thus contributing to the disease mechanism. Exploring differences in FcγRIII glycosylation between healthy and diseased individuals represents a fascinating avenue for further research.

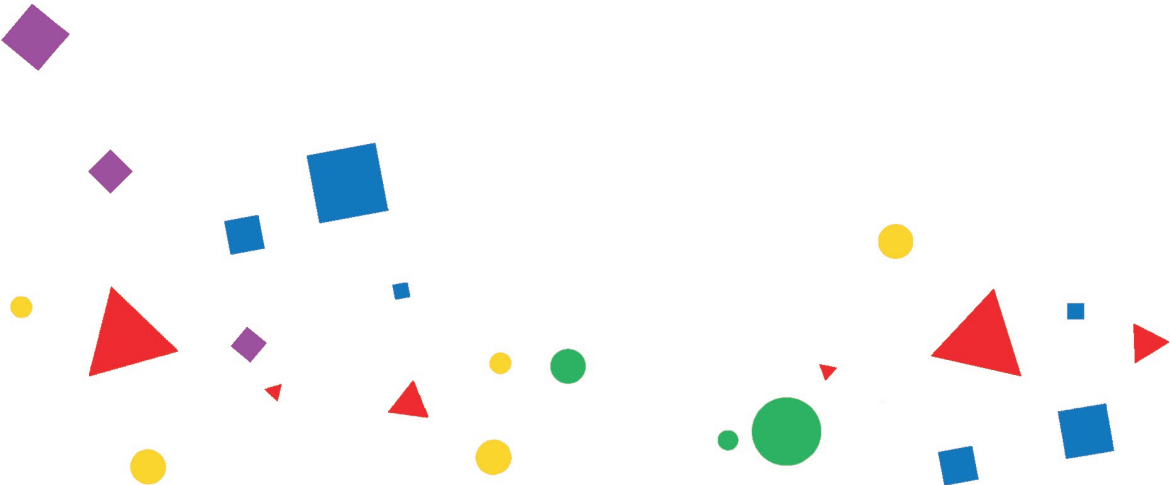
One key question pertains to the dynamics of N-glycosylation in FcγRIII. It raises the intriguing question whether potential glycosylation modulation is one the mechanisms by which neutrophils regulate their FcγR-dependent functions. For now, the data indicate that N-glycosylation of neutrophil-derived FcγRIIIb is rather consistent between healthy individuals. However, it significantly differs from the profiles of soluble FcγRIIIb, and that of recombinant or serum-derived and NK cell-derived FcγRIIIa profiles.(60, 64) This provides very interesting perspectives on the dynamic changes of FcγRIII upon activation and thus ground for future studies on the interaction between FcγRIIIb and IgG.

7.4 REFERENCES

1. Reiding KR, Ruhaak LR, Uh HW, El Bouhaddani S, van den Akker EB, Plomp R, et al. Human Plasma N-glycosylation as Analyzed by Matrix-Assisted Laser Desorption/Ionization-Fourier Transform Ion Cyclotron Resonance-MS Associates with Markers of Inflammation and Metabolic Health. *Mol Cell Proteomics*. 2017;16(2):228-42.
2. Ruhaak LR, Koeleman CA, Uh HW, Stam JC, van Heemst D, Maier AB, et al. Targeted biomarker discovery by high throughput glycosylation profiling of human plasma alpha1-antitrypsin and immunoglobulin A. *PLoS One*. 2013;8(9):e73082.
3. Bakovic MP, Selman MH, Hoffmann M, Rudan I, Campbell H, Deelder AM, et al. High-throughput IgG Fc N-glycosylation profiling by mass spectrometry of glycopeptides. *J Proteome Res*. 2013;12(2):821-31.
4. de Haan N, Pucic-Bakovic M, Novokmet M, Falck D, Lageveen-Kammeijer G, Razdorov G, et al. Developments and perspectives in high-throughput protein glycomics: enabling the analysis of thousands of samples. *Glycobiology*. 2022;32(8):651-63.
5. Trbojevic-Akmacic I, Lageveen-Kammeijer GSM, Heijs B, Petrovic T, Deris H, Wuhler M, et al. High-Throughput Glycomic Methods. *Chem Rev*. 2022;122(20):15865-913.
6. de Haan N, Wuhler M, Ruhaak LR. Mass spectrometry in clinical glycomics: The path from biomarker identification to clinical implementation. *Clin Mass Spectrom*. 2020;18:1-12.
7. Bladergroen MR, Reiding KR, Hipgrave Ederveen AL, Vreeker GC, Clerc F, Holst S, et al. Automation of High-Throughput Mass Spectrometry-Based Plasma N-Glycome Analysis with Linkage-Specific Sialic Acid Esterification. *J Proteome Res*. 2015;14(9):4080-6.
8. Reiding KR, Bondt A, Hennig R, Gardner RA, O'Flaherty R, Trbojevic-Akmacic I, et al. High-throughput Serum N-Glycomics: Method Comparison and Application to Study Rheumatoid Arthritis and Pregnancy-associated Changes. *Mol Cell Proteomics*. 2019;18(1):3-15.
9. Liang J, Zhu J, Wang M, Singal AG, Odewole M, Kagan S, et al. Evaluation of AGP Fucosylation as a Marker for Hepatocellular Carcinoma of Three Different Etiologies. *Sci Rep*. 2019;9(1):11580.
10. Wu Y, Hao M, Li W, Xu Y, Yan D, Xu Y, et al. N-glycomic profiling reveals dysregulated N-glycans of peripheral neuropathy in type 2 diabetes. *J Chromatogr B Analyt Technol Biomed Life Sci*. 2023;1220:123662.
11. Jannetto PJ, Fitzgerald RL. Effective Use of Mass Spectrometry in the Clinical Laboratory. *Clin Chem*. 2016;62(1):92-8.
12. Veillon L, Huang Y, Peng W, Dong X, Cho BG, Mechref Y. Characterization of isomeric glycan structures by LC-MS/MS. *Electrophoresis*. 2017;38(17):2100-14.
13. Lan Y, Hao C, Zeng X, He Y, Zeng P, Guo Z, et al. Serum glycoprotein-derived N- and O-linked glycans as cancer biomarkers. *Am J Cancer Res*. 2016;6(11):2390-415.
14. Wuhler M, de Boer AR, Deelder AM. Structural glycomics using hydrophilic interaction chromatography (HILIC) with mass spectrometry. *Mass Spectrom Rev*. 2009;28(2):192-206.
15. Bagdonaitė I, Malaker SA, Polasky DA, Riley NM, Schjoldager K, Vakhrushev SY, et al. Glycoproteomics. *Nature Reviews Methods Primers* 2022;2(48).
16. Vreeker GC, Wuhler M. Reversed-phase separation methods for glycan analysis. *Anal Bioanal Chem*. 2017;409(2):359-78.
17. Gudelj I, Lauc G, Pezer M. Immunoglobulin G glycosylation in aging and diseases. *Cell Immunol*. 2018;333:65-79.
18. Dotz V, Wuhler M. N-glycome signatures in human plasma: associations with physiology and major diseases. *FEBS Lett*. 2019;593(21):2966-76.
19. Reilly C, Stewart TJ, Renfrow MB, Novak J. Glycosylation in health and disease. *Nat Rev Nephrol*. 2019;15(6):346-66.
20. Haslund-Gourley BS, Wigdahl B, Comunale MA. IgG N-glycan Signatures as Potential Diagnostic and Prognostic Biomarkers. *Diagnostics (Basel)*. 2023;13(6).
21. Carr SA, Abbatiello SE, Ackermann BL, Borchers C, Domon B, Deutsch EW, et al. Targeted peptide measurements in biology and medicine: best practices for mass spectrometry-based assay development using a fit-for-purpose approach. *Mol Cell Proteomics*. 2014;13(3):907-17.
22. Etchebarria J, Reichardt NC. Methods for the absolute quantification of N-glycan biomarkers. *Biochim Biophys Acta*. 2016;1860(8):1676-87.
23. Delafield DG, Li L. Recent Advances in Analytical Approaches for Glycan and Glycopeptide Quantitation. *Mol Cell Proteomics*. 2021;20:100054.
24. van der Burgt Y, Wuhler M. The Role of Clinical Glyco(proteo)mics in Precision Medicine. *Mol Cell Proteomics*. 2023;22(6):100565.

25. Shipman JT, Nguyen HT, Desaire H. So You Discovered a Potential Glycan-Based Biomarker; Now What? We Developed a High-Throughput Method for Quantitative Clinical Glycan Biomarker Validation. *ACS Omega*. 2020;5(12):6270-6.
26. Sustic T, Van Coillie J, Larsen MD, Derksen NIL, Szittner Z, Nouta J, et al. Immunoassay for quantification of antigen-specific IgG fucosylation. *EBioMedicine*. 2022;81:104109.
27. Kapur R, Kustiawan I, Vestrhein A, Koeleman CA, Visser R, Einarsdottir HK, et al. A prominent lack of IgG1-Fc fucosylation of platelet alloantibodies in pregnancy. *Blood*. 2014;123(4):471-80.
28. Larsen MD, de Graaf EL, Sonneveld ME, Plomp HR, Nouta J, Hoepel W, et al. Afucosylated IgG characterizes enveloped viral responses and correlates with COVID-19 severity. *Science*. 2021;371(6532).
29. Demus D, Urbanowicz PA, Gardner RA, Wu H, Juszczak A, Stambuk T, et al. Development of an exoglycosidase plate-based assay for detecting alpha1-3,4 fucosylation biomarker in individuals with HNF1A-MODY. *Glycobiology*. 2022;32(3):230-8.
30. Serdarevic N. The Comparison Between Different Immunoassays for Serum Carbohydrate Antigen (CA 19-9) Concentration Measurement. *Acta Inform Med*. 2018;26(4):235-9.
31. Hata T, Chiba K, Mizuma M, Masuda K, Ohtsuka H, Nakagawa K, et al. Levels of tumor markers CEA/CA 19-9 in serum and peritoneal lavage predict postoperative recurrence in patients with pancreatic cancer. *Ann Gastroenterol Surg*. 2022;6(6):862-72.
32. Hess V, Glimelius B, Grawe P, Dietrich D, Bodoky G, Ruhstaller T, et al. CA 19-9 tumour-marker response to chemotherapy in patients with advanced pancreatic cancer enrolled in a randomised controlled trial. *Lancet Oncol*. 2008;9(2):132-8.
33. Scara S, Bottoni P, Scatena R. CA 19-9: Biochemical and Clinical Aspects. *Adv Exp Med Biol*. 2015;867:247-60.
34. An HJ, Kronewitter SR, de Leoz ML, Lebrilla CB. Glycomics and disease markers. *Curr Opin Chem Biol*. 2009;13(5-6):601-7.
35. Abu Bakar N, Lefeber DJ, van Scherpenzeel M. Clinical glycomics for the diagnosis of congenital disorders of glycosylation. *J Inherit Metab Dis*. 2018;41(3):499-513.
36. Shkunnikova S, Mijakovac A, Sironic L, Hanic M, Lauc G, Kavur MM. IgG glycans in health and disease: Prediction, intervention, prognosis, and therapy. *Biotechnol Adv*. 2023;67:108169.
37. Clerc F, Reiding KR, Jansen BC, Kammeijer GS, Bondt A, Wuhler M. Human plasma protein N-glycosylation. *Glycoconj J*. 2016;33(3):309-43.
38. Lauber MA, Yu YQ, Brousmiche DW, Hua Z, Koza SM, Magnelli P, et al. Rapid Preparation of Released N-Glycans for HILIC Analysis Using a Labeling Reagent that Facilitates Sensitive Fluorescence and ESI-MS Detection. *Anal Chem*. 2015;87(10):5401-9.
39. Tirumalai RS, Chan KC, Prieto DA, Issaq HJ, Conrads TP, Veenstra TD. Characterization of the low molecular weight human serum proteome. *Mol Cell Proteomics*. 2003;2(10):1096-103.
40. Callewaert N, Van Vlierberghe H, Van Hecke A, Laroy W, Delanghe J, Contreras R. Noninvasive diagnosis of liver cirrhosis using DNA sequencer-based total serum protein glycomics. *Nat Med*. 2004;10(4):429-34.
41. Lauc G, Essafi A, Huffman JE, Hayward C, Knezevic A, Kattla JJ, et al. Genomics meets glycomics-the first GWAS study of human N-Glycome identifies HNF1alpha as a master regulator of plasma protein fucosylation. *PLoS Genet*. 2010;6(12):e1001256.
42. Juszczak A, Pavic T, Vuckovic F, Bennett AJ, Shah N, Pape Medvidovic E, et al. Plasma Fucosylated Glycans and C-Reactive Protein as Biomarkers of HNF1A-MODY in Young Adult-Onset Nonautoimmune Diabetes. *Diabetes Care*. 2019;42(1):17-26.
43. Demus D, Jansen BC, Gardner RA, Urbanowicz PA, Wu H, Stambuk T, et al. Interlaboratory evaluation of plasma N-glycan antennary fucosylation as a clinical biomarker for HNF1A-MODY using liquid chromatography methods. *Glycoconj J*. 2021;38(3):375-86.
44. Ng BG, Sosicka P, Agadi S, Almannai M, Bacino CA, Barone R, et al. SLC35A2-CDG: Functional characterization, expanded molecular, clinical, and biochemical phenotypes of 30 unreported Individuals. *Hum Mutat*. 2019;40(7):908-25.
45. Chen J, Li X, Edmondson A, Meyers GD, Izumi K, Ackermann AM, et al. Increased Clinical Sensitivity and Specificity of Plasma Protein N-Glycan Profiling for Diagnosing Congenital Disorders of Glycosylation by Use of Flow Injection-Electrospray Ionization-Quadrupole Time-of-Flight Mass Spectrometry. *Clin Chem*. 2019;65(5):653-63.
46. Adamczyk B, Tharmalingam T, Rudd PM. Glycans as cancer biomarkers. *Biochim Biophys Acta*. 2012;1820(9):1347-53.
47. Li D, Satomura S. Biomarkers for Hepatocellular Carcinoma (HCC): An Update. *Adv Exp Med Biol*. 2015;867:179-93.

48. Yamagata Y, Shimizu K, Nakamura K, Henmi F, Satomura S, Matsuura S, et al. Simultaneous determination of percentage of Lens culinaris agglutinin-reactive alpha-fetoprotein and alpha-fetoprotein concentration using the LiBASys clinical auto-analyzer. *Clin Chim Acta*. 2003;327(1-2):59-67.
49. Wessels H, Kulkarni P, van Dael M, Suppers A, Willems E, Zijlstra F, et al. Plasma glycoproteomics delivers high-specificity disease biomarkers by detecting site-specific glycosylation abnormalities. *J Adv Res*. 2023.
50. Zhang Z, Wu J, Liu P, Kang L, Xu X. Diagnostic Potential of Plasma IgG N-glycans in Discriminating Thyroid Cancer from Benign Thyroid Nodules and Healthy Controls. *Front Oncol*. 2021;11:658223.
51. de Jong SE, Selman MH, Adegnik AA, Amoah AS, van Riet E, Kruize YC, et al. IgG1 Fc N-glycan galactosylation as a biomarker for immune activation. *Sci Rep*. 2016;6:28207.
52. Qian Y, Wang Y, Zhang X, Zhou L, Zhang Z, Xu J, et al. Quantitative analysis of serum IgG galactosylation assists differential diagnosis of ovarian cancer. *J Proteome Res*. 2013;12(9):4046-55.
53. Ackerman ME, Crispin M, Yu X, Baruah K, Boesch AW, Harvey DJ, et al. Natural variation in Fc glycosylation of HIV-specific antibodies impacts antiviral activity. *J Clin Invest*. 2013;123(5):2183-92.
54. Kapur R, Della Valle L, Sonneveld M, Hipgrave Ederveen A, Visser R, Ligthart P, et al. Low anti-RhD IgG-Fc-fucosylation in pregnancy: a new variable predicting severity in haemolytic disease of the fetus and newborn. *Br J Haematol*. 2014;166(6):936-45.
55. Oosterhoff JJ, Larsen MD, van der Schoot CE, Vidarsson G. Afucosylated IgG responses in humans - structural clues to the regulation of humoral immunity. *Trends Immunol*. 2022;43(10):800-14.
56. Pongracz T, Nouta J, Wang W, van Meijgaarden KE, Linty F, Vidarsson G, et al. Immunoglobulin G1 Fc glycosylation as an early hallmark of severe COVID-19. *EBioMedicine*. 2022;78:103957.
57. Aleman OR, Rosales C. Human neutrophil Fc gamma receptors: Different buttons for different responses. *J Leukoc Biol*. 2023.
58. Van Coillie J, Schulz MA, Bentlage AEH, de Haan N, Ye Z, Geerdes DM, et al. Role of N-Glycosylation in FcgammaRIIIa interaction with IgG. *Front Immunol*. 2022;13:987151.
59. Hayes JM, Frostell A, Cosgrave EF, Struwe WB, Potter O, Davey GP, et al. Fc gamma receptor glycosylation modulates the binding of IgG glycoforms: a requirement for stable antibody interactions. *J Proteome Res*. 2014;13(12):5471-85.
60. Wojcik I, Senard T, de Graaf EL, Janssen GMC, de Ru AH, Mohammed Y, et al. Site-Specific Glycosylation Mapping of Fc Gamma Receptor IIb from Neutrophils of Individual Healthy Donors. *Anal Chem*. 2020;92(19):13172-81.
61. Washburn N, Meccariello R, Duffner J, Getchell K, Holte K, Prod'homme T, et al. Characterization of Endogenous Human FcgammaRIII by Mass Spectrometry Reveals Site, Allele and Sequence Specific Glycosylation. *Mol Cell Proteomics*. 2019;18(3):534-45.
62. Yagi H, Takakura D, Roumenina LT, Fridman WH, Sautes-Fridman C, Kawasaki N, et al. Site-specific N-glycosylation analysis of soluble Fcgamma receptor IIb in human serum. *Sci Rep*. 2018;8(1):2719.
63. Maliepaard JCL, Damen JMA, Boons GPH, Reiding KR. Glycoproteomics-Compatible MS/MS-Based Quantification of Glycopeptide Isomers. *Anal Chem*. 2023;95(25):9605-14.
64. Lippold S, de Ru AH, Nouta J, van Veelen PA, Palmblad M, Wuhrer M, et al. Semiautomated glycoproteomics data analysis workflow for maximized glycopeptide identification and reliable quantification. *Beilstein J Org Chem*. 2020;16:3038-51.
65. Choo MS, Wan C, Rudd PM, Nguyen-Khuong T. GlycopeptideGraphMS: Improved Glycopeptide Detection and Identification by Exploiting Graph Theoretical Patterns in Mass and Retention Time. *Anal Chem*. 2019;91(11):7236-44.



Addendum

English Summary
Nederlandse Samenvatting
Curriculum Vitae
List of Publications
Acknowledgments



ENGLISH SUMMARY

The immune system comprises a complex network of organs, tissues and cells with various types of biomolecules of which glycoproteins are an important class. Glycoforms are variants of a specific glycoprotein (coded by a single gene) that differ in the composition and/or structure of the attached glycans. Moreover, the site-occupancy of each glycoprotein may be different. Glycans on immune molecules modulate protein structure and function, thereby facilitating cell-cell recognition, signal transduction and interactions with other glycoproteins or the extracellular matrix. In this manner, glycans play a vital role in initiating and regulating both adaptive and innate immune responses. Changes in protein glycosylation may originate from genetic, epigenetic or environmental factors and resulting aberrances can impact immune function and are associated with immunopathological processes. For example, it is known that changes in immunoglobulin G (IgG) glycosylation influence effector mechanisms such as complement activation and antibody-dependent cellular cytotoxicity. It is therefore important to develop methods that provide a detailed insight into protein glycosylation in order to gain a comprehensive understanding of key immune-related glycoproteins, and translate these findings into clinical applications. This knowledge could aid in deciphering immune-related processes in health and disease, establishing clinical markers for early disease detection, and optimizing the glycosylation of biopharmaceuticals for enhanced therapeutic benefits.

In this thesis the intricate associations between glycosylation on immune-related molecules and clinical features across diverse biological contexts are discussed. By integrating cutting-edge liquid chromatography (LC) and mass spectrometry (MS) methodologies for N-glycan analysis, the research described in this thesis revealed glycan signatures of antibodies in two population studies, but also extended this type of methodology to other proteins (Fc gamma receptors; FcγRs) and matrices (semen). Through a comprehensive analysis of glycosylation patterns, structural determinants, and pathophysiological changes, the thesis revealed new associations underpinning glycan-mediated immune modulation.

In **Chapter 1**, the significance of protein N-glycosylation in the immune system is discussed, with a particular focus on the influence of various proteoforms of IgG and FcγRs on immune responses. N-glycosylation, intricately regulated by cellular metabolic states and environmental conditions, is crucial for various immunological processes such as intrinsic and extrinsic recognition mechanisms, signal transduction pathways and effector functions. Alterations in glycosylation patterns profoundly impact fundamental immunological processes and their association with inflammatory and autoimmune diseases. Furthermore, in this chapter, advances in MS technology are discussed that enable the identification of disease-specific glycan signatures, followed by highlighting potential clinical implications of aberrant glycosylation of immune glycoproteins as markers for disease diagnosis and prognosis.

Regulation as well as function of IgG Fc-glycosylation is still not fully understood, despite substantial studies that have included various clinical conditions. **Chapter 2** endeavours to

address this gap by investigating the role of the spleen in IgG glycosylation. Utilizing a well-established LC-MS glycoproteomic workflow, it examines the effect of splenectomy on IgG Fc-glycopeptides sourced from plasma samples of individuals who underwent splenectomy due to trauma (n = 38), immune thrombocytopenia (ITP, n = 35), or spherocytosis (n = 16) in comparison to controls with intact spleens (n = 165). The findings revealed that splenectomy led to an increase in IgG1 and IgG2/3 fucosylation, particularly pronounced in trauma and ITP cases. Furthermore, ITP patients exhibited lower IgG1 fucosylation compared to healthy controls, suggesting an altered immune response in this autoimmune condition. Overall, the findings indicate the important role of the spleen in formation and maintenance of IgG afucosylated responses, with implications for autoimmune diseases and immune responses to infections. Further research is needed to understand the mechanisms underlying these changes and their clinical implications.

One aspect of using antibody glycosylation in a clinical application is the ability to discern diseased individuals from healthy ones. Alternatively, and equally vital, antibody glycosylation provides insight into specific disease types or the likelihood of disease relapse. This offers the opportunity for personalized monitoring of a patient's disease progression and response to treatment. In **Chapter 3** the potential of IgG Fc-glycosylation as prognostic marker for relapse prediction in patients with anti-neutrophil cytoplasmic antibody (ANCA)-associated vasculitis (AAV) is described. In this study, serum samples from 89 AAV patients were collected at up to six time points spanning from diagnosis to relapse or time-matched remission. Total IgG glycosylation was determined by LC-MS with a particular focus on its longitudinal dynamics during initial treatment, maintenance therapy, follow-up and relapse. The results revealed differences in IgG Fc-sialylation and bisection between relapsing and non-relapsing patients. The reduction in IgG sialylation was observed months before relapse, underscoring its utility as a relapse marker. While sialylation differed in the year ahead of the relapse, bisection already differed at the time of diagnosis between relapsing and non-relapsing patients and correlated with long-term treatment efficacy. Importantly, the differences in IgG fucosylation between relapsing patients and non-relapsing provided compelling evidence of orthogonality of ANCA-rise and IgG fucosylation, underlining the potential of combining these markers aiming to improve patient outcomes.

So far many glycosylation studies focused on IgG. This can be partially attributed to the high abundance of IgG in the blood and the relatively low complexity of its glycosylation, which simplifies the analysis. However, in the context of initiation and regulation of immune effector responses, the glycosylation of not only IgG, but also its respective receptors is crucial, such as Fc-receptor FcγRIIIb which is found exclusively on granulocytes. In **Chapter 4**, a novel glycoproteomic method for site-specific profiling of FcγRIIIb with four to six potential N-glycosylation sites is introduced, addressing previous methodological limitations. The methodology involves the isolation of FcγRIIIb from primary human neutrophils and subjecting it to in-gel digestion followed LC-MS/MS analysis. This approach allows for simultaneous mapping of almost all glycosylation sites in a single experiment,

providing detailed insights into glycosylation site occupancy, glycan composition, and structure. Results demonstrated the complexity of FcγRIIIb glycosylation, revealing site-specific variations in glycan composition and occupancy. For example, distinct glycosylation sites varied in positional isomerism and abundance of fucose residue. Specifically, site N45 exhibited solely core fucosylation, whereas sites N74 and N169 predominantly displayed antenna fucosylation. Additionally, site N162 demonstrated a concurrent presence of both core and antenna fucosylation. Moreover, the study identifies two previously unexplored glycosylation sites, N74 and N169, and elucidates differences between FcγRIIIb glycosylation profiles in neutrophils compared to its soluble form and the homologous FcγRIIIa. Neutrophil-bound and soluble FcγRIIIb differed in the occupancy of site N64. Specifically, in the neutrophil-bound form, site N64 was unoccupied, while in the soluble form, highly branched glycans were observed at this site. A major difference between cell-bound FcγRIIIb and FcγRIIIa was noted in the level of antennary fucosylation. Namely, FcγRIIIb exhibited a higher degree of antennary fucosylation at sites N74, N162 and N169. The findings highlight the importance of glycosylation in modulating FcγRIIIb function which may be implicated in antibody-mediated immune responses. Moreover, the presented methodology offers a robust platform for future investigations into the role of FcγRIIIb glycosylation in various physiological and pathological contexts, with implications for therapeutic interventions and personalized medicine.

Various workflows are currently employed for high-throughput N-glycan analysis, allowing for the identification and characterization of protein N-glycosylation at different levels. This can include the characterization of glycopeptides, as described in preceding chapters, or released glycans, as shown in the subsequent chapter. While methodologies for released N-glycan analysis continue to evolve, new advancements are consistently emerging. One such innovation applies RapiFluor-MS, a fluorescent tag incorporating a quinoline fluorophore and a tertiary amine. This tag simplifies the sample preparation process and enhances fluorescence and MS detection. **Chapter 5** details on the development and optimization of a hydrophilic interaction LC-MS method for the analysis of RapiFluor-MS labeled N-glycans from plasma and serum samples. The optimized method effectively profiles and separates N-glycans into 44 individual glycan peaks with 72 assigned compositions. Moreover, the method was applied to assess glycosylation in a population cohort, demonstrating its capability to detect biological variability of the serum N-glycome and suggesting its utility for biomarker discovery and biopharmaceutical development.

Next to IgG N-glycosylation analysis, the field of glycomics has largely expanded with regard to plasma or serum N-glycome analyses. N-glycome analysis can also be applied to alternative biofluids, such as seminal plasma, and was used to study the potential correlation of N-glycosylation with sperm function, semen abnormalities and male reproductive system disorders. Factors such as hormonal imbalances, genetic aberrations, and lifestyle habits, including smoking, alcohol consumption, and exposure to environmental and occupational hazards contribute to loss of sperm DNA integrity and male

infertility. However, there is a limited understanding of the association between seminal plasma N-glycome, semen DNA fragmentation (SDF) and environmental exposure in men. In **Chapter 6** these associations were explored among men with normal ($n = 82$) and abnormal semen parameters ($n = 84$). In subjects with normal semen parameters, significant and simultaneous associations of sialylated N-glycans eluting in SPGP5 ($p = 0.006$), SPGP17 ($p = 0.025$), and SPGP26 ($p = 0.038$) with SDF, exposure to photocopying and smoking were observed. In subjects with abnormal semen parameters, a significant simultaneous association of diantennary digalactosylated N-glycan with core and antennary fucose eluting in SPGP18 with SDF ($p = 0.001$), and smoking was detected. The study concludes that seminal plasma N-glycan profile disturbances are associated with reduced semen quality and exposure to environmental factors. The findings offer new insights into male infertility risk assessment and underscore the potential of N-glycans as clinical markers for exposure to environmental stressors, but also highlight the need for further research to validate these findings.

Chapter 7, the general discussion, concludes this thesis. The performed research is contextualized within the existing literature. The strengths of MS-based glycomics methodology for clinical marker discovery studies are discussed, such as high-throughput and high-sensitivity, as well as the challenges with regard to separating structural isomers. Following this, it critically evaluates the feasibility of transferring and implementing these approaches into clinical practise. In this chapter non-MS platforms are presented as potentially simpler and more cost-effective alternatives, thus enhancing the potential for successful implementation in clinical settings. Lastly, the chapter discusses the potential of plasma-derived glycan-based clinical markers in the realm of personalized medicine, emphasizing the importance of integrating these markers with existing ones into multifactor platforms to enhance sensitivity and specificity.

NEDERLANDSE SAMENVATTING

Het immuunsysteem bestaat uit een complex netwerk van organen, weefsels en lichaamscellen met verschillende biomoleculen waarvan glycoproteïnen een belangrijk onderdeel zijn. Elk glycoproteïne (gecodeerd door één gen) verschijnt in meerdere glycovormen die verschillen in compositie en/of structuur van de glycanen. Deze glycanen zijn covalent gebonden aan specifieke aminozuren op een specifieke locatie van het glycoproteïne (glycosyleringsplaats). Overigens hoeft niet elke glycosyleringsplaats in een glycoproteïne volledig geglycosyleerd te zijn (bezettingsgraad). Glycanen die zijn verbonden aan immunologisch relevante moleculen moduleren de eiwitstructuur en -functie, eigenschappen die belangrijk zijn bij cel-cel herkenning, signaaltransductie en interactie met andere glycoproteïnen of de extracellulaire matrix. Op deze manier spelen glycanen een rol bij het initiëren en reguleren van zowel de adaptieve als aangeboren immuunrespons. Veranderingen in eiwitglycosylering als gevolg van (epi)genetische of omgevingsfactoren hebben een impact op de immuunfunctie en zijn geassocieerd met immunopathologische processen. Een voorbeeld hiervan is glycosylering van immunoglobuline G (IgG), waarbij veranderingen gevolgen hebben voor complement-activering en antilichaam-gereguleerde cytotoxiciteit van cellen. Het is daarom belangrijk methodes te ontwikkelen die eiwitglycosylering gedetailleerd in kaart kunnen brengen en die bijdragen aan het begrip van immunologisch relevante glycoproteïnen en daarmee translatie naar klinische toepassingen mogelijk maken. Deze kennis zal helpen bij het ontcijferen van immunologische processen bij ziekte en gezondheid, het implementeren van klinische markers voor vroegdetectie, en het optimaliseren van glycosylering van biofarmaceutische producten voor verbeterde therapie.

In dit proefschrift zullen de complexe associaties tussen glycosylering van immunologisch relevante moleculen en klinische verschijnselen met verschillende biologische context worden besproken. Voor het onderzoek dat hier is beschreven wordt gebruikt gemaakt van de nieuwste analytische methoden op gebied van vloeistofchromatografie (LC) en massaspectrometrie (MS). Specifieke glycaansignaturen van antilichamen in verschillende populatiestudies worden gerapporteerd. Daarnaast zijn deze methoden ingezet bij het bestuderen van andere eiwitten (namelijk Fc gamma receptoren FcγRs) en de analyse van glycoproteïnen in een alternatieve matrix (zoals semen). Na uitvoerige analyses werden nieuwe associaties gevonden tussen glycosyleringspatronen, structuurdeterminanten en pathofysiologische veranderingen, die het belang van glycosylering in immuunmodulatie onderstrepen.

In **Hoofdstuk 1** wordt het belang van eiwitglycosylering in het immuunsysteem beschreven, met speciale aandacht voor verschillende proteovormen van IgG en FcγRs op immuunrespons. N-glycosylering is op een complexe manier gereguleerd door een combinatie van de metabole toestand van een cel en omgevingsfactoren. N-glycosylering speelt een belangrijke rol in immunologische processen zoals intrinsieke en extrinsieke herkenningsmechanismen, signaaltransductie en effectorfuncties. Afwijkingen in

glycosyleringspatronen hebben een grote invloed op fundamentele immunologische processen en hun associatie met ontstekings- en autoimmuunziekten. Daarnaast worden in dit hoofdstuk ontwikkelingen in MS-technologie besproken die geschikt zijn voor het bepalen van ziekte-specifieke signaturen. Tenslotte wordt een overzicht gegeven van de klinische implicaties van afwijkingen met betrekking tot glycosylering en het toepassen van immunologisch relevante glycoproteïnen als diagnostische of prognostische ziektemarker. Zowel de regulering als de functie van IgG Fc-glycosylering zijn niet volledig opgehelderd, ondanks vele studies die zijn uitgevoerd bij verschillende klinische condities. In **Hoofdstuk 2** is de rol van de milt en splenectomie op IgG Fc-glycosylering bestudeerd door gebruik te maken van een geavanceerde LC-MS *glycoproteomics* strategie. IgG uit plasmamonsters van gezonde individuen met intacte milt (n = 165) werd vergeleken met IgG van personen bij wie de milt verwijderd is na trauma (n = 38), of als gevolg van immuun trombocytopenie (ITP, n = 35) of sferocytose (n = 16). Er werd gevonden dat splenectomie resulteerde in een toegenomen hoeveelheid IgG1 en IgG2/3 fucosylering, met name in het geval van trauma en ITP. Daarnaast liet deze laatste groep lagere IgG1 fucosylering zien vergeleken met gezonde controles, dit impliceert een veranderde immuunrespons bij deze autoimmuunziekte. Samenvattend lieten deze resultaten zien dat de milt een belangrijke rol speelt bij het vormen en onderhouden van niet-gefucosyleerd IgG. Meer onderzoek is noodzakelijk teneinde de mechanismen te achterhalen die aan deze veranderingen ten grondslag liggen.

In het algemeen vormen glycosyleringspatronen van antilichamen een potentiële klinische applicatie voor het onderscheiden van zieke en gezonde individuen. Even belangrijk is echter dat zulke profielen inzicht kunnen geven in een bepaalde ziekte of de kans op terugkeren van een ziekte (recidive). Hiermee wordt het persoonlijk monitoren van het ziekteverloop en de behandeling van een patiënt mogelijk. In **Hoofdstuk 3** wordt bestudeerd welk potentieel IgG Fc-glycosylering heeft als prognostische marker voor recidive bij patiënten met *anti-neutrophil cytoplasmic antibody (ANCA)-associated vasculitis* (AAV). Hierbij zijn serummonsters van 89 AAV patiënten verzameld op verschillende tijdstippen in de periode tussen diagnose en terugkeer van ziekte. Totaal IgG glycosylering werd bepaald met LC-MS waarbij nauwkeurig de longitudinale verschillen tussen initiële behandeling, therapie, follow-up en recidive werden geëvalueerd. De resultaten lieten een verschil in IgG Fc-sialylering en *bisection* zien tussen patiënten met en zonder recidive. De afname in IgG sialylering werd reeds vastgesteld maanden vóór terugkomst van de ziekte, wat de bruikbaarheid als recidive-marker onderstreept. De hoeveelheid *bisection* verschilde tussen patiënten met en zonder recidive zelfs al op tijdstip van diagnose en correleerde met effectiviteit van de behandeling. Deze verschillen tussen patiënten met en zonder recidive zijn veelbelovend voor het verbeteren van patiëntperspectief door ANCA-detectie te combineren met IgG Fc-glycosylering.

Tot dusver beschreven de meeste glycosyleringsstudies IgG, wellicht omdat dit glycoproteïne in een relatief hoge concentratie in bloed voorkomt en de

glycosyleringsprofielen eenvoudig zijn. Echter, in het licht van initiatie en regulering van immuunrespons is het niet alleen belangrijk naar IgG glycosylering te kijken, maar ook naar de corresponderende receptoren, zoals Fc-receptor FcγRIIIb welke uitsluitend op granulocyten wordt aangetroffen. In **Hoofdstuk 4** wordt een nieuwe *glycoproteomics* methode ingezet om 4 tot 6 mogelijke glycosyleringsplaatsen van FcγRIIIb in kaart te brengen. Hierbij is FcγRIIIb geïsoleerd uit humane neutrofielen, gevolgd door in-gel digestie en LC-MS/MS analyse van (glyco)peptiden. De resultaten lieten een complex beeld van FcγRIIIb glycosylering zien, met variaties in glycaancompositie en -bezetting op elke afzonderlijke glycosyleringsplaats. Zo werd op plaats N45 uitsluitend core-fucosylering aangetroffen, terwijl aminozuren N74 en N169 voornamelijk antenne-fucosylering lieten zien (aminozuur N162 had beide vormen). Aan de hand van aminozuren N74 en N169, die niet eerder zijn bestudeerd, werd gevonden dat FcγRIIIb glycosyleringsprofielen van neutrofielen verschilden van de oplosbare vorm (in de circulatie) en homologe FcγRIIIa. Daarnaast werden er verschillen gevonden in de bezettingsgraad op aminozuur N64. Bij FcγRIIIb op neutrofielen was N64 niet geglycosyleerd, terwijl in de oplosbare vorm sterk vertakte glycaanstructuren werden aangetroffen. Daarnaast verschilden FcγRIIIb en FcγRIIIa voor wat betreft de hoeveelheid antennaire structuren, waarbij de eerste hoge niveaus van antennaire fucosylering liet zien op aminozuren N74, N162 en N169. Deze bevindingen onderstrepen het belang van glycosylering bij het moduleren van de functie van FcγRIIIb. Tenslotte dient opgemerkt dat de gebruikte methodologie geschikt is voor toekomstig onderzoek van de rol van FcγRIIIb glycosylering in verschillende fysiologische en pathologische context, met implicaties voor therapeutische interventie en precisiegeneeskunde in het algemeen.

Verschillende analytische strategieën worden toegepast voor *high-throughput* analyse van N-glycanen. In de voorgaande hoofdstukken werden glycanen geïdentificeerd in glycopeptide-vorm, in het volgende hoofdstuk worden deze gekarakteriseerd als van-eiwit-vrijgemaakte N-glycanen. Een innovatie op het gebied van vrijgemaakte N-glycanen past RapiFluor-MS toe, waarbij een fluorescent molecuul (met een quinoline fluorofoor) gekoppeld wordt aan een glycaan met als voordeel een vereenvoudigde monstervoorbewerking en detectie met behulp van fluorescentie. In **Hoofdstuk 5** wordt de ontwikkeling en optimalisering van een hydrofiele interactie LC-MS methode beschreven voor de analyse van met RapiFluor-MS gekoppelde N-glycanen uit serum- en plasmamonsters. Er konden 44 verschillende pieken worden gescheiden waarbij 72 composities werden vastgesteld. De methode is geschikt voor het evalueren van biologische variaties en biomarker kandidaten in grote cohorten, en kan tevens worden ingezet bij ontwikkeling van biofarmaceutische producten.

De beschreven N-glycoom strategieën zijn eveneens geschikt voor de analyse van alternatieve lichaamsvloeistoffen, zoals semen. In **Hoofdstuk 6** is de correlatie tussen N-glycosylering en het mannelijk reproductiesysteem bestudeerd aan de hand van afwijkend

semen materiaal. Factoren die een rol spelen bij kwaliteitsverlies van zaadcellen en onvruchtbaarheid bij mannen zijn afwijkingen in de hormoonhuishouding, leefstijl (roken, alcohol, omgevingsfactoren) en genetische afwijkingen. Heel specifiek is er gekeken naar de associatie tussen semen N-glycoomprofielen, semen DNA fragmentatie (SDF) en omgevingsparameters in mannen met normale ($n = 82$) en afwijkende ($n = 84$) semen parameters. In de eerste groep werden significante associaties waargenomen tussen gesialyleerde N-glycanen met SDF en blootstelling aan fotokopiëren en roken. In de tweede groep werd een significante associatie waargenomen tussen diantennaire digalactosyleerde N-glycanen met zowel core- als antenne-fucosylering en roken. Geconcludeerd werd dat een afgenomen kwaliteit van semen correleerde met afwijkingen in het N-glycaan profiel en dat deze bevindingen als startpunt kunnen fungeren voor het verder ontwikkelen van N-glycanen als potentiële marker voor blootstelling aan omgevingsfactoren met betrekking tot vruchtbaarheidsrisico's voor mannen.

Dit proefschrift sluit af met een algemene discussie in **Hoofdstuk 7**. Het beschreven onderzoek wordt in het licht van recente literatuur besproken evenals de voordelen van glycosyleringsanalyses met behulp van massaspectrometrie voor klinisch biomarker onderzoek. Vervolgens wordt er een kritische evaluatie gegeven over of en hoe deze analytische strategieën en glycosyleringsprofielen hun weg kunnen vinden in de klinische praktijk. Er wordt een inkijk gegeven in platforms die geen gebruik maken van MS en daarmee potentieel eenvoudiger en goedkoper te implementeren zijn in een klinische setting. Tenslotte worden nieuwe, potentiële glycosyleringsmarkers besproken in de context van precisiegeneeskunde ("zorg op maat") en wordt geconcludeerd dat deze geïntegreerd dienen te worden met bestaande markers teneinde sensitiviteit en specificiteit op een multiparameter manier te verbeteren.

CURRICULUM VITAE

Iwona Borošak (*née* Wójcik) was born on September 18th, 1989 in Sosnowiec, Poland. Her insatiable curiosity and endless fascination with the natural world manifested at an early stage, nurturing a profound interest in biology and chemistry.

Her passion for the natural sciences led her to pursue her academic career at Jagiellonian University, where she obtained both her Bachelor's and Master's degrees in Biotechnology. Her education was broadly focused on various aspects of molecular biology and biochemistry, equipping her with a versatile skill set that included techniques in analytical chemistry, molecular biology, and cell culture. During her Master's she specialized in proteomics and mass spectrometry while focusing her research on the proteomic analysis of *Staphylococcus aureus* virulence factors. This period solidified her fascination with the intricate biochemical processes within the human body.

Motivated by her desire to unravel the complexities of the human body, in 2017, she decided to pursue her scientific career in interdisciplinary and international research settings applying for the prestigious Marie Skłodowska-Curie fellowship. Upon approval, she joined the interdisciplinary European Industrial Doctorate program (GlySign) at Leiden University Medical Centre (LUMC) in the Netherlands. While primarily enrolled in a doctorate program at LUMC and engaged in research projects led by Prof. Manfred Wuhrer, she spent a significant portion of her time at the industrial partner Genos Ltd led by Prof. Gordan Lauc. This dual engagement in both industry and academia provided her with valuable experience. At Genos, supervised by Maja Pučić-Baković, she mastered high-throughput techniques for immunoglobulin G and plasma N-glycosylation analysis. She also contributed to developing novel methods for N-glycan analysis. At LUMC, mentored by Dr. David Falck, she refined her expertise in LC-MS N-glycosylation analysis. During her work there, she mapped the N-glycosylation of Fc gamma receptor IIIb and analyzed subclass-specific IgG N-glycosylation in different pathological conditions. Her research led to several publications in peer-reviewed journals.

Currently, Iwona is employed as a Researcher at Genos Ltd., Zagreb, within the group of Gordan Lauc, where she is deepening her understanding of glycans as potential biomarkers and leveraging high-throughput glycomic techniques. Her scientific interests are focused on glycobiology, mass-spectrometry-based proteomics, protein chemistry, and biomarker discovery.

LIST OF PUBLICATIONS

First author papers

- 1) **Site-Specific Glycosylation Mapping of Fc Gamma Receptor IIIb from Neutrophils of Individual Healthy Donors**
Iwona Wojcik, Thomas Sénard, Erik L de Graaf, George MC Janssen, Arnoud H de Ru, Yassene Mohammed, Peter A van Veelen, Gestur Vidarsson, Manfred Wuhrer and David Falck

Analytical Chemistry 92(19):13172-13181, 2022
- 2) **A functional spleen contributes to afucosylated IgG in humans**
Iwona Wojcik, David E. Schmidt, Lisa A. de Neef, Minke A.E. Rab, Bob Meek, Okke de Weerd, Manfred Wuhrer, C. Ellen van der Schoot, Jaap J. Zwaginga, Masja de Haas, David Falck and Gestur Vidarsson

Scientific Reports 15;11(1):24045, 2021
- 3) **Seminal plasma N-glycome as a new biomarker of environmental exposure associated with semen quality**
Maric T, Wójcik I, Katusic Bojanac A, Matijevic A, Ceppi M, Bruzzzone M, Evgeni E, Petrovic T, Trbojevic-Akmacic I, Lauc G, Jezek D and Fucic A

Reproductive Toxicology 113:96-102, 2022
- 4) **Specific IgG glycosylation differences precede relapse in PR3-ANCA PR3-ANCA-associated vasculitis patients with and without ANCA rise**
Iwona Wojcik^{1,2}, Manfred Wuhrer¹, Peter Heeringa³, Coen Stegeman⁴, Abraham Rutgers⁵, David Falck¹

Frontiers in Immunology 14:1214945, 2023

ACKNOWLEDGMENTS

Dear reader, thank you for taking the time to read my thesis and reaching this section, where I would like to acknowledge the exceptional individuals who made this thesis possible. From my esteemed promotors and co-promotors to my amazing friends. Thanks to all of them, I am about to defend my PhD thesis, filled with profound gratitude and appreciation. First, I would like to express my sincere gratitude to my promotor, Manfred, for allowing me to pursue my doctorate and explore the exciting field of glycobiology. I am deeply thankful for your immense support, expert guidance, and encouragement. Your brilliance, wisdom, and analytical knowledge command respect, while your care for students and remarkable organizational skills are truly admirable!

I wish to extend my deepest gratitude to my promotor, Gordan, for offering me the life-changing opportunity to relocate to Croatia and participate in the GlySign project. I could not have asked for a better mentor and ultimately a boss and I am profoundly grateful for your unwavering friendliness, genius, and support throughout my efforts.

I am immensely grateful for the unconditional guidance and exceptional support I received, even from a distance, from my co-promotor, David. I am deeply thankful for reading and re-reading my manuscripts, always providing insightful, constructive feedback and invaluable advice. I admire your analytical mind, and extensive knowledge, and consider myself truly fortunate to have had you as my supervisor!

I would like to extend my sincere thanks to Maja and Mislav, who have been great daily supervisors at Genos. I am grateful for their profound belief in my abilities, their helpful advice and practical suggestions. It has been an immense pleasure to work with you and I look forward to having an opportunity to collaborate with you in the future.

I would like to thank our collaborators from Sanquin, especially Gestur, for expanding my knowledge in immunology. I enjoyed our insightful discussions, and I found myself continually impressed by your expertise, knowledge and dedication. It was a pleasure to work with you.

I shared my PhD time between Leiden University Medical Center and Glycoscience Research Laboratory in Zagreb. A special thanks go to my Genos colleagues, Olga, Tomislav, Marija, and Anne-Marie for sharing the office with me, engaging in discussions, and offering words of advice and encouragement. I am also grateful to my colleagues at LUMC for their warm welcome, inspiring discussions, and tremendous support.

My PhD journey would not have been the same without my friends Aniela and Daniel. Aniela, you are an inspiring person and a very talented scientist, I learnt so much from you. Daniel, you are the most fun and intelligent person I know! Thank you for always being there

for me, and I am happy to have you by my side during my upcoming defence. I look forward to continuing to support each other through life's ups and downs.

A special thanks to Jan for being an incredible paranymph, and for being my ears and eyes in Leiden. Your support in the final steps of this journey has been invaluable. I am continually amazed by your kindness, positive energy, and professionalism. I know that with you and Daniel, I will have the best support during my PhD defence.

I would also like to thank my student Eva for her excellent work and for bringing out the best in me as a supervisor.

GlySign fellows, it was a great adventure exploring both the Netherlands and Croatia, and participating in various training sessions together. I truly enjoyed our time together, and wish you all the best in your careers.

I am grateful to my husband, not only for prioritizing my career alongside our lives, but also for sharing this incredible journey with me. Thank you for your unwavering support, smile and optimism over the long working weekends.

Mamo, Jacek, Leszek i Konrad, dziękuję Wam za wasze wsparcie w dążeniu do spełnienia moich marzeń. Nawet jeśli to doświadczenie nas trochę rozdzieliło, dla mnie zawsze byliście blisko.

Twona

